The Thesis Committee for Matthew Brian Stokley
Certifies that this is the approved version of the following thesis:

Development of an In-Core Neutron Monitoring System and Characterization of the University of Texas at Austin TRIGA Reactor Steady-State Neutron Flux Variations for use with Neutron Activation Analysis

APPROVED BY
SUPERVISING COMMITTEE:

Supervisor:

Derek Haas

Steven Biegalski

Development of an In-Core Neutron Monitoring System and Characterization of the University of Texas at Austin TRIGA Reactor Steady-State Neutron Flux Variations for use with Neutron Activation Analysis

by

Matthew Brian Stokley

Thesis

Presented to the Faculty of the Graduate School of

The University of Texas at Austin

in Partial Fulfillment

of the Requirements

for the Degree of

Master of Science in Engineering

The University of Texas at Austin

May 2018

Dedication

I would like to dedicate this work to my Family. To my wife, Christina, and my children, Evans and Nolan, thank you for allowing me to have the opportunity and providing the desire to do my very best. Your zeal for life, learning, and happiness is a beacon I try to follow everyday both professionally and personally. I am so much better for it. To my parents, Karon and Byron, thank you for giving me the tools and wherewithal to finish the tasks I have completed and attack the ones I have yet to do. The core-values that are my foundation, I owe to you. To Pat and Marie, I am very much appreciative of the love and support. I can never say it enough, thank you all.

Acknowledgements

There are many people to thank associated with my time at The University of Texas at Austin. First, I would like to thank my advisors Dr. Steven Biegalski and Dr. Derek Haas for their guidance and trust. This project was a great broadening experience professionally, intellectually and personally. I appreciate you providing me with the freedom to attack issues as I saw fit and for holding me accountable for the results. The success of this project and my time at The University of Texas at Austin are a direct result of your work and dedication.

I would like to thank Dr. Sheldon Landsberger for introducing me to the Nuclear and Radiation Engineering Program and his support and guidance throughout my time at The University of Texas at Austin. Our first meeting facilitated my attending the program and for that I am very grateful.

I would also like to thank everyone that helped with the technical and logistical aspects of this project. Dr. Edward Artnak for his help talking through issues and designing N-MS components with the utmost attention to detail. Mr. Larry Hall for always being available to conduct a reactor run and speak about things from a military point-of-view. Mr. Tracy Tipping for working the important health physics aspects needed for any radiological work. Mr. Greg Kline for providing a crash course in NI LabVIEW and initial system prototypes. Dr. Matt Paul for the skeptical discussions and dry erase board talks. I apologize as there are others needing to be named, but please accept my appreciation for the support.

Abstract

Development of an In-Core Neutron Monitoring System and Characterization of the University of Texas at Austin TRIGA Reactor Steady-State Neutron Flux Variations for use with Neutron Activation Analysis

Matthew Brian Stokley, M.S.

The University of Texas at Austin, 2018

Supervisor: Derek Haas

The pneumatic NAA facility within The University of Texas at Austin is widely used for the measurement of trace elemental concentrations. It has been shown for extremely short duration NAA irradiations, sample activation measurements can vary by up to 12% from normalized values. The typical university research reactor's external neutron monitoring instruments are unable to detect small, localized variations in neutron population likely resulting in the observed error. The primary method to reduce this uncertainty is to irradiate traceable flux monitor samples in addition to the experimental samples to be analyzed. This method doubles the required sample prep, measurement, and analysis effort. An in-core neutron monitoring system was designed and installed adjacent to the pneumatic NAA sample system terminus to track these localized fluctuations. This design consists of a miniature in-core fission chamber fitted through the upper grid plate of the reactor core. The system is controlled by a NI LabVIEW data logging application.

This system provides the capability of monitoring sample irradiance in real-time. In preliminary testing, the system was able to track short irradiation NAA sample variance to within 3% of normalized values. Thus, a significant reduction in the uncertainty of NAA measurements for trace elemental concentrations is achievable.

Table of Contents

List of Tables

List of Figures

List of Illustrations

Chapter 1: Introduction

The field of elemental analysis has become a key component of our world's everyday life. The better understanding of elemental compositions has enabled mankind to engineer superior materials and products, answer historical questions, solve and deter criminal activity, ensure environmental protection, develop safe medical treatments, and the list goes on and on. From improving the seemingly trivial time it takes your cellphone to charge to the potential development of new cryogenic fuel tanks for interplanetary travel, elemental analysis has a foundational role in the success of scientific endeavors.

One such elemental analysis technique is Neutron Activation Analysis (NAA). NAA is suitable for conducting both qualitative and quantitative analysis of major, minor, and trace elements in samples. It is an isotopic analytical technique that has the ability to distinguish between more than 30 elements in a sample and, depending on analytical parameters, can have extremely low detection limits on the order of 1 ppm to 0.1 ppt. [Chen, 2010; Hancock, 2015] NAA samples can be analyzed in any physical form, liquid, solid or gas, and often sample sizes can be on the order of milligrams of material. In addition, NAA is a non-destructive analytical technique which allows a single sample to tested multiple times if desired.

All of these benefits make NAA a very attractive tool for scientific research. University and government research reactors are the primary method used to perform NAA irradiation. The University of Texas at Austin has a General Atomics TRIGA Mark II Research Reactor used for NAA and researchers can conduct such analysis at UT Austin's Nuclear Engineering Teaching Laboratory.

The University of Texas at Austin's Nuclear Engineering Teaching Laboratory (NETL) is an experimental research and teaching facility housing a 1.1 MW General

Atomics TRIGA Mark II reactor. The laboratory has multiple experimental facilities used to perform research centered around the utilization of the reactor. Experimental facilities include beam ports that penetrate the reactor reflector and shielding to provide external irradiation capabilities and internal core irradiation facilities using a Rotary Specimen Rack (RSR), fuel element replacement cavities and pneumatic sample delivery systems.

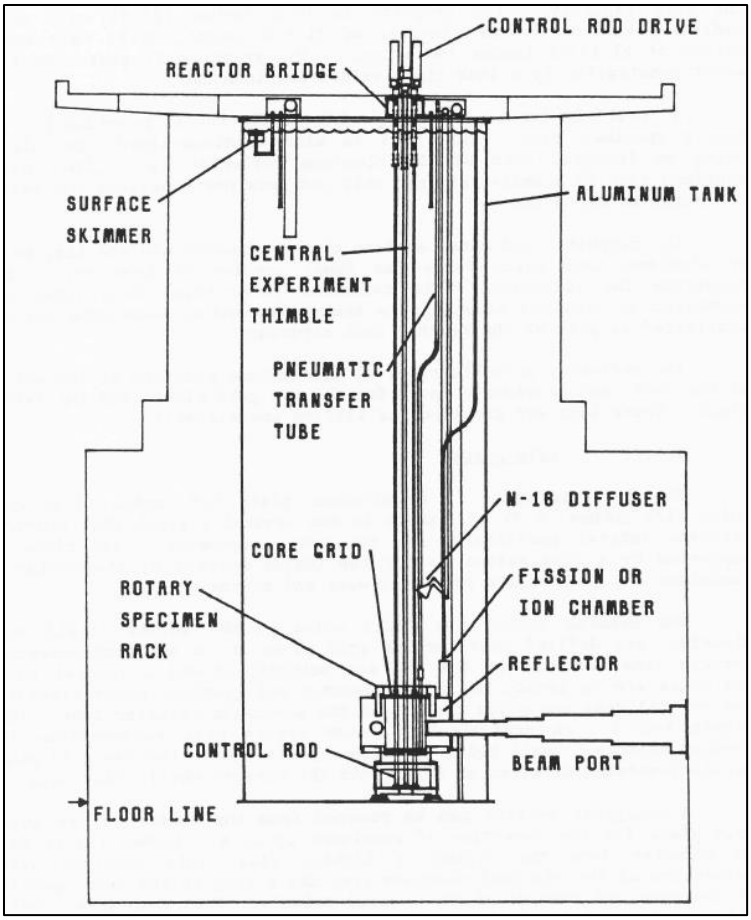

Figure 1.1: General Atomics TRIGA Mark II Research Reactor Layout [NETL SAR, 1991]

These irradiation facilities can be used to perform NAA in a multitude of ways. From long duration, low intensity neutron irradiations of large samples with the external

beam ports to rapid in-core, high neutron irradiations of milligram size samples with the pneumatic transfer systems (PTS).

1.1 Project Motivation

The NAA PTS is a highly utilized experimental facility within The University of Texas at Austin's Nuclear Engineering Teaching Laboratory. The NAA PTS is located within the G-ring of the NETL TRIGA Mark II Nuclear Reactor. The reactor power and neutron flux monitoring instruments, an NM-1000 and two NP(P)-1000 fission chambers, are located on the outside of the reactor's graphite reflector.

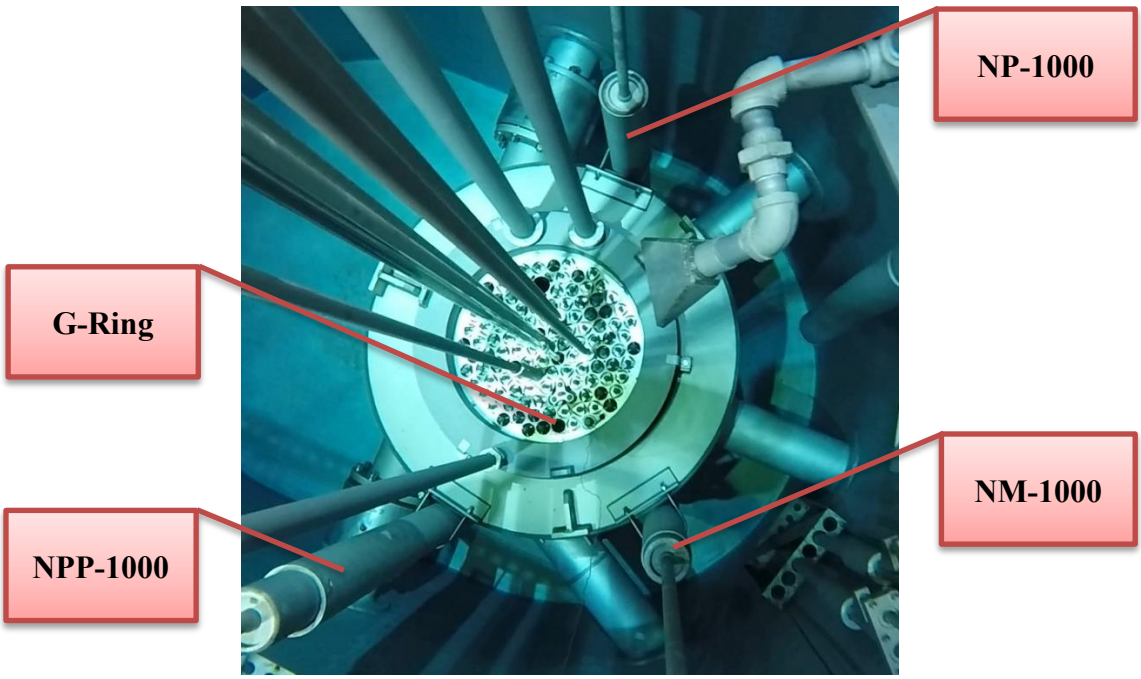

Figure 1.2: NETL TRIGA Mark II Research Reactor

This location, though an ideal placement for overall reactor power monitoring and detector longevity, does not allow for the sensitive localized inner core measurements needed to detect minute neutron flux variations at steady state power that can influence experimental sample irradiation activation. [Knoll, 2010] A reactor's neutron population is heavily dependent on many core configuration parameters.[DiLuzio, 2017] The neutron population internally can shift with control rod movement, temperature changes, and xenon buildup. This can cause a divergence in a given locations neutron flux compared to another location. [Kaiba, 2015] These steady state power neutron flux variations can become a significant source of experimental error when performing short duration irradiations. The reactor Instrument Control System (ICS) controlled steady state power can potentially have localized neutron flux variations up to 8-12% of nominal levels. [Landsberger, 2012] To reduce this induced error, natural sulfur powder flux monitors can be made and sent with experimental samples to detect the neutron flux during irradiation. This method can reduce experimental error significantly but requires additional sample preparation, reactor irradiation, processing, analysis time, and cost.

A solution was proposed to design a Neutron Monitoring System (N-MS) capable of detecting the localized neutron flux variations in real-time and within a neutron path-length of the NAA PTS terminus. With the N-MS essentially collocated with the NAA sample, accurate neutron flux measurements can be made allowing significant experimental error reduction without the added time, resources, and cost of using natural sulfur powder flux monitors. [Landsberger, 2012; Braisted, 2008]

Chapter 2: Reactor Theory

The University of Texas at Austin's (UT Austin) Nuclear Engineering Teaching Laboratory (NETL) TRIGA Mark II nuclear reactor can achieve up to 1.1 MW steady state power and can Pulse to power levels reaching 1600 MW. The fuel used at NETL is a Uranium-Zirconium-Hydride (UZrH) fuel enriched to 19.75% ^{235}U. The ^{235}U is the primary fuel fissioned during NETL TRIGA reactor operations and starting the reactor begins with the introduction of free neutrons. Free neutrons diffuse and collide with other atoms within the reactor core until they reach an energy conducive to being absorbed by the ^{235}U fuel. This is called moderation. Moderators used in the NETL TRIGA are H_2O and the UZrH fuel itself. Neutrons are produced from fission at energies averaging around 2 MeV and can range from sub-MeV up to about ten MeV. The most likely energy for a neutron in the reactor is approximately 0.025 eV. This is the thermal energy region and improves the likelihood of fission due to the large absorption cross-section for ^{235}U at this energy. Hydrogen components of both moderators allow the neutron energy spectrum to be reduced to thermal equilibrium through elastic scattering.

When struck by an incoming neutron, the ^{235}U atom can absorb the neutron and split releasing fission products, free neutrons, and energy. The released neutrons can then go on to interact with other ^{235}U atoms within the fuel to cause more fission, thereby releasing more fission products, neutrons and energy. This is called a chain reaction that can build, leading to critically where the reaction is self-sustaining. The reaction is controlled and monitored at the NETL TRIGA Instrument Control Station (ICS) by inserting or removing control rods designed to absorb free neutrons. The control rods can break the chain reaction cycle and return the reactor to a subcritical state when inserted or allow more neutrons to flow within the core to increase reactor reactivity when withdrawn.

The reactor core also has graphite reflectors to moderate and return free neutrons back into the core allowing them to fission more fuel. Other neutrons can leak out of the core and are absorbed by structural shielding designed to keep the reactor bay safe for students, staff, and researchers. The shieling is composed of the reactor pool water and finally the concrete structure of the reactor vessel.

The time rate of change of a nuclear reactor can be represented as the change in neutron population.

$$\frac{\partial n(t)}{\partial t} = \dot{n}(t) = \alpha n(t) \qquad \text{Eq. 2.1}$$

Where α is the Inverse Period of the reactor. The solution to the time rate of change of the reactor neutron population with a constant period is below.

$$n(t) = n_o e^{\alpha t} \qquad \text{Eq. 2.2}$$

Inhomogeneity within the reactor core influences the neutron population's ability to propagate evenly throughout the core. Neutron leakage rate will change with core design and level of inhomogeneity. Core inhomogeneity and the resulting relative flux distortion that can be a result is depicted in the figure below.

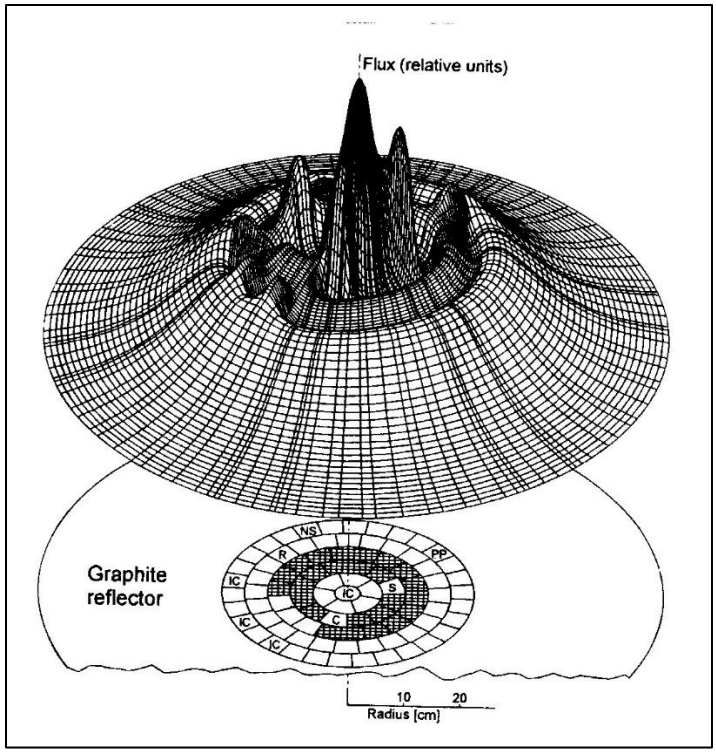

Figure 2.1. Core inhomogeneity neutron flux. [Ravnik, 1990]

The UT Austin NETL TRIGA reactor was modeled to capture the system's specific neutron population localized variation. Figure 2.2 and 2.3 show the modeled relative neutron population effects of the reactor's core inhomogeneity at a centerline core height of 12 to 13 inches from the upper grid plate at moderate critical power. This is the approximate height of pneumatic transfer system's sample terminus. During long runs or after multiple days of running the control rods are withdrawn further from the core to compensate for xenon buildup and other reactor poisons. As a result, this region's neutron population can change significantly from one experiment to another.

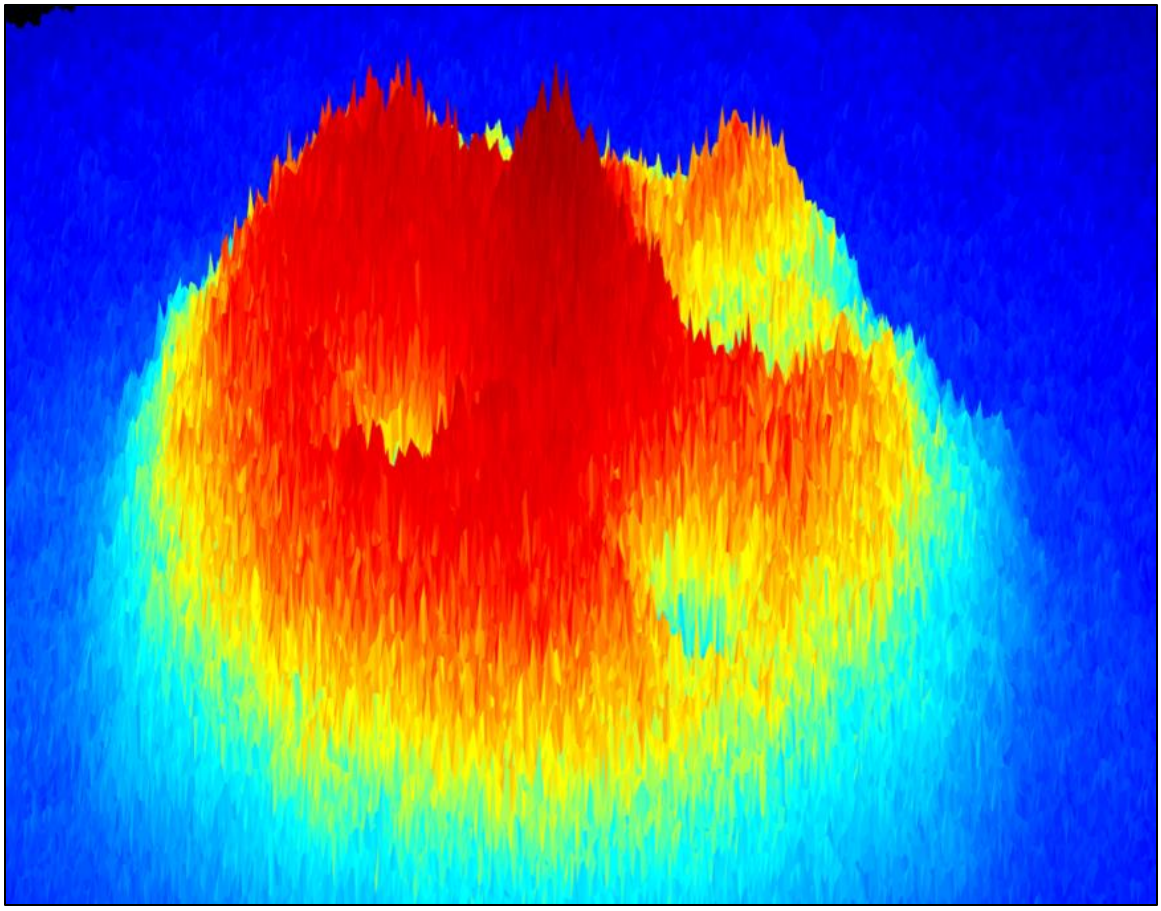

Figure 2.2. UT NETL TRIGA MCNP Modeled Core Inhomogeneity neutron flux.

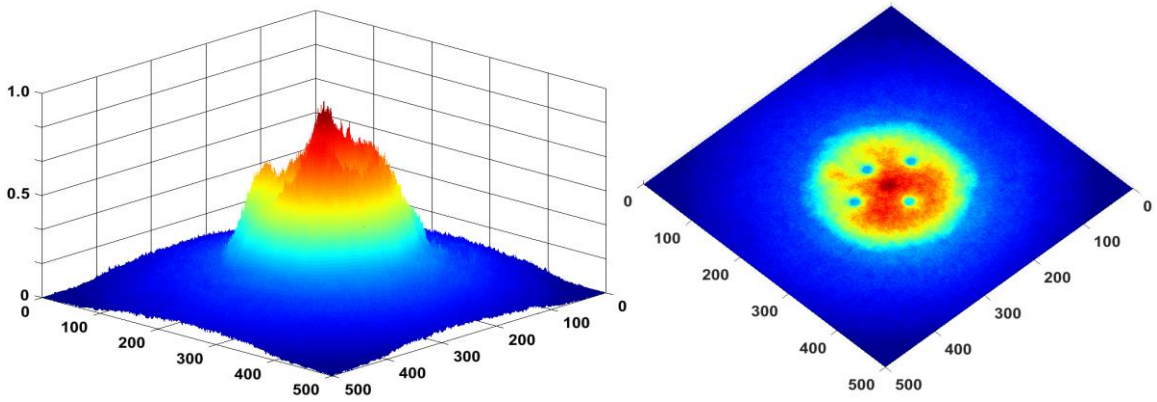

Figure 2.3. UT NETL TRIGA MCNP Modeled Core Inhomogeneity neutron flux.

Figures 2.1-2.3 show the core inhomogeneity effect on neutron flux in a static manner but it is important to remember that any changes within the core during operation can dynamically cause neutron flux changes. The main source of these dynamic neutron flux changes under normal operating conditions is by control rod manipulation. This can be seen below in Figure 2.4. This data was captured during automatic reactor power operation of the UT Austin NETL TRIGA and shows the neutron population fluctuation with control rod movement approaching steady state power of 100 kW.

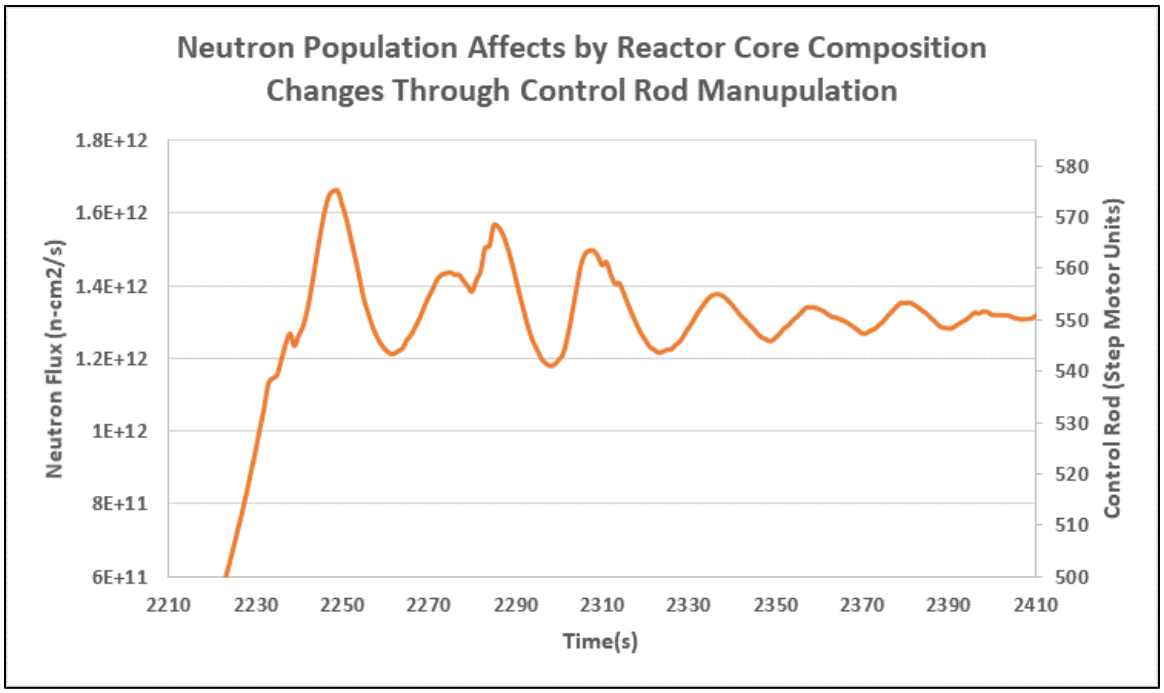

Figure 2.4. Control Rod Movement with Resulting Neutron Population Change.

Monitoring these flux changes are of great importance to reactor experimental studies. [Geslot, 2011]

Chapter 3: Neutron Activation Analysis

Neutron Activation Analysis (NAA) is a non-destructive analytical technique for determining elemental and isotopic compositions of sample media. It plays an important role due to its sensitivity and selectiveness during analysis. [Trkov, 2015] When a sample is bombarded with a neutron source, the isotopic constituents can capture a free neutron and become another isotope. This is called neutron activation.

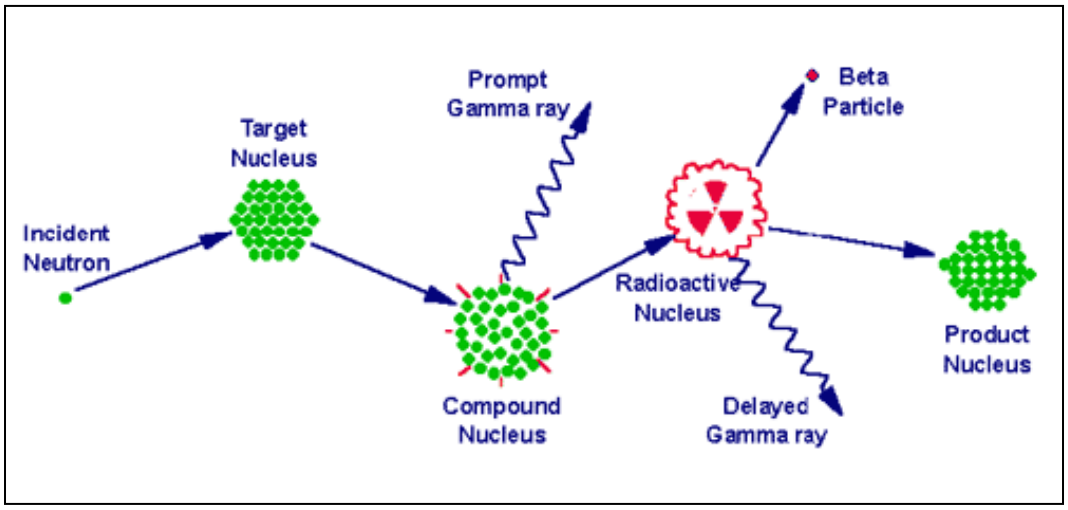

Illustration 3.1. Graphical representation of the NAA process. [Glascock, 2017]

The above figure can also be expressed as written below.

$$n + {}^{A}Z \rightarrow {}^{A+1}Z^{*} \rightarrow {}^{A+1}Z + \gamma \qquad \text{Eq. 3.1.}$$

Where ${}^{A}Z$ is the target nucleus, ${}^{A+1}Z^{*}$ is the compound nucleus, and ${}^{A+1}Z$ is the resulting neutron activated nucleus. Various neutron reactions can occur during sample bombardment. [Frontasyeva, 2011]

An (n, γ) reaction is when a neutron is captured by the target nucleus and a prompt gamma-ray is emitted from the excited compound nucleus. The target atom is then changed into another isotope of the same element by the addition of one nucleon to the atomic number.

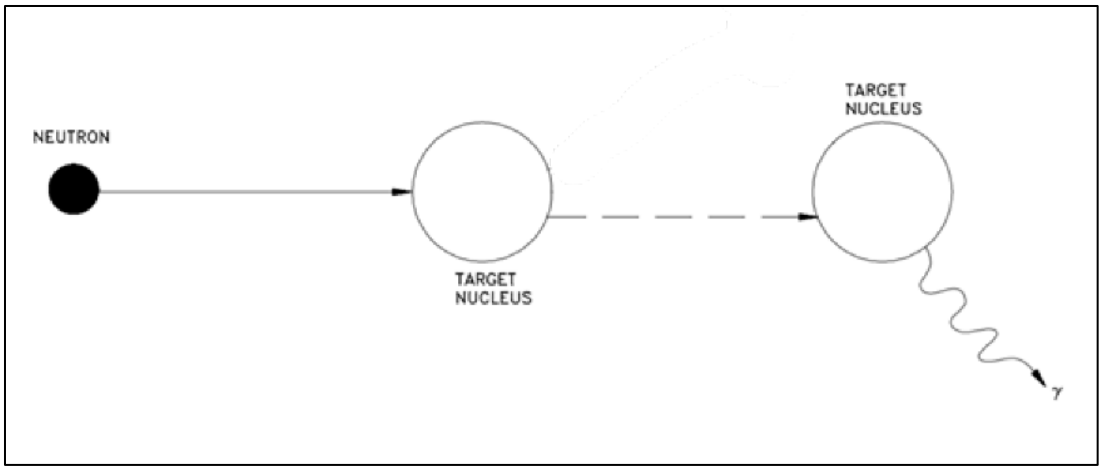

Illustration 3.2. (n, γ) Reaction. [U.S. DOE V.1, 1993 (Modified)]

An (n,p) reaction is when a neutron is captured by the target nucleus and a proton is emitted from the excited compound nucleus. The target atom is transformed into a different element by the loss of one proton.

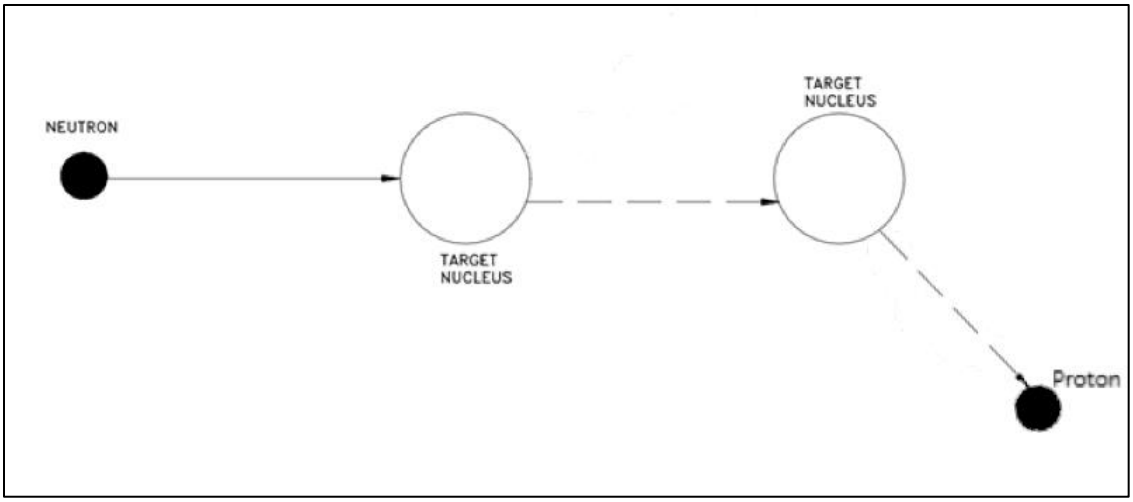

Illustration 3.3. (n,p) Reaction [U.S. DOE V.1, 1993 (Modified)]

An (n,α) reaction is when a neutron is captured by the target nucleus and an alpha particle (2-p, 2-n) is emitted from the excited compound nucleus. This reaction also produces a different element from the target atom differing by the loss two protons.

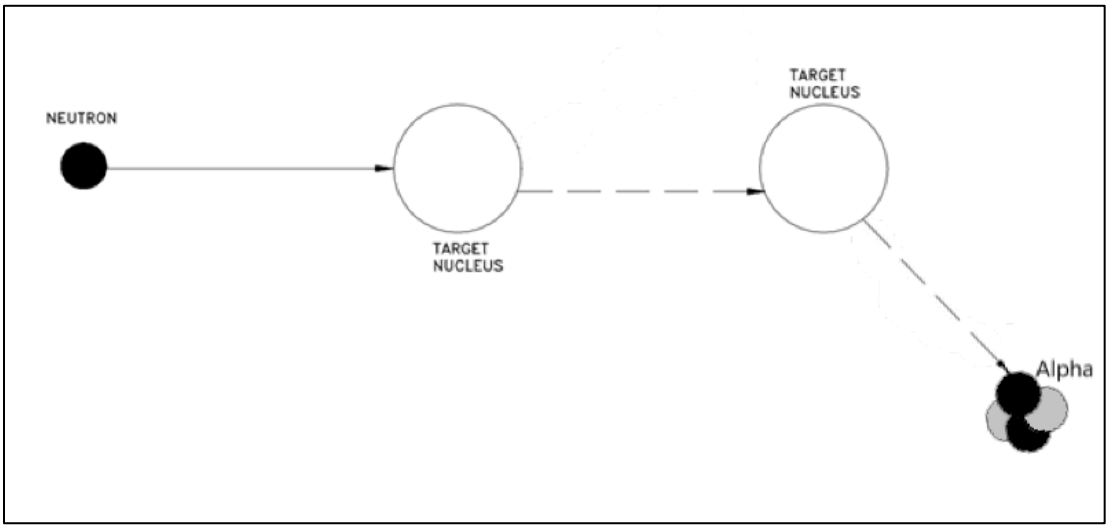

Illustration 3.4. (n,α) Reaction [U.S. DOE V.1, 1993 (Modified)]

These are the main reactions for non-fissionable isotopes but there are other possibilities. The rate and likelihood of a reaction occurring is determined by the amount of target material, the neutron energy and flux bombarding the sample, and the respective isotopic cross-sections for each reaction.

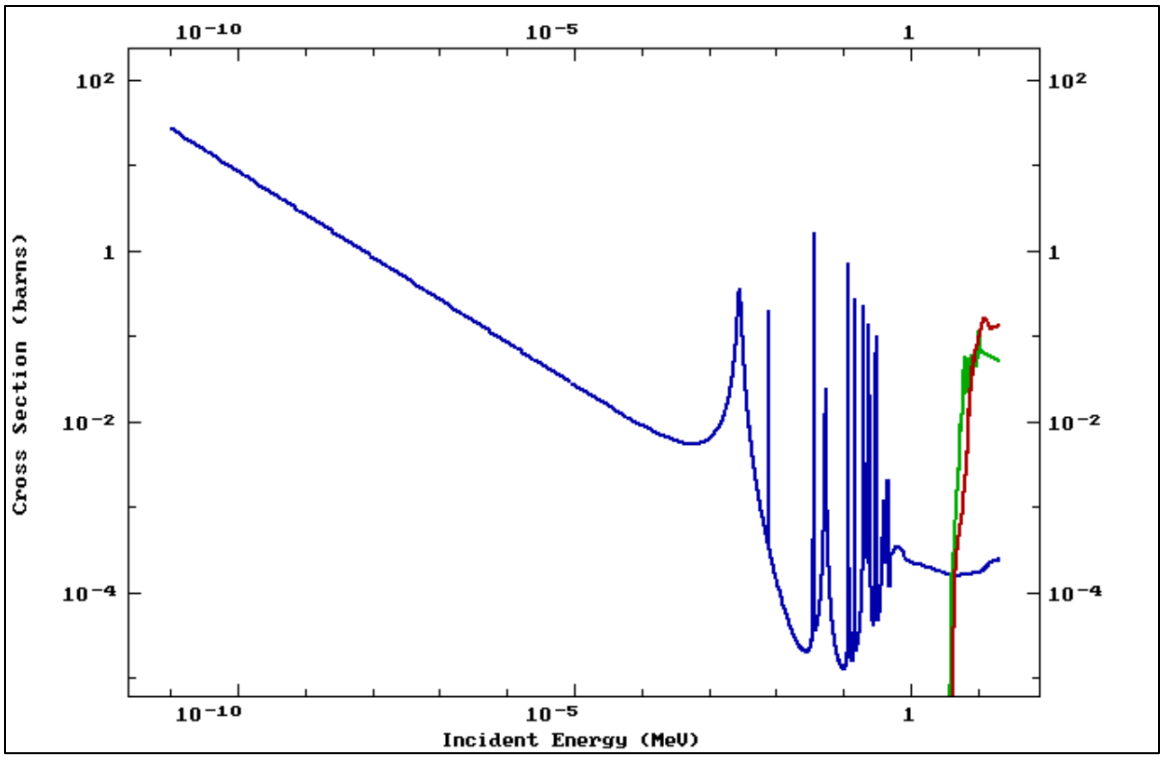

Figure 3.1. IAEAA ENDF Cross Section Plot for ^{23}Na neutron reactions.

The ^{23}Na cross section plot in Figure 3.2 shows the (n, γ) reaction (Blue) dominates the (n,p) (Red) and (n,α) (Green) reactions until much higher neutron incident energy. Using the information from these plots allows an experimenter to choose what energy best obtains the reaction desired.

3.1 NAA SAMPLE ANALYSIS

The resulting atoms produced from the neutron activation can be calculated the equation below. This equation assumes the (n, γ) reaction is dominant. [ASTM E 262-03, 2003]

$$N = \frac{N_o \sigma_1 \phi (e^{-(\phi\sigma_1 t_i)} - e^{-(\phi\sigma_2 + \lambda)t_i})}{(\phi(\sigma_2 - \sigma_1) + \lambda)e^{-\lambda t_w}} \quad \text{Eq. 3.2}$$

Where N is the number of produced atoms (^{A+1}Z), N_0 is the original number of target atoms (^{A}Z), σ_1 is ^{A}Z (n, γ) cross-section, σ_2 is ^{A+1}Z (n, γ) cross-section, λ is ^{A+1}Z decay constant, φ is the neutron flux, t_i is exposure time, and t_w is the elapsed time after the end of the exposure.

3.1.1 Gamma-Ray Spectroscopy

After activation, the NAA samples are placed in a gamma-ray detector system for further analysis. Radioactive emissions in the form of gamma-ray photons from the NAA samples interact with the detector material. The interaction of the photons with the detector falls within three main areas; photoelectric effect, Compton scatter, and pair production.

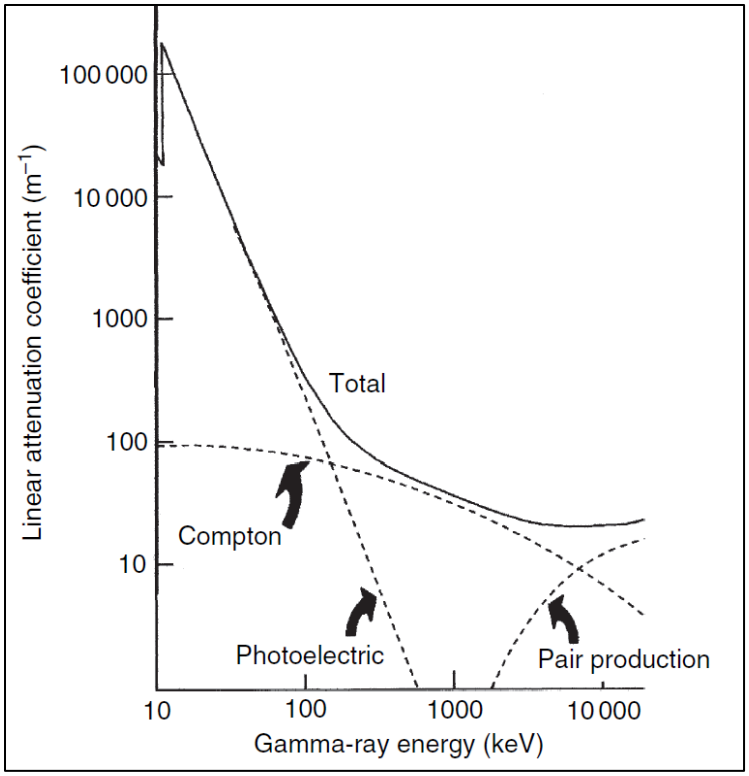

Figure 3.2. Photon interaction curves. [Gilmore, 2008]

These three interaction methods vary how the energy from the radiative gamma ray emission deposits energy within the detector material. When an interaction occurs within a solid-state detector such as high-purity germanium (HPGe), electron-hole pairs are produced. The image below depicts the gamma-ray Compton scattering interaction with an electron.

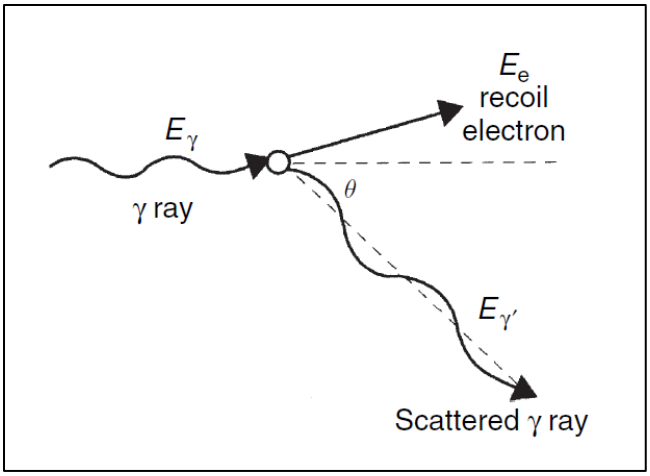

Illustration 3.5. Gamma-Ray Compton scattering interaction. [Gilmore, 2008]

The number of electron-hole pairs produced is proportional to the energy deposited. This event produces a signal that is then amplified, processed and counted. The counts are then binned into various channels roughly according to signal magnitude to produce a spectrum.

A gamma-ray detection system is energy calibrated by using a reference source of a known material with known energy peaks. A europium-152 spectrum, often used to calibrate gamma-ray detector systems, is shown below.

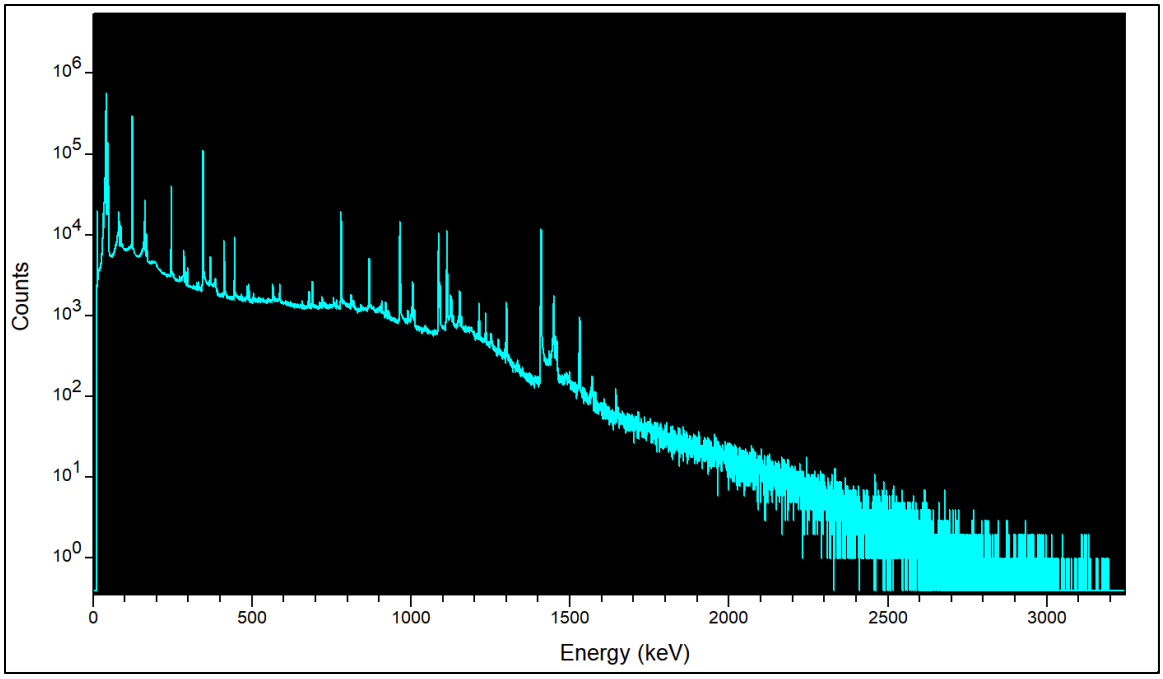

Figure 3.3. HPGe ^{152}Eu Energy Calibrated Gamma-Ray Spectrum.

To accurately determine sample activity with gamma-ray spectroscopy an efficiency curve must be developed. Using a reference source with known activity, net peak counts can be associated with the gamma-ray energy and intensity present in the spectrum to yield an energy depended efficiency calibrated fit or curve. For a radioactive source with a half-life that is much longer than the count time, the expected gammas produced, $\gamma_{E,}$ by the known source is calculated with the equation below where A_{Curr} is the current activity of the source, T_C is count time and $I\gamma$ is gamma-ray intensity.

$$\gamma_E = A_{Curr} \times T_C \times (I_\gamma/100) \qquad \text{Eq. 3.3}$$

The equation below then calculates the efficiency, ε, of each peak where C_N is net peak counts.

$$\varepsilon = {C_N}/{\gamma_E} \qquad \text{Eq. 3.4}$$

The developed efficiency curve fit from the above is used to determine specific energy peak efficiencies associated with fission product isotopes. The determined efficiency is utilized in the equation below to estimate the unknown activities of isotopes, $A\gamma$, within the sample.

$$A_\gamma = {C_N}\Big/{(I_\gamma \times \epsilon_\gamma \times T_C)} \qquad \text{Eq. 3.5}$$

3.1.2 NAA Concentration Calculations

Once you have a gamma-ray spectrum of the neutron activated sample, you can analyze the peaks generated to determine the mass of the element(s) of concern. The number of counts seen in the spectrum is directly proportional to the number of atoms within the sample and thus the mass. [Greenberg et al., 2011]

$$m = C \frac{\lambda}{(1-e^{-\lambda t_i})e^{-\lambda t_w}(1-e^{-\lambda t_m})\phi_{th}\sigma_{eff}\Gamma\varepsilon} \times \frac{M}{\theta N_{Av}} \qquad \text{Eq. 3.6}$$

Where the C is the net gamma-ray counts from ^{A+1}Z, N_{Av} is Avogadro's Constant, θ is the isotopic abundance of ^{A}Z, M is atomic mass, m is the mass of ^{A+1}Z, Γ is the gamma-ray abundance of the ^{A+1}Z peak analyzed, σ_{eff} is the effective activation cross-section considering neutron spectrum energies and resonance integral, φ_{th} is the thermal neutron flux, t_m is the gamma-ray spectrum measurement time. [Greenberg et al., 2011]

NAA often uses a direct comparator method to determine the unknown sample constituents. [Huang, 2017] For this method, a sample with a known isotopic concentration of element of interest is irradiated and functions as a calibrator for the unknown sample. Both samples are typically irradiated under similar conditions using the sample detector system to mitigate any differences and simplify analysis. Using this method, the comparator sample peaks can be contrasted to determine the unknown element mass. [Greenberg et al., 2011]

$$m_u = m_k \frac{\frac{C_u}{t_m e^{-\lambda t_{d_u}} \left(1 - e^{-\lambda t_{m_u}}\right)}}{\frac{C_k}{t_m e^{-\lambda t_{d_k}} \left(1 - e^{-\lambda t_{m_k}}\right)}} \quad \text{Eq. 3.7}$$

Where the u subscript represents the unknown sample and the k subscript represents the known sample.

Taking note of Equation 3.5, converting from activity to number of atoms ($A_i = \lambda N_i$), and maintaining the same sample counting parameters for both and known and unknown samples allows further simplification yeilding an equation for sample concentration.

$$Concentration_u = Concentration_k \frac{m_k}{m_u} \frac{N^*{}_u}{N^*{}_k} \frac{e^{-\lambda t_{dk}}}{e^{-\lambda t_{du}}} \quad \text{Eq. 3.8}$$

Chapter 4: NETL Delayed NAA Pneumatic Transfer Systems

4.1 Manual Pneumatic Transfer System

The University of Texas at Austin operates a Manual PTS for delayed NAA sample irradiation. The PTS has two rabbit transfer tube irradiation facilities that extend from the reactor pool surface to core.

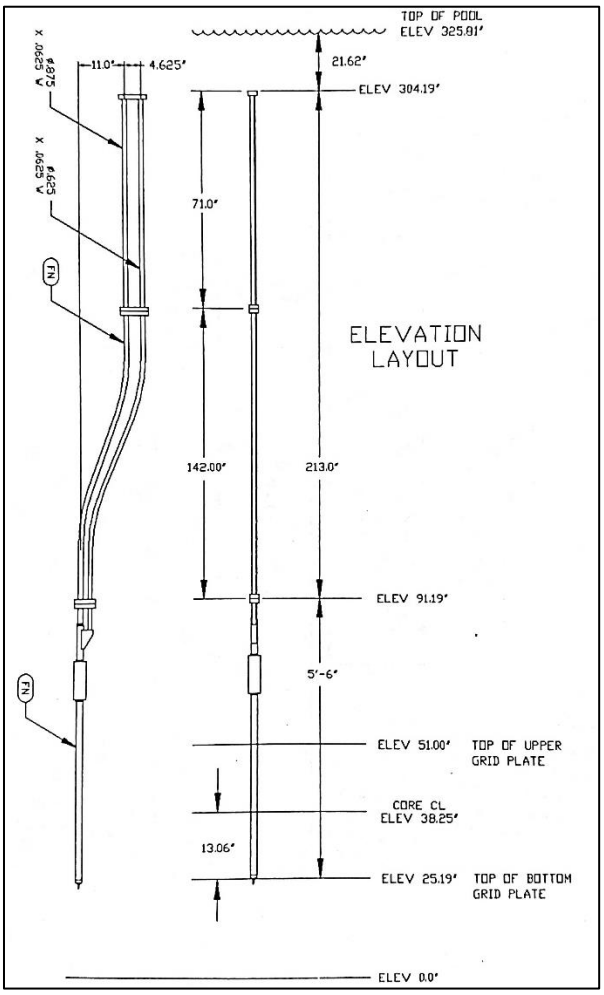

Figure 4.1. PTS Rabbit Transfer tube Irradiation Facility Diagram. [Pneumatic Transfer System Design Schematics, 1997 / Appendix A]

One rabbit transfer tube irradiation facility is lead-lined and capable thermal neutron irradiation at reactor powers up to 950 kW yielding a neutron flux up to 2.7×10^{12} $\frac{n}{cm^2 s}$. The second rabbit transfer tube irradiation facility is cadmium-lined and allows for epithermal neutron irradiations at reactor powers up to 500 kW producing 5×10^{11} $\frac{n}{cm^2 s}$.

The Manual PTS sample loading chamber is located within a laboratory fume hood and all samples are individually loaded by the experimenter.

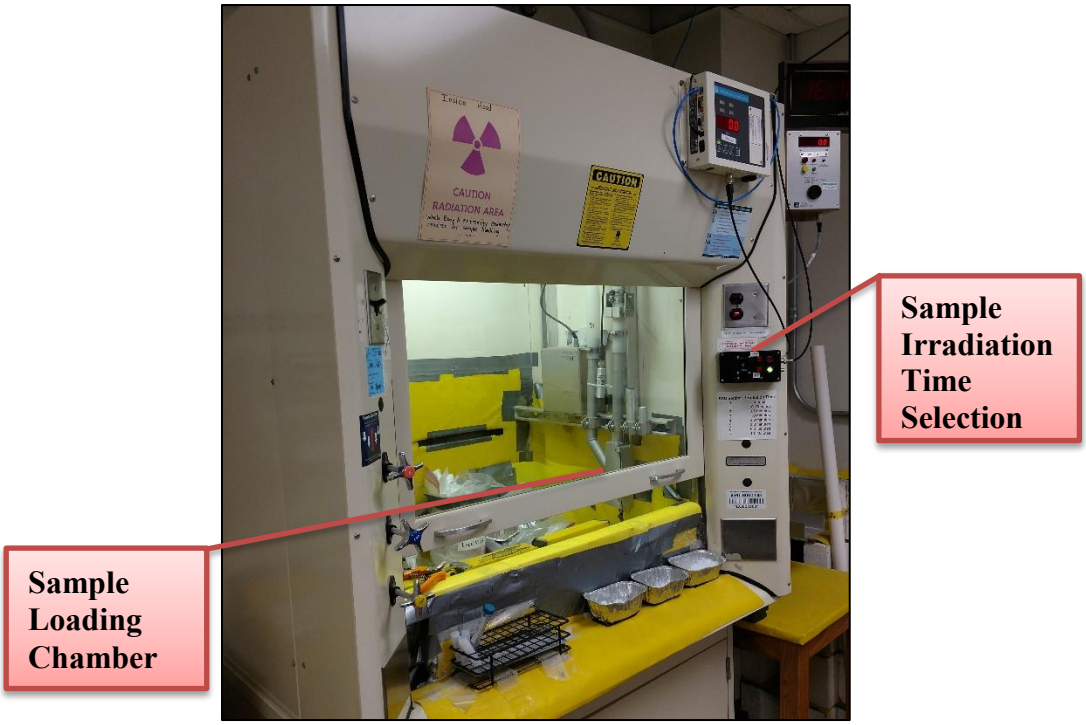

Figure 4.2. Manual PTS Fume Hood and Sample Loading Chamber.

After the sample is loaded, an irradiation time is selected from a preprogramed system timer. Sample irradiation settings range from 10 seconds to 10 minutes. The system transfers the sample from the loading chamber to the reactor core and returns to the fume hood after irradiation for sample processing. A set of electronic timers track sample irradiation time and decay time with diffuse photo sensors along the sample transit path.

[Copple, 2014] After the sample is returned to the fume hood, the experimenter can process the sample for analysis. This involves removing the sample from the potentially contaminated sample HDPE vial.

The main drawback for the Manual PTS is the user interaction and time required for sample processing after the irradiation. This handling and additional processing time precludes using this system with extremely short-lived activated isotopes and has potential to insert human error. [Coople, 2014]

4.2 AUTOMATIC PNEUMATIC TRANSFER SYSTEM

The Automatic PTS expands on the functionality of the Manual PTS by removing the potential for human error. The Automatic PTS makes the entire process of irradiation, sample counting and the sample transfer in-between automated. The system uses a network of pneumatic tubes and solenoid controlled vales to move the sample from a sample holder magazine, to the reactor core, on a shielded HPGE detector for counting, and then to a sample ejection bin. A switch in the system allows the Automatic PTS to use the same rabbit transfer tube irradiation facility as the Manual PTS.

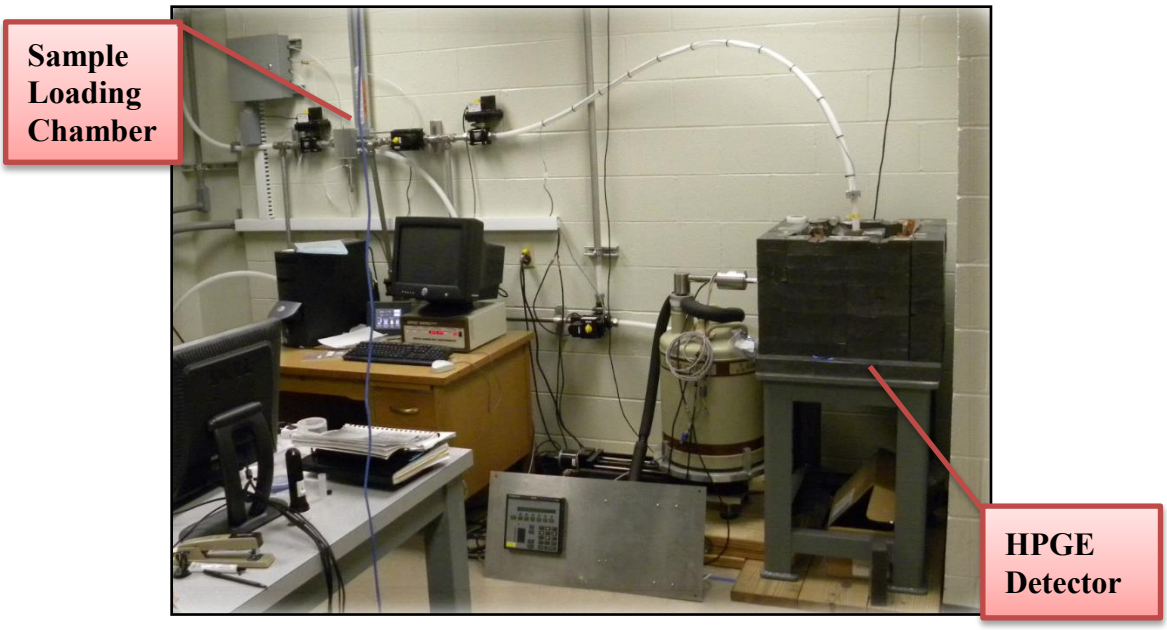

Figure 4.3. UT Austin NETL Automatic PTS.

The Automatic PTS is able to place the irradiated sample directly on a detector after leaving the core. This enables the system to capture the activation of extremely short-lived isotopes. [Khamis, 2001] The Automatic PTS has a programmable logic controller (PLC) with a graphical user interface enabling the experimenter to input all of the desired experimental parameters before allowing the system to run. The system can independently run up to 30 consecutive samples.

4.3 NAA Pneumatic System Sample Variance

When conducting elemental sample characterization with NAA, the neutron fluence during sample irradiation is of primary concern for accurate analysis. The University of Texas at Austin's Nuclear Engineering Teaching Laboratory uses the $^{36}S(n,\gamma)^{37}S$ reaction from sulfur powder as a short-irradiation flux monitor to account for this neutron fluence variation. [Landsberger, 2012; Vieira, 2006] This requires additional

preparation, irradiation time, detector time and analysis for each monitor on top of time required for the unknown sample.

The sulfur used at NETL for short-duration NAA flux monitoring is produced by Sigma-Aldrich and is a laboratory grade natural sulfur power assayed at greater than 99%.[MilliporeSigma, 2016]

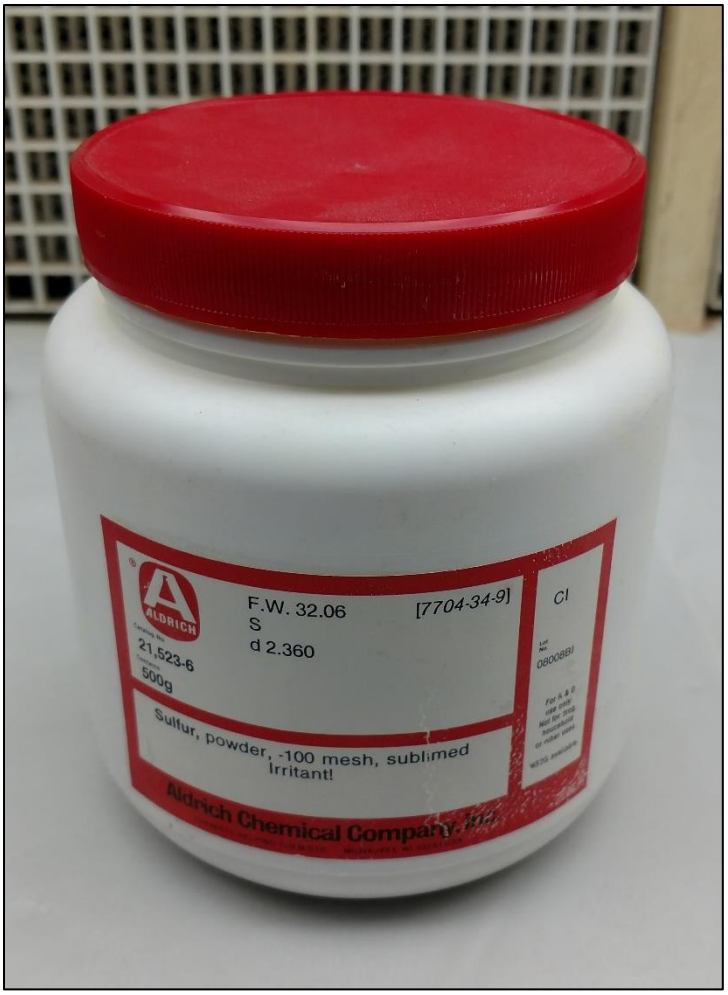

Figure 4.4. MilliporeSigma Sulfur CAS-No:7704-34-9

The sulfur powder is sampled, weighed, and placed within 1.65 mL high density polyethylene (HDPE) vials and centered within a larger 7.5 mL HDPE vials for pneumatic injection into the reactor core. Typical sample and HPDE vials used are shown in the figure below.

Figure 4.5. Sulfur powder sample and HPDE vials used for NAA sample delivery into the reactor core.

Due to the orientation of the sample within the Automatic PTS, it is possible for the HPDE vial cap to become dislodged when returning from the reactor core and landing on the detector stop. To prevent this, all samples injected for irradiation using the Automatic PTS must be heat-sealed. This is not required for use of the Manual PTS as the sample momentum is not as great upon return. A completed sulfur flux monitor that has been heat-sealed for use within the Automatic PTS can be seen in Figure 4.6.

Figure 4.6. Finished sulfur flux monitor HPDE vial (Heat-sealed).

The activated ^{37}S 3103.4 keV net peak area is used to determine a monitor's relative fluence through UT Austin's Neutron Activation Data Analysis (NADA) program. [Landsberger, 1992] As you can see from Figure 4.7 below, the ^{37}S 3103.4 keV peak is at a high enough energy to minimize Compton continuum net area peak effects. This ensures typical activation products within a sample will not cause error in the neutron flux determination.

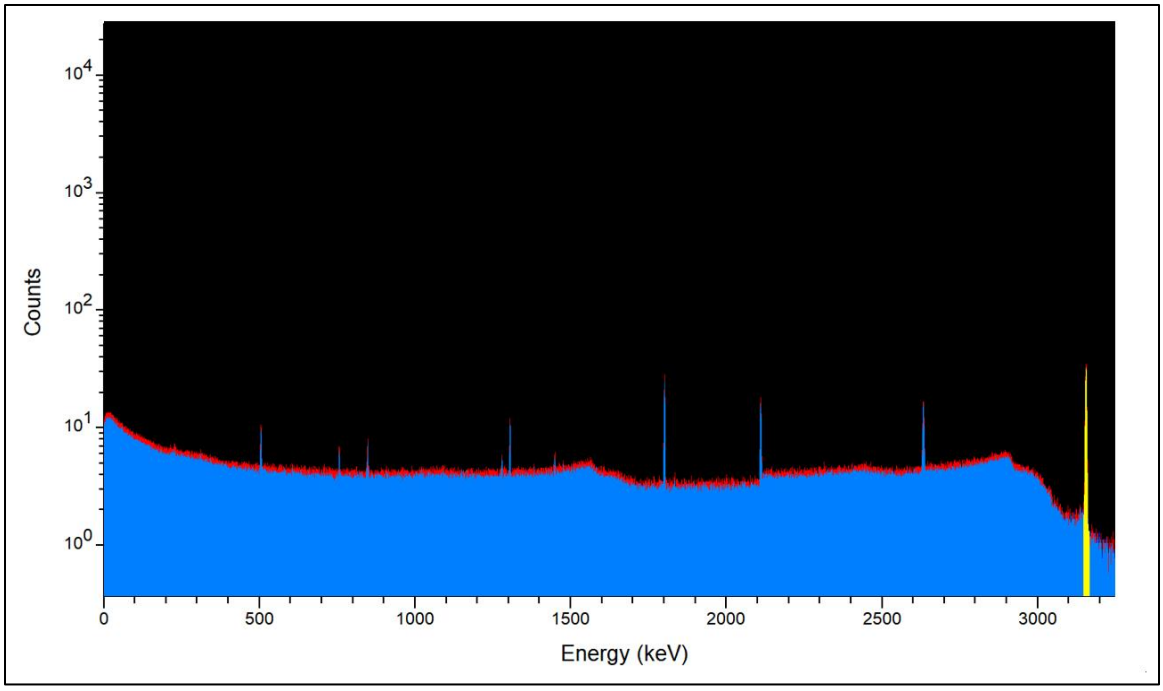

Figure 4.7. Sulfur flux monitor comparison (^{37}S 3103.4 keV peak highlighted)

Figure 4.8 shows the activation difference in ^{37}S 3103.4 keV net peak area caused by neutron flux variation within the Manual PTS. The red (background) peak is one sample ans the blue (foreground) peak is a second sample. Both samples shared the same irradiation, decay, and data acquisition times.

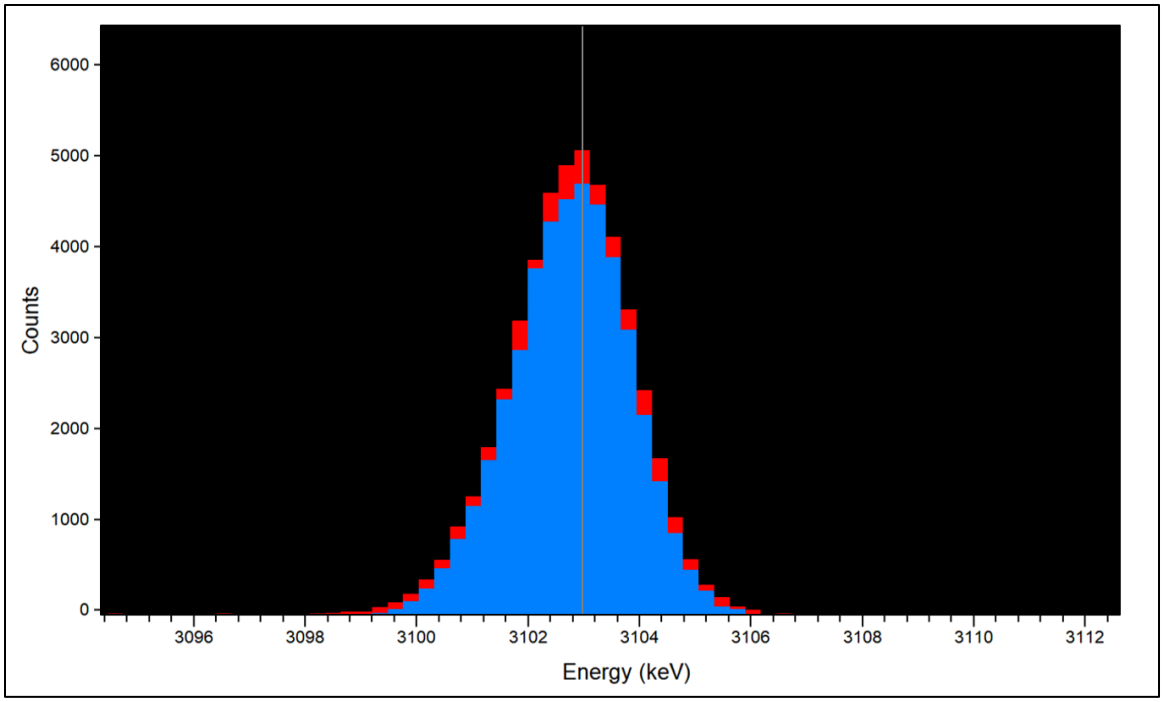

Figure 4.8. Sulfur flux monitor ^{37}S 3103.4 keV peak comparison between samples with identical experimental parameters.

It has been shown the natural variance in neutron source fluence can induce up to a 12% error in sample irradiation. [Landsberger, 2012] During testing, short irradiation NAA sample variance showed a flux difference up to 8% as seen in Figure 4.9.

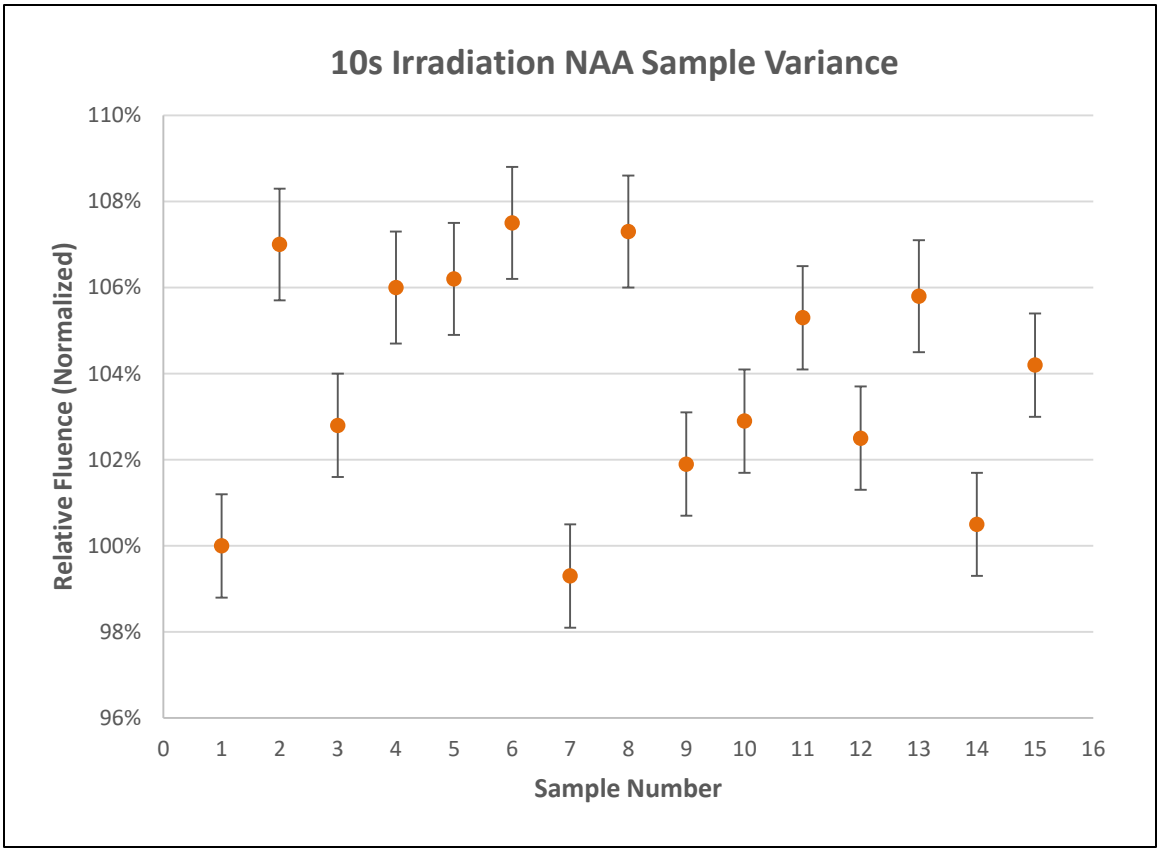

Figure. 4.9. The relative sample flux irradiation for consecutive 10-second samples (1σ-Error).

Chapter 5: Neutron Monitoring System (N-MS)

In designing the N-MS, the objective was to design a system capable of tracking neutron population in real time at a localized point commensurate with the UT Austin NETL NAA Manual and Automatic PTS. Meeting this design objective could remove the requirement for passive flux monitors and save substantial amounts of laboratory time. The installation location chosen for the N-MS was a 5/8'' diameter access hole within the upper grid plate of the NETL TRIGA reactor.

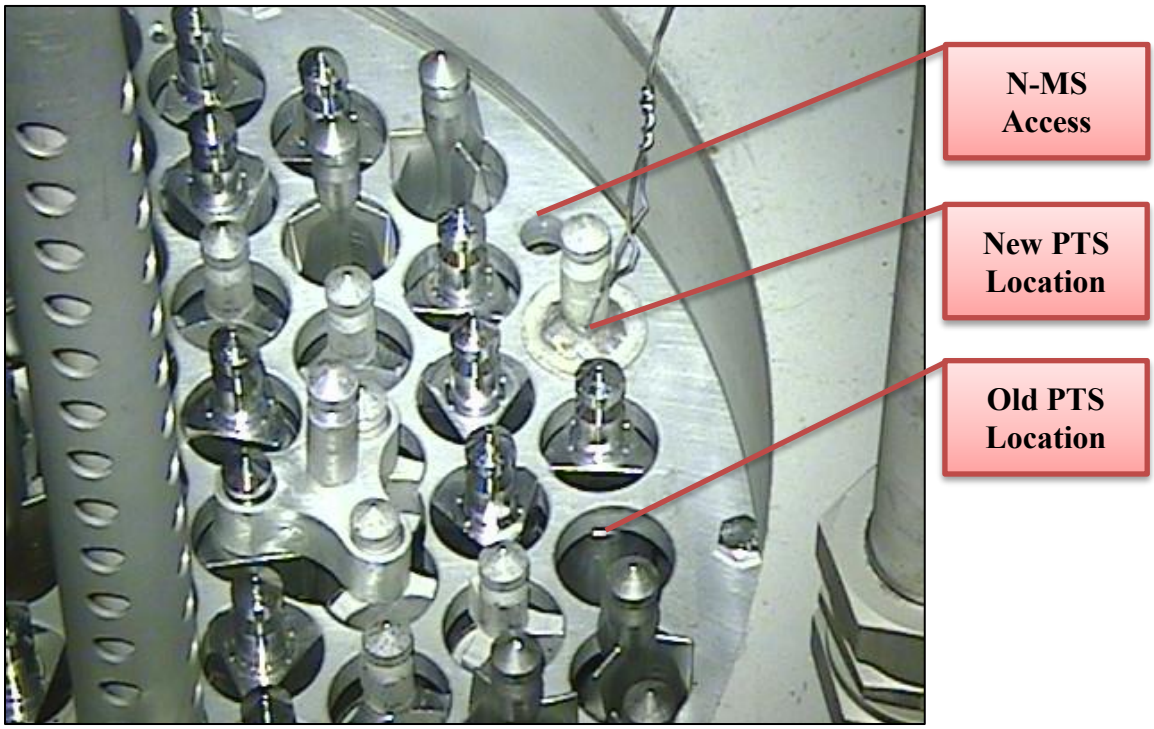

Figure 5.1. N-MS grid plate access location.

This access hole is intended to be utilized for activation foil and wire irradiations in order to determine neutron flux within the core. The original PTS facility is installed in the G38 grid location. This would cause the sample centerline to be 12.8 cm horizontally

from the N-MS centerline. The N-MS needs to be as close to the PTS terminus as possible to obtain an accurate localized reading of the neutron flux during sample irradiation. In order to have the N-MS system as close to the PTS sample terminus as possible, the PTS facility was moved to a new location in the G36 grid location.

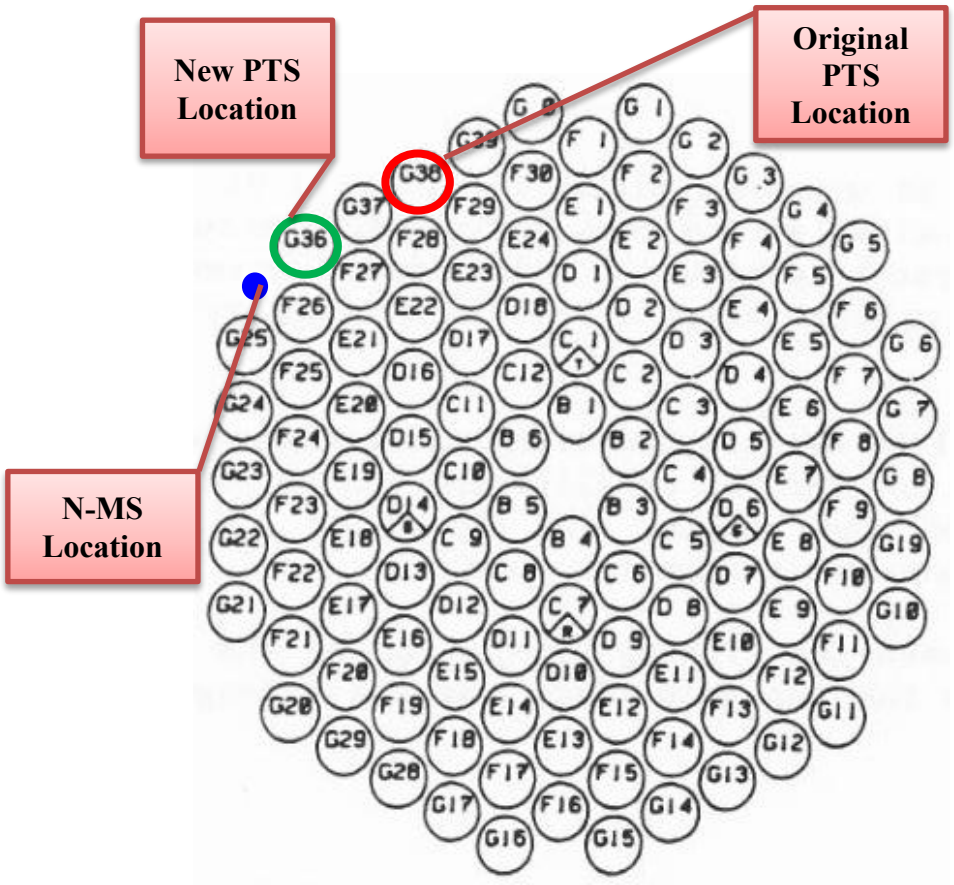

Figure 5.2. UT Austin NETL TRIGA Reactor Core Arrangement

In this location, the centerline horizontal distance is reduced to 3.7 cm. From edge to edge, the systems are 2.6 cm apart and within a neutron path length in a light water moderator. [Mosgovoy, 1962; DeJuren, 1953] The relative positions as modeled with MCNP can be seen in Figure 5.3 below.

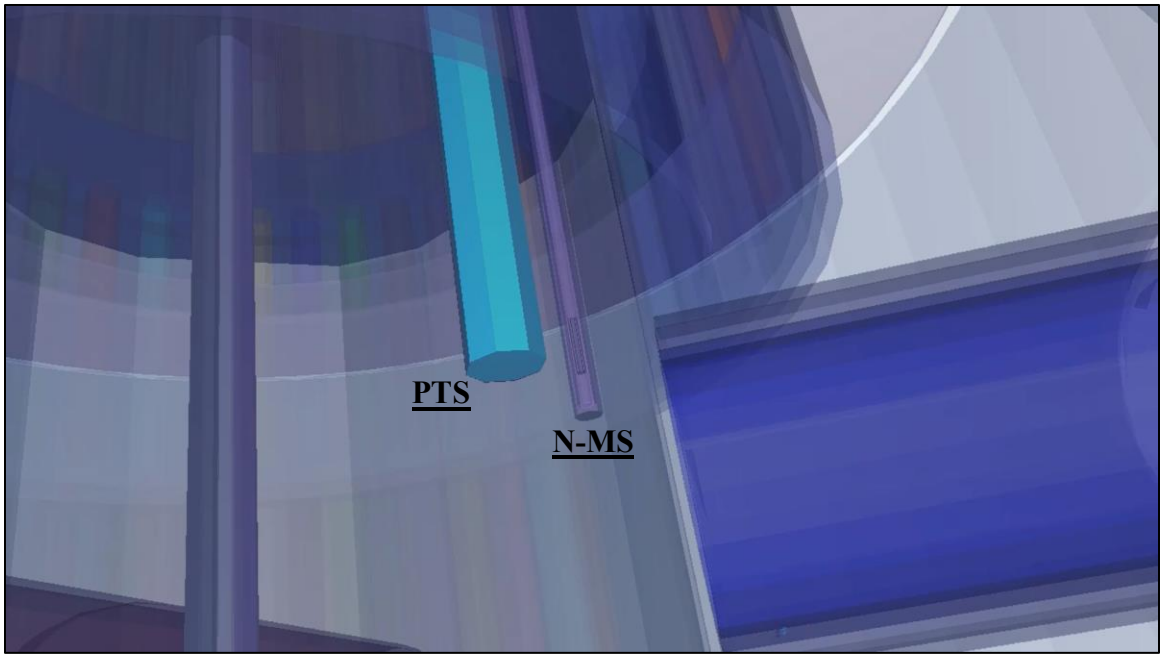

Figure 5.3. N-MS Position with respect to PTS Terminus.

5.1 N-MS System Components

The N-MS constructed utilizes a high voltage power supply, signal splitter box, a picoammeter, in-core fission chamber, and a detector isolating holder. The system is controlled with a laptop through a LabVIEW data acquisition and logging application.

5.1.1 In-Core Fission Chamber

A Photonis CFUF43 inner-core fission chamber was chosen to be the neutron detection probe for the N-MS. The fission chamber is shown in Figure 5.4.

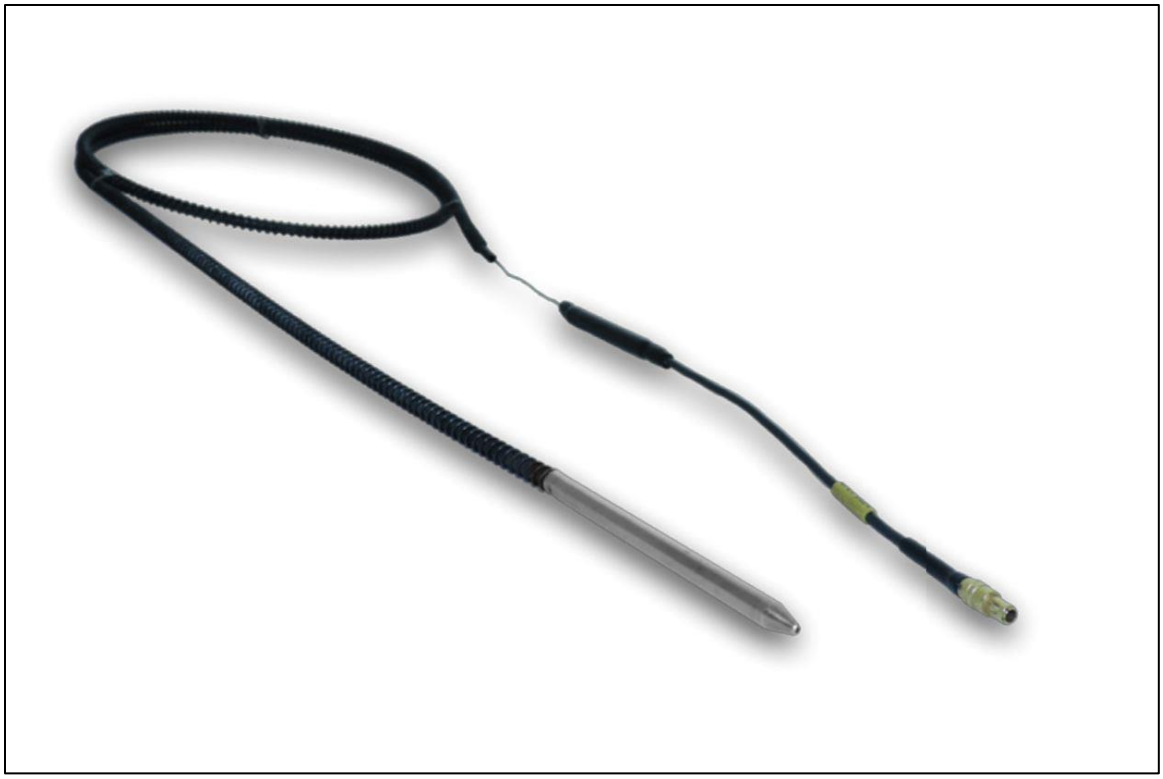

Figure 5.4. Photonis CFUF43 In-Core Fission Chamber [Photonis, 2018]

The Photonis CFUF43 is a concentric cylindrical fission chamber constructed of coaxial electrodes. The anode and cathode are separated by a pressurized fill gas. [Chabod, 2006] The Photonis CFUF43 uses an argon fill gas pressurized to 110 kPa. The outer case is 4.7 mm in diameter, 86 mm in length, and is constructed from hardened stainless steel contining less than 0.05% cobalt. Detailed measurements of the detector can be seen in Figure 5.5. [Photonis, 2015]

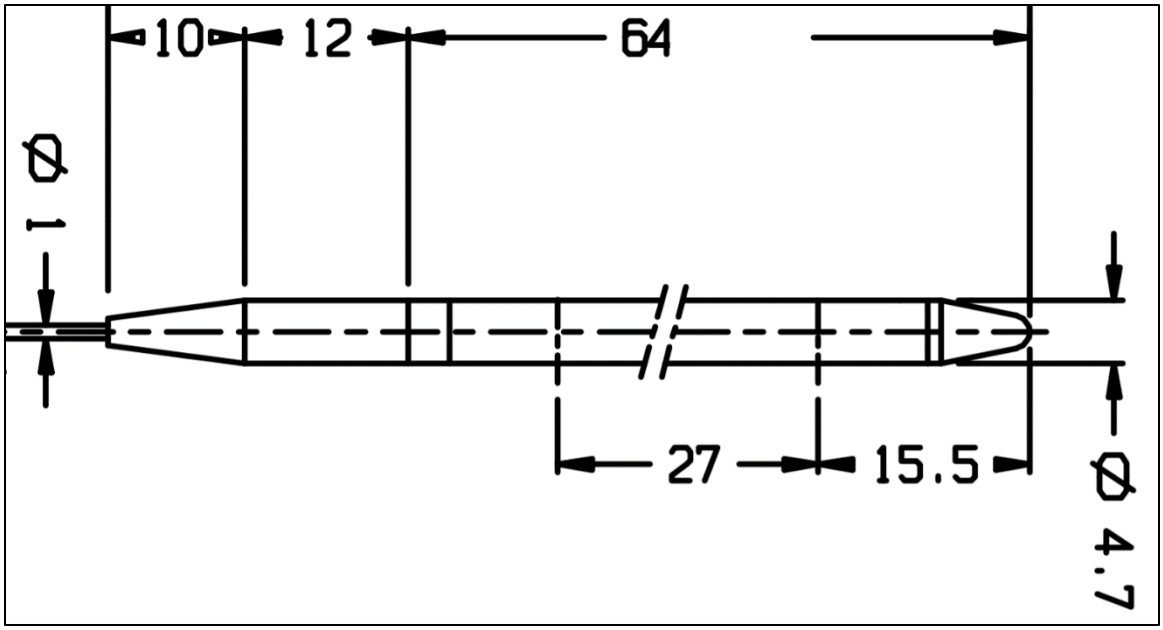

Figure 5.5. Photonis CFUF43 In-Core Fission Chamber(mm). [Photonis, 2015]

The detector's sensitive region is 27 mm in length and located 15.5 mm above the detector's base. The anode is doped with >90% ^{235}U enriched uranium. The total amount of uranium within the detector is 374μg with 349μg of ^{235}U. Figure 5.6 is a neutron radiography image of the fission chamber taken at UT Austin's NETL. The image shows the internal fission chamber cylinder containing the enriched uranium sensitive region to the lower right. In the upper left of Figure 5.6 the inner electrode connects to the integrated mineral coaxial cable junction. The Al_2O_3 insulated coaxial cable is 1mm in diameter, 30 meters long, and capped with a single male BNC connector. At its nominal operating voltage of 150V, the detector is rated up to 350°C. [Photonis, 2015]

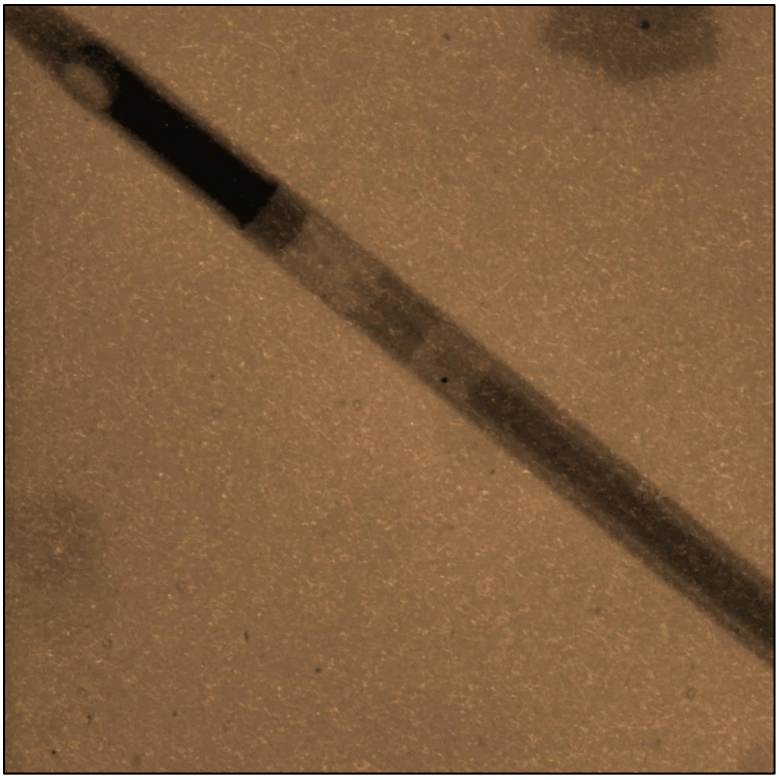

Figure 5.6. Neutron Radiography Image of Photonis CFUF43.

When the fission chamber is irradiated with neutrons, fissions are induced in the sensitive region containing the ^{235}U enriched uranium. The fission products then ionize the fill gas creating an avalanche of election-ion pairs. [Geslot, 2009] With the bias voltage applied to the detector, the electron-ion pairs can be collected by the system producing an electrical current. Fission chambers can be designed to operate in low neutron flux environments in pulse mode or, conversely, in high neutron flux regions in current mode. [Antolínez, 2006] The Photonis CFUF43 is designed to operate in current mode and has a measurement range of 10^{10}–10^{14} $\frac{n}{cm^s s}$. Figure 5.7 depicts the processes of detection with a fission chamber as discussed above.

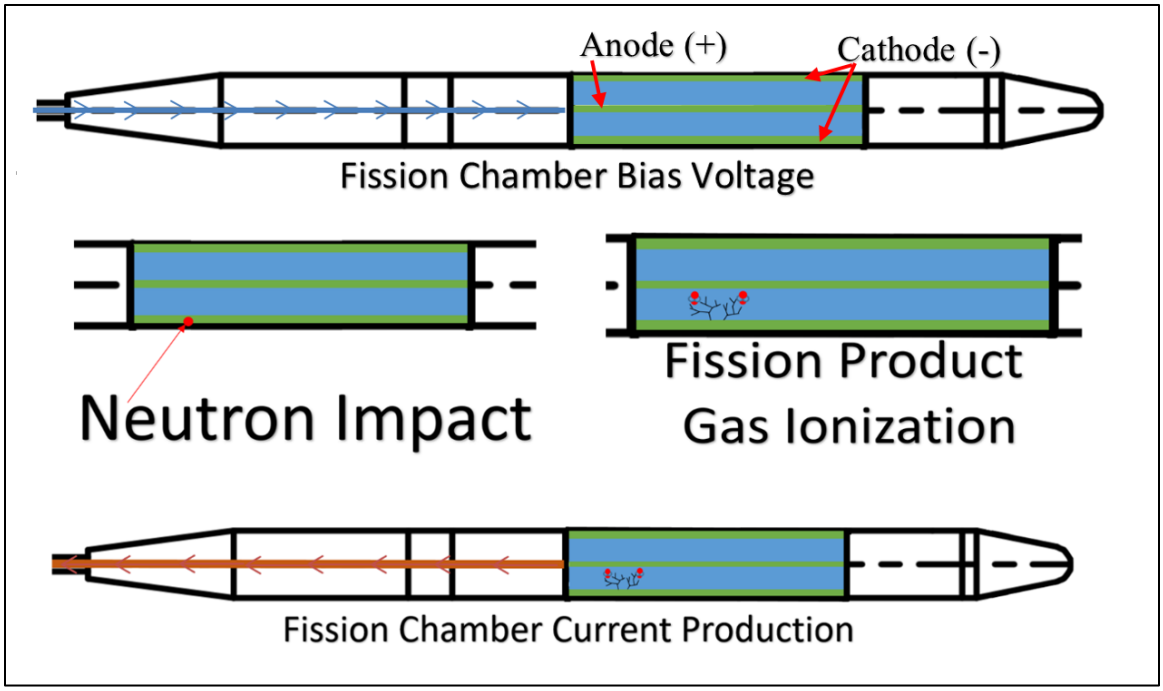

Illustration 5.7. Fission Chamber Current Production Process

5.1.2 Fission Chamber Isolating Holder

An aluminum casing was designed to position the CFUF43's sensitive region, semi-permanently, at the same vertical position of the NAA PTS terminus within the core. The isolating holder was needed due to the turbulent nature of the light water moderator within the reactor core. As fuel temperature increases, the coolant flow rate surging from the bottom of the core increases. This, along with the added pressure at the lower regions of the reactor pool, causes the Photonis CFUF43 to be subject to a turbulent upward buoyancy.

The PTS design schematics were used to determine the required holder length and positioning required to accurately locate the fission chamber's sensitive region. The PTS

locates the center of the injected sample 12.8 inches into the reactor core. The PTS blueprints can be found Appendix A. The overall length of the fission chamber isolating holder's outer case is 16 inches with approximately 14 inches extending into the reactor core. The holder has a chamfered internal base that places the bottom of the fission chamber at 13.94 inches from the top of the upper reactor gridplate as seen in Figure 5.8. This positions the center of the fission chamber's sensitive region at 12.8 inches into the core.

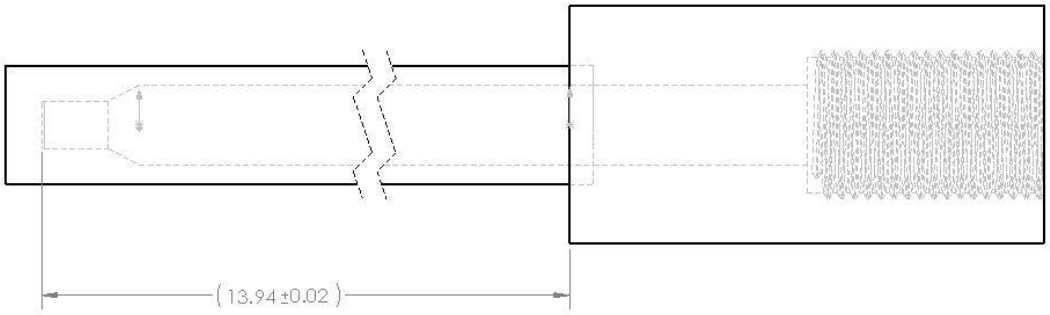

Figure 5.8. Fission chamber holder outer case schematic.

Aluminum 6061-T6 was chosen as the material for the holder for its resistance to corrosion, strength, availability, and dose reduction characteristics. A model of the outer case can be seen in Figure 5.9.

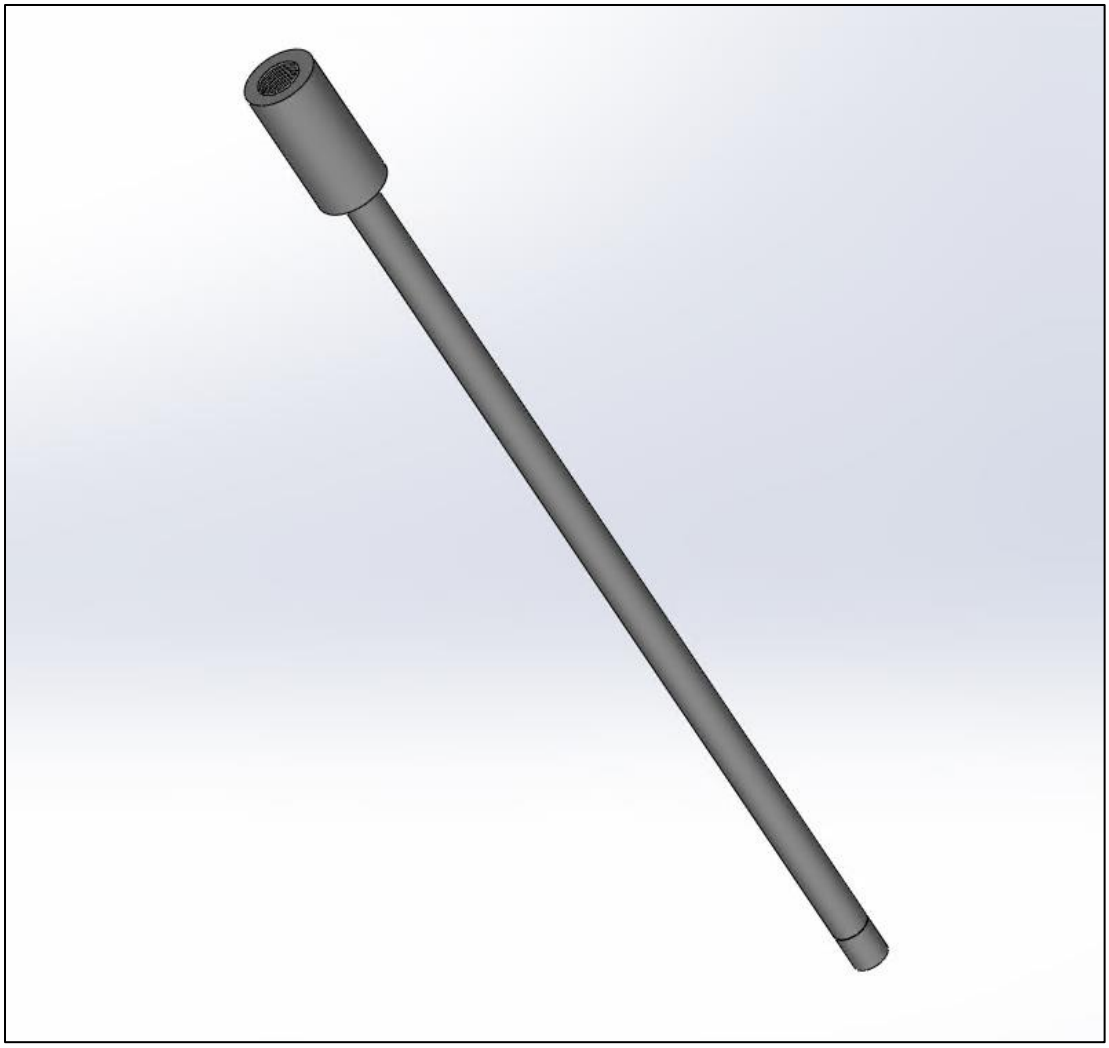

Figure 5.9. N-MS Aluminum 6061-T6 holder outer case model.

To ensure the Photonis CFUF43 is firmly seated within the isolating holder at all times, a 9 inch compression spring is used. The spring has a rate of 2.7 lbs/in and is made of standard corrosion resistant spring steel. [Century Spring Corp., 2018] The compression spring is captured between an aluminum cap within the neck of the outer case and a 3.5 inch aluminum billet seated directly on top of the fission chamber. This compresses the spring by approximately 1 inch and results in a constant pressure of 2 lbs holding the fission chamber in position. This method of retention was chosen to provide flexibility. The entire

system is able to be moved in and out of the reactor as needed and the potential for the signal cable to be caught during transfer is moderate. Also, the system is able to accept other Photonis in-core fission chambers with different operational modes and sensitivities depending on experimental need, such as the Photonis CFUF34 fission chamber capable of pulse mode detecting neutron fluxes ranging between 10^3–10^9 $\frac{n}{cm^2 s}$. The entire isolating holder assembly is shown in Figure 5.10.

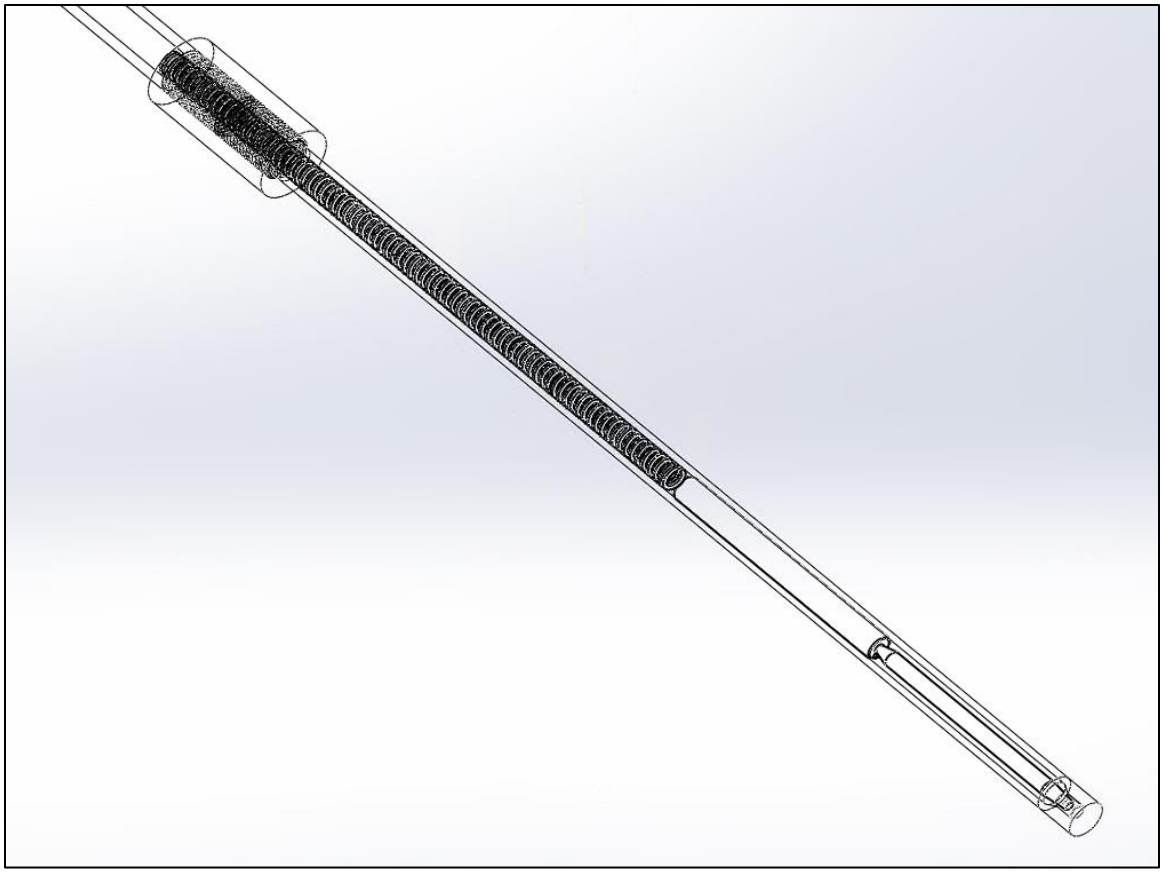

Figure 5.10. N-MS isolating holder assembly and CFUF43 Fission Chamber.

All components of the isolating holder, with the exception of the compression spring, were 3-D printed using a FormLabs Form 2 printer for fitment and testing. The

Form 2 printer is a high resolution 3-D printer that utilizes an optically hardened resin. The resin used for the build was FormLabs' White resin supporting print resolutions down to 50 microns. The printed model can be seen in Figure 5.11 below.

Figure 5.11. 3-D Printed N-MS Testing Model.

5.1.3 N-MS Electrical Components

The N-MS is powered by a Keithley 6487 Voltage Source. The operational voltage of +150 volts is applied through an electrical junction box made for the system.

Figure 5.12. Electrical Junction Box.

The junction box allows the bias voltage and detector output signal to be transferred along the Phontonis CFUF43's single BNC mineral coaxial cable. The electrical junction box and its wiring diagram can be seen in Figure 5.12 above and Figure 5.13 below.

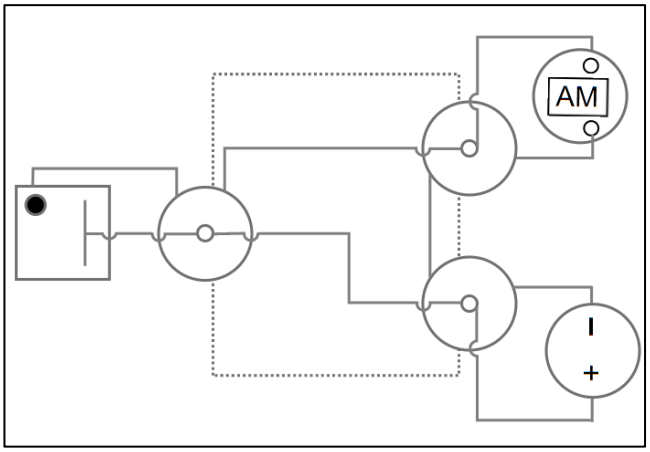

Figure 5.13. Electrical Junction Box Wiring Diagram.

The junction box routes the Photnonis CFUF4's return signal to a Keithley 6485 picoammeter. The Keithley 6485 picoammeter is a programmable high-resolution picoammeter capable of current measurements ranging between 2nA to 20mA. [Tektronix, 2015] With the system operational and installed in the reactor core during shutdown, the average leakage current is $8.89 \times 10^{-09} \pm 6.26 \times 10^{-11}$ amperes.

5.1.4 System Automation and Data Logging Software

The N-MS is initialized through a National Instruments (NI) Laboratory Virtual Instrument Engineering Workbench (LabVIEW) Virtual Instrument (VI) application designed and written for this system at NETL. LabVIEW is a programing language that uses a graphical interface to produce applications and virtual instruments. The graphical interface is similar to a traditional block wiring diagram and the order of operation is determined by wiring layout within the application. [National Instruments, 2017] This programming language was chosen to allow the N-MS the ability to easily be modified for additional instruments, functions and/or operations, if needed.

A National Instruments GPIB-USB interface is used to connect the N-MS LabVIEW application to the Keithley 6485 Picoammeter allowing the application to remotely initialize the system, set all desired instrument parameters, begin measurements, and log all data during operation. The GPIB-USB interface is capable of being easily configurable through the NI LabView Software. [National Instruments, 2015] The N-MS LabVIEW Application is a uses a Producer/Consumer Loop architecture. This Producer/Consumer Loop architecture synchronizes the Consumer Loop to the Producer Loop. This executes Consumer Loop only when data is available from the competed

Producer Loop saving computational power and increasing system speed. The N-MS LabView application block diagram is shown in figure 5.14.

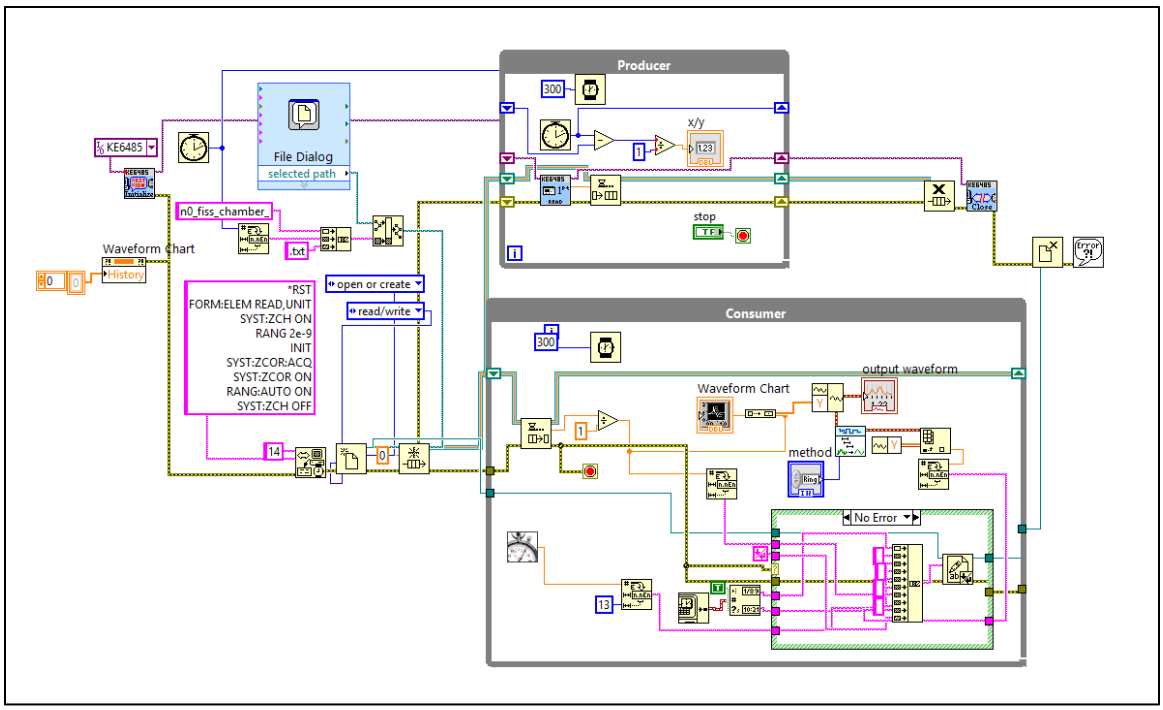

Figure 5.14. National Instruments LabVIEW N-MS Block Diagram Overview

The N-MS LabVIEW application is composed of four main blocks of VIs. The Initializing and Data Logging Block calls the Keithley 6485 picoammeter and transmits the commands within a string box to set up the instrument. The commands issued to the unit perform a system parameter reset, defines the element type to be read, zeros the current channel, sets current measurement range, and initializes measurement. The application then creates a text file for logging the data and initiates a data queue with the Obtain Queue function. Initializing and Data Logging Block of application can be seen in detail below in Figure 5.15.

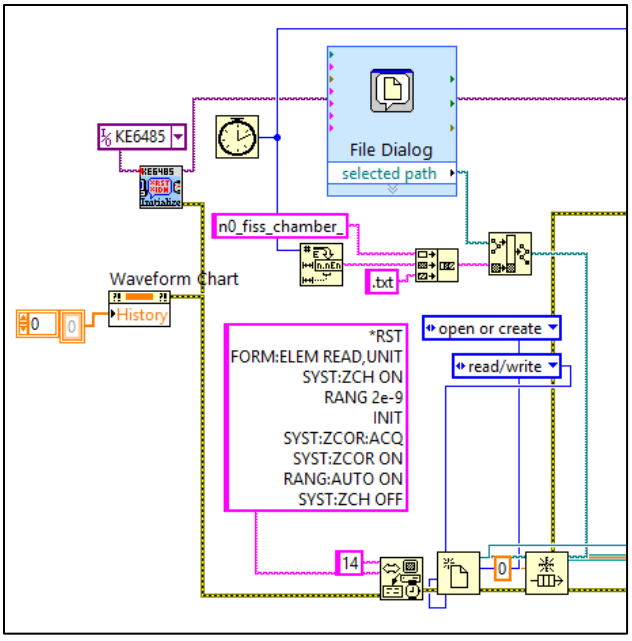

Figure 5.15. N-MS Initiating and Data Logging Block Diagram

The Producer Block calls the picoammeter and performs the signal measurement with the Read Function VI. The collected data is stored in the Enqueue Element function to be accessed by the Consumer Loop. This loop can also be used to measure the system sample rate. The Producer Block diagram can be seen in detail in Figure 5.16.

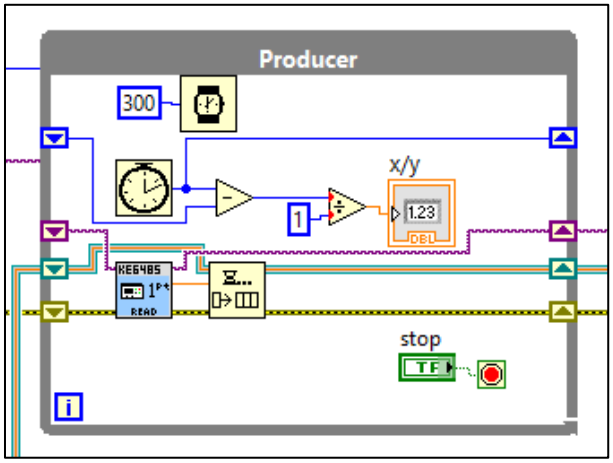

Figure 5.16. N-MS Producer Block Diagram

The Consumer Block calls the Dequeue Element function and withdraws the data from the queue. The data is then used to produce a waveform chart on the application's front panel. The Consumer Loop simultaneously takes the data from the queue and places it in the file initialized with the Initializing and Data Logging Block. The parameters for the logged data can be chosen by the experimenter. The application as written logs Date, Time, Sample Interval Time, and N-MS Current. This loop can also be used to perform a running system signal average. The Consumer Block diagram can be seen in detail in Figure 5.17.

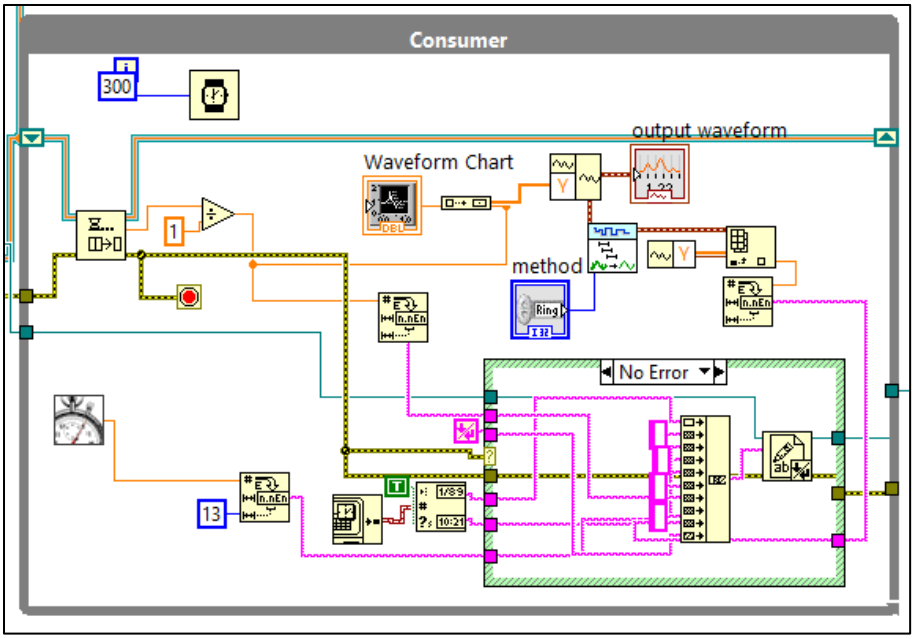

Figure 5.17. N-MS Consumer Block Diagram

The last block is the Closing Block. This block uses the Release Queue function to remove the Producer/Consumer Loops from the queue and allows the application to close

the connection with the KE6485 and report any error, if any. The Closing Block diagram can be seen in detail in Figure 5.18.

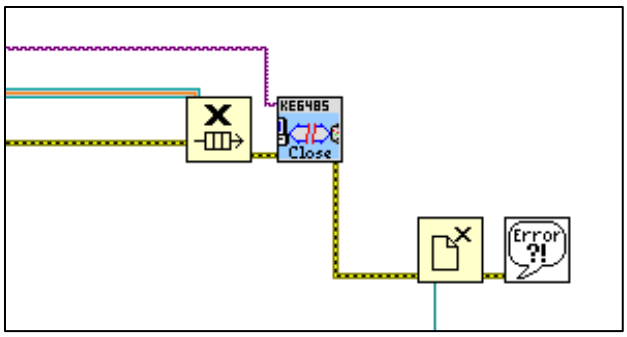

Figure 5.18. N-MS Closing Block Diagram

The application front panel can be seen in Figure 5.19. This shows the waveform generated during N-MS operation, as well as a 2-second running average. The front panel can be used to develop multiple virtual instrument readouts tailorable to the experiment, if desired.

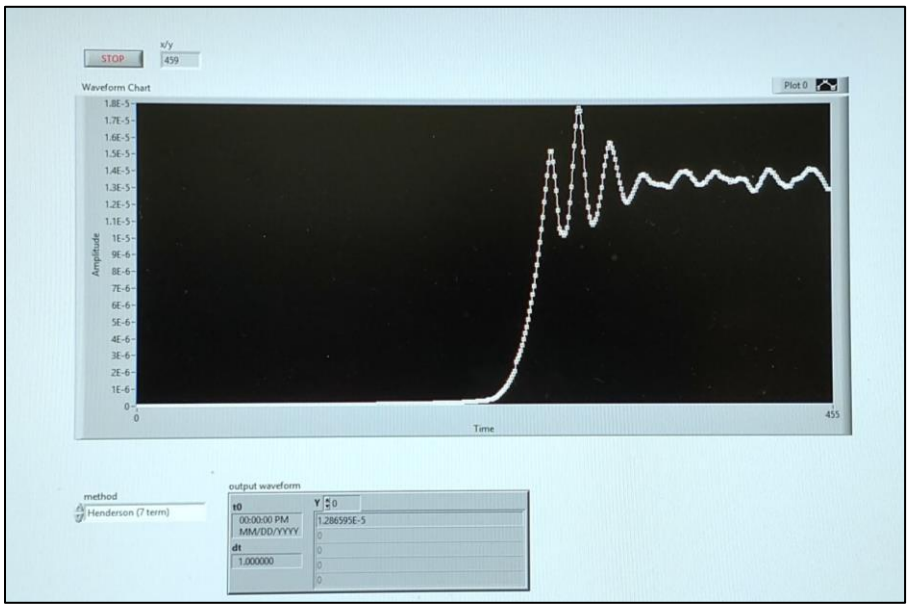

Figure 5.19. N-MS NI LabVIEW Application Front Panel.

An N-MS component layout diagram is shown in in Figure 5.20 and an image of the system in operation during testing is provided in Figure 5.21.

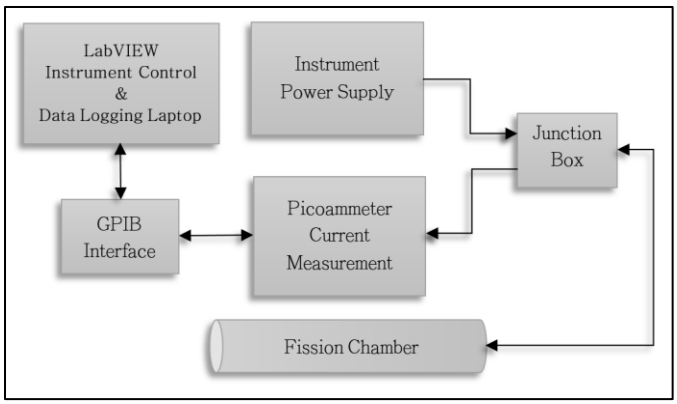

Figure 5.20. N-MS Diagram

Figure 5.21. N-MS in Operation (Photonis CFUF43 w/ Holder installed in reactor core)

Chapter 6: System Testing and Validation

The N-MS system was put through a series of testing measures. The sections below discuss the reason each test chosen, how each experiment was conducted, and the results.

6.1 MCNP6 Modelling

An MCNP model was used to estimate the reactivity changes caused by the new N-MS and PNT experimental designs and materials. This was to ensure the system design would not violate UT Austin NETL TRIGA Technical Specifications. [NETL, 1990] This modeling was in addition to a Radiation Operation Committee (ROC) Safety Analysis Report generated for experimental approval. The ROC experiment safety analysis report can be found in Appendix D.

The reactor model code used for MCNP analysis was originally developed by Dr. Alex Fay and later further developed by Dr. William Wilson. The MCNP Model is a detailed reproduction of the UT NETL TRIGA reactor an is provided in Appendix E. MCNP6.2.2 was used to run the model and produce images to verify system design measurements. MCNPX Visual Editor (Vised) Version 2.7E was also used to produce visual reproductions of the modeled systems.

The N-MS geometry was developed from the Photonis CFUF43 system literature and the isolating holder design schematics developed at NETL. The engineering design schematics have been included in the reference section and appendices. The N-MS surface cards added to The MCNP NETL TRIGA Model input deck are shown below.

```
c Fission Chamber Exp Surface Cards (MBS)
c ==========================================
c
c   -- 91 is Outer cylinder representing Fission Chamber Case
c   -- 92 is Inner cylinder representing Fission Chamber Holder
c   -- 93 is Outer cylinder representing Fission Chamber Holder
c   -- 94 is cylinder representing Fission Chamber Wire
c   -- 95 is Outer cylinder representing Billet
c   -- 96 is Inner cylinder representing Billet
c   -- 97 is Outer cylinder representing 90%+ HEU
c   -- 98 is Outer cylinder representing Fission Chamber Top Holder
c   -- 99 is Inner cylinder representing Fission Chamber Top Holder
c   -- 910 is Fission Chamber Fill Gas
c   -- 911 is Fission Chamber Inner Electrode
c   -- 912 is Fission Chamber Holder Bottom
c
 91       RCC -2.17170E+01 1.25476E+01 -5.004   0 0 8.6    0.235
 92       RCC -2.17170E+01 1.25476E+01 -6.004   0 0 38.39  0.424
 93       RCC -2.17170E+01 1.25476E+01 -5.504   0 0 37.89  0.635
 94       RCC -2.17170E+01 1.25476E+01 3.596    0 0 35     0.05
 95       RCC -2.17170E+01 1.25476E+01 3.596    0 0 8.8    0.406
 96       RCC -2.17170E+01 1.25476E+01 3.596    0 0 8.8    0.177
 97       RCC -2.17170E+01 1.25476E+01 -3.454   0 0 2.7    0.000005
 98       RCC -2.17170E+01 1.25476E+01 32.386   0 0 5.08   1.27
 99       RCC -2.17170E+01 1.25476E+01 32.386   0 0 5.08   0.424
 910      RCC -2.17170E+01 1.25476E+01 -3.454   0 0 2.7    0.22
 911      RCC -2.17170E+01 1.25476E+01 -3.454   0 0 2.7    0.12
 912      RCC -2.17170E+01 1.25476E+01 -5.504   0 0 0.5    0.635
c
```

Figure 6.1. MCNP Model N-MS Surface Cards.

The PNT geometry was developed from the UT NETL design schematics and the established PNT system in the MCNP Model of the UT NETL TRIGA reactor. The engineering design schematics have been included in the appendices. The PNT surface cards within the MCNP NETL TRIGA Model input deck are shown below. These surfaces were designed into the model and only needed slight modification to be included. The original model PNT geometry needed to be moved to the new location in grid location G36 to place the N-MS and PNT sample terminus as close as possible.

```
c Surface cards defining the boundaries of the
c pneumatic transfer system irradiation facility:
c ------------------------------------------------
c
c The following surface cards define the boundaries of the pneumatic transfer
c system irradiation facility.
c
c    nnnn AAA  D.DDDDDE+DD  x.xxxxxE+xx  y.yyyyyE+yy  R.RRRRRE+RR
c    ---- ---  -----------  -----------  -----------  -----------
0121      C/Z              -1.88519E+01  1.52375E+01  8.69950E-01
0122      C/Z              -1.88519E+01  1.52375E+01  1.11125E+00
0123      C/Z              -1.88519E+01  1.52375E+01  1.16205E+00
0124      C/Z              -1.88519E+01  1.52375E+01  1.53543E+00
0125      C/Z              -1.88519E+01  1.52375E+01  1.74625E+00
0126      PZ  -3.58275E+00
0127      PZ  -3.37193E+00
0128      PZ  -2.99855E+00
0129      PZ  -2.94775E+00
0130      PZ  -2.07645E+00
0131      PZ   5.00000E+01
c
```

Figure 6.2. MCNP Model PNT Surface Cards.

The N-MS was added to the model geometry as shown below. The reactor pool water cell, 0411, required modification to allow for the addition of the N-MS while still filling the inner portions of the N-MS holder with water.

```
c Fission Chamber Exp Cell Cards (MBS)
c ================================================
c
0691    91 -19.1 -97 910                                          $ Fission Chamber HEU
0692    01 -8.05 -91 #0691 #0697 #0698                            $ Fission Chamber Case
0693    95 -2.7 -94                                               $ Fission Chamber Wire
0694    09 -2.7 (-95 96)                                          $ Billet
0696    09 -2.7 (-93 92):(-912):(-98 99) #0691 #0692 #0693 #0694  $ Fission Chamber Holder
0697    96 -0.0018261048 (-910 911)                               $ Fission Chamber Gas
0698    01 -8.05 -911                                             $ Fission Chamber Inner Electrode
```

Figure 6.3. MCNP Model N-MS Cell Cards.

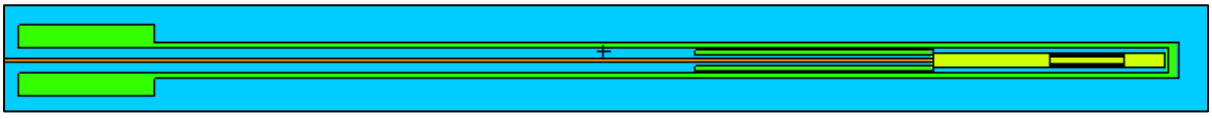

Figure 6.4. MCNP Model of Fission Chamber Neutron Monitoring System(2-D).

The PNT cell cards within the MCNP NETL TRIGA Model input deck are shown below. These cells were designed into the model similarly to the PNT surface cards and only require slight modification to be included in the model geometry as required. The reactor pool water cell, 0411, again required modification to allow for the addition of the PNT and accommodation in the new location.

```
c     m         d                    geom
c     --   -----------  ----------------------------------
0271  02  -1.20500E-03  -0131 -0121  0130
0272  09  -2.70000E+00  -0131 -0122  0129 ( -0130 :  0121 )
0273  13  -8.65000E+00  -0131 -0123  0128 ( -0129 :  0122 )
0274  02  -1.20500E-03  -0131 -0124  0127 ( -0128 :  0123 )
0275  09  -2.70000E+00  -0131 -0125  0126 ( -0127 :  0124 )
c
```

Figure 6.5. MCNP Model PNT Cell Cards.

The following figures show the MCNP NETL TRIGA Model geometry. The high level of detail can be seen throughout the model geometry.

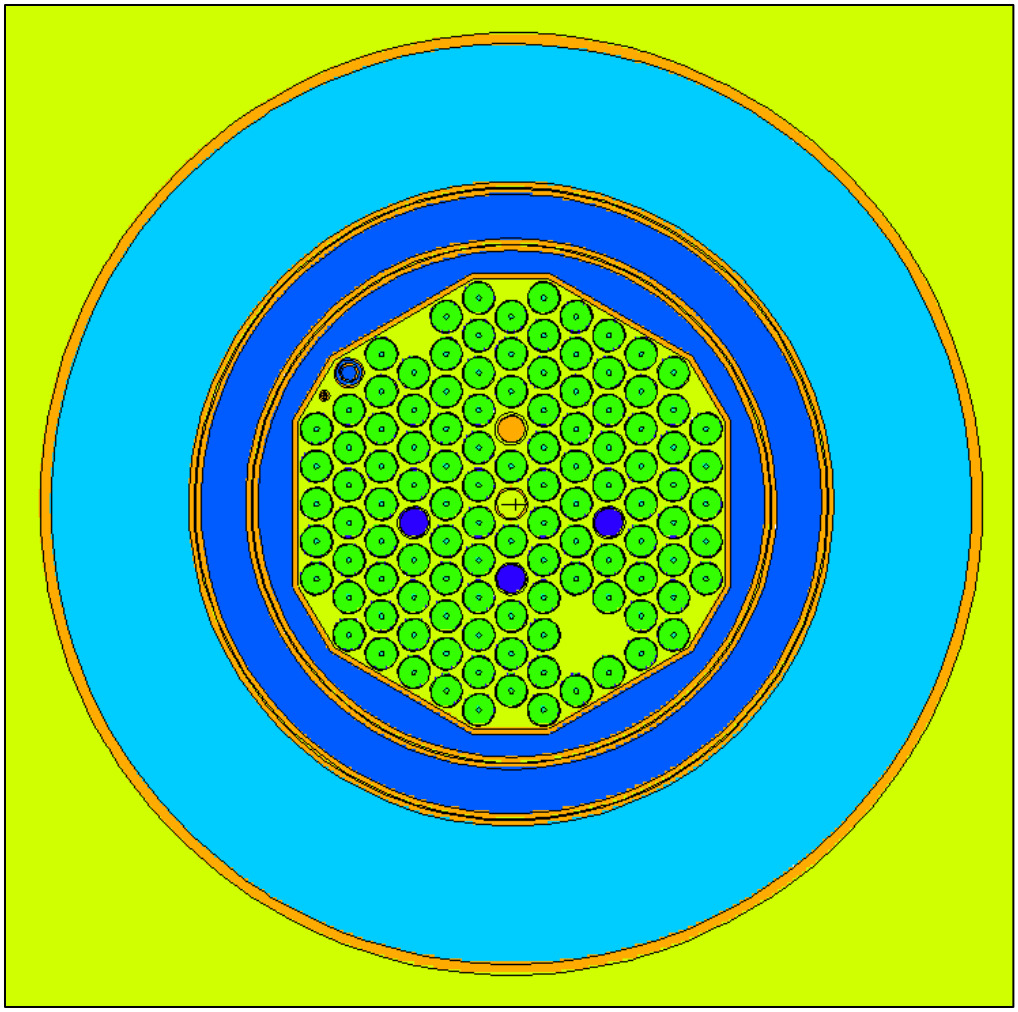

Figure 6.6. MCNP Model of NETL TRIGA Reactor, XY View.

The X-Y axis correctional view in the figure above shows the current UT Austin NETL TRIGA Core configuration when using the N-MS to track NAA PTS samples. The view shows the current fuel loading, 3-Element facility in the lower right, four control rods, and the N-MS adjacent to the PTS in the upper left.

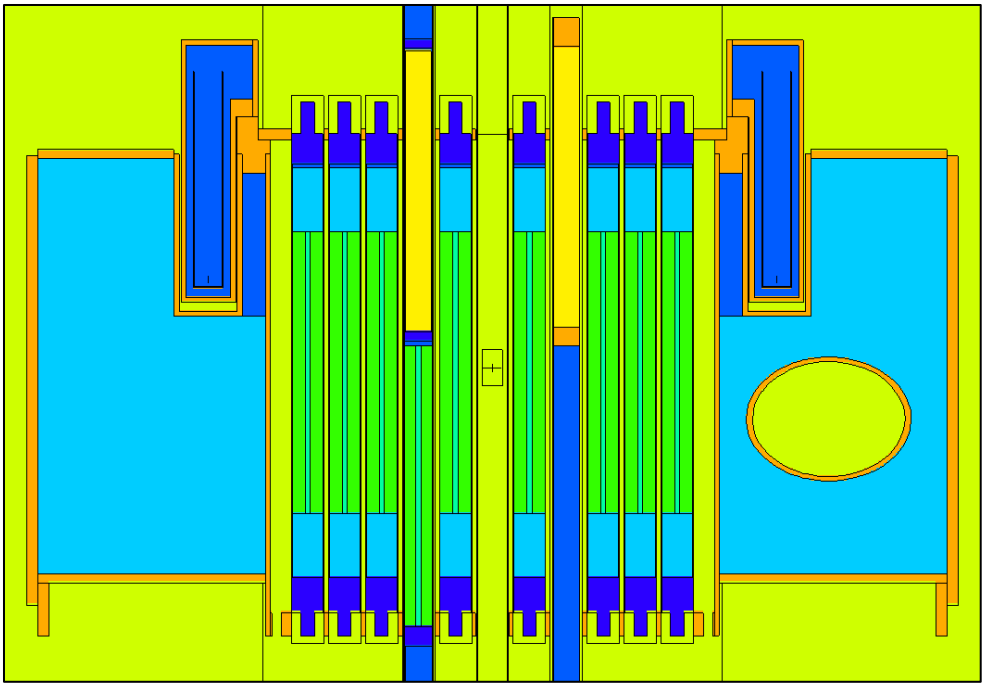

Figure 6.7. MCNP Model of NETL TRIGA Reactor, XZ View.

The X-Z axis correctional view in the figure above shows the UT Austin NETL TRIGA Core configuration, Rotary Sample Rack (RSR), and reflector assembly. A fuel followed control rod configuration can be seen on the left with the air followed transient rod on the right. A beam port can be seen on the right within the reflector.

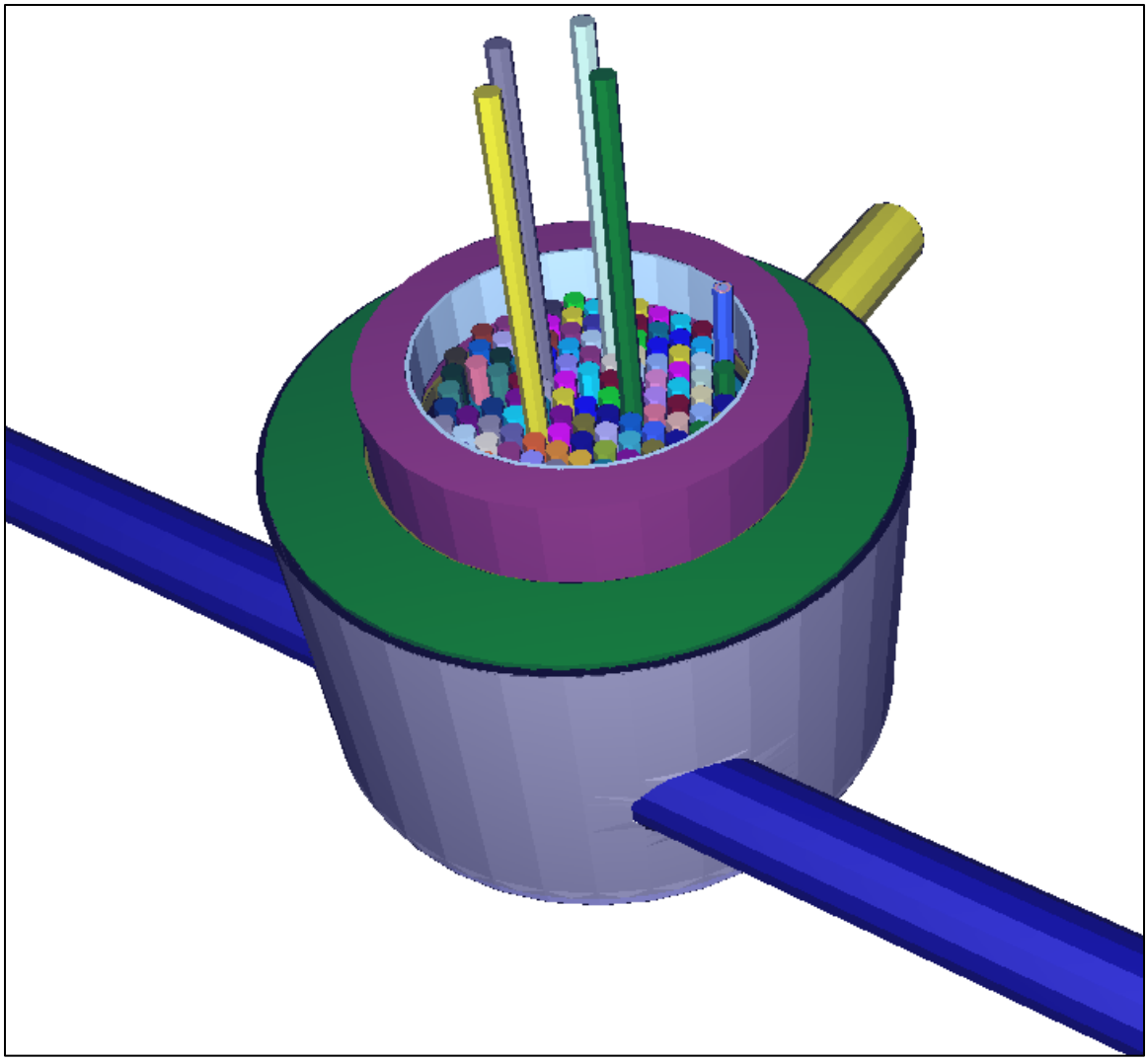

Figure 6.8. MCNP Model of NETL TRIGA Reactor, 3D View.

The entire reactor core is immersed within the reactor containment pool and vessel. The beam ports protrude from the reflector and extend through the containment pool and vessel as shown in Figure 6.8 above.

The N-MS and PNT system geometries as installed in the model are shown in detail below.

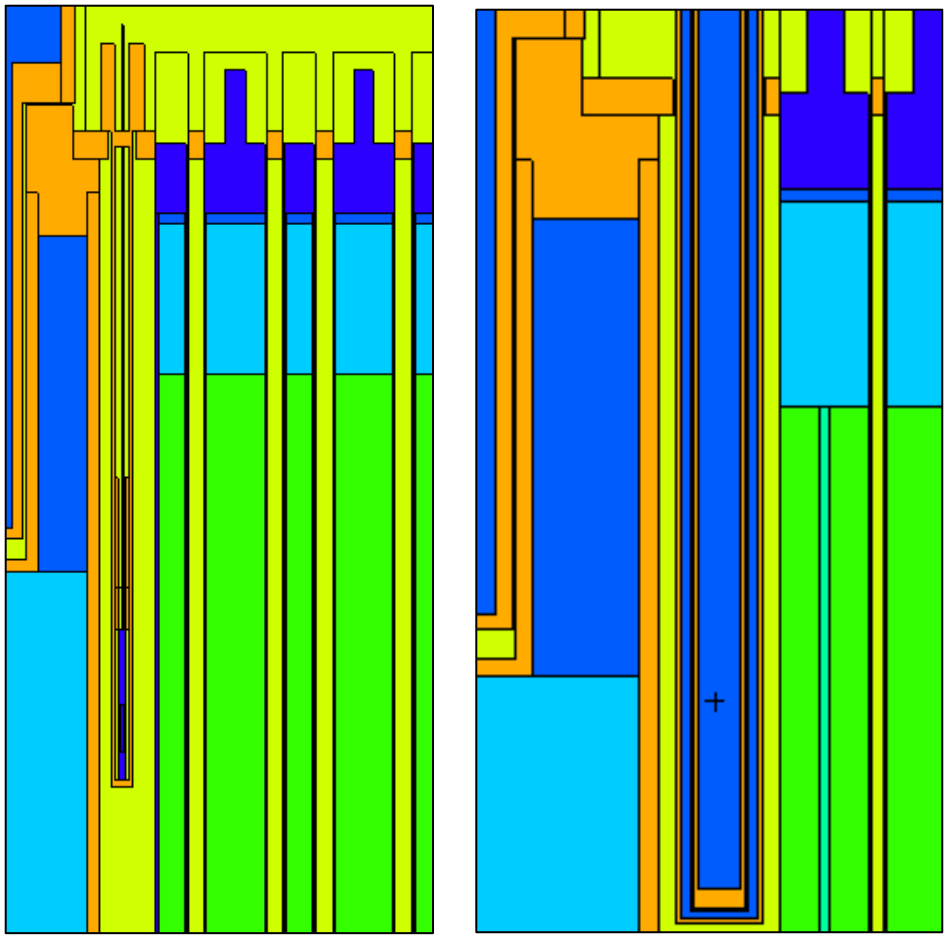

Figure 6.9. MCNP Model of N-MS (Left) and the PNT System (Right), XZ View.

The N-MS and PTS images provided in Figure 6.9 were generated after inserting the specific geometry code into the UT Austin NETL TRIGA MCNP deck. The PTS system actually extends further down into the core but this model stops at the PTS sample terminus.

A 3-dimentianal view of the installed N-MS and PTS within the core is provided in Figure 6.10 and 6.11. Both figures were produced with the MCNP6.2.2 modified code and the Vised v2.7E software.

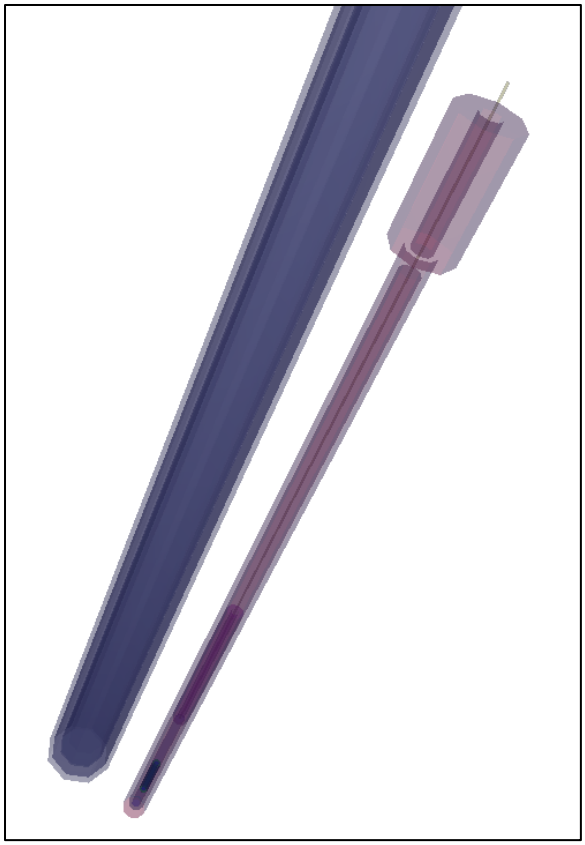

Figure 6.10. MCNP Model of N-MS (Right) and the PNT System (Left), 3D View.

Figure 6.10 was made by removing all reactor code cells from the visualization to confirm the precise location of the coded systems after installation. From the image it can be seen the N-MS is as close as possible to the PTS sample terminus.

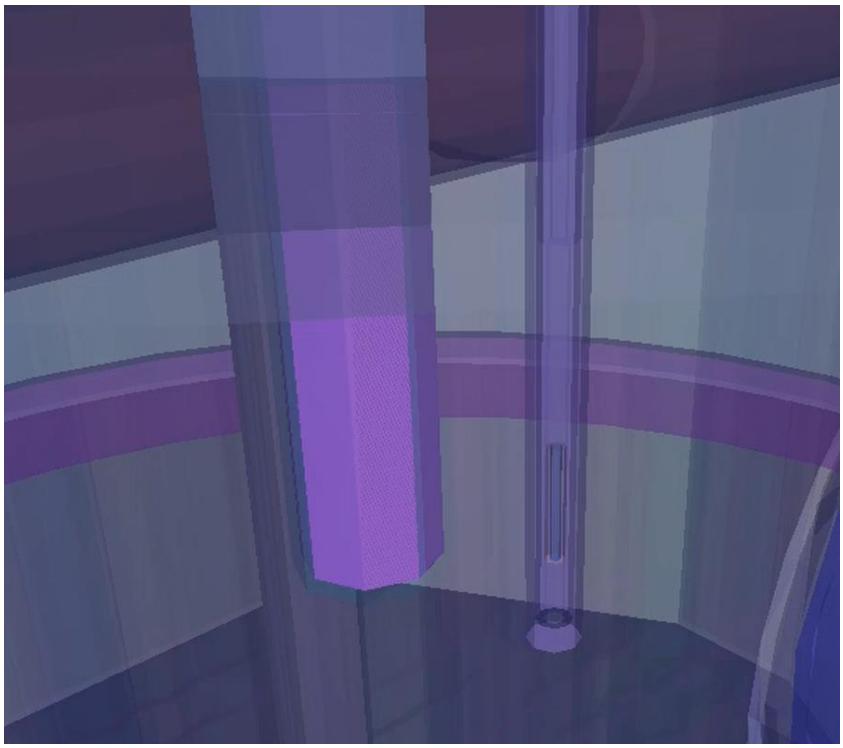

Figure 6.11. MCNP Model N-MS Sensitive Region N-MS (Right) and PNT System (Left).

The visualization in Figure 6.11 above shows the sensitive region of the N-MS fission chamber. Care was taken to ensure the sensitive region is at the same height as the NAA sample when injected with the PTS. The system is also close to the reflector cut out for beam port 3. The edge of the beam port 3 can be seen in the lower right of the image.

The model showed the N-MS system will have a negligible effect of reactor operation as the reactivity change was on the order of nominal burnup. The N-MS change was often indistinguishable from the baseline model without any experimental facilities installed. The 100,000 particle run produced the most stable and clear separation of the three geometries. These results are presented in Figure 6.12 below.

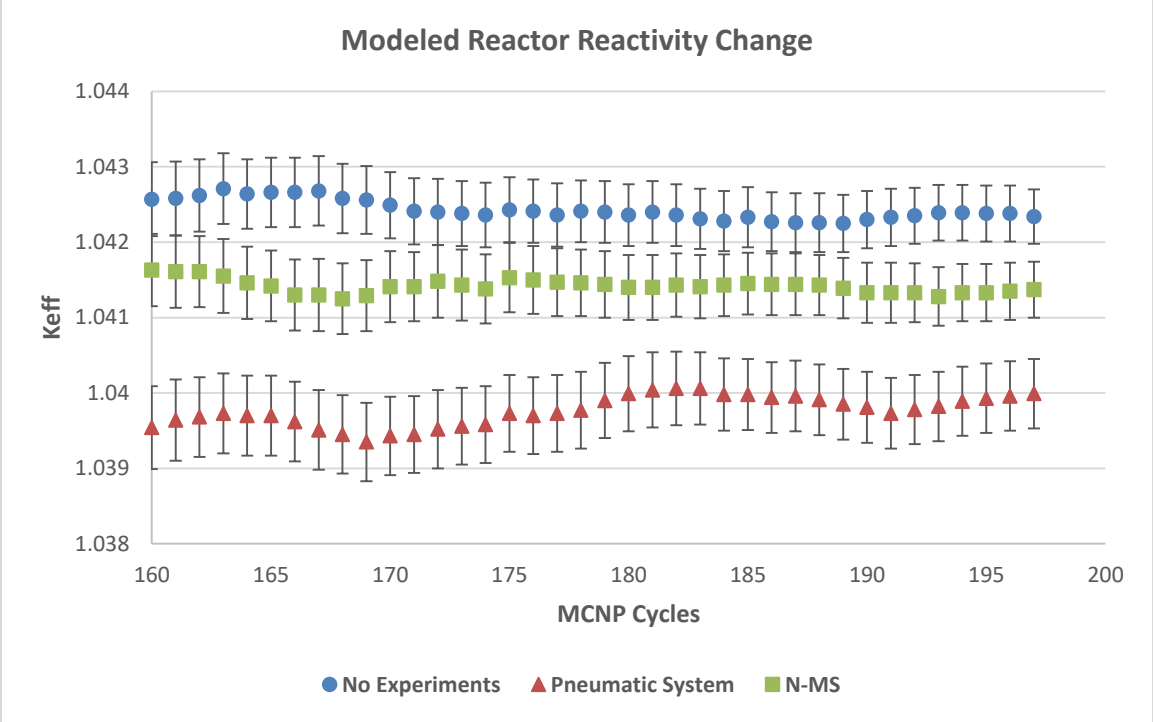

Figure 6.12. UT Austin NETL TRIGA MCNP Modeled Reactivity Change: N-MS and ePNT (1σ-Error).

For model verification, results were compared to the epithermal PNT (ePNT) reactivity worth. The ePNT has been in use for many years and has a well-documented reactivity worth of -$0.30. Reactivity changes were modeled to within 10% of determined values of established experiments. N-MS subsequent testing has shown a reactivity worth range of -$0.08 to -$0.15. This may seem contrary to what is expected from inserting HEU

within the reactor core. The relatively small amount of HEU within the fission chamber does not produce a positive reactivity change strong enough to overcome the negative moderator reactivity change due to the N-MS displacing water from the core of the TRIGA Mk II Reactor. This also showed the N-MS can likely be a mobile monitoring system during operation as the reactivity effect is well less than $1.00. The N-MS model geometry created is easy to move the around the reactor model geometry to test the effect at other locations and powers. The final model summary is provided in Table 6.1 below.

Modeled Reactor Reactivity Change

	Keff	σ	Δρ($)	σ
No Experiment	1.0419 - 1.0425	3.6E-4		
ePNT	1.0396 - 1.0399	4.6 E-4	-0.306 - -0.330	0.04
N-MS	1.0414 - 1.0415	3.7 E-4	-0.133 - -0.062	0.03

Table 6.1. Modeled Reactor Reactivity Change Summary

6.2 3-Element Experimental Facility Testing

Preliminary testing of the N-MS was conducted in the 3-Element (3-EL) irradiation facility. The 3-EL facility is location with the reactor core where three elements can be removed and an experiment inserted for irradiation. This location was easily accessible for quick testing of the N-MS system signal and activation calibration.

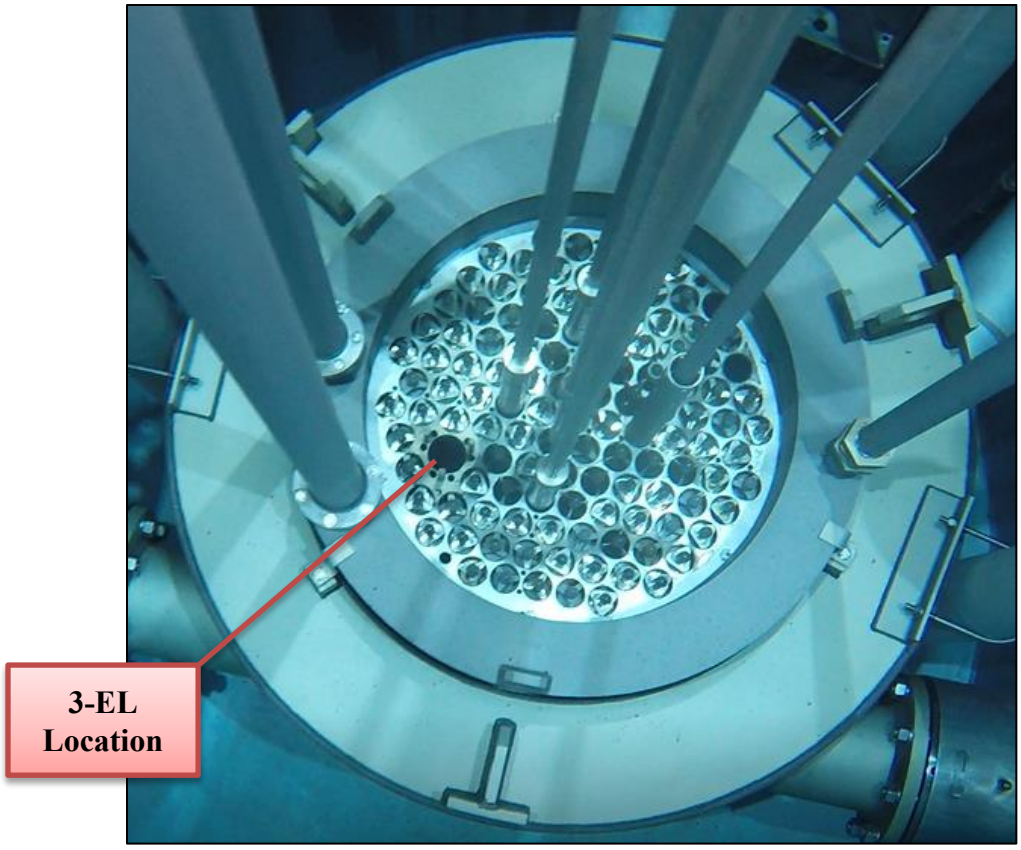

Figure 6.13. 3-Element Irradiation Facility Location

Figure 6.13 shows the 3-EL access location. The N-MS was attached to a temporary experimental jig for irradiation. To perform the activation calibration test, a neutron density monitor wire was irradiation with the N-MS. National Institute of Standards and Technology (NIST) Standard Reference Material (SRM) number 953 was chosen for activation calculations. The NIST SRM 953 wire is an aluminum-cobalt flux wire 0.116±0.002 percent cobalt by weight. Flux wire monitors were approximately 1cm long, 0.5mm in diameter, and an average weight of 0.00584 ± 0.0002 grams. The $^{59}Co(n,\gamma)^{60}Co$ reaction was used to determine neutron fluence. Calculations were performed as per ASTM E 262-03.

Five irradiations were performed and each irradiation was at a specific power level and maintained for 1 hour. The N-MS and SRM 953 wire was placed within the 3-EL facility before reactor startup and removed after reactor shutdown. The N-MS system captured each rector run and logged all data for further processing after the irradiations.

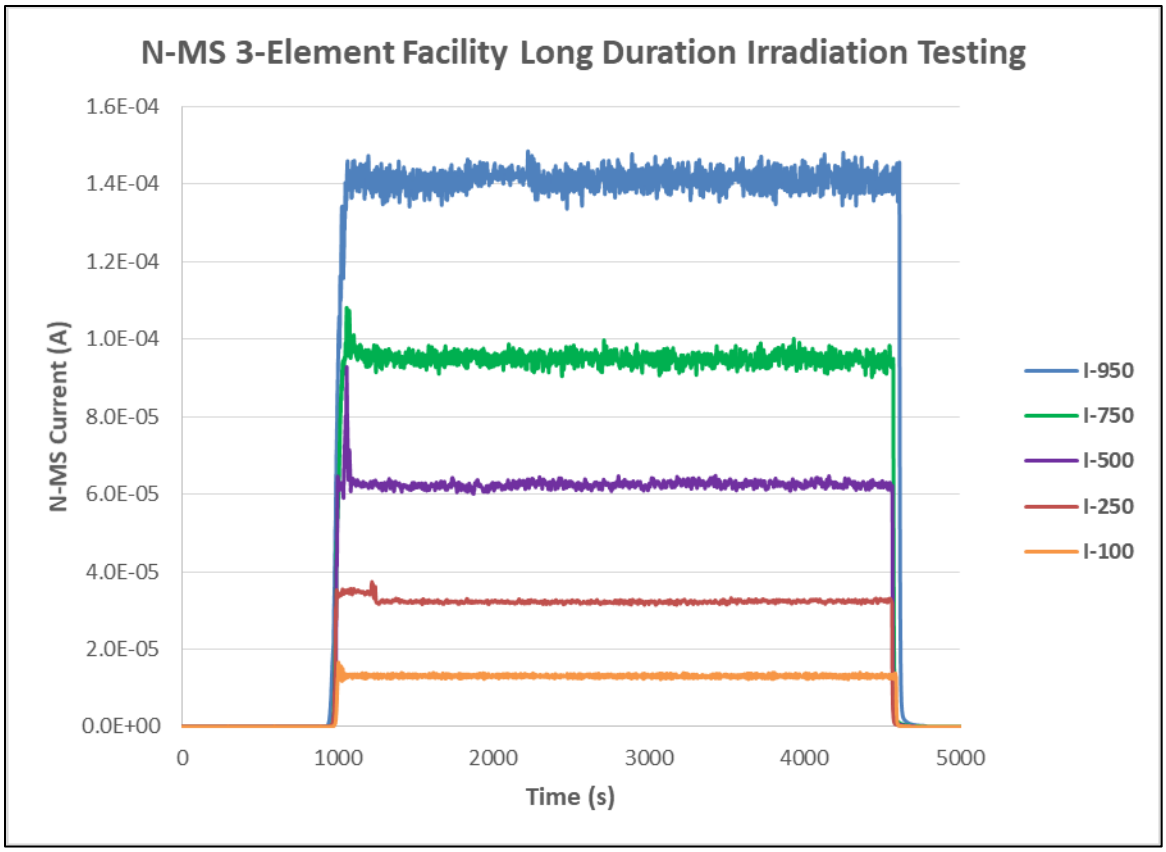

Figure 6.14. N-MS Reactor Power Response 3-Element Irradiation Facility Location

The reactor powers used to irradiate the NIST SRM 953 wires and N-MS were 100kW, 250kW, 500kW, 750kW, and 950kW. The figure above shows each reactor power level N-MS response current versus time. As the power level increases, the standard deviation of the signal increases as well. Each section of the signal representing the steady

state power 1 hour irradiation was parsed and compared to the ^{60}Co 1332.5 keV peak net counts.

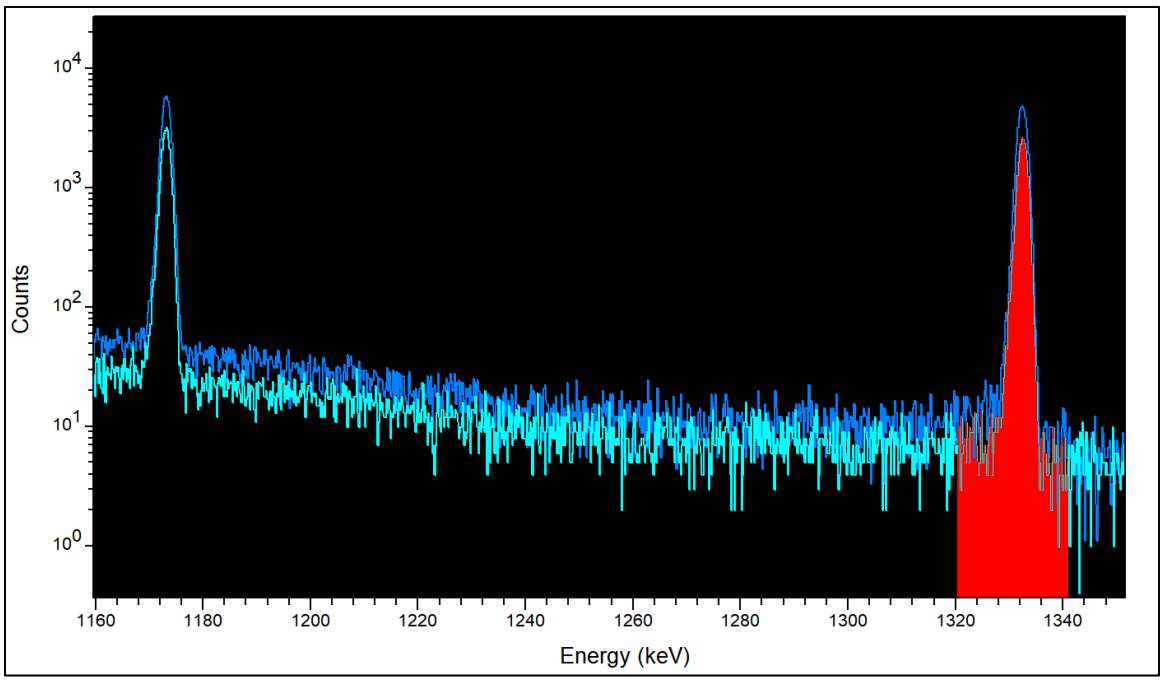

Figure 6.15. NIST SRM 953 Neutron Density Monitor Wire Activation 100kW vs 950kW

The activated NIST SRM 953 wire spectra were obtained using an HPGE gamma-ray spectroscopy system with a lead clamshell shield. Each sample was allowed to decay for a set time depending on irradiation power level to ensure the HPGE system dead time remained below 10%. Figure 6.15 above shows the spectra from both the 100kW irradiation counted for 14 hours and the 950kW irradiation counted for 2 hours. Taking Equation 3.2 and solving for neutron flux gives Equation 6.1 below.

$$\phi = \frac{\lambda(\text{Net Counts}_{1332})}{\sigma N_o \xi \Theta P_\gamma \, [1-e^{-\lambda t_c}][1-e^{-\lambda t_i}][e^{-\lambda t_d}]} \qquad \text{Eq 6.1}$$

Using the Activated NIST SRM 953 spectra, the required neutron flux for each sample was calculated. The resultant N-MS calibrated conversion factor for the 3-EL experimental test was determined to be $1.197\text{x}10^{-17}\frac{A}{ncm^2s}$. This experimentally derived conversion factor was very close to the standard conversion factor provided by the Photonis CFUF43 manufacturer, $1.\text{x}10^{-17}\frac{A}{ncm^2s}$. The resulting activation flux was able to be tracked to within 1% of the activated NIST SRM 953 wires. The resulting data is presented in Figure 6.16 below.

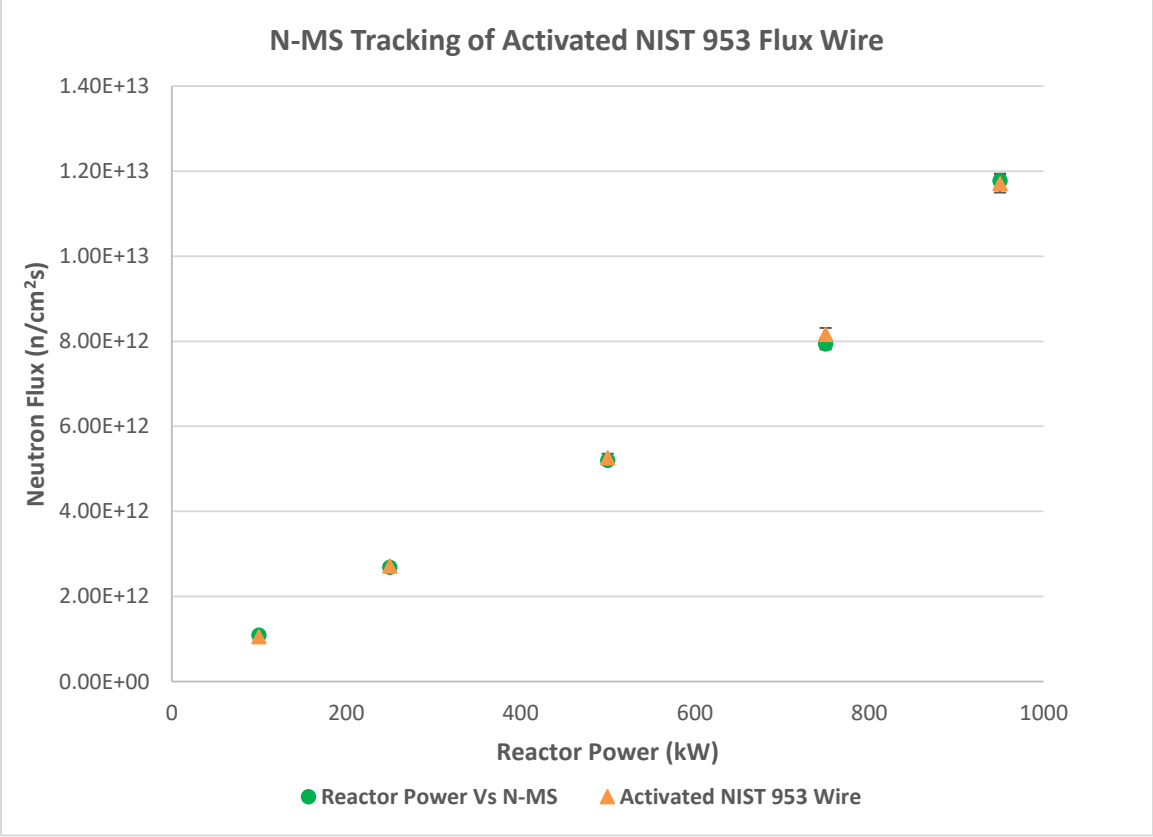

Figure 6.16. N-MS Activation Response 3-Element Irradiation Facility Location, (1σ-Error).

To perform a detailed test of the N-MS response to power across the full reactor power range, the system was placed within the 3-EL facility to track reactor power from startup to full power at 950kW and back to shutdown. Reactor power was increased in 100kW increments until the final 50kW increase to arrive at 950kW. The reactor was then tilted to force a higher neutron flux into the 3-EL facility while maintaining total reactor power at 950kW. The tilting of the reactor was conducted as a preliminary measurement for an upcoming experimental irradiation not related to the N-MS test. The full test signal for the test can be seen in Figure 6.17 below.

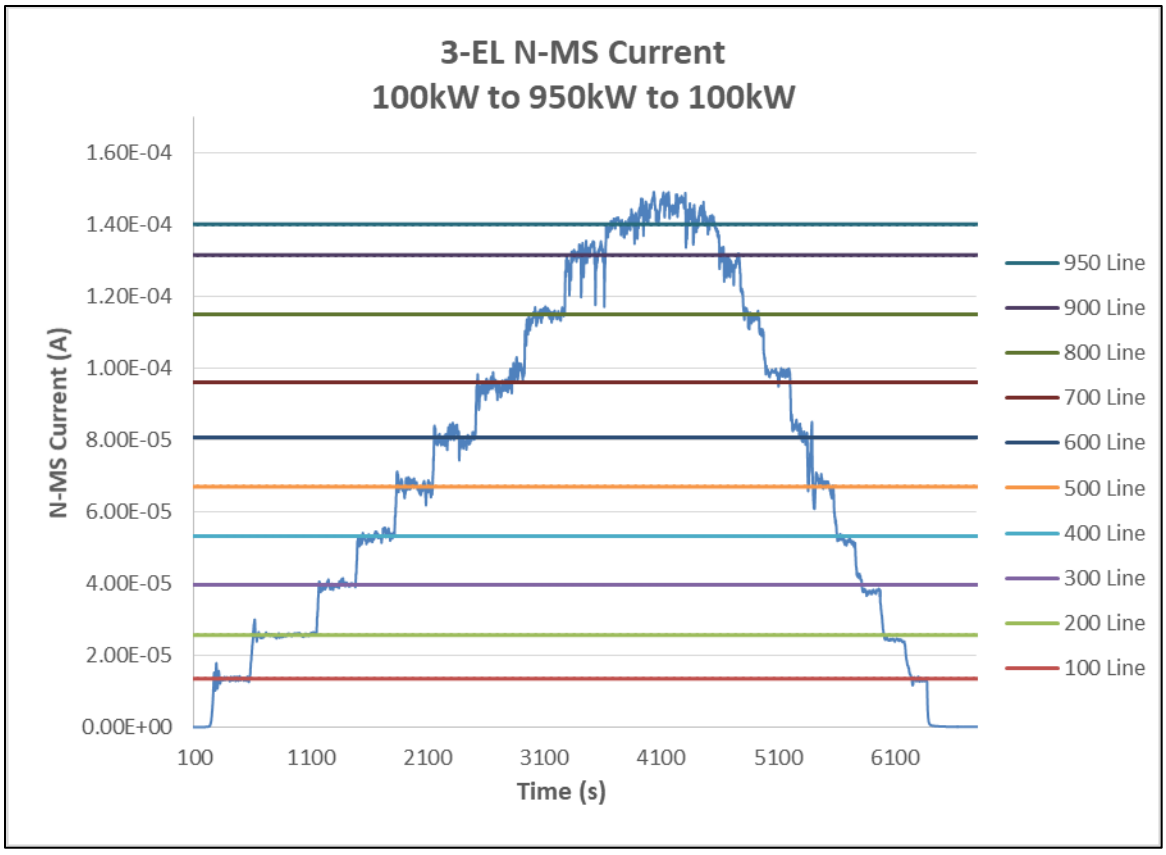

Figure 6.17. N-MS Reactor Power Response 3-Element Irradiation Facility Location

The N-MS response was linear with reactor power. The system linearity was not dependent on increasing reactor power trends or shutdown trends as can be seen from Figure 6.17. The linearity test data is present in Figure 6.18 below. Some of the reactor power levels seemed to have more variance than others. Namely reactor power levels 700kW and 900kW. This could be due to the reactor operator adjusting or "banking" the reactor control rod positions during automatic reactor power mode. The small deviations from linearity are most likely attributed to small N-MS movements within the 3-EL during measurement.

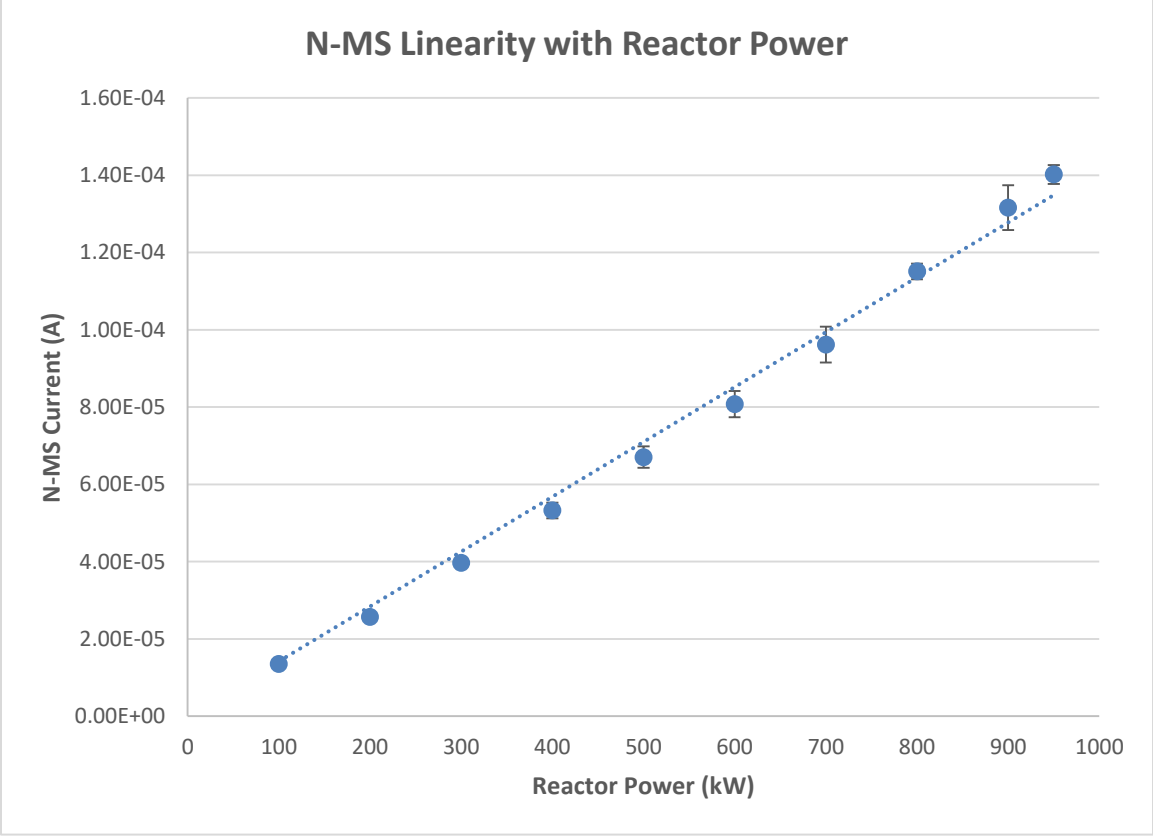

Figure. 6.18. N-MS System Response with Increasing Power in 3-Element Facility, (1σ-Error).

6.3 N-MS PTS Facility Testing

The next sequence of tests were conducted with the N-MS installed in the 5/8in upper grid plate access hole as shown in Figures 5.1 and 5.2. The system was tested again for linearity with reactor power. The N-MS is held firmly in this position not allowing the small movements that caused the minor linearity deviations in the 3-EL testing. This test included a reactor power range of 100kW to 950kW in 50kW increments. Also a rapid shutdown from full power using a planned SCRAM of the reactor was conducted. The N-MS system response is show in Figure 6.19 below.

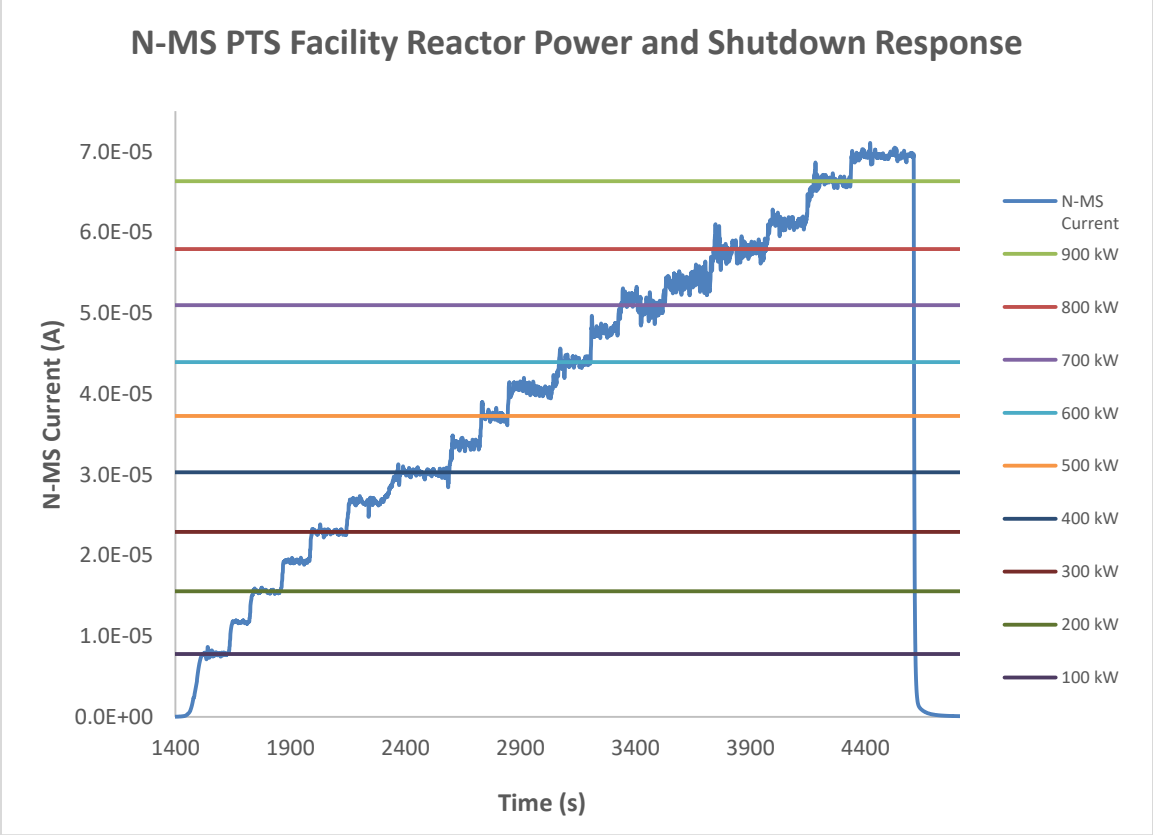

Figure. 6.19. N-MS PTS Facility Response with Incremental Power Increase to Shutdown

The system response was linear and capable of easily discerning the 50kW power increments. The reactor SCRAM was also captured without incident. The N-MS resolution is capable of capturing localized neutron flux changes on the order of typical irradiation experiments.

The N-MS linearity with reactor power in this test was much more stable than in the 3-EL testing as can be seen in Figure 6.20 below. The linear trend line fitted to the data had an R-value of 0.999. The N-MS response was linear with reactor power as expected and was very responsive to individual control rod movements. [Goricanec, 2018; Zerovnik 2015]

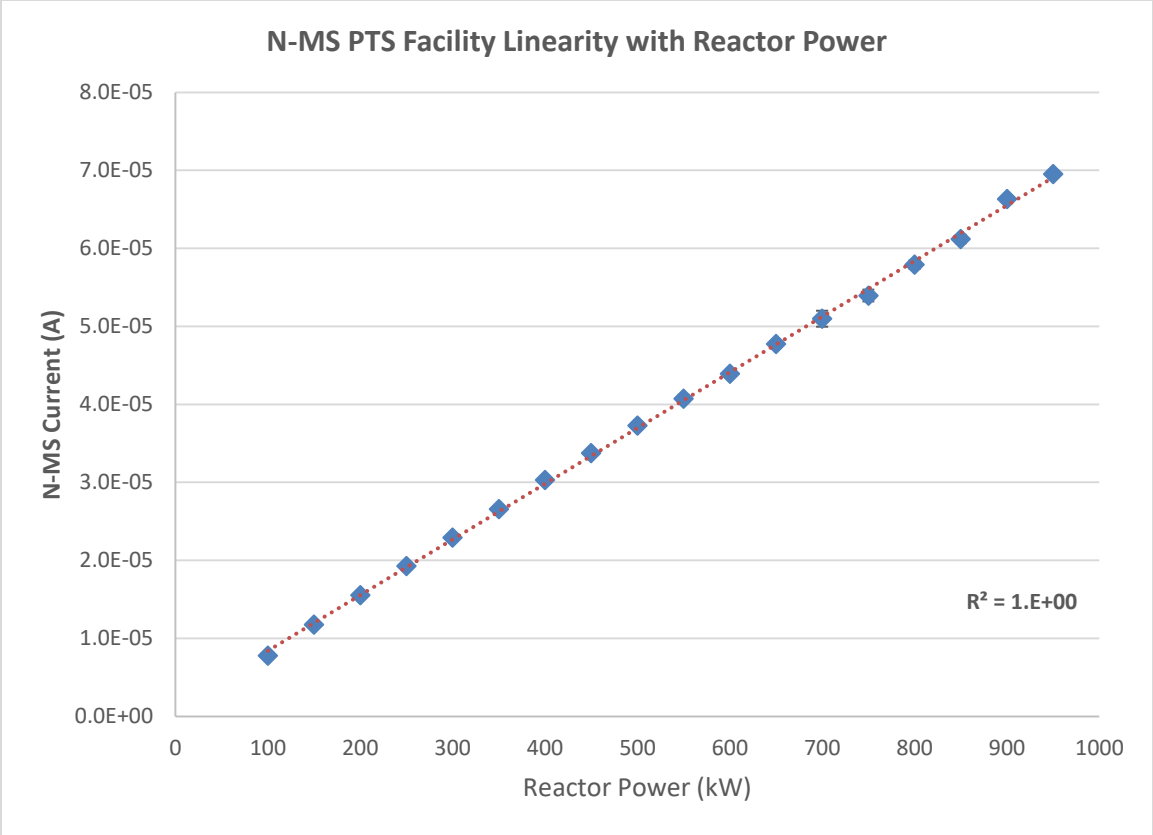

Figure. 6.20. N-MS PTS Facility Linearity with Increasing Power, (1σ-Error).

6.3.1 Manual Pneumatic Transfer System Testing

The ultimate test was to verify the N-MS's ability to track neutron fluence of NAA samples. To test the N-MS with the Manual PTS, multiple sulfur flux monitors were placed in NAA polyethylene vials for irradiation. Each monitor was injected into the reactor core using the Manual PTS and irradiated for 10 seconds in UT Austin NETL's TRIGA reactor at 950 kW sequentially to gather flux variance at steady state power. The N-MS was tracking and logging measurements within the core while the NAA sulfur flux monitors were irradiated. The activated sulfur flux monitors were allowed to decay for 300 seconds before being placed on a shielded high purity germanium detector for measurement. All samples were counted for a live time of 300 seconds ensuring regimented counting geometry and dead times below 10%. Neutron flux data logged by the N-MS was parsed for each irradiation period and normalized for comparison with the Manual PTS injected NAA sulfur flux monitors. The data is presented in Figures 6.21 and 6.22 below.

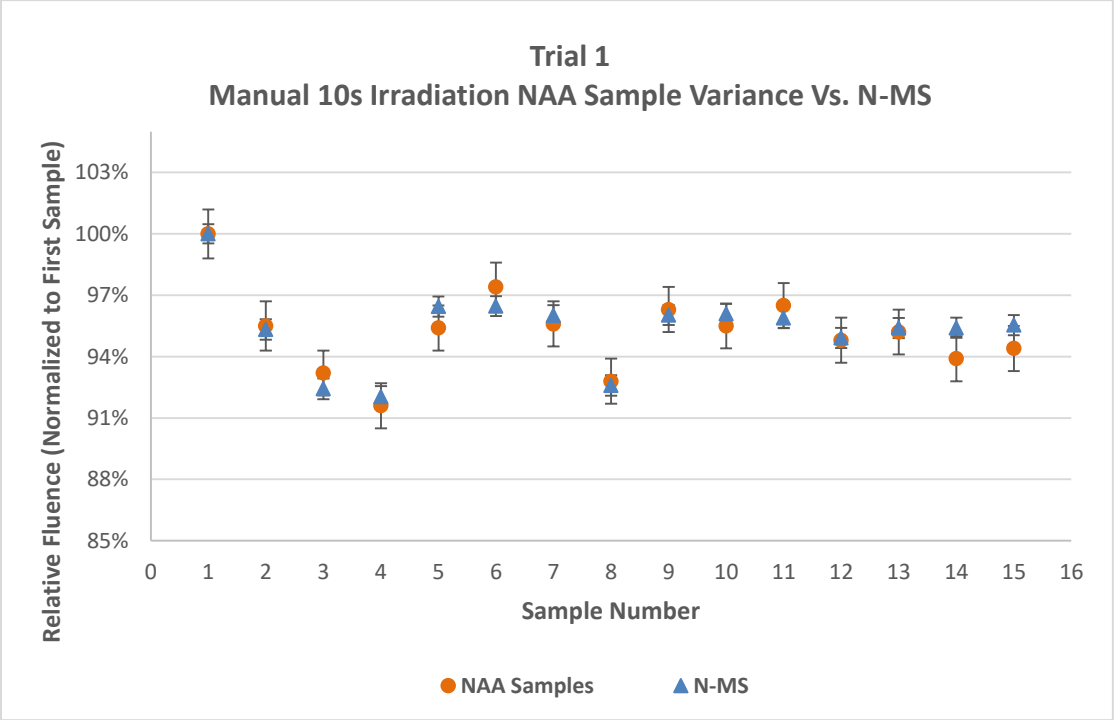

Figure 6.21. Consecutive Manual 10s Irradiation NAA samples with N-MS tracking data, (1σ-Error).

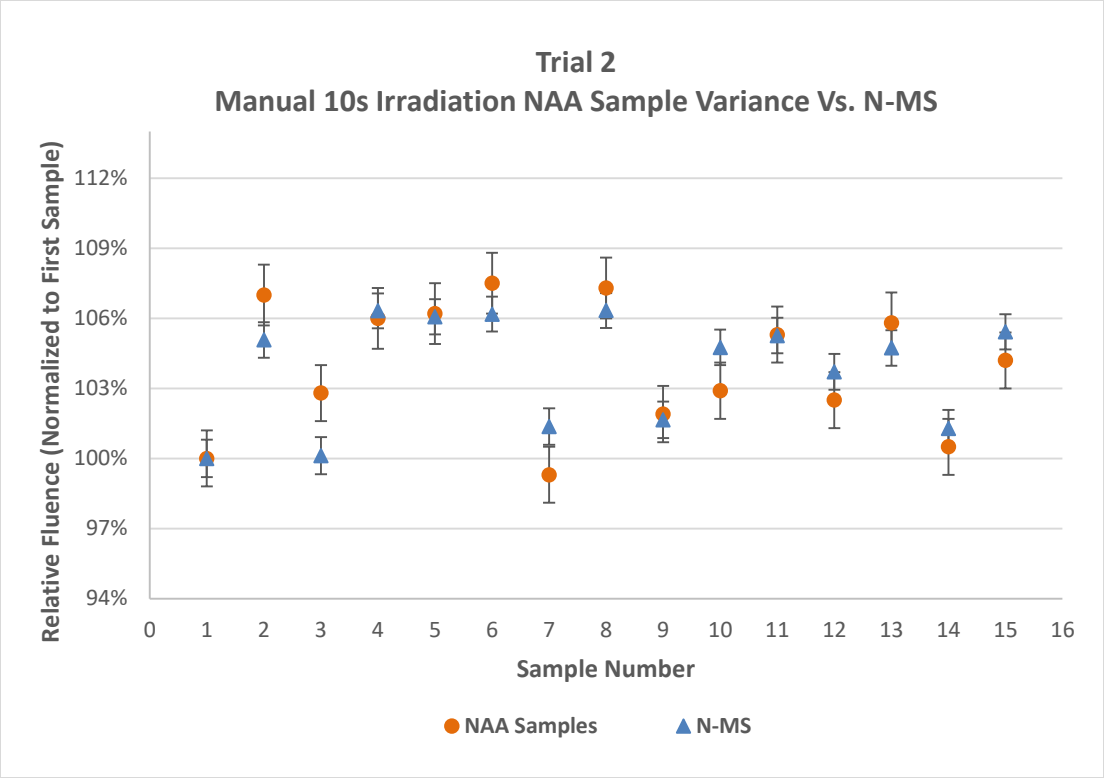

Figure 6.22. Consecutive Manual 10s Irradiation NAA samples with N-MS tracking data, (1σ-Error).

Both trials with the Manual PTS showed the N-MS system was able to track the short duration irradiations with the Manual PTS to within 3% of the activated variance. The Manual PTS system requires manual post irradiation processing before counting the sample and has potential, especially with rapidly decaying isotopes, to induce human error. The experimenter is required to manually maintain regimented redundancy between all samples.

6.3.2 Automatic Pneumatic Transfer System Testing

The Auto PTS was tested in much the same way as the Manual PTS but with the ability to perform automated testing at multiple irradiation times. The Auto PTS removes the experimenter involvement between irradiation and sample counting. This reduces the potential for induced sample post processing error and is a rapid, repeatable process. Samples were injected and counted with the Auto PTS system at irradiation times of 10, 60, and 180 seconds. The sample decay times were maintained within each group and chosen to allow for a deadtime below 10%. The Auto PTS testing results are summarized below in Figure 6.23 thru 6.25.

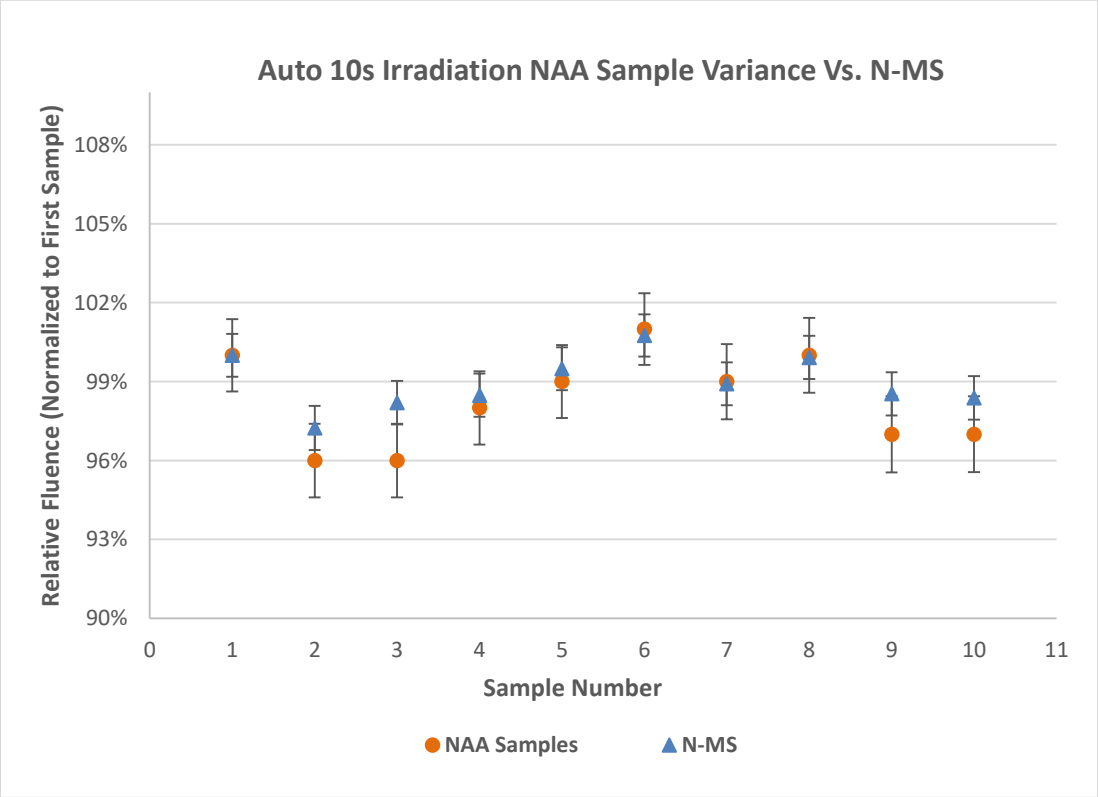

Figure 6.23. Consecutive Auto 10s Irradiation NAA samples with N-MS tracking data, (1σ-Error).

The 10-Second short irradiation is the fastest irradiation time allowed with the Auto PTS. The samples during the 10-Second irradiation Auto PTS trial showed 5% NAA sample activation variation. The N-MS was able to track samples within 2%. Most samples were tracked to within 1% with 4 samples outside of the normalization sample within 0.5%.

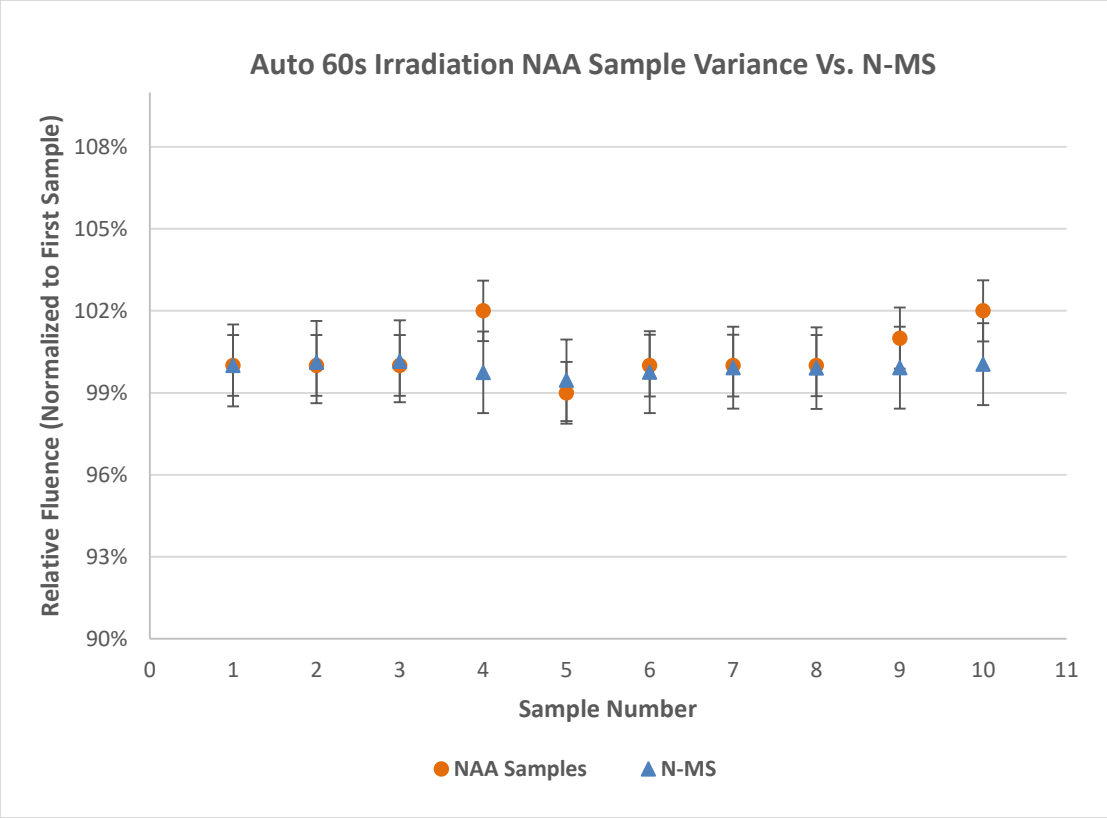

Figure 6.24. Consecutive Auto 60s Irradiation NAA samples with N-MS tracking data, (1σ-Error).

The 60-Second irradiations were expected to begin showing an tighter trend as the neutron fluence each sample received should approach an average the longer the irradiation

time. This was the case as can be seen in Figure 6.24 above. Sample variance began collapsing towards an average activation fluence.

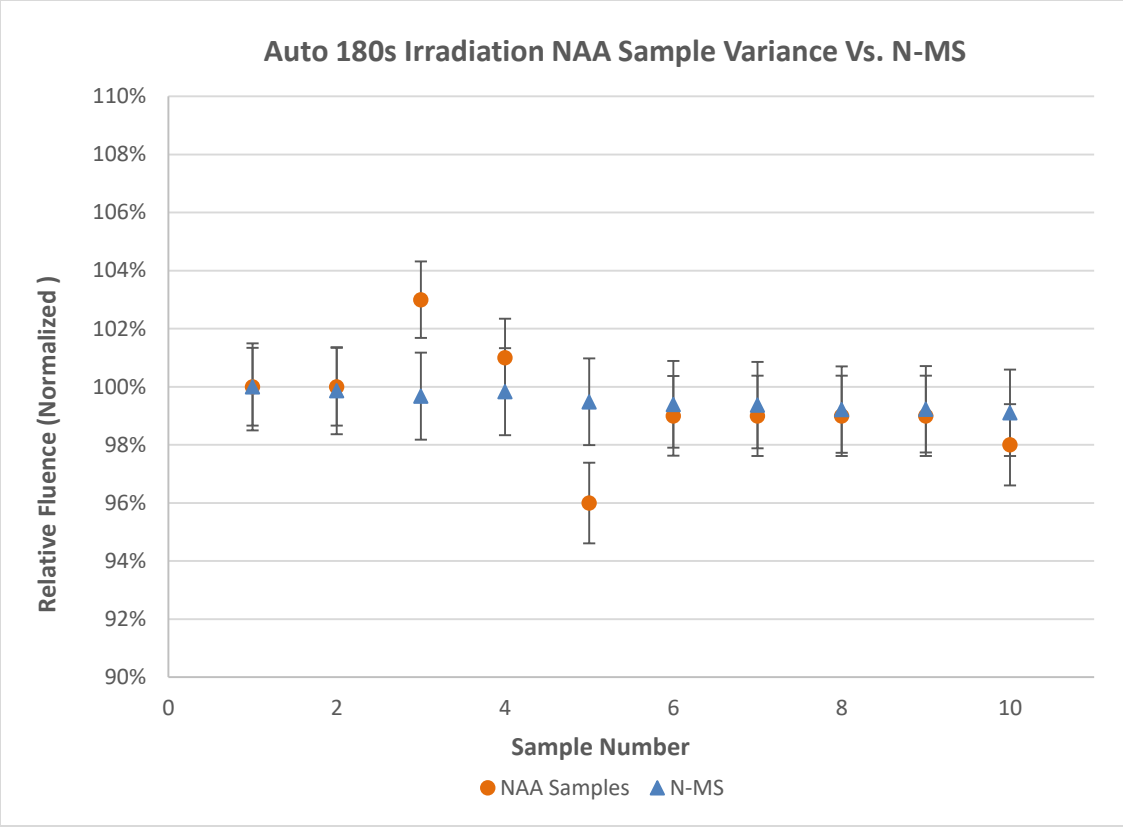

Figure 6.25. Consecutive Auto 180s Irradiation NAA samples with N-MS tracking data, (1σ-Error).

The 180-Second irradiation continued the same trend as shown with the 60-Second irradiations. The N-MS was able to track the vast majority, 80%, of the automatic pneumatic transfer system samples to within 1%. In each trial a few NAA samples were out of bounds in comparison to the average and the neutron detector. This may be due to a size difference in prepared HPDE vials effecting sample transfer times within the system tubing. The other possibility is the sulfur powder compressing upon impact within the

pneumatic transfer system if the powder was not sufficiently packed during preparation. Both of these scenarios need to be investigated further to rule out any systematic variation in the pneumatic transfer system. Overall, the N-MS remained able to track all samples to within 1-3%.

For all trials, the normalized NAA sulfur monitor values and N-MS values show good correlation as seen in Figure 6.26 below.

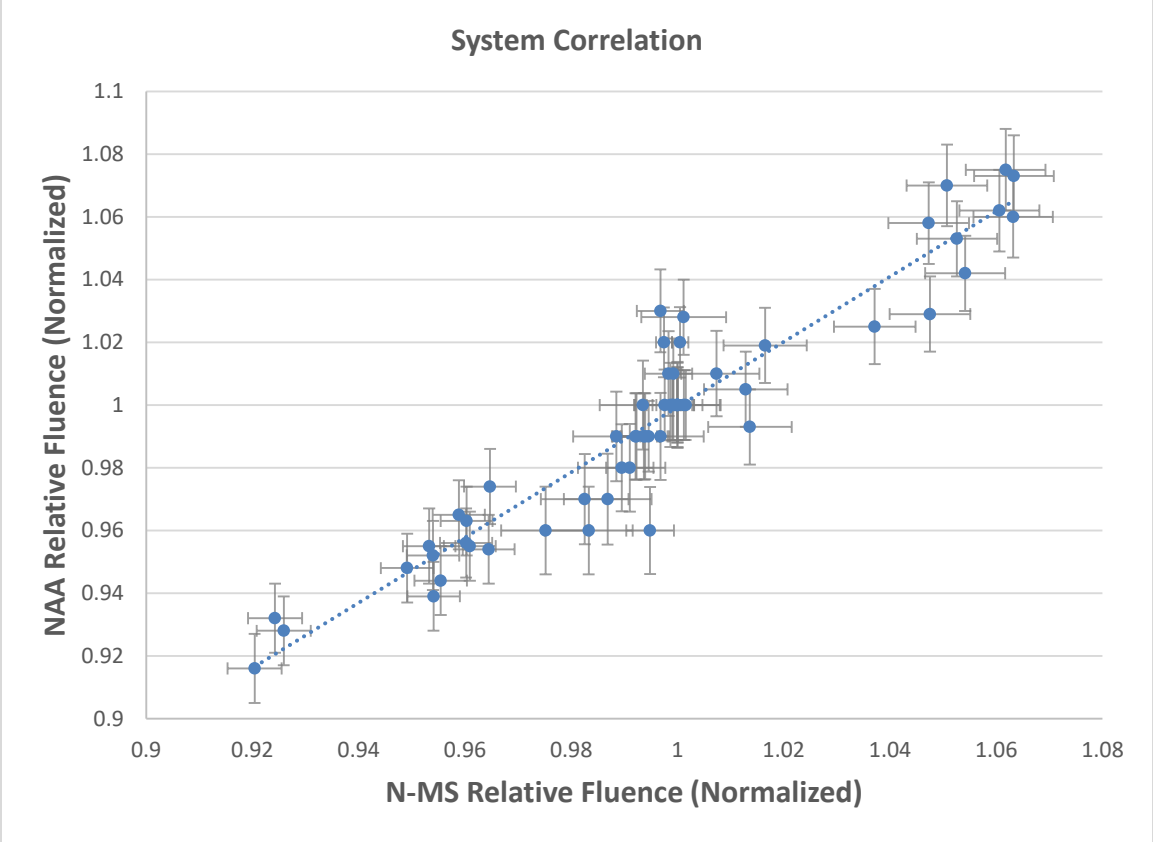

Figure 6.26. N-MS and NAA Sample Irradiation Correlation, (1σ-Error).

Chapter 7: Conclusions

7.1 Summary of Results

The results above show the designed system is capable of monitoring sample activation in real-time and is able to track NAA sample variance to within 1-3% of normalized values. A significant reduction in the uncertainty of NAA measurements for trace elemental concentrations is achievable without co-located flux monitor samples. This can considerably cut down on sample preparation, reactor operation, and laboratory analysis time. Both the manual and automatic pneumatic transfer systems at UT Austin were used for these measurements and some error in the tracking irradiation times could account for the few outliers seen in the data. [Stopic, 2016] Further evaluation of possible systematic errors within the pneumatic transfer systems could allow error isolation and potentially allow the N-MS system tracking capability to reach sub 3% error values. In addition to the N-MS being used for NAA tracking, the versatility of the system has led to further use as a reactor calibration instrument for core configuration measurements and axial neutron flux tilt characterization. The system also has a potential benefit for reactor model verification. [Zerovnik, 2015] Further work is currently underway to fully evaluate the N-MS's utility in these areas.

7.2 Future Work

The N-MS setup enables the system to be used for future sample delivery and retrieval automation based on N-MS readings, if deemed necessary. Future work would be to integrate the N-MS with the automated NAA pneumatic sample system and increasing the sampling resolution for finer detail. If done, this system has the potential to allow for fully automated sample irradiation independent of reactor power and irradiation

time constraints but targeted at total sample fluence alone. A reactor pulse was also captured during testing but the time scale exceeded that if the current LabVIEW-GPIB-Keithley 6485 sample rate. As a result, the peak of the pulse was unable to be captured fully. This could be resolved by exchanging current Keithly 6485 picoammeter with a direct current reading LabVIEW interface or writing a simplified VI for the Keithley 6485 enabling a quicker read rate. This system could also be used to better asses the reactor fast neutron population with use of two fission chambers with differing sensitivities to thermal and fast neutrons. This concept is discussed in detail in Geslot,2009;2011 and the N-MS could be easily modified to perform such tasks given the appropriate fission chamber detectors were added to the holder.

Appendices

APPENDIX A: PNEUMATIC TRANSFER SYSTEM SCHEMATICS

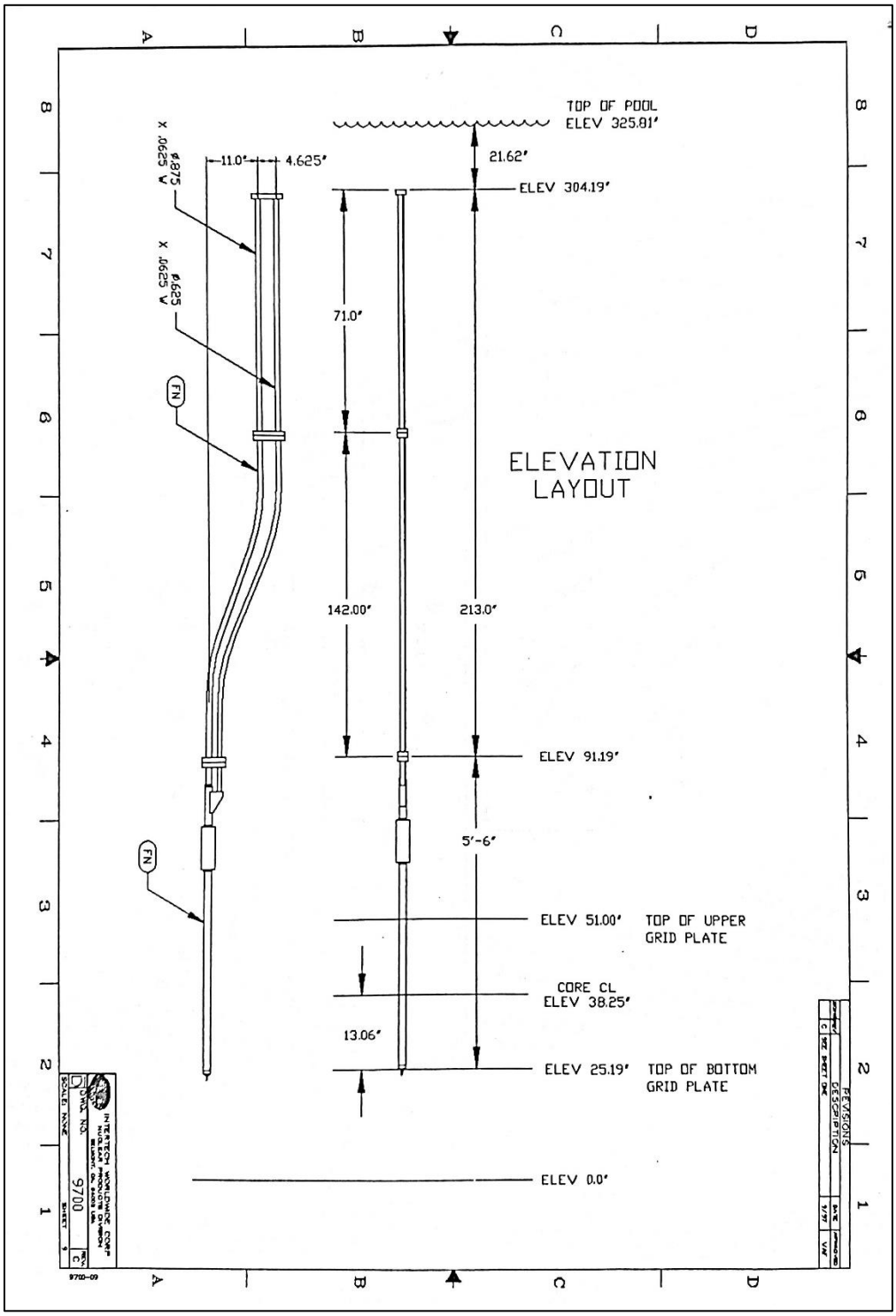

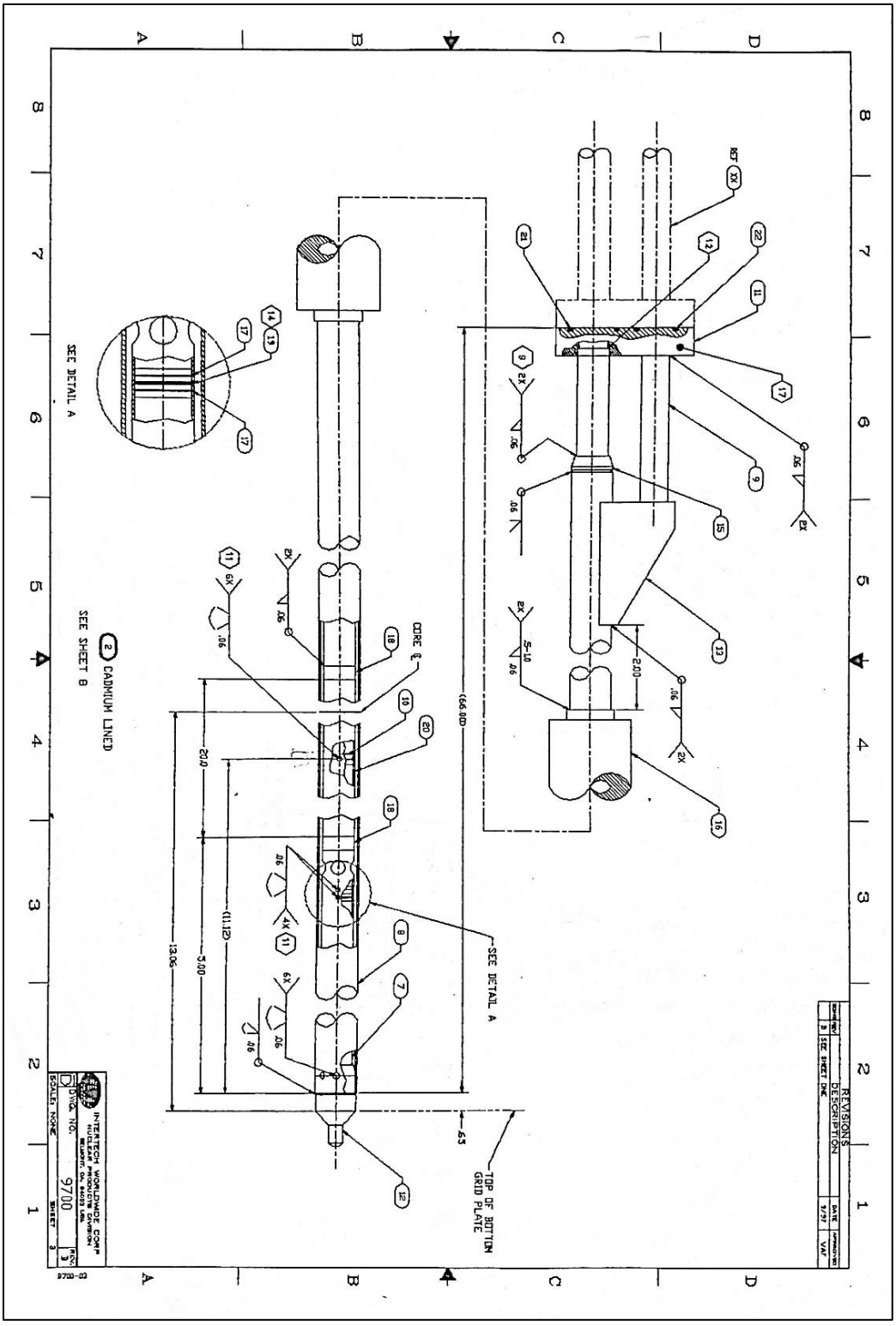
SEE DETAIL A
(2) CADMIUM LINED
SEE SHEET 8
CORE ℄
SEE DETAIL A
TOP OF BOTTOM GRID PLATE
66.00
20.0
13.06
3.00
(11.12)
2.00
.65
REVISIONS
DESCRIPTION
SEE SHEET ONE
INTERTECH WORLDWIDE CORP
NUCLEAR PRODUCTS DIVISION
SCALE: NONE
DWG. NO.
9700
SHEET 2
REV 3

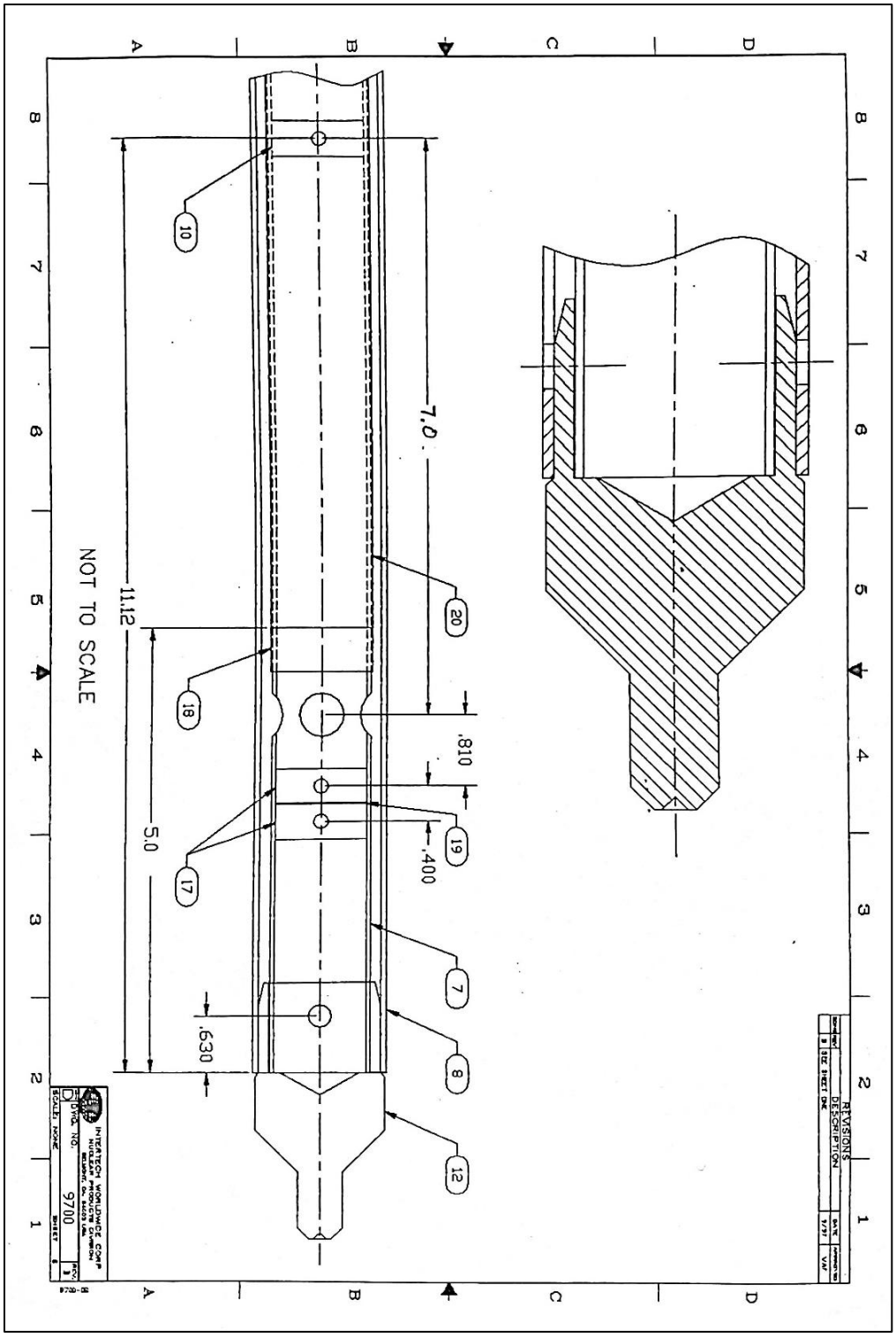
NOT TO SCALE
11.12
7.0
5.0
.810
.400
.630
10
18
17
20
19
7
8
12
REVISIONS
DESCRIPTION
INTERTECH WORLDWIDE CORP
DWG. NO. 9700

APPENDIX B: N-MS ISOLATING HOLDER SCHEMATICS

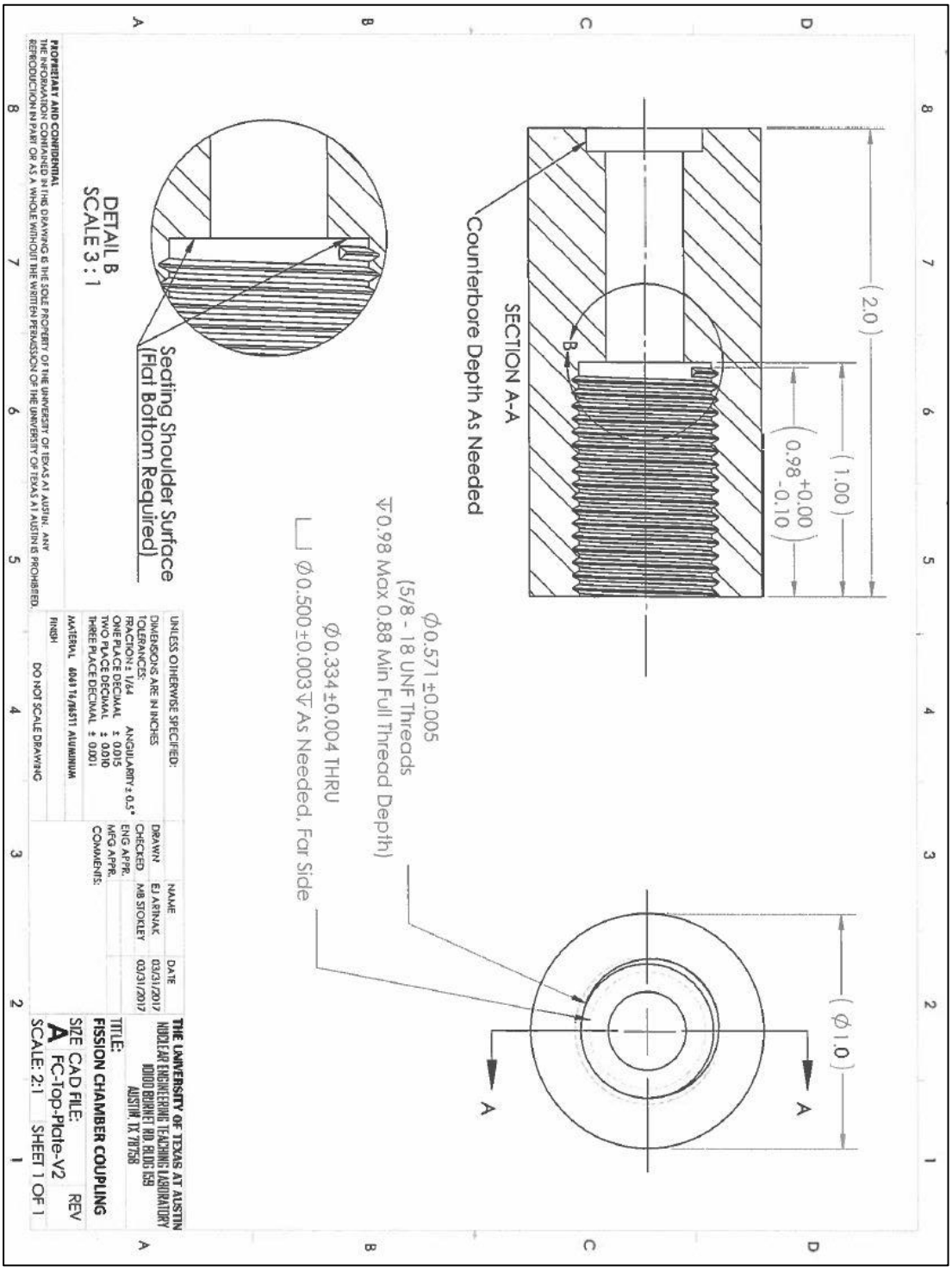

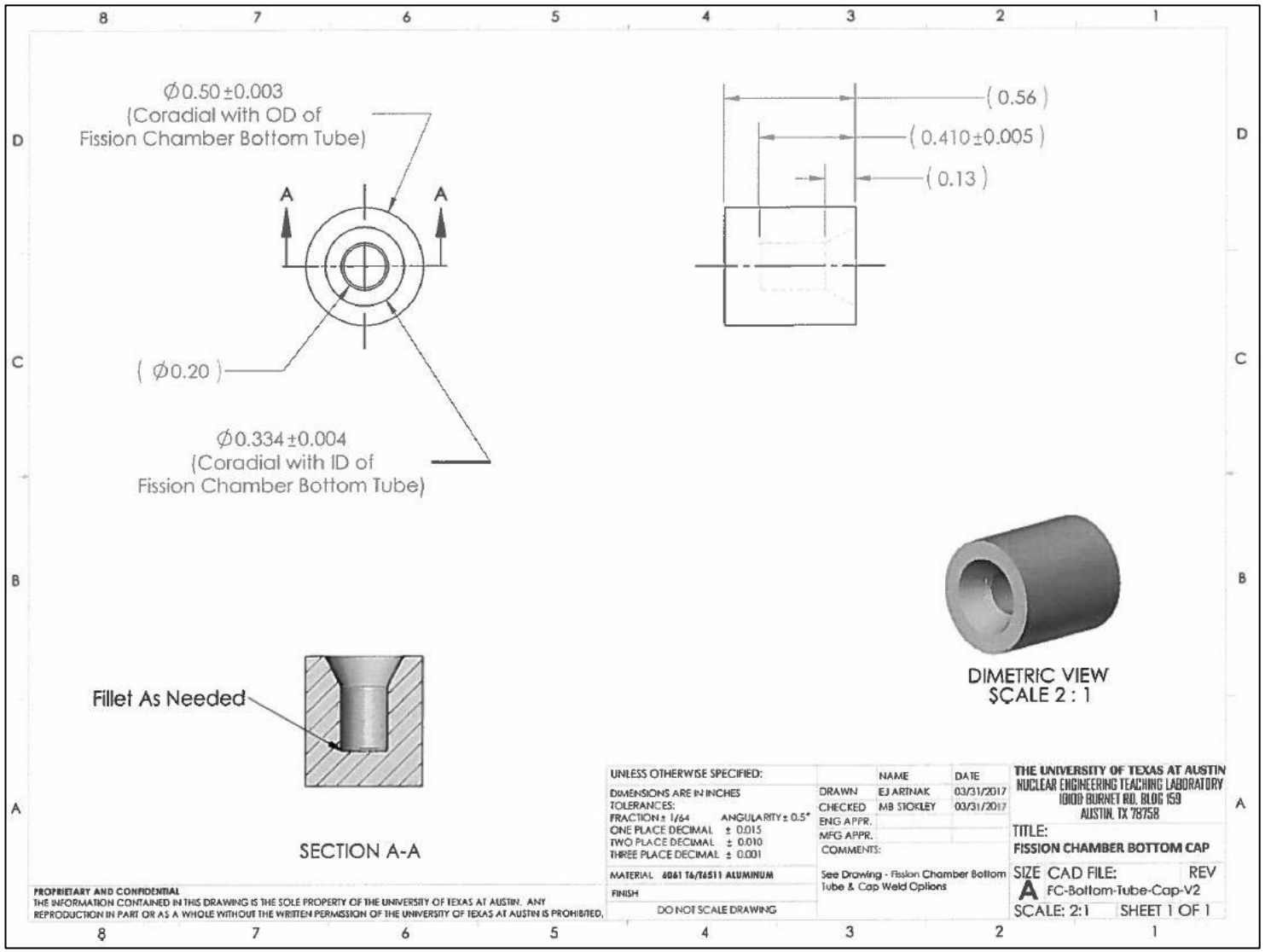
Ø0.50 ±0.003
(Coradial with OD of
Fission Chamber Bottom Tube)
A
A
(Ø0.20)
Ø0.334 ±0.004
(Coradial with ID of
Fission Chamber Bottom Tube)
(0.56)
(0.410±0.005)
(0.13)
Fillet As Needed
SECTION A-A
DIMETRIC VIEW
SCALE 2 : 1
UNLESS OTHERWISE SPECIFIED:
DIMENSIONS ARE IN INCHES
TOLERANCES:
FRACTION ± 1/64 ANGULARITY ± 0.5°
ONE PLACE DECIMAL ± 0.015
TWO PLACE DECIMAL ± 0.010
THREE PLACE DECIMAL ± 0.001
MATERIAL 6061 T6/T6511 ALUMINUM
FINISH
DO NOT SCALE DRAWING
NAME DATE
DRAWN EJ ARTNAK 03/31/2017
CHECKED MB STOKLEY 03/31/2017
ENG APPR.
MFG APPR.
COMMENTS:
See Drawing - Fission Chamber Bottom Tube & Cap Weld Options
THE UNIVERSITY OF TEXAS AT AUSTIN
NUCLEAR ENGINEERING TEACHING LABORATORY
10100 BURNET RD. BLDG 159
AUSTIN, TX 78758
TITLE:
FISSION CHAMBER BOTTOM CAP
SIZE A
CAD FILE: FC-Bottom-Tube-Cap-V2
REV
SCALE: 2:1
SHEET 1 OF 1
PROPRIETARY AND CONFIDENTIAL
THE INFORMATION CONTAINED IN THIS DRAWING IS THE SOLE PROPERTY OF THE UNIVERSITY OF TEXAS AT AUSTIN. ANY REPRODUCTION IN PART OR AS A WHOLE WITHOUT THE WRITTEN PERMISSION OF THE UNIVERSITY OF TEXAS AT AUSTIN IS PROHIBITED.

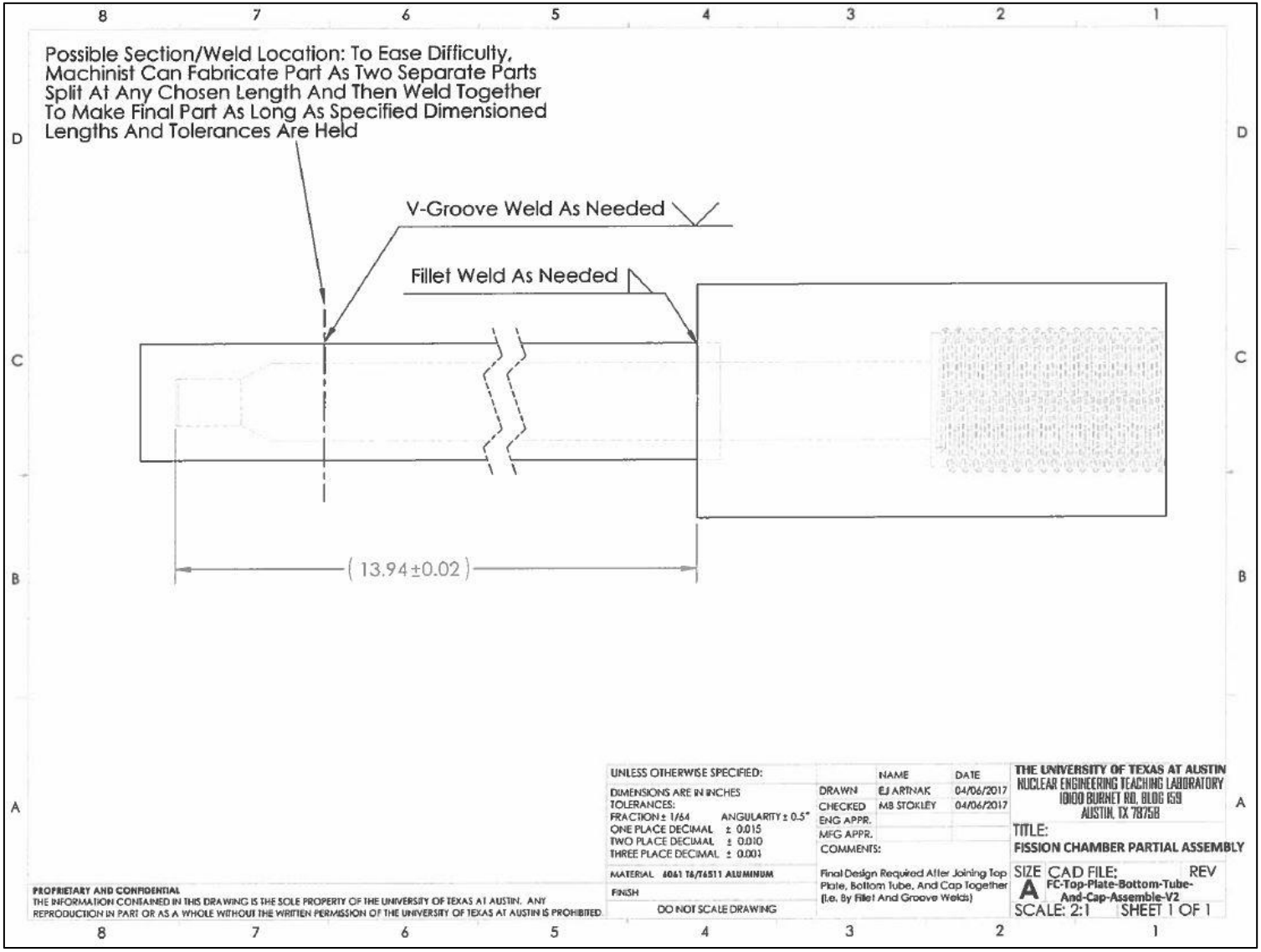
Possible Section/Weld Location: To Ease Difficulty, Machinist Can Fabricate Part As Two Separate Parts Split At Any Chosen Length And Then Weld Together To Make Final Part As Long As Specified Dimensioned Lengths And Tolerances Are Held
V-Groove Weld As Needed
Fillet Weld As Needed
(13.94 ±0.02)
UNLESS OTHERWISE SPECIFIED:
DIMENSIONS ARE IN INCHES
TOLERANCES:
FRACTION ± 1/64 ANGULARITY ± 0.5°
ONE PLACE DECIMAL ± 0.015
TWO PLACE DECIMAL ± 0.010
THREE PLACE DECIMAL ± 0.003
MATERIAL 6061 T6/T6511 ALUMINUM
FINISH
DO NOT SCALE DRAWING
NAME DATE
DRAWN EJ ARTNAK 04/06/2017
CHECKED MB STOKLEY 04/06/2017
ENG APPR.
MFG APPR.
COMMENTS:
Final Design Required After Joining Top Plate, Bottom Tube, And Cap Together (i.e. By Fillet And Groove Welds)
THE UNIVERSITY OF TEXAS AT AUSTIN
NUCLEAR ENGINEERING TEACHING LABORATORY
10100 BURNET RD. BLDG 159
AUSTIN, TX 78758
TITLE:
FISSION CHAMBER PARTIAL ASSEMBLY
SIZE A
CAD FILE: FC-Top-Plate-Bottom-Tube-And-Cap-Assemble-V2
REV
SCALE: 2:1
SHEET 1 OF 1
PROPRIETARY AND CONFIDENTIAL
THE INFORMATION CONTAINED IN THIS DRAWING IS THE SOLE PROPERTY OF THE UNIVERSITY OF TEXAS AT AUSTIN. ANY REPRODUCTION IN PART OR AS A WHOLE WITHOUT THE WRITTEN PERMISSION OF THE UNIVERSITY OF TEXAS AT AUSTIN IS PROHIBITED.

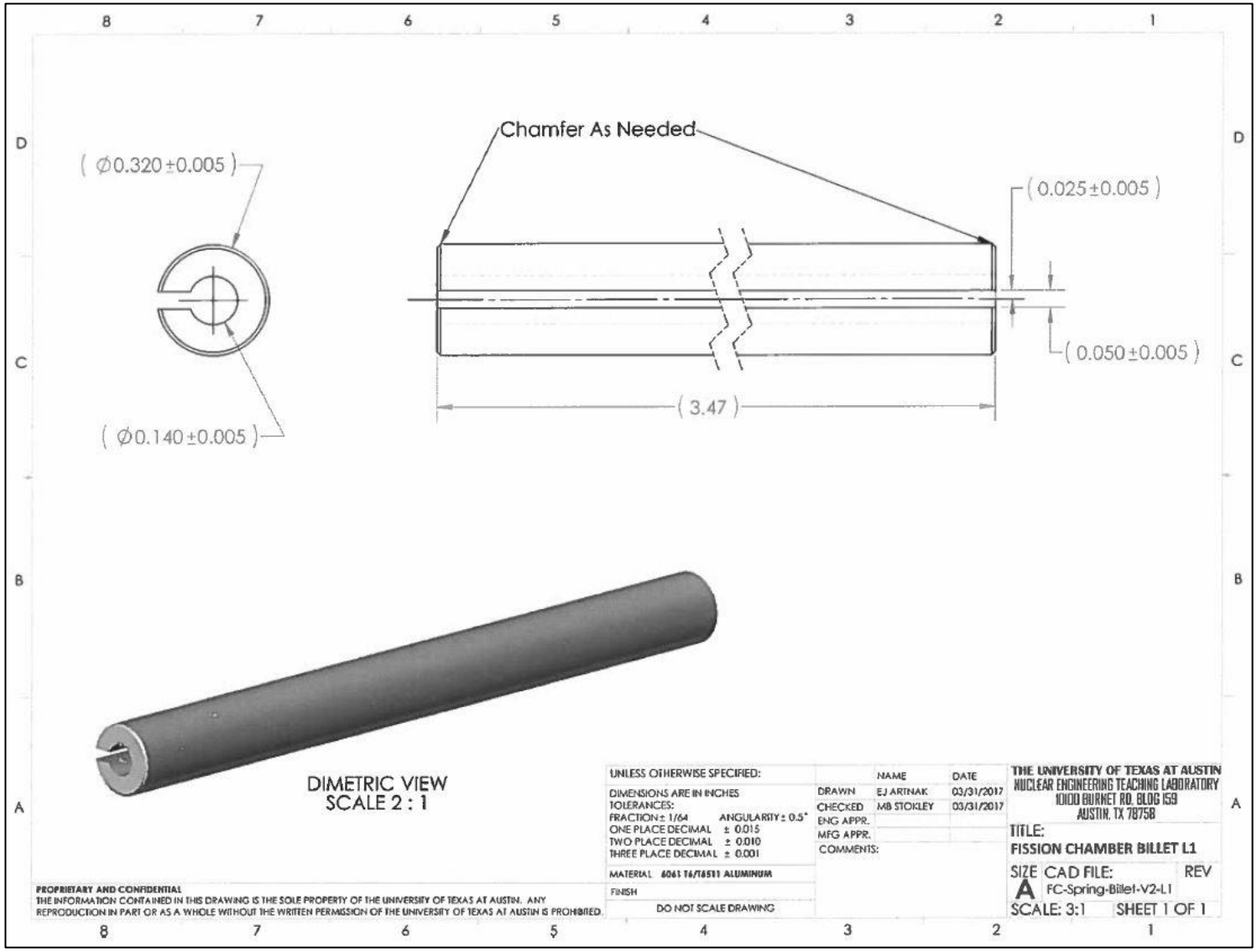
Chamfer As Needed
(Ø0.320 ±0.005)
(Ø0.140 ±0.005)
(0.025 ±0.005)
(0.050 ±0.005)
(3.47)
DIMETRIC VIEW
SCALE 2 : 1
UNLESS OTHERWISE SPECIFIED:
DIMENSIONS ARE IN INCHES
TOLERANCES:
FRACTION ± 1/64 ANGULARITY ± 0.5°
ONE PLACE DECIMAL ± 0.015
TWO PLACE DECIMAL ± 0.010
THREE PLACE DECIMAL ± 0.001
MATERIAL 6061 T6/T6511 ALUMINUM
FINISH
DO NOT SCALE DRAWING
NAME DATE
DRAWN EJ ARTNAK 03/31/2017
CHECKED MB STOKLEY 03/31/2017
ENG APPR.
MFG APPR.
COMMENTS:
THE UNIVERSITY OF TEXAS AT AUSTIN
NUCLEAR ENGINEERING TEACHING LABORATORY
10100 BURNET RD. BLDG 159
AUSTIN, TX 78758
TITLE:
FISSION CHAMBER BILLET L1
SIZE A
CAD FILE: FC-Spring-Billet-V2-L1
REV
SCALE: 3:1
SHEET 1 OF 1
PROPRIETARY AND CONFIDENTIAL
THE INFORMATION CONTAINED IN THIS DRAWING IS THE SOLE PROPERTY OF THE UNIVERSITY OF TEXAS AT AUSTIN. ANY REPRODUCTION IN PART OR AS A WHOLE WITHOUT THE WRITTEN PERMISSION OF THE UNIVERSITY OF TEXAS AT AUSTIN IS PROHIBITED.

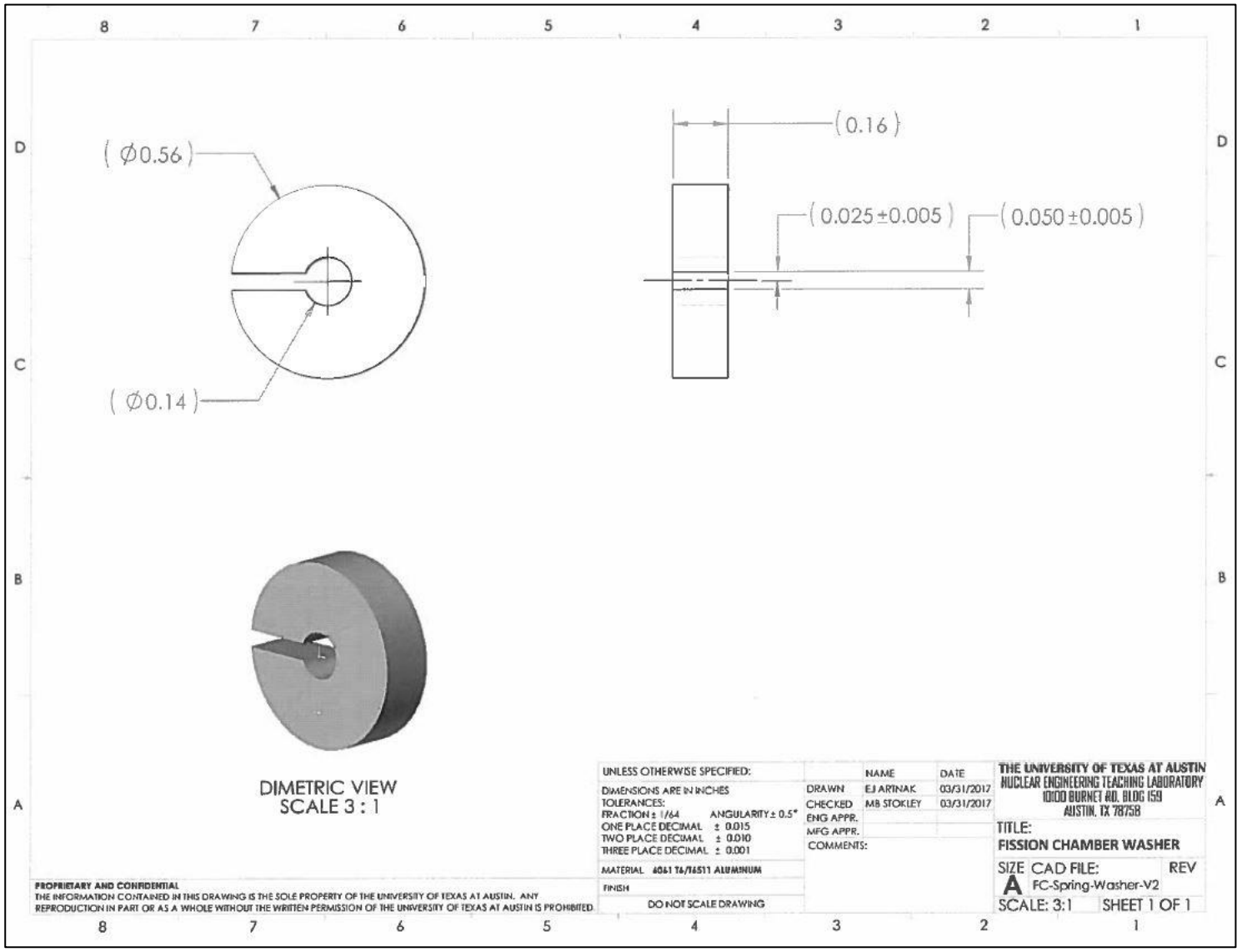
(Ø0.56)
(Ø0.14)
(0.16)
(0.025 ±0.005)
(0.050 ±0.005)
DIMETRIC VIEW
SCALE 3 : 1
UNLESS OTHERWISE SPECIFIED:
DIMENSIONS ARE IN INCHES
TOLERANCES:
FRACTION ± 1/64 ANGULARITY ± 0.5°
ONE PLACE DECIMAL ± 0.015
TWO PLACE DECIMAL ± 0.010
THREE PLACE DECIMAL ± 0.001
MATERIAL 6061 T6/T6511 ALUMINUM
FINISH
DO NOT SCALE DRAWING
NAME DATE
DRAWN EJ ARTNAK 03/31/2017
CHECKED MB STOKLEY 03/31/2017
ENG APPR.
MFG APPR.
COMMENTS:
PROPRIETARY AND CONFIDENTIAL
THE INFORMATION CONTAINED IN THIS DRAWING IS THE SOLE PROPERTY OF THE UNIVERSITY OF TEXAS AT AUSTIN. ANY REPRODUCTION IN PART OR AS A WHOLE WITHOUT THE WRITTEN PERMISSION OF THE UNIVERSITY OF TEXAS AT AUSTIN IS PROHIBITED.
THE UNIVERSITY OF TEXAS AT AUSTIN
NUCLEAR ENGINEERING TEACHING LABORATORY
10100 BURNET RD. BLDG 159
AUSTIN, TX 78758
TITLE:
FISSION CHAMBER WASHER
SIZE A
CAD FILE: FC-Spring-Washer-V2
REV
SCALE: 3:1
SHEET 1 OF 1

APPENDIX C: PHOTONIS CFUF43/30 FISSION CHAMBER SCHEMATICS

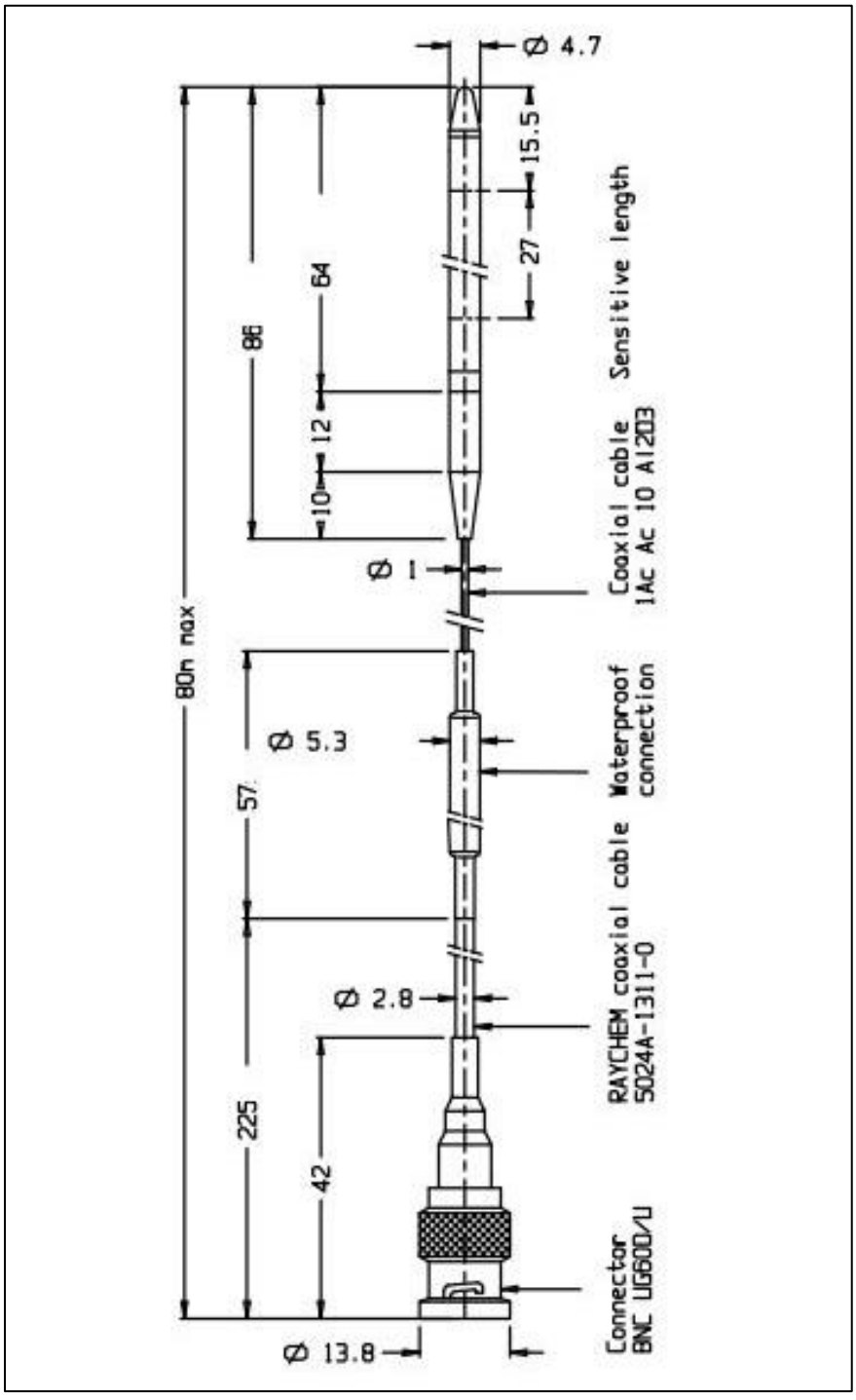

APPENDIX D: EXPERIMENT SAFETY ANALYSIS REPORT

Safety Analysis of Experiment

Photonis CFUF43 Fission Chamber

Report Prepared by: Matthew Stokley
April 10, 2017

Description and Purpose of Experiment

The Neutron Activation Analysis NAA facility is a highly utilized facility within The University of Texas at Austin TRIGA reactor. The NAA lab air pneumatic tube sample delivery system is located within the outer grid plate ring of the NETL TRIGA core. Neutron flux monitors are located at distances from the pneumatic tube sample delivery system that they are not reliably able to perform flux measurements with respect to the NAA sample location and/or short duration irradiation. By installing a fission chamber closer to the NAA sample location, the goal is to be able to better monitor sample irradiance.

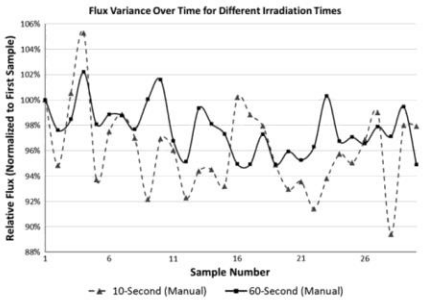

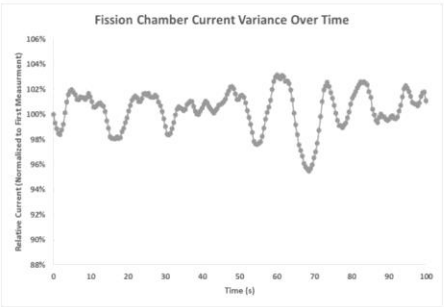

It is the goal of this safety analysis to formulate an approved experiment for the installation of the Photonis CFUF43 Fission Chamber to monitor neutron flux within the reactor.

1

Experimental Requirements

Experiment Facility and Location

The experimental facility under consideration in this document is an in core fission chamber for neutron flux measurement in conjunction with the NAA pneumatic tube delivery system. The experiment may be placed in the small 5/8'' hole within the upper grid plate located closest to the NAA pneumatic tube delivery system. The location within the core is as shown in Figure 1. Component assembly diagrams are provided in the appendices of this document.

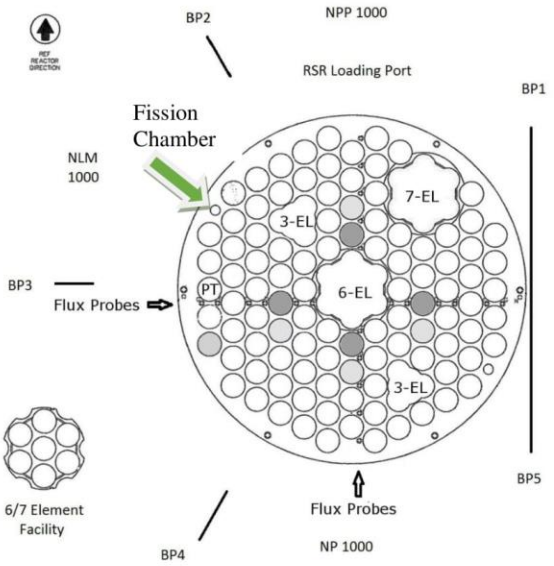

Figure 1. Diagram of NETL reactor core showing experimental locations.

Maximum Reactor Power

The fission chamber installation is intended to be utilized up to the full licensed power for the reactor.

Maximum Operation Time

Nominal run times are assumed to be contained within one operational day. Operational days are nominally eight hours or less. Some operational days extend to 12 hours. However, this safety analysis does not set a limit on the length of the operational day. The safety analysis assumed a full 24-hour day irradiation for one full year.

Physical Experiment Effects

Reactivity

As defined under Technical Specifications 3.4.1.b:

> *The reactivity worth of any single secured experiment shall be less than 2.50 dollars.*

Pervious experiments within the 3-EL facility have shown the fission chamber reactivity to be negligible and well below $2.50. This experimental approval can be verified when installed in its final disposition to ensure reactivity is as expected.

Thermal Hydraulic and Experiment Temperature

The aluminum and stainless steel fission chamber assembly will be constantly cooled by the pool water (~ 25 ˚C). It is expected that the maximum temperature will stay significantly below the melting temperature of any experimental material and that the materials being irradiated are relatively inert with respect to chemistry.

Mechanical Stress

Mechanical stresses are expected to be minimal. The fission chamber assembly will not any have mechanical stresses placed on it while installed other than its own weight.

Material Evaluation

Radioactivity

The worst-case scenario evaluated for this event would be to remove the fission chamber after a full year's operation at full power, 950 kW. This is not intended to be done as the fission chamber will potentially be a permanent installation. The results are presented in the attached appendix. All values are below any specified restriction for experimental radioactivity.

Material Hazards

Trace Element Impurities Which May Represent a Significant Radiological Hazard

No trace element impurities are known that will present this hazard.

High Cross-Section Elements

This experiment is internal to the reactor and 349 micrograms of U-235 is contained within the fission chamber, but experience has shown a minimal reactivity concern.

As part of normal NETL protocols, the reactivity worth of each experiment will be measured during the reactor start-up. The reactor will be brought to 50 W where there are no fuel temperature effects in the core. The control rod positions will be compared to a reference position and the difference in reactivity will be calculated from the control rod calibrations. Experiments will not be run if reactivity is greater than the $2.50 limit for secure experiments.

Flammable, Volatile, or Liquid Materials

The fission chamber does not contain volatile or liquid materials. If such materials are part of the experiment, a new safety analysis report is required and experimenters must show that Technical Specifications are met for the experiment.

Explosive Chemicals

No explosive chemicals in this experiment. If such materials are part of the experiment, a new safety analysis report is required and experimenters must show that Technical Specifications are met for the experiment.

Corrosive Chemicals

No corrosive chemicals are used in this experiment. If such materials are part of the experiment, a new safety analysis report is required and experimenters must show that Technical Specifications are met for the experiment.

Radiation Sensitive Materials Which When Exposed to Radiation Exhibit Degradation of Mechanical Properties, Decomposition, Chemical Changes, or Gas Evolution

Materials will be evaluated and chosen to minimize these effects. If such materials are part of the experiment, a new safety analysis report is required and experimenters must show that Technical Specifications are met for the experiment.

Toxic Compounds

No toxic compounds are used in this experiment. If such materials are part of the experiment, a new safety analysis report is required and experimenters must show that Technical Specifications are met for the experiment.

Cryogenic Liquids

No cryogenic liquids are used in this experiment. If such materials are part of the experiment, a new safety analysis report is required and experimenters must show that Technical Specifications are met for the experiment.

Unknown Materials

All materials used in this experiment are known. If such materials are part of the experiment, a new safety analysis report is required and experimenters must show that Technical Specifications are met for the experiment.

Experiment Classification

This experiment should be a Class A experiment. A Senior Reactor Operator must review and approve each experiment task prior to continuation of operation.

Appendix 1

Fission Chamber Activation & Decay

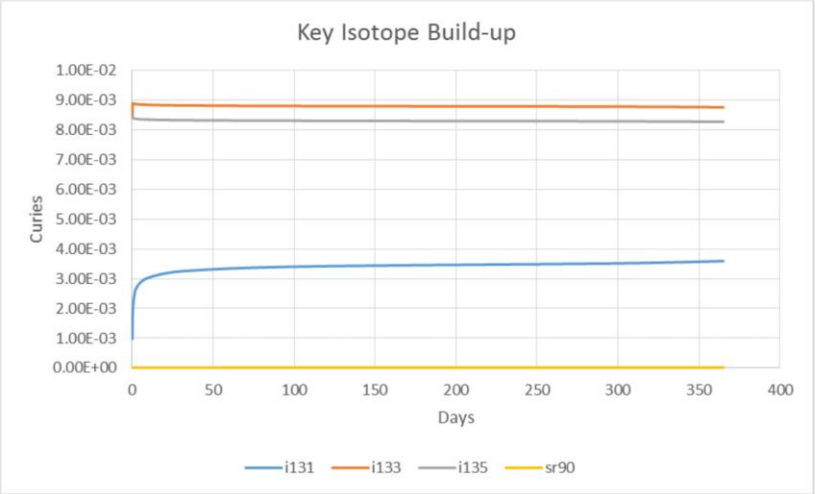

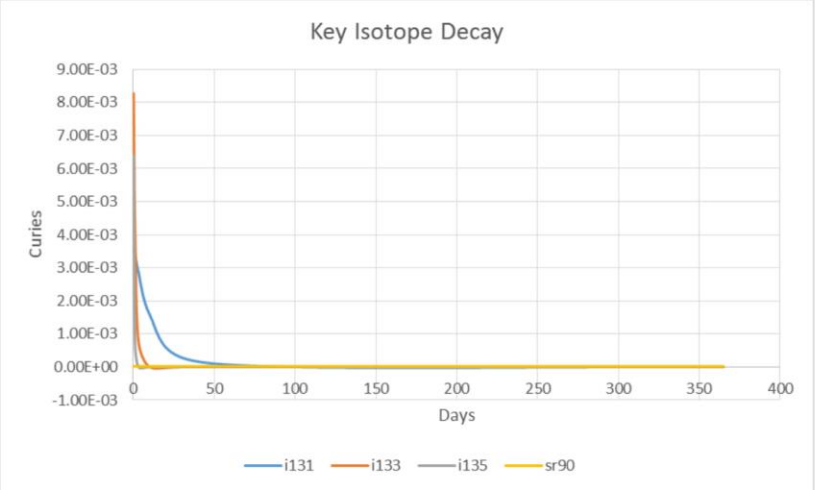

6

Appendix

Fission Chamber Assembly

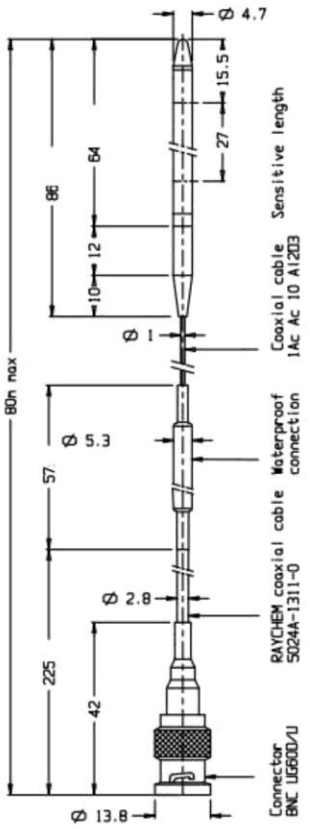

Figure 2. Fission Chamber Instrument

7

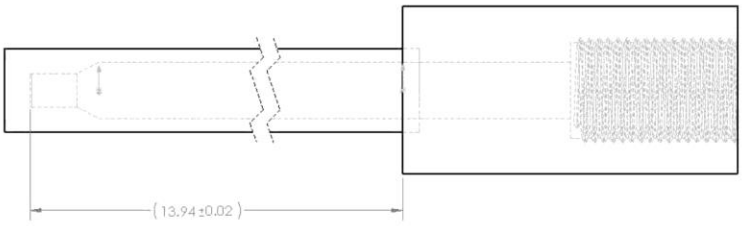

Figure 3. Fission Chamber Instrument Holder Assembly

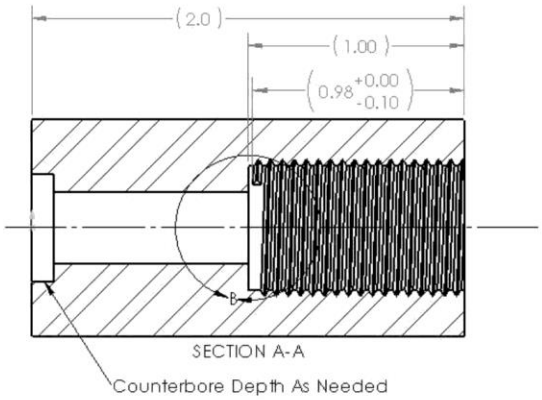

Figure 4. Fission Chamber Instrument Holder Assembly Top Cap

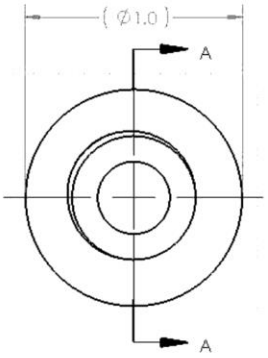

Figure 5. Fission Chamber Instrument Holder Assembly Top Cap

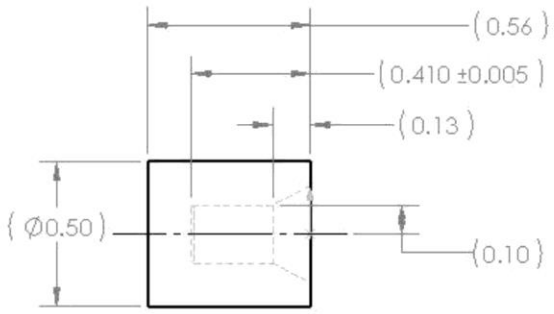

Figure 6. Fission Chamber Instrument Holder Assembly Bottom Cap

Nuclide Input

HELP

IMPORT | ------- Select Sample Data ------- | RESET

Original Element / Nuclide	Mass (g)	Original Element / Nuclide	Mass	Original Element / Nuclide	Mass	Original Element / Nuclide	Mass
Fe	0.008520						
Cr	0.002280						
Ni	0.001200						
U	0.000385						
Al	120						
Si	0.49						
Fe	.85						
Cu	.18						
Mg	.98						
Cr	.005						
Zn	.3						
Ti	.18						

Output Parameters

HELP

1e13 Neutron flux [per $cm^2 s$] - or - Point source neutron emission rate [per s] / Distance from point source [m]

- [x] use IAEA 2003 cross sections, where available
- [x] thermal neutrons (n,Gamma)
- [ ] fast neutrons (n,2n) (n,3n) (n,p) (n,t) (n,Alpha)

1 Duration of irradiation [a]

1 Time delay since end of irradiation [d]

Max. half-life for consideration of progeny [years]

Ci Activation Product Unit

10

System 1 year irradiation with no decay

Neutron flux = 10.00e12 per cm2s
Irradiation = 1 a; Delay = 0 a

8.520 mg Iron:

477.2 µg Fe-54 (n,G) -> 732.9 µCi Fe-55 (2.700 a)

26.51 µg Fe-58 (n,G) -> 96.41 µCi Fe-59 (44.53 d)

2.280 mg Chromium:

95.26 µg Cr-50 (n,G) -> 4.910 mCi Cr-51 (27.70 d)

1.200 mg Nickel:

808.7 µg Ni-58 (n,G) -> 94.36 nCi Ni-59 (75.00e3 a)

45.46 µg Ni-62 (n,G) -> 12.42 µCi Ni-63 (96.00 a)

11.89 µg Ni-64 (n,G) -> 49.30 µCi Ni-65 (2.520 h)

385.0 µg Uranium:

20.55 ng U-234 (n,G) -> 1.384e-15 Ci U-235 (703.8e6 a)
~> 1.378e-15 Ci Th-231 (25.52 h)

2.737 µg U-235 (n,G) -> 5.434 pCi U-236 (23.41e6 a)

382.2 µg U-238 (n,G) -> 700.3 µCi U-239 (23.54 m)
~> 700.3 µCi Np-239 (2.355 d)
~> 19.99 nCi Pu-239 (24.06e3 a)
~> 9.753e-18 Ci U-235 (703.8e6 a)
~> 9.671e-18 Ci Th-231 (25.52 h)

120.0 g Aluminum:

120.0 g Al-27 (n,G) -> 167.1 Ci Al-28 (2.240 m)

490.0 mg Silicon:

16.21 mg Si-30 (n,G) -> 9.415 mCi Si-31 (157.3 m)

850.0 mg Iron:

47.61 mg Fe-54 (n,G) -> 73.11 mCi Fe-55 (2.700 a)

2.645 mg Fe-58 (n,G) -> 9.618 mCi Fe-59 (44.53 d)

180.0 mg Copper:

123.3 mg Cu-63 (n,G) -> 1.438 Ci Cu-64 (12.70 h)

56.70 mg Cu-65 (n,G) -> 308.0 mCi Cu-66 (5.100 m)

5.000 mg Chromium:

208.9 µg Cr-50 (n,G) -> 10.76 mCi Cr-51 (27.70 d)

300.0 mg Zinc:

142.5 mg Zn-64 (n,G) -> 257.5 mCi Zn-65 (243.9 d)

58.58 mg Zn-68 (n,G) -> 10.10 mCi Zn-69 (57.00 m)

System 1 year irradiation with no decay

System 1 year irradiation with 1 day decay

Neutron flux = 10.00e12 per cm2s
Irradiation = 1 a; Delay = 1 d

8.520 mg Iron:

477.2 µg Fe-54 (n,G) -> 732.3 µCi Fe-55 (2.700 a)

26.51 µg Fe-58 (n,G) -> 94.92 µCi Fe-59 (44.53 d)

2.280 mg Chromium:

95.26 µg Cr-50 (n,G) -> 4.789 mCi Cr-51 (27.70 d)

1.200 mg Nickel:

808.7 µg Ni-58 (n,G) -> 94.36 nCi Ni-59 (75.00e3 a)

45.46 µg Ni-62 (n,G) -> 12.42 µCi Ni-63 (96.00 a)

11.89 µg Ni-64 (n,G) -> 66.98 nCi Ni-65 (2.520 h)

385.0 µg Uranium:

20.55 ng U-234 (n,G) -> 1.384e-15 Ci U-235 (703.8e6 a)
~> 1.381e-15 Ci Th-231 (25.52 h)

2.737 µg U-235 (n,G) -> 5.434 pCi U-236 (23.41e6 a)

382.2 µg U-238 (n,G) -> 0 Ci U-239 (23.54 m)
~> 525.3 µCi Np-239 (2.355 d)
~> 20.03 nCi Pu-239 (24.06e3 a)
~> 9.807e-18 Ci U-235 (703.8e6 a)
~> 9.725e-18 Ci Th-231 (25.52 h)

120.0 g Aluminum:

120.0 g Al-27 (n,G) -> 0 Ci Al-28 (2.240 m)

490.0 mg Silicon:

16.21 mg Si-30 (n,G) -> 16.52 µCi Si-31 (157.3 m)

850.0 mg Iron:

47.61 mg Fe-54 (n,G) -> 73.06 mCi Fe-55 (2.700 a)

2.645 mg Fe-58 (n,G) -> 9.469 mCi Fe-59 (44.53 d)

180.0 mg Copper:

123.3 mg Cu-63 (n,G) -> 388.2 mCi Cu-64 (12.70 h)

5.000 mg Chromium:

208.9 µg Cr-50 (n,G) -> 10.50 mCi Cr-51 (27.70 d)

300.0 mg Zinc:

142.5 mg Zn-64 (n,G) -> 256.8 mCi Zn-65 (243.9 d)

58.58 mg Zn-68 (n,G) -> 250.8 pCi Zn-69 (57.00 m)

System 1 year irradiation with 1 year decay

Neutron flux = 10.00e12 per cm2s
Irradiation = 1 a; Delay = 1 a

8.520 mg Iron:

477.2 µg Fe-54 (n,G) -> 566.9 µCi Fe-55 (2.700 a)

26.51 µg Fe-58 (n,G) -> 327.3 nCi Fe-59 (44.53 d)

2.280 mg Chromium:

95.26 µg Cr-50 (n,G) -> 527.7 nCi Cr-51 (27.70 d)

1.200 mg Nickel:

808.7 µg Ni-58 (n,G) -> 94.36 nCi Ni-59 (75.00e3 a)

45.46 µg Ni-62 (n,G) -> 12.33 µCi Ni-63 (96.00 a)

385.0 µg Uranium:

20.55 ng U-234 (n,G) -> 1.384e-15 Ci U-235 (703.8e6 a)
~> 1.384e-15 Ci Th-231 (25.52 h)
~> 43.88e-21 Ci Pa-231 (32.76e3 a)

2.737 µg U-235 (n,G) -> 5.434 pCi U-236 (23.41e6 a)

382.2 µg U-238 (n,G) -> 0 Ci U-239 (23.54 m)
~> 20.17 nCi Pu-239 (24.06e3 a)
~> 29.62e-18 Ci U-235 (703.8e6 a)
~> 29.54e-18 Ci Th-231 (25.52 h)

120.0 g Aluminum:

120.0 g Al-27 (n,G) -> 0 Ci Al-28 (2.240 m)

490.0 mg Silicon:

850.0 mg Iron:

47.61 mg Fe-54 (n,G) -> 56.56 mCi Fe-55 (2.700 a)

2.645 mg Fe-58 (n,G) -> 32.65 µCi Fe-59 (44.53 d)

180.0 mg Copper:

5.000 mg Chromium:

208.9 µg Cr-50 (n,G) -> 1.157 µCi Cr-51 (27.70 d)

300.0 mg Zinc:

142.5 mg Zn-64 (n,G) -> 91.22 mCi Zn-65 (243.9 d)

APPENDIX E: MCNP6.2 UT AUSTIN NETL TRIGA MODEL SCRIPT

```
UT NETL TRIGA Mark II Nuclear Research Reactor MCNP Input Deck
c
c Created by: William H. Wilson (Modified by Matthew B. Stokley)
c Created on: 1 October 2014
c Last updated on: 31 July 2017 By Matthew B. Stokley
c
c ====================
c GENERAL INFORMATION:
c ====================
c
c Abut this MCNP input deck:
c ==========================
c
c This MCNP input deck was created by William H. Wilson. It was created using
c MCNP version 6.1.1beta.
c
c This MCNP input deck was developed from an MCNP input deck that was created by
c Dr. Alexander G. Fay. William H. Wilson received the original input deck as
c an attachment to an email from Dr. Fay on 1 October 2014. For more information
c on the original input deck created by Dr. Fay, refer to Dr. Fay's doctoral
c dissertation, which is titled "Characterization of sources of radioargon in
c a research reactor."
c
c The geometry associated with the original MCNP input deck created by Dr. Fay
c has largely been retained in this input deck, but some geometry changes have
c been incorporated into this input deck. Additionally, several other aspects
c of the original input deck have been modified and some new features have
c been incorporated into this input deck.
c
c The University of Texas at Austin's TRIGA Mark II nuclear research reactor:
c ============================================================================
c
c This MCNP input deck models the TRIGA Mark II nuclear research reactor housed
c at The University of Texas at Austin's (UT's) The Nuclear Engineering Teaching
c Laboratory (NETL). The NETL is situated in the north-eastern corner of UT's
c JJ Pickle Research Campus in Austin, Texas, USA. The reactor itself is a
c TRIGA Mark II nuclear research reactor with an effective full-power
c steady-state operating limit of about 1 MWt.
c
c The core associated with UT's TRIGA Mark II nuclear research reactor has a
c hexagonal structure with seven hexagonal "rings." The center "ring," consists
c of only one reactor core location designated A01. The second ring, the B ring,
c consists of six reactor core locations designated B01 through B06. The third
c ring, the C ring, consists of 12 reactor core locations designated C01 through
c C12. The fourth ring, the D ring, consists of 18 reactor core locations
c designated D01 through D18. The fifth ring, the E ring, consists of 24 reactor
c core locations designated E01 through E24. The sixth ring, the F ring,
c consists of 30 reactor core locations designated F01 through F30. And finally,
c the seventh ring, the G ring, also consists of 30 reactor core locations
c designated G02 through G06, G08 through G12, G14 through G18, G20 through G24,
c G26 through G30, and G32 through G36. Note that the corners of the G-ring
c hexagon are missing, and the designators that would have been associated with
c the missing core locations are skipped. In total there are 121 reactor core
c locations in UT's TRIGA Mark II nuclear research reactor. That said, only 111
c reactor core locations typically contain fuel elements; the other reactor core
c locations are either left empty (i.e. they are filled with water) or they
c contain irradiation facilities.
c
c UT's TRIGA Mark II nuclear research reactor contains a few different types of
c TRIGA fuel elements, but all of them have the same basic design. The fuel
c elements are cylindrical and have an outer diameter of about 3.73 cm and an
```

```
c overall length of about 72.06 cm. That said, the fueled region of the fuel
c elements is only about 38.10 cm long and consists of three UZrH fuel slugs
c stacked on top of each other. The UZrH is 8.5 % uranium, by weight, and the
c uranium is enriched to 19.7 % in U-235. Graphite slugs are situated at the
c top and bottom ends of the UZrH fuel slugs. The fuel elements are clad in
c stainless steel alloy 304. The top and bottom ends of the fuel elements have
c stainless steel alloy 304 fittings on them. For more information pertaining to
c the fuel elements, refer to section 4.4.5 of the Safety Analysis Report for
c The University of Texas at Austin's TRIGA Mark II nuclear research reactor
c (the version dated May 1991).
c
c The center reactor core location, reactor core location A01, typically
c contains the central thimble irradiation facility, which is basically a long
c aluminum tube that extends from about 19.0 cm below the bottom grid plate up
c to the reactor pool surface. The volume inside the central thimble irradiation
c facility is typically completely filled with water, but the upper portion of
c the central thimble irradiation facility may be blown dry so that a collimated
c beam of neutrons or gamma-rays can be made available to irradiate samples near
c the reactor pool surface.
c
c Reactor core location C01 contains the transient control rod, while reactor
c core locations C07, D06, and D14 contain the three fuel-followed control rods:
c the regulating rod and shim rods 1 and 2, respectively. The fuel-followed
c control rods are driven by stepping motors while the transient control rod,
c which is followed by an air-filled aluminum canister, is driven pneumatically.
c The neutron absorbing material in the control rods is boron carbide. For more
c information pertaining to the control rods, refer to section 4.4.8 of the
c Safety Analysis Report for The University of Texas at Austin's TRIGA Mark II
c nuclear research reactor (the version dated May 1991).
c
c Reactor core locations E11, F13, and F14 typically contain only a rack used to
c hold the 3-Element (3L) irradiation facility in position and are effectively
c filled with water, not the 3L irradiation facility or fuel elements. However,
c these reactor core locations may be occupied by either the 3L irradiation
c facility or three fuel elements depending on the configuration of the reactor
c core. Two different 3L irradiation facilities are available at UT's TRIGA
c Mark II nuclear research reactor: (1) the thermal 3L irradiation facility
c contains a lead sleeve and thus supports irradiating samples with both thermal
c and epithermal neutrons and (2) the epithermal 3L irradiation facility
c contains a cadmium sleeve and thus supports irradiating samples with
c only epithermal neutrons.
c
c Reactor core location G32 contains the AmBe startup source for a brief period
c each time the reactor startup procedure is performed, but the source is
c removed from the reactor core during reactor operations at power and reactor
c core location G32 is thus typically filled only with water.
c
c Reactor core location G34 is typically left empty (i.e. it is filled with
c water). However, it sometimes contains the pneumatic transfer system
c irradiation facility depending on the configuration of the reactor core.
c The pneumatic transfer system irradiation facility consists of a sender/
c receiver station, a blower, several meters of aluminum tubing, and an
c in-core terminus that allow for the rapid transfer of samples from the
c sender/receiver station to the in-core terminus and back again. The pneumatic
c transfer system irradiation facility is thus typically used to support
c irradiations producing radioisotopes with very short half-lives. For more
c information pertaining to the pneumatic transfer system irradiation facility,
c refer to section 8.1.3 of the Safety Analysis Report for The University of
c Texas at Austin's TRIGA Mark II nuclear research reactor (the version dated
c May 1991).
c
c A reactor reflector assembly surrounds the outer edges of the reactor core
c radially. The reactor reflector assembly is essentially a cylindrical graphite
c shell surrounded by an aluminum shroud. There are a number of penetrations and
c air volumes in the reactor reflector assembly that allow neutrons to stream
c from the reactor core out through the five beam ports. The beam ports are
```

```
c essentially aluminum and steel tubes that extend from the reactor reflector
c assembly out through the reactor pool water to the outer edges of the
c biological shield. For more information pertaining to the reactor reflector
c assembly, refer to section 4.4.2 of the Safety Analysis Report for The
c University of Texas at Austin's TRIGA Mark II nuclear research reactor
c (the version dated May 1991).
c
c A Rotary Specimen Rack (RSR) irradiation facility sits on top of the reactor
c reflector assembly. The RSR irradiation facility consists of 40 sample tubes
c in an aluminum housing. The sample tubes are about 3.18 cm in diameter  and
c about 27.4 cm deep. For more information pertaining to the RSR irradiation
c facility, refer to section 8.1.2 of the Safety Analysis Report for The
c University of Texas at Austin's TRIGA Mark II nuclear research reactor
c (the version dated May 1991).
c
c The reactor pool is an oblong cylinder that is filled with deionized water.
c The reactor core is positioned such that it is offset within the reactor pool
c and sits not in the center of the reactor pool, but off to the southern side
c of the reactor pool. A thin sheet of aluminum lines the inner surface of the
c biological shield and provides a barrier between the inner surface of the
c biological shield and the deionized reactor pool water.
c
c The biological shield itself has two levels that vary both geometrically and
c in composition. The cross-section associated with the lower level of the
c biological shield has a dodecagonal shape, while the cross-section associated
c with the upper level of the biological shield has an octagonal shape.
c The lower level of the biological shield consists of steel rebar reinforced
c high density concrete with a magnetite aggregate. The upper level of the
c biological shield on the other hand consists of a steel rebar reinforced
c standard density concrete, also with a magnetite aggregate. For more
c information pertaining to the biological shield, refer to section 7.2.1 of
c the Safety Analysis Report for The University of Texas at Austin's TRIGA
c Mark II nuclear research reactor (the version dated May 1991).
c
c The sections that follow provide additional information pertaining to the
c coordinate system employed in this MCNP input deck, and the way the fuel
c elements, the control rods, and the irradiation facilities available at
c The University of Texas at Austin's TRIGA Mark II nuclear research reactor
c are modeled in this input deck. Subsequent sections discuss features of UT's
c TRIGA Mark II nuclear research reactor that are not modeled in this input
c deck, variance reduction techniques employed in this input deck, and the
c warnings and comments generated during execution of this input deck.
c
c The coordinate system employed in this MCNP input deck:
c ======================================================
c
c The geometric origin of the rectangular coordinate system employed in this
c MCNP input deck (x0 = 0.0 cm, y0 = 0.0 cm, and z0 = 0.0 cm) is placed near the
c vertical center of the central axis of the reactor core. The positive-x axis
c of the coordinate system is defined such that it runs parallel to, and points
c in the opposite direction of, beam port 3. The positive-y axis of the
c coordinate system is defined such that it runs parallel to beam ports 1 and 5
c and points in the direction of beam port 1. The positive-z axis of the
c coordinate system is defined such that it points upward towards the surface
c of the reactor pool.
c
c Additional information pertaining to the modeling of the fuel elements:
c ======================================================================
c
c To model the fuel elements, an initial fuel element is first created as an
c MCNP universe (U=1) in reactor core location B01. This MCNP universe is
c composed of a fuel element surrounded by an infinite volume of water.
c MCNP surface coordinate transformations 0082 through 0198 are then used to
c define the displacements required to create additional fuel elements in
c other reactor core locations, where the required displacements are specified
c relative to the location of the fuel element in reactor core location B01.
```

```
c These MCNP surface coordinate transformations instruct MCNP to fill each of
c the fuel element cells (MCNP cells 0082 through 0198) with the portion of the
c fuel element universe (U=1) that actually contains the fuel element (as
c opposed to the infinite water volume). If we simply filled the fuel element
c cells with the fuel element universe and did not include the MCNP surface
c coordinate transformations MCNP would fill the fuel element cells with water.
c
c Additional information pertaining to the modeling of the
c fuel-followed control rods and the transient control rod:
c ========================================================
c
c The fuel-followed control rods and the transient control rod are created
c as MCNP universes. The fuel-followed control rods are the regulating rod,
c shim rod 1, and shim rod 2. The transient rod is not a fuel-followed control
c rod; the transient rod is followed by an aluminum canister filled with air.
c The fuel-followed control rod universe (MCNP universe U=2) is created in the
c reactor core location occupied by the regulating rod (C07). The o1 and o2
c keywords associated MCNP surface coordinate transformation cards TR0104 and
c and TR0112 are used to displace MCNP universe U=2 and create shim rod 1 and
c shim rod 2 in reactor core locations D06 and D14, respectively. The transient
c rod universe (MCNP universe U=3) is created in the reactor core location
c occupied by the transient rod (C01).
c
c Using MCNP universes to create the fuel-followed and transient control rods
c makes it easy to adjust the vertical positions of the control rods. To adjust
c the vertical position of a given control rod the user needs only to modify the
c value assigned to the o3 keyword associated with the MCNP surface
c transformation card associated with the control rod of interest. The MCNP cell
c numbers and surface transformation numbers associated with each of the four
c control rods are summarized below along with the MCNP surface transformation
c card o3 keyword values corresponding to the full-in and full-out control
c rod positions:
c
c Control Rod   MCNP Cell #   MCNP Surf. Trans. #   Full-In o3   Full-Out o3
c -----------   -----------   -------------------   ----------   -----------
c Regulating       0093             0093             0.0 cm       38.1 cm
c   Shim 1         0104             0104             0.0 cm       38.1 cm
c   Shim 2         0112             0112             0.0 cm       38.1 cm
c Transient        0087             0087             0.0 cm       38.1 cm
c
c It should be noted that when the fuel-followed control rods are fully
c withdrawn from the reactor core their respective fuel-followers are vertically
c aligned with the fueled region of the reactor core. However, when the control
c rods are fully inserted their poison volumes do not vertically align with the
c fueled region of the reactor core - there is a slight offset. This aspect of
c this MCNP model is physically realistic and consistent with the positioning of
c the control rods in UT's TRIGA MARK II nuclear research reactor.
c
c Additional information pertaining to the modeling
c of the central thimble irradiation facility:
c ============================================
c
c Reactor core location A01 typically contains the central thimble irradiation
c facility, and the volume inside the central thimble irradiation facility is
c typically completely filled with water. However, when the central thimble
c irradiation facility is in use, the volume inside the portion of the central
c thimble irradiation facility above the top of the top grid plate may be filled
c with air, allowing a highly collimated beam of radiation to stream upward from
c the reactor core to a sample placed at the upper end of the central thimble
c irradiation facility, somewhere just above the reactor pool surface. The
c central thimble irradiation facility may also be removed from the reactor core
c entirely. The instructions that follow provide some basic guidance that may be
c used to fill reactor core location A01 with the central thimble irradiation
c facility or water. It should be noted that thought should be given to
c additional modifications beyond those listed below that may be required to
c support more specialized changes in the reactor core configuration.
```

```
c
c How to fill reactor core location A01 with
c the central thimble irradiation facility:
c ----------------------------------------
c
c Note that additional instructions specific to filling the volume inside
c the central thimble irradiation facility with either water or air are
c provided with the central thimble irradiation facility cell cards.
c
c (1) Verify that MCNP cells 0221, 0222, 0223, 0224, and 0225 are active.
c (2) Verify that MCNP surfaces 0071 through 0078 are active.
c (3) Verify that MCNP compliments 0221, 0222, 0223, 0224, and 0225 (#0221,
c     #0222, #0223, #0224, and #0225, respectively) are included in the list
c     of compliments associated with MCNP cell 0411.
c (4) Verify that any MCNP cells used to model samples inside the air/water-
c     filled volume inside the central thimble irradiation facility (MCNP cells
c     0223 and/or 0224) are active. Also verify that any MCNP surfaces used
c     exclusively to define these MCNP cells are active. Additionally, verify
c     that any MCNP compliments associated with MCNP cells used to model
c     samples inside the air/water-filled volume inside the central thimble
c     irradiation facility are included in the list of compliments associated
c     with MCNP cells 0223 and/or 0224.
c (5) Verify that any tallies evaluated in MCNP cells used to model samples
c     inside the air/water-filled volume inside the central thimble irradiation
c     facility are active.
c (6) Verify that the WWINP file called at the execution line includes an
c     appropriate number of lower weight-window bounds. This verification is
c     especially important if the central thimble irradiation facility
c     is just being introduced to the reactor core.
c
c How to fill reactor core location A01 with water:
c -------------------------------------------------
c
c (1) Verify that MCNP cells 0221, 0222, 0223, 0224, and 0225 are commented out.
c (2) Verify that MCNP surfaces 0071 through 0078 are commented out.
c (3) Verify that MCNP compliments 0221, 0222, 0223, 0224, and 0225 (#0221,
c     #0222, #0223, #0224, and #0225, respectively) are not included in the
c     list of compliments associated with MCNP cell 0411.
c (4) Verify that any MCNP cells that may have been used to model samples
c     inside the air/water-filled volume inside the central thimble irradiation
c     facility (MCNP cells 0223 and/or 0224) are commented out. Also verify that
c     any MCNP surfaces used exclusively to define these MCNP cells are
c     commented out. Additionally, verify that any MCNP compliments associated
c     with MCNP cells that may have been used to model samples inside the air/
c     water-filled volume inside the central thimble irradiation facility are
c     not included in the list of compliments associated with MCNP cells 0223
c     and/or 0224.
c (5) Verify that any tallies that may have been evaluated in MCNP cells
c     used to model samples inside the air/water-filled volume inside the
c     central thimble irradiation facility are commented out.
c (6) Verify that the WWINP file called at the execution line includes an
c     appropriate number of lower weight-window bounds. This verification is
c     especially important if the central thimble irradiation facility
c     is just being removed from the reactor core.
c
c Additional information pertaining to the modeling
c of the 3-Element (3L) irradiation facility:
c ===============================================
c
c The reactor core locations E11, F13, and F14 typically contain only a rack
c used to hold the 3L irradiation facility in position and are effectively
c filled with water, not the 3L irradiation facility or fuel elements. However,
c these reactor core locations may be occupied by either the 3L irradiation
c facility or three fuel elements depending on the configuration of the
c reactor core. The instructions that follow provide some basic guidance that
c may be used to fill the 3L irradiation facility reactor core locations with
```

```
c water, the 3L irradiation facility, or three fuel elements. It should be
c noted that thought should be given to additional modifications beyond those
c listed below that may be required to support more specialized changes in
c the reactor core configuration.
c
c How to fill reactor core locations E11, F13, and F14 with water:
c ---------------------------------------------------------------
c
c  (1) Verify that MCNP cells 0127, 0153, and 0154 are commented out.
c  (2) Verify that MCNP surface coordinate transformation cards 0127,
c      0153, and 0154 (TR0127, TR30153, and TR0154, respectively) are
c      commented out.
c  (3) Verify that MCNP compliments 0127, 0153, and 0154 (#0127, #0153,
c      and #0154, respectively) are not included in the list of
c      compliments associated with MCNP cell 0411.
c  (4) Verify that MCNP cells 0231 through 0237 are commented out.
c  (5) Verify that MCNP compliment 0237 (#0237) is not included in the
c      list of compliments associated with MCNP cell 0411.
c  (6) Verify that MCNP surfaces 0081 through 0094 are commented out.
c  (7) Verify that MCNP surfaces 0086, 0258, 0284, and 0285 are not
c      included in the list of surfaces used to define MCNP cell 0371.
c  (8) Verify that any MCNP cells that may have been used to model samples
c      inside the inner CO2-purged volume of the 3L irradiation facility
c      (MCNP cell 0235) are commented out. Also verify that any MCNP surfaces
c      used exclusively to define these MCNP cells are commented out.
c      Additionally, verify that any MCNP compliments associated with MCNP
c      cells that may have been used to model samples inside the inner
c      CO2-purged volume of the 3L irradiation facility are not included
c      in the list of compliments associated with MCNP cell 0235.
c  (9) Verify that the initial source point locations specified on the KSRC
c      card for reactor core locations E11, F13, and F14 are commented out.
c (10) Verify that any tallies that may have been evaluated in MCNP cells
c      used to model samples inside the inner CO2-purged volume of the
c      3L irradiation facility are commented out.
c (11) Verify that the WWINP file called at the execution line includes an
c      appropriate number of lower weight-window bounds. This verification is
c      especially important if either the three fuel elements or the
c      3L irradiation facility are just being removed from the reactor
c      core locations associated with the 3L irradiation facility.
c
c How to fill reactor core locations E11, F13,
c and F14 with the 3L irradiation facility:
c -------------------------------------------
c
c Note that additional instructions specific to selecting either the
c cadmium (epithermal) 3L irradiation facility sleeve or the lead
c (thermal) 3L irradiation facility sleeve are provided with the
c 3L irradiation facility cell cards.
c
c  (1) Verify that MCNP cells 0127, 0153, and 0154 are commented out.
c  (2) Verify that MCNP surface coordinate transformation cards 0127,
c      0153, and 0154 (TR0127, TR30153, and TR0154, respectively) are
c      commented out.
c  (3) Verify that MCNP compliments 0127, 0153, and 0154 (#0127, #0153,
c      and #0154, respectively) are not included in the list of
c      compliments associated with MCNP cell 0411.
c  (4) Verify that MCNP cells 0231 through 0237 are active.
c  (5) Verify that MCNP compliment 0237 (#0237) is included in the
c      list of compliments associated with MCNP cell 0411.
c  (6) Verify that MCNP surfaces 0081 through 0094 are active.
c  (7) Verify that MCNP surface 0086 is included in the list of surfaces used
c      to define MCNP cell 0371. Verify that MCNP surfaces 0258, 0284, and 0285
c      are not included in the list of surfaces used to define MCNP cell 0371.
c  (8) Verify that any MCNP cells used to model samples inside the inner
c      CO2-purged volume of the 3L irradiation facility (MCNP cell 0235)
c      are active. Also verify that any MCNP surfaces used exclusively to
```

```
c      define these MCNP cells are active. Additionally, verify that the MCNP
c      compliments associated with MCNP cells used to model samples inside the
c      inner CO2-purged volume of the 3L irradiation facility are included in
c      the list of compliments associated with MCNP cell 0235.
c  (9) Verify that the initial source point locations specified on the KSRC
c      card for reactor core locations E11, F13, and F14 are commented out.
c (10) Verify that any tallies evaluated in MCNP cells used to model samples
c      inside the inner CO2-purged volume of the 3L irradiation facility
c      are active.
c (11) Verify that the WWINP file called at the execution line includes an
c      appropriate number of lower weight-window bounds. This verification is
c      especially important if the 3L irradiation facility is just being
c      introduced to the reactor core locations associated with the
c      3L irradiation facility.
c
c How to fill reactor core locations E11, F13, and F14 with three fuel elements:
c ------------------------------------------------------------------------------
c
c  (1) Verify that MCNP cells 0127, 0153, and 0154 are active.
c  (2) Verify that MCNP surface coordinate transformation cards 0127,
c      0153, and 0154 (TR0127, TR30153, and TR0154, respectively) are active.
c  (3) Verify that MCNP compliments 0127, 0153, and 0154 (#0127, #0153,
c      and #0154, respectively) are included in the list of compliments
c      associated with MCNP cell 0411.
c  (4) Verify that MCNP cells 0231 through 0237 are commented out.
c  (5) Verify that MCNP compliment 0237 (#0237) is not included in the
c      list of compliments associated with MCNP cell 0411.
c  (6) Verify that MCNP surfaces 0081 through 0094 are commented out.
c  (7) Verify that MCNP surface 0086 is not included in the list of
c      surfaces used to define MCNP cell 0371. Verify that MCNP surfaces
c      0258, 0284, and 0285 are included in the list of surfaces used
c      to define MCNP cell 0371.
c  (8) Verify that any MCNP cells that may have been used to model samples
c      inside the inner CO2-purged volume of the 3L irradiation facility
c      (MCNP cell 0235) are commented out. Also verify that any MCNP surfaces
c      used exclusively to define these MCNP cells are commented out.
c      Additionally, verify that any MCNP compliments associated with MCNP
c      cells that may have been used to model samples inside the inner
c      CO2-purged volume of the 3L irradiation facility are not
c      included in the list of compliments associated with MCNP cell 0235.
c  (9) Verify that the initial source point locations specified on
c      the KSRC card for reactor core locations E11, F13, and active.
c (10) Verify that any tallies that may have been evaluated in MCNP cells
c      used to model samples inside the inner CO2-purged volume of
c      the 3L irradiation facility are commented out.
c (11) Verify that the WWINP file called at the execution line includes an
c      appropriate number of lower weight-window bounds. This verification is
c      especially important if the three fuel elements are just being
c      introduced into the reactor core locations associated with
c      the 3L irradiation facility.
c
c Additional information pertaining to the modeling
c of the pneumatic transfer system irradiation facility:
c ======================================================
c
c Reactor core location G34 is typically left empty (i.e. it is filled
c with water). However, it sometimes contains the pneumatic transfer system
c irradiation facility, depending on the configuration of the reactor core.
c The instructions that follow provide some basic guidance that may be used to
c fill reactor core location G34 with water or the pneumatic transfer system
c irradiation facility irradiation facility. It should be noted that thought
c should be given to additional modifications beyond those listed below that
c may be required to support more specialized changes in the reactor
c core configuration.
c
c How to fill reactor core location G34 with water:
```

```
c ------------------------------------------------
c
c (1) Verify that MCNP cells 0271, 0272, 0273, 0274, and 0275 are commented out.
c (2) Verify that MCNP surfaces 0121 through 0131 are commented out.
c (3) Verify that MCNP compliments 0271, 0272, 0273, 0274, and 0275 (#0271,
c     #0272, #0273, #0274, and #0275, respectively) are not included in
c     the list of compliments associated with MCNP cell 0411.
c (4) Verify that any MCNP cells used to model samples inside the air-filled
c     inner volume of the pneumatic transfer system irradiation facility
c     (MCNP cell 0271) are commented out. Also verify that any MCNP surfaces
c     used exclusively to define these MCNP cells are commented out.
c     Additionally, verify that any MCNP compliments associated with MCNP
c     cells used to model samples inside the air-filled inner volume of
c     the pneumatic transfer system irradiation facility are not included
c     in the list of compliments associated with MCNP cell 0271.
c (5) Verify that any tallies evaluated in MCNP cells used to model samples
c     inside the inner air-filled volume of the pneumatic transfer system
c     irradiation facility are commented out.
c (6) Verify that the WWINP file called at the execution line includes an
c     appropriate number of lower weight-window bounds. This verification is
c     especially important if the pneumatic transfer system irradiation
c     facility is just being removed from the reactor core.
c
c How to fill reactor core location G34 with the
c pneumatic transfer system irradiation facility:
c ------------------------------------------------
c
c Note that additional instructions specific to selecting either the cadmium
c (epithermal) pneumatic transfer system irradiation facility sleeve or the
c lead (thermal) pneumatic transfer system irradiation facility sleeve are
c provided with the pneumatic transfer system irradiation facility cell cards.
c
c (1) Verify that MCNP cells 0271, 0272, 0273, 0274, and 0275 are active.
c (2) Verify that MCNP surfaces 0121 through 0131 are active.
c (3) Verify that MCNP compliments 0271, 0272, 0273, 0274, and 0275 (#0271,
c     #0272, #0273, #0274, and #0275, respectively) are included in the list
c     of compliments associated with MCNP cell 0411.
c (4) Verify that any MCNP cells used to model samples inside the air-filled
c     inner volume of the pneumatic transfer system irradiation facility
c     (MCNP cell 0271) are active. Also verify that any MCNP surfaces used
c     exclusively to define these MCNP cells are active. Additionally, verify
c     that any MCNP compliments associated with MCNP cells used to model
c     samples inside the air-filled inner volume of the pneumatic transfer
c     system irradiation facility are included in the list of compliments
c     associated with MCNP cell 0271.
c (5) Verify that any tallies evaluated in MCNP cells used to model samples
c     inside the inner air-filled volume of the pneumatic transfer system
c     irradiation facility are active.
c (6) Verify that the WWINP file called at the execution line includes an
c     appropriate number of lower weight-window bounds. This verification is
c     especially important if the pneumatic transfer system irradiation
c     facility is just being introduced to the reactor core.
c
c Features of the UT TRIGA Mark II nuclear research
c reactor that are not modeled in this MCNP input deck:
c ================================================
c
c While a considerable amount of effort has been expended to incorporate the
c majority of the major features of the UT TRIGA Mark II nuclear research
c reactor into this MCNP input deck, there are several features of the UT TRIGA
c Mark II nuclear research reactor that are not included in this MCNP input
c deck. Some of the more notable features that are not modeled in this MCNP
c input deck include the following:
c
c (1) The fuel element composition assumed in this MCNP input deck is the fuel
c     element composition representative of a clean reactor core. That is to say
```

```
c     that the composition of each modeled fuel element is assumed to be that of
c     a brand new, never burned fuel element. Additionally, the fuel element
c     composition is assumed to be uniform throughout the volume of a given
c     fuel element, and all of the fuel elements are assumed to have the same
c     composition regardless of their location within the reactor core.
c     In reality the UT TRIGA Mark II nuclear research reactor has been
c     operational since 1992, and a large portion of the fuel elements were also
c     burned in UT's original research reactor which operated from August 1963
c     until the TRIGA Mark II nuclear research reactor went into operation in
c     1992, so the fuel elements contain less uranium than brand new, never
c     burned fuel elements. They also contain various neutron fission products
c     that would not be present in brand new, never burned fuel elements.
c     Assuming a fuel element composition representative of a clean reactor core
c     as opposed to the fuel element composition specific to a given time in
c     core life introduces some error into the output generated by this MCNP
c     model. That said, the magnitude of the error is difficult to estimate.
c
c (2) The temperature profile across the geometry of the UT TRIGA Mark II
c     nuclear research reactor is essentially assumed to be uniform at
c     T = 293.6 K. One notable exception is the temperature of the uranium
c     zirconium hydride material in each of the fuel elements, which is assumed
c     to be uniform at T = 600 K. Assuming a uniform temperature profile across
c     the geometry of the UT TRIGA Mark II nuclear research reactor introduces
c     some error into the output generated by this MCNP model. That said, the
c     magnitude of the error is difficult to estimate.
c
c (3) With the exception of the air cavity common to stage 1 of beam ports 1
c     and 5, the beam ports are modeled simply as air-filled tubes. Some notable
c     features of the UT TRIGA Mark II nuclear research reactor beam ports that
c     are not modeled in this MCNP input deck include the shield plugs that are
c     typically installed in beam ports 1 and 4 and the neutron wave guide that
c     is typically installed in beam port 3.
c
c (4) This MCNP input deck models the portion of the UT TRIGA Mark II nuclear
c     research reactor that extends from the bottom of the reactor pool up
c     through an elevation of 95 cm above the vertical center of the reactor
c     core. Horizontally the model extends out to the outer edges of the lower
c     level of the biological shield. It is thus important to note that this
c     MCNP input deck does not model the entire vertical extent of the UT TRIGA
c     Mark II nuclear research reactor, nor does it model any of the
c     experimental facilities outside of the biological shield.
c
c
c Information pertaining to the variance reduction
c techniques employed in this MCNP input deck:
c ================================================
c
c The principal variance reduction technique employed in this MCNP input deck is
c the weight-window population control technique. An initial set of cell-based
c lower weight-window bounds must be provided by the user in a separate WWINP
c file. The name of the WWINP file containing the cell-based lower weight-window
c bounds must be communicated to MCNP at the execution line using the WWINP
c keyword. The MCNP weight-window generator then generates a new, improved set
c of cell-based lower weight-window bounds that may be utilized by a subsequent
c continue run. The process of executing an MCNP run, generating a new, improved
c set of lower weight window bounds and then utilizing the new, improved set of
c lower weight window bounds in a continue run may be repeated a number of times
c to ensure that an optimal set of lower weight-window bounds has been
c generated. Then, once an optimal set of lower weight-window bounds has been
c generated, a final continue run requesting that a relatively large number of
c particle histories be run may be executed to minimize the variances associated
c with the tallies requested in a manner that is as efficient as possible. This
c variance reduction technique is particularly powerful when tallies are
c requested in MCNP cells that have volumes that are very small relative to the
c volume associated with the overall problem geometry.
c
```

```
c The WWINP file that supports this MCNP input deck must contain a lower
c weight-window bound for each of the cells associated with the problem
c geometry. The lower weight-window bound associated with the particle graveyard
c should be set equal to zero so that particles entering the particle graveyard
c will be killed. It is difficult to estimate what the lower weight-window
c bounds associated with the other cells associated with the problem geometry
c should be (this is, after all, why we are using the weight window generator
c to establish the lower weight-window bounds for us). Experience has shown that
c setting the lower weight-window bounds associated with the other cells
c associated with the problem geometry to 0.5 (one half of the weight that
c source particles are born with by default) allows MCNP to run the particle
c histories requested herein relatively quickly and efficiently without
c introducing any spatial bias to the output generated by this MCNP input deck.
c
c Additional weight-window generator options may be set using the WWP and
c cards. See the comments associated with the WWP and WWG cards for more
c information pertaining to these options.
c
c For more information pertaining to the weight-window population control
c variance reduction technique and the MCNP weight window generator refer to
c section 3.3.6 of the MCNP6 User's Manual (LA-CP-14-00745, Rev. 0) and
c volume I, chapter 2, section VII.B.5 of "MCNP — A General Monte Carlo
c N-Particle Transport Code, Version 5" (LA-UR-03-1987). Additionally, the
c "MCNP Reference Collection," which is available at https://laws.lanl.gov/...
c vhosts/mcnp.lanl.gov/references.shtml also includes several references on the
c weight-window population control technique and the MCNP weight window
c generator.
c
c Warnings and comments generated during execution of this MCNP input deck:
c ==========================================================================
c
c Warnings generated during the execution of this MCNP input deck:
c ----------------------------------------------------------------
c
c Three warnings are generated during the execution of this MCNP input deck.
c A summary of the warnings generated and their respective meanings follows.
c None of the warnings are cause for concern.
c
c (1) Warning: Physics models disabled.
c
c     Warning resolution: The MODE card in this MCNP input deck includes only
c     an "N" designator to specify that MCNP should transport only neutrons.
c     All MODE N, P, and E problems run with model physics turned off by
c     default. See section 3.3.3.7 of the MCNP6 User's Manual (LA-CP-14-00745,
c     Rev. 0) for more information. This warning may be disregarded.
c
c (2) Warning: Energy of the top neutron weight-window bound set to emax.
c
c     Warning resolution: This MCNP input deck does not employ a WWE card, so
c     a single weight-window energy interval is established with lower and
c     upper energy bounds equal to the energy limits of the problem. See
c     section 3.3.6.3 of the MCNP6 User's Manual (LA-CP-14-00745, Rev. 0)
c     for more information. This warning may be disregarded.
c
c (3) Warning: 001001.80c and 001001.81c are both called for.
c
c     Warning resolution: ZAID 001001.80c specifies that continuous energy
c     neutron data for H-1 in several materials, including the reactor pool
c     water and the high density concrete associated with the biological
c     shield, should be extracted from data library 80. H-1 data library 80
c     provides H-1 data for H-1 at T = 293.6 K. ZAID 001001.81c specifies that
c     continuous energy neutron data for H-1 in the UZrH fuel elements should
c     be extracted from data library 81. H-1 data library 81 provides H-1 data
c     for H-1 at T = 600 K. 001001.80c and 001001.81c are both called for
c     intentionally because H-1 data is needed for both of the aforementioned
c     temperatures. This warning may be disregarded.
```

```
c
c Comments generated during the execution of this MCNP input deck:
c ---------------------------------------------------------------
c
c Six comments are generated during the execution of this MCNP input deck.
c A summary of the comments generated and their respective meanings follows.
c None of the comments are cause for concern.
c
c (1) Comment: Total fission nubar data are being used.
c
c     Comment resolution: This KCODE card in this MCNP input deck specifies the
c     MCNP criticality source that is used for determining k-effective. The
c     criticality source uses total fission nubar data unless a TOTNU card is
c     used to specify that only prompt nubar data should be used. This MCNP
c     input deck does not employ a TOTNU card. See section 3.3.2.6 of the MCNP6
c     User's Manual (LA-CP-14-00745, Rev. 0) for more information. This comment
c     may be disregarded.
c
c (2) Comment: 117 surfaces were deleted for being the same as others.
c
c     Comment resolution: To create the 40 RSR sample tubes, a single RSR
c     sample tube, RSR sample tube 01, is first modeled using cell card form 1.
c     The remaining 39 RSR sample tubes are then modeled using cell card form 2
c     with cell coordinate transformations applied. This essentially creates
c     39 copies of RSR sample tube 01 transformed to the appropriate positions
c     within the RSR. Each time a copy of sample tube 01 is created and then
c     transformed, the three horizontal MCNP surfaces used to define the
c     boundaries of RSR sample tube 01 are copied and transformed to the
c     appropriate positions within the RSR. Because the z-component associated
c     with each of the transformations is zero, the copied and transformed
c     horizontal MCNP surfaces end up being the same as the original horizontal
c     MCNP surfaces used to define the boundaries of RSR sample tube 01.
c     MCNP recognizes that the surfaces are the same, deletes the duplicates,
c     and generates a comment to notify the user that the duplicate surfaces
c     were deleted. This comment may be disregarded.
c
c (3) Comment: Using random number generator 1, initial seed = 219008682294439.
c
c     Comment resolution: The "GEN" keyword on the RAND card is set equal to 1
c     to specify that random number generator 1, the MCNP Lehmer 48-bit
c     congruential pseudorandom number generator, should be used (this is the
c     default pseudorandom number generator in MCNP 6.1.1b). Also, the "SEED"
c     keyword on the RAND card is set equal to 219,008,682,294,439 to set the
c     pseudorandom number generator seed equal to 219,008,682,294,439. The
c     reason for setting the pseudorandom number generator seed equal to
c     219,008,682,294,439 is discussed in the comments near the RAND card;
c     refer to the discussion there for more information. Additional information
c     may also be found in section 3.3.7.3.1 of the MCNP6 User's Manual
c    (LA-CP-14-00745, Rev. 0). This comment may be disregarded.
c
c (4) Comment: Nine cross-sections modified by free-gas thermal treatment.
c
c     Comment resolution: This MCNP input deck employs four thermal neutron
c     scattering cards, or MT cards. These four MT cards override the free-gas
c     treatment associated with nine cross-sections at low energies where
c     thermal neutron scattering data is available: (1) MT card MT03 provides
c     thermal neutron scattering data for natural carbon in graphite at
c     T = 293.6 K; (2) MT card MT05 provides thermal neutron scattering data
c     for H-1, Zr-90, Zr-91, Zr-92, Zr-94, and Zr-96 in zirconium hydride at
c     T = 600 K; (3) MT card MT07 provides thermal neutron scattering data
c     for H-1 in water at T = 293.6 K; and (4) MT card MT09 provides thermal
c     neutron scattering data for Al-27 at T = 293.6 K. In order to properly
c     model the scattering of thermal neutrons, it is essential that the
c     free-gas treatment be overridden at low energies where thermal neutron
c     scattering data is available. See section 3.3.2.2 of the MCNP6 User's
c     Manual (LA-CP-14-00745, Rev. 0) for more information. This comment may
```

```
c     be disregarded.
c
c (5) Comment: Setting up hash-based fast table search for xsec tables.
c
c     Comment resolution: MCNP6.1.1 beta employs a new hash-based cross-section
c     lookup algorithm. The new hash-based cross-section lookup algorithm is
c     15-20 faster than the conventional algorithm employed by older versions
c     of MCNP. For more information see the presentation by Dr. Forrest Brown
c     (Senior Research Scientist, Los Alamos National Laboratory) titled
c     "New Hash-based Energy Lookup Algorithm for Monte Carlo Codes"
c     (LA-UR-14-27037). This comment may be disregarded.
c
c (6) Comment: Entropy of the fission source distribution will be computed.
c
c     Comment resolution: MCNP computes a quantity called the Shannon entropy
c     of the fission source distribution to assist in assessing the convergence
c     of the fission source distribution. To compute the Shannon entropy of the
c     fission source distribution a three-dimensional grid encompassing all of
c     the fissionable regions is superimposed on the problem geometry and then
c     the number of fission sites that fall into each of the grid boxes is
c     tallied. The user may use the HSRC card to request that a particular grid
c     be used to evaluate the Shannon entropy. This MCNP input deck does not
c     employ an HSRC card, so MCNP automatically determines a grid that encloses
c     all of the fission sites. The grid is expanded as necessary if fission
c     source sites for a given KCODE cycle fall outside of the grid. See
c     section 3.3.4.12 of the MCNP6 User's Manual (LA-CP-14-00745, Rev. 0)
c     for more information. This comment may be disregarded.
c
c ================
c MCNP CELL CARDS:
c ================
c
c Cell cards modeling the particle graveyard:
c ========================================
c
c A single cell card, cell card 0001, is used to model the particle graveyard.
c
c     m                           geom
c     --  ------------------------------------------------------
0001  00  -0547 :  0541 :  0544 : -0550 :  0552 :  0551 :  0542 :
           0543 :  0548 :  0549 :  0546 :  0545 :  0519 : -0518
c
c Cell cards modeling the fuel element universe:
c ==============================================
c
c Ten cell cards are used to model the fuel element universe:
c  (1) Cell 0011 represents the stainless steel tri-flute at the upper
c      end of the fuel element.
c  (2) Cell 0012 represents the stainless steel cladding that covers the
c      outer cylindrical surfaces of the fuel element.
c  (3) Cell 0013 represents the air gap above the graphite slug at the
c      upper end of the fuel element.
c  (4) Cell 0014 represents the graphite slug at the upper end of
c      the fuel element.
c  (5) Cell 0015 represents the zirconium rod that runs the length of
c      the fueled region of the fuel element.
c  (6) Cell 0016 represents the uranium zirconium hydride fuel that
c      constitutes the fueled region of the fuel element.
c  (7) Cell 0017 represents the molybdenum disk that separates the
c      fueled region of the fuel element from the graphite slug at
c      the lower end of the fuel element.
c  (8) Cell 0018 represents the graphite slug at the lower end of
c      the fuel element.
c  (9) Cell 0019 represents the stainless steel tri-flute at the lower
c      end of the fuel element.
c (10) Cell 0020 represents the reactor pool water that surrounds the
```

```
c      fuel element.
c
c     m         d                 geom           params
c     --   -----------  ----------------------  ------
0011  01  -8.00000E+00  ( -0012 -0004  0011 ) :
                         ( -0013 -0002  0012 )    u=1
0012  01  -8.00000E+00  -0011 -0004  0003  0006  u=1
0013  02  -1.20500E-03  -0011 -0003  0010        u=1
0014  03  -1.70000E+00  -0010 -0003  0009        u=1
0015  04  -6.50600E+00  -0009 -0001  0008        u=1
0016  05  -6.13115E+00  -0009 -0003  0001  0008  u=1
0017  06  -1.02200E+01  -0008 -0003  0007        u=1
0018  03  -1.70000E+00  -0007 -0003  0006        u=1
0019  01  -8.00000E+00  ( -0006 -0004  0194 ) :
                         ( -0194 -0002  0193 )    u=1
0020  07  -9.98207E-01  -0193 :
                         ( -0194  0002  0193 ) :
                         ( -0012  0004  0194 ) :
                         ( -0013  0002  0012 ) : 0013  u=1
c
c Cell cards modeling the fuel-followed control rod universe:
c ============================================================
c
c Fifteen cell cards are used to model the fuel-followed control rod universe:
c  (1) Cell 0031 represents the stainless steel fitting at the upper end of
c      the control rod.
c  (2) Cell 0032 represents the stainless steel cladding that covers the
c      outer cylindrical surfaces of the control rod.
c  (3) Cell 0033 represents the air gap at the upper end of the control rod.
c  (4) Cell 0034 represents the stainless steel plug that separates the air gap
c      at the upper end of the control rod from the boron carbide poison.
c  (5) Cell 0035 represents the air gap that surrounds the boron carbide poison.
c  (6) Cell 0036 represents the boron carbide poison.
c  (7) Cell 0037 represents the stainless steel plug that separates the boron
c      carbide poison from the air gap above the upper end of the fueled region
c      of the control rod.
c  (8) Cell 0038 represents the air gap above the upper end of the fueled
c      region of the control rod.
c  (9) Cell 0039 represents the zirconium rod that runs the length of the
c      fueled region of the control rod.
c (10) Cell 0040 represents the uranium zirconium hydride fuel that constitutes
c      the fueled region of the control rod.
c (11) Cell 0041 represents the stainless steel plug that separates the fueled
c      region of the control rod from the air gap at the lower end of the
c      control rod.
c (12) Cell 0042 represents the aluminum sleeve that surrounds the air gap at
c      the lower end of the control rod.
c (13) Cell 0043 represents the air gap at the lower end of the control rod.
c (14) Cell 0044 represents the stainless steel fitting at the lower end of
c      the control rod.
c (15) Cell 0045 represents the reactor pool water that surrounds the
c      control rod.
c
c     m         d                      geom              params
c     --   -----------  ----------------------------------  ------
0031  01  -8.00000E+00  -0036 -0025  0035                   u=2
0032  01  -8.00000E+00  -0035 -0025  0024  0027             u=2
0033  02  -1.20500E-03  -0035 -0024  0034                   u=2
0034  01  -8.00000E+00  -0034 -0024  0033                   u=2
0035  02  -1.20500E-03  -0033 -0024  0031 (  0022 :  0032 )  u=2
0036  08  -2.52000E+00  -0032 -0022  0031                   u=2
0037  01  -8.00000E+00  -0031 -0024  0030                   u=2
0038  02  -1.20500E-03  -0030 -0024  0008                   u=2
0039  04  -6.50600E+00  -0021 -0008  0029                   u=2
0040  05  -6.13115E+00  -0024 -0008  0021  0029             u=2
0041  01  -8.00000E+00  -0029 -0024  0028                   u=2
```

```
0042  09  -2.70000E+00  -0028 -0024  0023  0027              u=2
0043  02  -1.20500E-03  -0028 -0023  0027                    u=2
0044  01  -8.00000E+00  -0027 -0025  0026                    u=2
0045  07  -9.98207E-01  ( -0026 :  0025 :  0036 )           u=2
c
c Cell cards modeling the transient control rod universe:
c ========================================================
c
c Eight cell cards are used to model the transient control rod universe:
c (1) Cell 0061 represents the aluminum fitting at the upper end of the
c     control rod.
c (2) Cell 0062 represents the aluminum cladding that covers the outer
c     cylindrical surfaces of the control rod.
c (3) Cell 0063 represents the air gap that surrounds the boron carbide poison.
c (4) Cell 0064 represents the boron carbide poison.
c (5) Cell 0065 represents the aluminum plug that separates the boron carbide
c     from the air-filled volume at the lower end of the control rod.
c (6) Cell 0066 represents the air-filled volume at the lower end of the
c     transient control rod. This air-filled volume replaces the zirconium
c     hydride fuel that constitutes the fueled region of the fuel-followed
c     control rod control rods.
c (7) Cell 0067 represents the aluminum fitting at the lower end of
c     the control rod.
c (8) Cell 0068 represents the reactor pool water that surrounds
c     the control rod.
c
c     m         d                 geom            params
c     --   -----------  ------------------------  ------
0061  09  -2.70000E+00  -0058 -0052  0057          u=3
0062  09  -2.70000E+00  -0058 -0053  0052  0054    u=3
0063  02  -1.20500E-03  -0057 -0052  0051  0056    u=3
0064  08  -2.52000E+00  -0057 -0051  0056          u=3
0065  09  -2.70000E+00  -0056 -0052  0008          u=3
0066  02  -1.20500E-03  -0052 -0008  0055          u=3
0067  09  -2.70000E+00  -0055 -0052  0054          u=3
0068  07  -9.98207E-01  ( -0054 :  0053 :  0058 )  u=3
c
c Cell cards modeling the fuel elements and control rods in the reactor core:
c ============================================================================
c
c 118 cell cards are used to model the fuel elements and control rods in the
c reactor core. 114 of the cell cards are used to model fuel elements. Three of
c the 114 cell cards (cell cards 0127, 0153, and 0154) are commented out when
c the 3L irradiation facility is in the reactor core. The other four cell cards
c (cell cards 0087, 0093, 0104, and 0112) are used to model the transient rod,
c the regulating rod, and the two shim rods, respectively.
c
c B-ring fuel element cells:
c --------------------------
c
c     m         geom            params
c     --  -----------------  -------------
0081  00  -0212 -0014  0005  FILL=1         $ Fuel element in location B01.
0082  00  -0213 -0014  0005  FILL=1 (0082)  $ Fuel element in location B02.
0083  00  -0214 -0014  0005  FILL=1 (0083)  $ Fuel element in location B03.
0084  00  -0215 -0014  0005  FILL=1 (0084)  $ Fuel element in location B04.
0085  00  -0216 -0014  0005  FILL=1 (0085)  $ Fuel element in location B05.
0086  00  -0217 -0014  0005  FILL=1 (0086)  $ Fuel element in location B06.
c
c C-ring fuel element and control rod cells:
c ------------------------------------------
c
c     m         geom            params
c     --  -----------------  -------------
0087  00  -0218 -0519  0518  FILL=3 (0087)  $ Transient rod in location C01.
0088  00  -0219 -0014  0005  FILL=1 (0088)  $ Fuel element in location C02.
```

```
0089  00  -0220 -0014  0005  FILL=1 (0089)  $ Fuel element in location C03.
0090  00  -0221 -0014  0005  FILL=1 (0090)  $ Fuel element in location C04.
0091  00  -0222 -0014  0005  FILL=1 (0091)  $ Fuel element in location C05.
0092  00  -0223 -0014  0005  FILL=1 (0092)  $ Fuel element in location C06.
0093  00  -0224 -0519  0518  FILL=2 (0093)  $ Regulating rod in location C07.
0094  00  -0225 -0014  0005  FILL=1 (0094)  $ Fuel element in location C08.
0095  00  -0226 -0014  0005  FILL=1 (0095)  $ Fuel element in location C09.
0096  00  -0227 -0014  0005  FILL=1 (0096)  $ Fuel element in location C10.
0097  00  -0228 -0014  0005  FILL=1 (0097)  $ Fuel element in location C11.
0098  00  -0229 -0014  0005  FILL=1 (0098)  $ Fuel element in location C12.
c
c D-ring fuel element and control rod cells:
c ----------------------------------------
c
c     m         geom          params
c     --  -----------------  -------------
0099  00  -0230 -0014  0005  FILL=1 (0099)  $ Fuel element in location D01.
0100  00  -0231 -0014  0005  FILL=1 (0100)  $ Fuel element in location D02.
0101  00  -0232 -0014  0005  FILL=1 (0101)  $ Fuel element in location D03.
0102  00  -0233 -0014  0005  FILL=1 (0102)  $ Fuel element in location D04.
0103  00  -0234 -0014  0005  FILL=1 (0103)  $ Fuel element in location D05.
0104  00  -0235 -0519  0518  FILL=2 (0104)  $ Shim rod 1 in location D06.
0105  00  -0236 -0014  0005  FILL=1 (0105)  $ Fuel element in location D07.
0106  00  -0237 -0014  0005  FILL=1 (0106)  $ Fuel element in location D08.
0107  00  -0238 -0014  0005  FILL=1 (0107)  $ Fuel element in location D09.
0108  00  -0239 -0014  0005  FILL=1 (0108)  $ Fuel element in location D10.
0109  00  -0240 -0014  0005  FILL=1 (0109)  $ Fuel element in location D11.
0110  00  -0241 -0014  0005  FILL=1 (0110)  $ Fuel element in location D12.
0111  00  -0242 -0014  0005  FILL=1 (0111)  $ Fuel element in location D13.
0112  00  -0243 -0519  0518  FILL=2 (0112)  $ Shim rod 2 in location D14.
0113  00  -0244 -0014  0005  FILL=1 (0113)  $ Fuel element in location D15.
0114  00  -0245 -0014  0005  FILL=1 (0114)  $ Fuel element in location D16.
0115  00  -0246 -0014  0005  FILL=1 (0115)  $ Fuel element in location D17.
0116  00  -0247 -0014  0005  FILL=1 (0116)  $ Fuel element in location D18.
c
c E-ring fuel element cells:
c ---------------------------
c
c Note that the cell representing the fuel element in reactor
c core location E11, cell 0127, should be commented out
c if the 3L irradiation facility is in the reactor core.
c
c     m         geom          params
c     --  -----------------  -------------
0117  00  -0248 -0014  0005  FILL=1 (0117)  $ Fuel element in location E01.
0118  00  -0249 -0014  0005  FILL=1 (0118)  $ Fuel element in location E02.
0119  00  -0250 -0014  0005  FILL=1 (0119)  $ Fuel element in location E03.
0120  00  -0251 -0014  0005  FILL=1 (0120)  $ Fuel element in location E04.
0121  00  -0252 -0014  0005  FILL=1 (0121)  $ Fuel element in location E05.
0122  00  -0253 -0014  0005  FILL=1 (0122)  $ Fuel element in location E06.
0123  00  -0254 -0014  0005  FILL=1 (0123)  $ Fuel element in location E07.
0124  00  -0255 -0014  0005  FILL=1 (0124)  $ Fuel element in location E08.
0125  00  -0256 -0014  0005  FILL=1 (0125)  $ Fuel element in location E09.
0126  00  -0257 -0014  0005  FILL=1 (0126)  $ Fuel element in location E10.
c 0127  00  -0258 -0014  0005  FILL=1 (0127)  $ Fuel element in location E11.
0128  00  -0259 -0014  0005  FILL=1 (0128)  $ Fuel element in location E12.
0129  00  -0260 -0014  0005  FILL=1 (0129)  $ Fuel element in location E13.
0130  00  -0261 -0014  0005  FILL=1 (0130)  $ Fuel element in location E14.
0131  00  -0262 -0014  0005  FILL=1 (0131)  $ Fuel element in location E15.
0132  00  -0263 -0014  0005  FILL=1 (0132)  $ Fuel element in location E16.
0133  00  -0264 -0014  0005  FILL=1 (0133)  $ Fuel element in location E17.
0134  00  -0265 -0014  0005  FILL=1 (0134)  $ Fuel element in location E18.
0135  00  -0266 -0014  0005  FILL=1 (0135)  $ Fuel element in location E19.
0136  00  -0267 -0014  0005  FILL=1 (0136)  $ Fuel element in location E20.
0137  00  -0268 -0014  0005  FILL=1 (0137)  $ Fuel element in location E21.
0138  00  -0269 -0014  0005  FILL=1 (0138)  $ Fuel element in location E22.
```

```
0139  00  -0270 -0014  0005  FILL=1 (0139)  $ Fuel element in location E23.
0140  00  -0271 -0014  0005  FILL=1 (0140)  $ Fuel element in location E24.
c
c F-ring fuel element cells:
c --------------------------
c
c Note that the cells representing the fuel elements in reactor core
c locations F13 and F14, cells 0153 and 0154, respectively, should be
c commented out if the 3L irradiation facility is in the reactor core.
c
c     m         geom           params
c     --  -----------------  -------------
0141  00  -0272 -0014  0005  FILL=1 (0141)  $ Fuel element in location F01.
0142  00  -0273 -0014  0005  FILL=1 (0142)  $ Fuel element in location F02.
0143  00  -0274 -0014  0005  FILL=1 (0143)  $ Fuel element in location F03.
0144  00  -0275 -0014  0005  FILL=1 (0144)  $ Fuel element in location F04.
0145  00  -0276 -0014  0005  FILL=1 (0145)  $ Fuel element in location F05.
0146  00  -0277 -0014  0005  FILL=1 (0146)  $ Fuel element in location F06.
0147  00  -0278 -0014  0005  FILL=1 (0147)  $ Fuel element in location F07.
0148  00  -0279 -0014  0005  FILL=1 (0148)  $ Fuel element in location F08.
0149  00  -0280 -0014  0005  FILL=1 (0149)  $ Fuel element in location F09.
0150  00  -0281 -0014  0005  FILL=1 (0150)  $ Fuel element in location F10.
0151  00  -0282 -0014  0005  FILL=1 (0151)  $ Fuel element in location F11.
0152  00  -0283 -0014  0005  FILL=1 (0152)  $ Fuel element in location F12.
c 0153  00  -0284 -0014  0005  FILL=1 (0153)  $ Fuel element in location F13.
c 0154  00  -0285 -0014  0005  FILL=1 (0154)  $ Fuel element in location F14.
0155  00  -0286 -0014  0005  FILL=1 (0155)  $ Fuel element in location F15.
0156  00  -0287 -0014  0005  FILL=1 (0156)  $ Fuel element in location F16.
0157  00  -0288 -0014  0005  FILL=1 (0157)  $ Fuel element in location F17.
0158  00  -0289 -0014  0005  FILL=1 (0158)  $ Fuel element in location F18.
0159  00  -0290 -0014  0005  FILL=1 (0159)  $ Fuel element in location F19.
0160  00  -0291 -0014  0005  FILL=1 (0160)  $ Fuel element in location F20.
0161  00  -0292 -0014  0005  FILL=1 (0161)  $ Fuel element in location F21.
0162  00  -0293 -0014  0005  FILL=1 (0162)  $ Fuel element in location F22.
0163  00  -0294 -0014  0005  FILL=1 (0163)  $ Fuel element in location F23.
0164  00  -0295 -0014  0005  FILL=1 (0164)  $ Fuel element in location F24.
0165  00  -0296 -0014  0005  FILL=1 (0165)  $ Fuel element in location F25.
0166  00  -0297 -0014  0005  FILL=1 (0166)  $ Fuel element in location F26.
0167  00  -0298 -0014  0005  FILL=1 (0167)  $ Fuel element in location F27.
0168  00  -0299 -0014  0005  FILL=1 (0168)  $ Fuel element in location F28.
0169  00  -0300 -0014  0005  FILL=1 (0169)  $ Fuel element in location F29.
0170  00  -0301 -0014  0005  FILL=1 (0170)  $ Fuel element in location F30.
c
c G-ring fuel element cells:
c --------------------------
c
c Note that there are no fuel element cells associated with the G01, G07, G13,
c G19, G25, or G31 reactor core locations because there are not cutouts in the
c top or bottom grid plates in any of these reactor core locations. Reactor
c core locations G32 and G34 sometimes contain the AmBe startup source and the
c pneumatic transfer system irradiation facility, respectively, depending on
c the reactor core configuration. When the G32 and G34 reactor core locations
c do not contain the AmBe startup source or the pneumatic transfer system
c irradiation facility they are typically left empty (i.e. they are filled
c with water, not fuel elements).
c
c     m         geom           params
c     --  -----------------  -------------
0171  00  -0302 -0014  0005  FILL=1 (0171)  $ Fuel element in location G02.
0172  00  -0303 -0014  0005  FILL=1 (0172)  $ Fuel element in location G03.
0173  00  -0304 -0014  0005  FILL=1 (0173)  $ Fuel element in location G04.
0174  00  -0305 -0014  0005  FILL=1 (0174)  $ Fuel element in location G05.
0175  00  -0306 -0014  0005  FILL=1 (0175)  $ Fuel element in location G06.
0176  00  -0307 -0014  0005  FILL=1 (0176)  $ Fuel element in location G08.
0177  00  -0308 -0014  0005  FILL=1 (0177)  $ Fuel element in location G09.
0178  00  -0309 -0014  0005  FILL=1 (0178)  $ Fuel element in location G10.
```

```
0179  00  -0310 -0014  0005  FILL=1 (0179)  $ Fuel element in location G11.
0180  00  -0311 -0014  0005  FILL=1 (0180)  $ Fuel element in location G12.
0181  00  -0312 -0014  0005  FILL=1 (0181)  $ Fuel element in location G14.
0182  00  -0313 -0014  0005  FILL=1 (0182)  $ Fuel element in location G15.
0183  00  -0314 -0014  0005  FILL=1 (0183)  $ Fuel element in location G16.
0184  00  -0315 -0014  0005  FILL=1 (0184)  $ Fuel element in location G17.
0185  00  -0316 -0014  0005  FILL=1 (0185)  $ Fuel element in location G18.
0186  00  -0317 -0014  0005  FILL=1 (0186)  $ Fuel element in location G20.
0187  00  -0318 -0014  0005  FILL=1 (0187)  $ Fuel element in location G21.
0188  00  -0319 -0014  0005  FILL=1 (0188)  $ Fuel element in location G22.
0189  00  -0320 -0014  0005  FILL=1 (0189)  $ Fuel element in location G23.
0190  00  -0321 -0014  0005  FILL=1 (0190)  $ Fuel element in location G24.
0191  00  -0322 -0014  0005  FILL=1 (0191)  $ Fuel element in location G26.
0192  00  -0323 -0014  0005  FILL=1 (0192)  $ Fuel element in location G27.
0193  00  -0324 -0014  0005  FILL=1 (0193)  $ Fuel element in location G28.
0194  00  -0325 -0014  0005  FILL=1 (0194)  $ Fuel element in location G29.
0195  00  -0326 -0014  0005  FILL=1 (0195)  $ Fuel element in location G30.
0196  00  -0328 -0014  0005  FILL=1 (0196)  $ Fuel element in location G33.
0197  00  -0330 -0014  0005  FILL=1 (0197)  $ Fuel element in location G35.
0198  00  -0331 -0014  0005  FILL=1 (0198)  $ Fuel element in location G36.
c
c Cell cards modeling the central thimble irradiation facility:
c ============================================================
c
c Five cell cards are used to model the central thimble irradiation facility:
c (1) Cell 0221 represents the plug at the bottom of the central thimble
c     irradiation facility.
c (2) Cell 0222 represents the cylindrical walls of the central thimble
c     irradiation facility.
c (3) Cell 0223 represents the water-filled volume inside the lower portion of
c     the central thimble irradiation facility. Note that there are holes in
c     the cylindrical walls of the central thimble irradiation facility that
c     prevent the lower portion of the central thimble below the upper grid
c     plate from being blown dry and filled with air even when the central
c     thimble irradiation is blown dry to support sample irradiations.
c (4) Cell 0224 represents the air/water-filled volume inside the upper portion
c     of the central thimble irradiation facility. Note that the upper portion
c     of the central thimble irradiation facility may be blown dry and filled
c     with air to support sample irradiations and that switching the between the
c     air-filled volume and the water-filled volume is as simple as modifying
c     the material number on cell card 0224; set the material number to the
c     material number associated with the air material data card to select the
c     air-filled volume, or set the material number to the material number
c     associated with the water material data card to select the
c     water-filled volume.
c (5) Cell 0225 represents the sample location within the air/water-filled
c     volume inside the central thimble irradiation facility. As is the case
c     with cell card 0224, note that switching the between the air-filled volume
c     inside the central thimble irradiation facility and the water-filled
c     volume inside the central thimble irradiation facility is as simple as
c     modifying the material number on cell card 0225.
c
c     m         d                   geom
c     --   -----------  ----------------------------
0221  09  -2.70000E+00  -0075 -0072  0074
0222  09  -2.70000E+00  -0519 -0073  0072  0074
0223  07  -9.98207E-01  -0519 -0078 -0072  0075 #0225
0224  07  -9.98207E-01  -0519 -0072  0078
0225  07  -9.98207E-01  -0077 -0071  0076
c
c Cell cards modeling the three element (3L) irradiation facility universe:
c ========================================================================
c
c Seven cell cards are used to model the 3L irradiation facility universe:
c (1) Cell 0231 represents the outer aluminum casing of
c     the 3L irradiation facility.
```

```
c (2) Cell 0232 represents the air gap between the outer aluminum casing
c     and the cadmium/lead sleeve of the 3L irradiation facility.
c (3) Cell 0233 represents the cadmium/lead sleeve of the 3L irradiation
c     facility. Note that switching between the cadmium 3L irradiation facility
c     sleeve and the lead 3L irradiation facility sleeve is as simple as
c     modifying the material number on cell card 0233; set the material number
c     to the material number associated with the cadmium material data card to
c     select the cadmium 3L irradiation facility sleeve, or set the material
c     number to the material number associated with the lead material data
c     card to select the lead 3L irradiation facility sleeve.
c (4) Cell 0234 represents the aluminum sleeve between the cadmium/lead sleeve
c     of the 3L irradiation facility and the inner CO2-purged volume of the
c     3L irradiation facility where samples are located.
c (5) Cell 0235 represents the inner CO2-purged volume of the 3L irradiation
c     facility where samples are located. Note that in this model the inner
c     CO2-purged volume is actually filled with air rather than CO2.
c (6) Cell 0236 represents the reactor pool water that surrounds
c     the 3L irradiation facility.
c (7) Cell 0237 is a cylindrical cell centered at a location corresponding
c     to the position of the 3L irradiation facility in the reactor core.
c     This cell is filled with the 3L irradiation facility universe,
c     effectively placing the 3L irradiation facility in the appropriate
c     location within the reactor core.
c
c     m         d                 geom            params
c     --   -----------  -------------------------  ------
c 0231  09  -2.70000E+00  -0094 -0085  0087
c                         (  0084 :  0093 : -0088 )  u=4
c 0232  02  -1.20500E-03  -0093 -0084  0081  0088
c                         (  0083 :  0091 )
c                         (  0082 :  0092 )          u=4
c 0233  10  -1.13500E+01  -0091 -0083  0088
c                         ( -0089 :  0082 )          u=4
c 0234  09  -2.70000E+00  -0092 -0082  0089
c                         ( -0090 :  0081 )          u=4
c 0235  02  -1.20500E-03  -0093 -0081  0090
c                        #0256 #0257 #0255 #0254
c                       #0253 #0252 #0251          u=4
c 0236  07  -9.98207E-01  ( -0087 :  0085 :  0094 )  u=4
c 0237  00                -0519 -0086  0194          FILL=4
c
c Cell cards modeling the Swagelok PFA plug
c valve in the 3L irradiation facility:
c ========================================
c
c Seven cell cards are used to model the Swagelok PFA plug valve
c in the 3L irradiation facility:
c (1) Cell 0251 represents the Ar, Xe, etc. gas trapped
c     in the Swagelok PFA plug valve end-cap section.
c (2) Cell 0252 represents the PFA portion of the bottom end
c     of the Swagelok PFA plug valve that has an end-cap on
c     it to trap the Ar, Xe, etc. gas to be irradiated.
c (3) Cell 0253 represents the Ar, Xe, etc. gas trapped in
c     the Swagelok PFA plug valve central body section.
c (4) Cell 0254 represents the thin PFA portion of the
c     Swagelok PFA plug valve central body section.
c (5) Cell 0255 represents the thick PFA portion of the
c     Swagelok PFA plug valve central body section.
c (6) Cell 0256 represents the open portion of the top end of the
c     Swagelok PFA plug valve that has no end-cap on it and is open
c     to the CO2 purge gas in the 3L irradiation facility.
c (7) Cell 0257 represents the PFA portion of the top end of the
c     Swagelok PFA plug valve that has no end-cap on it and is open
c     to the CO2 purge gas in the 3L irradiation facility.
c
c     m         d                     geom                 params
```

```
c     --   -----------  ---------------------------------  ------
c 0251  12   3.29400E-06  ( -0113 -0104  0102  0112 ) :
c                        ( -0113 -0112 -0105  0111 )          u=4
c 0252  11  -2.15000E+00  ( -0113 -0105  0103  0104  0112 ) :
c                        ( -0113 -0107  0103  0105  0111 ) :
c                        ( -0113 -0111 -0107  0090 )          u=4
c 0253  12   3.29400E-06  -0102 -0101                          u=4
c 0254  11  -2.15000E+00  ( -0110 -0102  0108 ) #0253          u=4
c 0255  11  -2.15000E+00  -0109 -0103  0102  0108 #0256 #0251  u=4
c 0256  02  -1.20500E-03  ( -0114 -0104  0102  0113 ) :
c                        ( -0115 -0105  0113  0114 )          u=4
c 0257  11  -2.15000E+00  ( -0114 -0105  0103  0104  0113 ) :
c                        ( -0115 -0106  0103  0105  0113 )    u=4
c
c Cell cards modeling the pneumatic transfer system irradiation facility:
c ========================================================================
c
c Five cell cards are used to model the pneumatic
c transfer system irradiation facility:
c (1) Cell 0271 represents the air cavity at the interior of the
c     pneumatic transfer system irradiation facility.
c (2) Cell 0272 represents the aluminum sleeve between the air cavity at
c     the interior of the pneumatic transfer system irradiation facility
c     and the cadmium/lead sleeve of the pneumatic transfer system
c     irradiation facility.
c (3) Cell 0273 represents the cadmium/lead sleeve of the pneumatic
c     transfer system irradiation facility. Note that switching between the
c     cadmium pneumatic transfer system irradiation facility sleeve and the
c     lead pneumatic transfer system irradiation facility sleeve is as simple
c     as modifying the material number on cell card 0273; set the material
c     number to the material number associated with the cadmium material
c     data card to select the cadmium pneumatic transfer system irradiation
c     facility sleeve, or set the material number to the material number
c     associated with the lead material data card to select the lead
c     pneumatic transfer system irradiation facility sleeve.
c (4) Cell 0274 represents the air gap between the cadmium/lead sleeve
c     and the outer aluminum casing of the pneumatic transfer system
c     irradiation facility.
c (5) Cell 0275 represents the outer aluminum casing of the pneumatic
c     transfer system irradiation facility.
c
c It should be noted that the pneumatic transfer system irradiation facility is
c only modeled to a height of 50 cm above the vertical center of the reactor
c core, but in reality it extends all the way to the surface of the reactor pool.
c
c     m         d                      geom
c     --   -----------  ---------------------------------
c 0271  02  -1.20500E-03  -0131 -0121  0130
c 0272  09  -2.70000E+00  -0131 -0122  0129 ( -0130 :  0121 )
c 0273  13  -8.65000E+00  -0131 -0123  0128 ( -0129 :  0122 )
c 0274  02  -1.20500E-03  -0131 -0124  0127 ( -0128 :  0123 )
c 0275  09  -2.70000E+00  -0131 -0125  0126 ( -0127 :  0124 )
c
c Cell cards modeling the Rotary Specimen Rack (RSR):
c ================================================
c
c Cell cards modeling the outer casing and inner volume of the RSR:
c ------------------------------------------------------------------
c
c Two cell cards are used to model the outer casing and inner volume of the RSR:
c (1) Cell 0291 represents the outer casing of the RSR.
c (2) Cell 0292 represents the inner volume of the RSR where the sample tubes
c     are located.
c
c     m         d                          geom
c     --   -----------  ------------------------------------------
```

```
0293  09  -2.70000E+00  ( -0152 -0142  0141  0149 )
0291  09  -2.70000E+00  ( -0150 -0143  0142  0149 ) :
                        ( -0150 -0144  0143  0147 ) :
                        ( -0148 -0145  0144  0147 ) :
                        ( -0152 -0146  0145  0147 ) :
                        ( -0145  0142  0151 -0152 )
0292  02  -1.20500E-03  ( -0151 -0144  0142  0150 ) :
                        ( -0151 -0145  0148  0144 )
                       #0301 #0302 #0303 #0304 #0305 #0306 #0307 #0308
                       #0309 #0310 #0311 #0312 #0313 #0314 #0315 #0316
                       #0317 #0318 #0319 #0320 #0321 #0322 #0323 #0324
                       #0325 #0326 #0327 #0328 #0329 #0330 #0331 #0332
                       #0333 #0334 #0335 #0336 #0337 #0338 #0339 #0340
                       #0351 #0352 #0353 #0354
c
c Cell cards modeling the RSR sample tubes:
c ----------------------------------------
c
c 40 cell cards, cell cards 0301 through 0340, are used to model the 40 RSR
c sample tubes. MCNP cell card form 1 is used on cell card 0301 to model RSR
c sample tube 01 and MCNP cell card form 2 is used on cell cards 0302 through
c 0340 to model RSR sample tubes 02 through 40.
c
c     m         d                      geom
c     --   -----------  ----------------------------------
0301  09  -2.70000E+00  -0165 -0161  0163 ( -0164 :  0162 )  $ Sample tube 01.
c
c     LIKE   n    BUT                      list
c     ----  ----  ---  ---------------------------------------------
0302  like  0301  but  TRCL=(-4.11900E-01  5.23371E+00  0.00000E+00)  $ Tube 02.
0303  like  0301  but  TRCL=(-1.63747E+00  1.03386E+01  0.00000E+00)  $ Tube 03.
0304  like  0301  but  TRCL=(-3.64652E+00  1.51888E+01  0.00000E+00)  $ Tube 04.
0305  like  0301  but  TRCL=(-6.38958E+00  1.96651E+01  0.00000E+00)  $ Tube 05.
0306  like  0301  but  TRCL=(-9.79912E+00  2.36572E+01  0.00000E+00)  $ Tube 06.
0307  like  0301  but  TRCL=(-1.37912E+01  2.70667E+01  0.00000E+00)  $ Tube 07.
0308  like  0301  but  TRCL=(-1.82675E+01  2.98098E+01  0.00000E+00)  $ Tube 08.
0309  like  0301  but  TRCL=(-2.31177E+01  3.18188E+01  0.00000E+00)  $ Tube 09.
0310  like  0301  but  TRCL=(-2.82226E+01  3.30444E+01  0.00000E+00)  $ Tube 10.
0311  like  0301  but  TRCL=(-3.34563E+01  3.34563E+01  0.00000E+00)  $ Tube 11.
0312  like  0301  but  TRCL=(-3.86900E+01  3.30444E+01  0.00000E+00)  $ Tube 12.
0313  like  0301  but  TRCL=(-4.37949E+01  3.18188E+01  0.00000E+00)  $ Tube 13.
0314  like  0301  but  TRCL=(-4.86451E+01  2.98098E+01  0.00000E+00)  $ Tube 14.
0315  like  0301  but  TRCL=(-5.31214E+01  2.70667E+01  0.00000E+00)  $ Tube 15.
0316  like  0301  but  TRCL=(-5.71135E+01  2.36572E+01  0.00000E+00)  $ Tube 16.
0317  like  0301  but  TRCL=(-6.05230E+01  1.96651E+01  0.00000E+00)  $ Tube 17.
0318  like  0301  but  TRCL=(-6.32661E+01  1.51888E+01  0.00000E+00)  $ Tube 18.
0319  like  0301  but  TRCL=(-6.52751E+01  1.03386E+01  0.00000E+00)  $ Tube 19.
0320  like  0301  but  TRCL=(-6.65007E+01  5.23372E+00  0.00000E+00)  $ Tube 20.
0321  like  0301  but  TRCL=(-6.69126E+01  0.00000E+00  0.00000E+00)  $ Tube 21.
0322  like  0301  but  TRCL=(-6.65007E+01 -5.23372E+00  0.00000E+00)  $ Tube 22.
0323  like  0301  but  TRCL=(-6.52751E+01 -1.03386E+01  0.00000E+00)  $ Tube 23.
0324  like  0301  but  TRCL=(-6.32661E+01 -1.51888E+01  0.00000E+00)  $ Tube 24.
0325  like  0301  but  TRCL=(-6.05230E+01 -1.96651E+01  0.00000E+00)  $ Tube 25.
0326  like  0301  but  TRCL=(-5.71135E+01 -2.36572E+01  0.00000E+00)  $ Tube 26.
0327  like  0301  but  TRCL=(-5.31214E+01 -2.70667E+01  0.00000E+00)  $ Tube 27.
0328  like  0301  but  TRCL=(-4.86451E+01 -2.98098E+01  0.00000E+00)  $ Tube 28.
0329  like  0301  but  TRCL=(-4.37949E+01 -3.18188E+01  0.00000E+00)  $ Tube 29.
0330  like  0301  but  TRCL=(-3.86900E+01 -3.30444E+01  0.00000E+00)  $ Tube 30.
0331  like  0301  but  TRCL=(-3.34563E+01 -3.34563E+01  0.00000E+00)  $ Tube 31.
0332  like  0301  but  TRCL=(-2.82226E+01 -3.30444E+01  0.00000E+00)  $ Tube 32.
0333  like  0301  but  TRCL=(-2.31177E+01 -3.18188E+01  0.00000E+00)  $ Tube 33.
0334  like  0301  but  TRCL=(-1.82675E+01 -2.98098E+01  0.00000E+00)  $ Tube 34.
0335  like  0301  but  TRCL=(-1.37912E+01 -2.70667E+01  0.00000E+00)  $ Tube 35.
0336  like  0301  but  TRCL=(-9.79912E+00 -2.36572E+01  0.00000E+00)  $ Tube 36.
0337  like  0301  but  TRCL=(-6.38958E+00 -1.96651E+01  0.00000E+00)  $ Tube 37.
0338  like  0301  but  TRCL=(-3.64652E+00 -1.51888E+01  0.00000E+00)  $ Tube 38.
```

```
0339  like  0301  but  TRCL=(-1.63747E+00 -1.03386E+01  0.00000E+00)  $ Tube 39.
0340  like  0301  but  TRCL=(-4.11900E-01 -5.23372E+00  0.00000E+00)  $ Tube 40.
c
c Cell cards modeling the cobalt RSR flux wires:
c ==============================================
c
c Four cell cards, cell cards 0351, 0352, 0353, and 0354, are used to model four
c cobalt RSR flux wires, one in each of four rotary specimen rack sample tubes.
c
c     m         d             geom
c     --   -----------  -----------------
0351  14  -8.90000E+00  -0176 -0171  0175
0352  14  -8.90000E+00  -0176 -0174  0175
0353  14  -8.90000E+00  -0176 -0173  0175
0354  14  -8.90000E+00  -0176 -0172  0175
c
c Cell cards modeling the top and bottom grid plates:
c ==================================================
c
c One cell card, cell card 0361, is used to model the bottom grid plate,
c and one card, cell card 0371, is used to model the top grid plate.
c
c     m         d                           geom
c     --   -----------  ------------------------------------------------
0361  09  -2.70000E+00  -0194 -0192 -0191 -0189 -0188 -0186 -0185 -0184
                        -0183 -0182 -0181  0187  0190  0193  0211  0212
                         0213  0214  0215  0216  0217  0218  0219  0220
                         0221  0222  0223  0224  0225  0226  0227  0228
                         0229  0230  0231  0232  0233  0234  0235  0236
                         0237  0238  0239  0240  0241  0242  0243  0244
                         0245  0246  0247  0248  0249  0250  0251  0252
                         0253  0254  0255  0256  0257  0258  0259  0260
                         0261  0262  0263  0264  0265  0266  0267  0268
                         0269  0270  0271  0272  0273  0274  0275  0276
                         0277  0278  0279  0280  0281  0282  0283  0284
                         0285  0286  0287  0288  0289  0290  0291  0292
                         0293  0294  0295  0296  0297  0298  0299  0300
                         0301  0302  0303  0304  0305  0306  0307  0308
                         0309  0310  0311  0312  0313  0314  0315  0316
                         0317  0318  0319  0320  0321  0322  0323  0324
                         0325  0326  0327  0328  0329  0330  0331  0351
                         0352  0353  0354  0355  0356  0357  0358  0359
                         0360  0371  0372  0373  0374  0375  0376  0377
                         0378  0379  0380  0381  0382  0383  0384  0385
                         0386  0387  0388  0389  0390  0391  0392  0393
                         0394  0395
0371  09  -2.70000E+00  -0202 -0200        0201  0211  0212  0213  0214
                         0215  0216  0217  0218  0219  0220  0221  0222
                         0223  0224  0225  0226  0227  0228  0229  0230
                         0231  0232  0233  0234  0235  0236  0237  0238
                         0239  0240  0241  0242  0243  0244  0245  0246
                         0247  0248  0249  0250  0251  0252  0253  0254
                         0255  0256  0257        0259  0260  0261  0262
                         0263  0264  0265  0266  0267  0268  0269  0270
                         0271  0272  0273  0274  0275  0276  0277  0278
                         0279  0280  0281  0282  0283              0286
                         0287  0288  0289  0290  0291  0292  0293  0294
                         0295  0296  0297  0298  0299  0300  0301  0302
                         0303  0304  0305  0306  0307  0308  0309  0310
                         0311  0312  0313  0314  0315  0316  0317  0318
                         0319  0320  0321  0322  0323  0324  0325  0326
                         0327  0328  0329  0330  0331  0371  0372  0373
                         0374  0375  0376  0377  0378  0379  0380  0381
                         0382  0383  0384  0385  0386  0387  0388  0389
                         0390  0391  0392  0393  0394  0395  0411  0412
                         0413  0414  0415  0416  0417  0418  0419  0420
```

```
c
c Cell cards modeling the reactor reflector assembly:
c ================================================
c
c Fifteen cell cards are used to model the reactor reflector assembly:
c  (1) Cell 0381 represents the aluminum shroud on the top surface of the
c      reactor reflector assembly.
c  (2) Cell 0382 represents the thick portion of the aluminum shroud on the top
c      surface of the reactor reflector assembly where the top grid plate and
c      the rotary specimen rack attach to the reactor reflector assembly.
c  (3) Cell 0383 represents the recessed portion of the aluminum shroud on the
c      top surface of the reactor reflector assembly where the rotary specimen
c      rack rests inside the upper portion of the reactor reflector assembly.
c  (4) Cell 0384 represents the air gap that fills the upper portion of the
c      reactor reflector assembly between the rotary specimen rack and the
c      aluminum shroud on the inner cylindrical surface of the reactor
c      reflector assembly.
c  (5) Cell 0385 represents the aluminum shroud on the inner cylindrical
c      surface of the reactor reflector assembly.
c  (6) Cell 0386 represents the aluminum shroud on the outer cylindrical
c      surface of the reactor reflector assembly.
c  (7) Cell 0387 represents the graphite that fills the reactor
c      reflector assembly.
c  (8) Cell 0388 represents the aluminum shroud that surrounds the water-filled
c      cavity that runs parallel to beam port 2 in the reactor
c      reflector assembly.
c  (9) Cell 0389 represents the water-filled cavity that runs parallel to
c      beam port 2 in the reactor reflector assembly.
c (10) Cell 0390 represents the aluminum shroud that surrounds the water-filled
c      sleeve that surrounds the portion of beam port 3 that extends into the
c      the reactor reflector assembly.
c (11) Cell 0391 represents the water-filled sleeve that surrounds the portion
c      of beam port 3 that extends into the reactor reflector assembly.
c (12) Cell 0392 represents the aluminum shroud that surrounds the water-filled
c      cavity that runs parallel to beam port 4 in the reactor
c      reflector assembly.
c (13) Cell 0393 represents the water-filled cavity that runs parallel to
c      beam port 4 in the reactor reflector assembly.
c (14) Cell 0394 represents the aluminum shroud on the
c      bottom surface of the reactor reflector assembly.
c (15) Cell 0395 represents the lip that extends downward from the outer
c      edges of the aluminum shroud on the bottom surface of the reactor
c      reflector assembly.
c
c     m         d                              geom
c     --   -----------  ------------------------------------------------
0381  09  -2.70000E+00  -0480 -0451  0474  0479
0382  09  -2.70000E+00  -0478 -0472  0477
                         ( -0201 :  0200 ) ( -0471 :  0443 )
                         ( -0190 : -0187 :  0181 :  0182 :
                            0183 :  0184 :  0185 :  0186 :
                            0188 :  0189 :  0191 :  0192 ) #0385
0383  09  -2.70000E+00  -0474 -0443  0471  0475
                         ( -0476 : -0472 :  0473 )
0384  02  -1.20500E-03  -0477 -0471  0475
                         ( -0440 : -0437 :  0431 :  0432 :  0433 :
                            0434 :  0435 :  0436 :  0438 :  0439 :
                            0441 :  0442 )
0385  09  -2.70000E+00  -0443  0193
                         ( -0442 -0441 -0439 -0438 -0436 -0435
                           -0434 -0433 -0432 -0431  0437  0440 )
                         ( -0190 : -0187 :  0181 :  0182 :  0183 :
                            0184 :  0185 :  0186 :  0188 :  0189 :
                            0191 :  0192 )
0386  09  -2.70000E+00  -0454 -0452  0451  0453  0562
                         (  0437 :  0492 )
```

```
0387  03  -1.70000E+00  -0479 -0451  0462  0562
                         ( -0475 :  0474 ) (  0437 :  0492 )
                         ( -0439 :  0652 ) (  0612 :  0615 )
                         ( -0504 : -0502 : -0431 :  0501 :  0503 :  0505 )
                         ( -0440 : -0437 :  0431 :  0432 :  0433 :
                            0434 :  0435 :  0436 :  0438 :  0439 :
                            0441 :  0442 )
0388  09  -2.70000E+00  -0615 -0612 -0451  0611
0389  07  -9.98207E-01  -0615 -0611 -0451
0390  09  -2.70000E+00  -0492 -0452 -0437  0491
0391  07  -9.98207E-01  -0491 -0452 -0437  0632
0392  09  -2.70000E+00  -0652 -0451  0439  0651
0393  07  -9.98207E-01  -0651 -0451  0439  0664
0394  09  -2.70000E+00  -0462 -0451  0461
                         ( -0440 : -0437 :  0431 :  0432 :  0433 :  0434 :
                            0435 :  0436 :  0438 :  0439 :  0441 :  0442 )
0395  09  -2.70000E+00  -0461 -0451  0193  0463
c
c Cell cards modeling the reactor pool water:
c ==========================================
c
c Three cell cards are used to model the reactor pool water in a piecewise
c fashion: (1) Cell 0411 is used to model the fraction of the reactor pool water
c in the cylindrical column shared by the reactor core. (2) Cell 0412 is used
c to model the largest fraction of the reactor pool water, the fraction of the
c pool water that is not in the cylindrical column shared by the reactor core.
c This fraction of the reactor pool water is modeled as two large cylinders that
c extend out to the curved sections of the aluminum pool liner. (3) Cell 0413
c is used to model the remainder of the reactor pool water, the fraction that
c extends out from the outer edges of the two cylinders associated with
c cell 0412 to the straight sections of the aluminum pool liner.
c
c     m         d                          geom
c     --   -----------  ------------------------------------------
0411  07  -9.98207E-01  -0519 -0511  0518 #0081 #0082 #0083 #0084 #0085
                         #0086 #0087 #0088 #0089 #0090 #0091 #0092 #0093
                         #0094 #0095 #0096 #0097 #0098 #0099 #0100 #0101
                         #0102 #0103 #0104 #0105 #0106 #0107 #0108 #0109
                         #0110 #0111 #0112 #0113 #0114 #0115 #0116 #0117
                         #0118 #0119 #0120 #0121 #0122 #0123 #0124 #0125
                         #0126 #0128 #0129 #0130 #0131 #0132 #0133 #0134
                         #0135 #0136 #0137 #0138 #0139 #0140 #0141 #0142
                         #0143 #0144 #0145 #0146 #0147 #0148 #0149 #0150
                         #0151 #0152 #0155 #0156 #0157 #0158 #0159 #0160
                         #0161 #0162 #0163 #0164 #0165 #0166 #0167 #0168
                         #0169 #0170 #0171 #0172 #0173 #0174 #0175 #0176
                         #0177 #0178 #0179 #0180 #0181 #0182 #0183 #0184
                         #0185 #0186 #0187 #0188 #0189 #0190 #0191 #0192
                         #0193 #0194 #0195 #0196 #0197 #0198 #0221 #0222
                         #0223 #0224 #0225 $ #0271 #0272 #0273 #0274 #0275 $ 0271-0275
added or removed for Pneumatic Tube System (MBS)
                               #0361 #0371 #0381 #0382 #0383 #0384 #0385
                         #0387 #0390 #0391 #0392 #0393 #0394 #0395 #0441
                         #0451 #0471 #0472 #0491 #0492  $ 0700  0711 0708 0710 $EDIT--
                         #0691 #0692 #0693 #0694 #0696 #0697 #0698         $Fission
Chamber Edit (MBS)
c 0700  24 -8.650000E+00  -0700 0701 0702 0703 0704 $Cd Shell
c 0701  21 -2.700000E+00  -0701 0702 0703 0704 $Al Shell
c 0702  22 -2.340000E+00  -0702 0703 0704 $Boron Powder
c 0703  23 -2.000000E+00  -0703 0704 $BN Shell
c 0704  02 -1.205000E-03  -0704 0706 $Air Shell
c 0706  25 -2.230000E+00  -0706 0707 $borosilicate glass sample
c 0707  02 -1.205000E-03  -0707 $air or material inside sample ampoule
c 0708  21 -2.700000E+00  -0708 0709 $pneumatic part 1
c 0709  26 -2.340000E+00  -0709 0710 $pneumatic part 2
c 0710  02 -1.205000E-03  -0710 $transfer part 1
```

```
c 0705  02 -1.205000E-03  -0705 $ Air Shell for Fast Neutrons
c 0711  21 -2.700000E+00  -0711 0705 $Al shell surrounding in core air shell
0412  07  -9.98207E-01  ( -0513 : -0512 ) -0519  0511  0518
                        #0291 #0292 #0293 #0301 #0302 #0303 #0304 #0305 #0306
                        #0307 #0308 #0309 #0310 #0311 #0312 #0313 #0314
                        #0315 #0316 #0317 #0318 #0319 #0320 #0321 #0322
                        #0323 #0324 #0325 #0326 #0327 #0328 #0329 #0330
                        #0331 #0332 #0333 #0334 #0335 #0336 #0337 #0338
                        #0339 #0340 #0351 #0352 #0353 #0354 #0371 #0381
                        #0382 #0383 #0384 #0385 #0386 #0387 #0388 #0389
                        #0390 #0391 #0392 #0393 #0394 #0395 #0441 #0442
                        #0451 #0461 #0462 #0471 #0472 #0491 #0492 #0501
                        #0502 #0503 #0504 #0505 $reEDIT 0700----------
0413  07  -9.98207E-01  -0519 -0517 -0515  0512  0513  0514  0516  0518
                        #0441 #0442  $reEDIT 0700----------------------
c
c Cell cards modeling the pool liner:
c ===================================
c
c A single cell card, cell card 0421, is used to model the aluminum reactor
c pool liner that lines the inner surfaces of the biological shield and
c separates the biological shield from the reactor pool water. The cell
c consists of four sections: (1) Section 1 is the curved section of the
c reactor pool liner that lines the southern edge of the biological shield.
c (2) Section 2 is the straight section of the reactor pool liner that lines
c the eastern edge the biological shield. (3) Section 3 is the curved section
c of the reactor pool liner that lines the northern edge of the biological
c shield. (4) Section 4 is the straight section of the reactor pool liner
c that lines the western edge of the biological shield.
c
c     m         d                                 geom
c     --   -----------   ------------------------------------------------------
0421  09  -2.70000E+00  ( -0532 -0519  0513  0515  0518 ) :
                        ( -0534 -0519 -0515  0514  0517  0518  0562 ) :
                        ( -0531 -0519 -0514  0512  0518  0612  0632  0652 ) :
                        ( -0519 -0516 -0515  0514  0518  0533  0562 )
c
c Cell cards modeling the biological shield:
c ==========================================
c
c Six cell cards are used to model the biological shield:
c (1) Cell 0431 represents the cylindrical portion of the biological shield
c     that surrounds beam port 1.
c (2) Cell 0432 represents the cylindrical portion of the biological shield
c     that surrounds beam port 2.
c (3) Cell 0433 represents the cylindrical portion of the biological shield
c     that surrounds beam port 3.
c (4) Cell 0434 represents the cylindrical portion of the biological shield
c     that surrounds beam port 4.
c (5) Cell 0435 represents the cylindrical portion of the biological shield
c     that surrounds beam port 5.
c (6) Cell 0436 represents the remainder of the biological shield.
c
c     m         d                             geom
c     --   -----------  ------------------------------------------------------
0431  15  -2.89000E+00  -0553 -0544  0534 #0441 #0442 #0443 #0444
0432  15  -2.89000E+00  -0615 -0554 -0546  0531 #0461 #0462 #0463 #0464 #0465
0433  15  -2.89000E+00  -0555 -0514  0531  0547 #0471 #0472 #0473 #0474 #0475
                        #0476 #0477 #0478
0434  15  -2.89000E+00  -0556 -0549  0439  0531 #0491 #0492 #0493 #0494 #0449
0435  15  -2.89000E+00  -0553 -0533  0550 #0441 #0442 #0445 #0446 #0447 #0448
                        #0449 #0450 #0511 #0512 #0513 #0514 #0515 #0516 #0517
                        #0518 #0519
0436  15  -2.89000E+00  -0552 -0551 -0549 -0548 -0546 -0545 -0544
                        -0543 -0542 -0541 -0519  0518  0547  0550
                        (  0531  0532 ) (  0534 : -0533: -0514:  0515 )
```

```
                        #0431 #0432 #0433 #0434 #0435 #0441 #0442 #0443 #0444
                        #0445 #0446 #0447 #0448 #0449 #0450 #0461 #0462 #0463
                        #0464 #0465 #0471 #0472 #0473 #0474 #0475 #0476 #0477
                        #0478 #0491 #0492 #0493 #0494 #0511 #0512 #0513 #0514
                        #0515 #0516 #0517 #0518 #0519
c
c Cell cards modeling the beam ports:
c ==================================
c
c Cell cards modeling beam ports 1 and 5:
c --------------------------------------
c
c Eleven cells are used to model beam ports 1 and 5:
c  (1) Cell 0441 represents the aluminum tube common to stage 1 of
c      beam ports 1 and 5.
c  (2) Cell 0442 represents the air cavity common to stage 1 of
c      beam ports 1 and 5.
c  (3) Cell 0443 represents the stainless steel tube that forms
c      stage 2 of beam port 1.
c  (4) Cell 0444 represents the air cavity in stage 2 of beam port 1.
c  (5) Cell 0445 represents the stainless steel tube that forms
c      stage 2 of beam port 5.
c  (6) Cell 0446 represents the air cavity in stage 2 of beam port 5.
c  (7) Cell 0447 represents the stainless steel tube that forms
c      stage 3 of beam port 5.
c  (8) Cell 0448 represents the air cavity in stage 3 of beam port 5.
c  (9) Cell 0449 represents the stainless steel tube that forms
c      stage 4 of beam port 5.
c (10) Cell 0450 represents the air cavity in stage 4 of beam port 5.
c (11) Cell 0451 represents the graphite scattering block in the air cavity
c      common to stage 1 of beam ports 1 and 5. The graphite scattering block
c      serves to scatter neutrons down beam ports 1 and 5 and is said to
c      increase the intensity of the neutron beam at the neutron radiography
c      imaging plane in beam port 5 by a factor of 1.7 (according to a document
c      titled "Beam_Scatterer_Notes.pdf" that was provided by Mr. Michael Krause
c      on 17 November 2015).
c
c     m         d               geom
c     --   -----------  ----------------------
0441  09  -2.70000E+00  -0572 -0562  0561  0571
0442  02  -1.20500E-03  -0572 -0561  0571 #0451
                        #0501 #0505 #0511 #0512
                        #0513 #0514 #0515 #0516
0443  01  -8.00000E+00  -0564 -0544  0563  0572
0444  02  -1.20500E-03  -0563 -0544  0572
0445  01  -8.00000E+00  -0571 -0564  0563  0570
0446  02  -1.20500E-03  -0571 -0563  0570 #0516
                        #0517 #0518 #0519
0447  01  -8.00000E+00  -0570 -0566  0565  0569
0448  02  -1.20500E-03  -0570 -0565  0569
0449  01  -8.00000E+00  -0569 -0568  0550  0567
0450  02  -1.20500E-03  -0569 -0567  0550
0451  03  -1.70000E+00  -0582 -0581  0504
c
c Cell cards modeling beam port 2:
c -------------------------------
c
c Five cells are used to model beam port 2:
c (1) Cell 0461 represents the aluminum tube that forms
c     stage 1 of beam port 2.
c (2) Cell 0462 represents the air cavity in stage 1 of beam port 2.
c (3) Cell 0463 represents the stainless steel tube that forms
c     stage 2 of beam port 2.
c (4) Cell 0464 represents the air cavity in stage 2 of beam port 2.
c (5) Cell 0465 represents the sapphire filter at the end of
c     the first stage of beam port 2.
```

```
c
c     m         d                   geom
c     --   -----------  ----------------------------
0461  09  -2.70000E+00  -0615 -0612  0452  0611  0616
0462  02  -1.20500E-03  -0615 -0611  0452  0617 #0502
0463  01  -8.00000E+00  -0616 -0614 -0546  0613
0464  02  -1.20500E-03  -0616 -0613 -0546
0465  16  -3.97000E+00  -0617 -0611  0616
c
c Cell cards modeling beam port 3:
c --------------------------------
c
c Eight cells are used to model beam port 3:
c (1) Cell 0471 represents the aluminum tube that forms
c     stage 1 of beam port 3.
c (2) Cell 0472 represents the air cavity in stage 1 of beam port 3.
c (3) Cell 0473 represents the stainless steel tube that forms
c     stage 2 of beam port 3.
c (4) Cell 0474 represents the air cavity in stage 2 of beam port 3.
c (5) Cell 0475 represents the stainless steel tube that forms
c     stage 3 of beam port 3.
c (6) Cell 0476 represents the air cavity in stage 3 of beam port 3.
c (7) Cell 0477 represents the stainless steel tube that forms
c     stage 4 of beam port 3.
c (8) Cell 0478 represents the air cavity in stage 4 of beam port 3.
c
c     m         d                geom
c     --   -----------  ------------------------
0471  09  -2.70000E+00  -0632  0631 -0437  0641
0472  02  -1.20500E-03  -0631 -0437  0641 #0503
0473  01  -8.00000E+00  -0641 -0634  0633  0640
0474  02  -1.20500E-03  -0641 -0633  0640
0475  01  -8.00000E+00  -0640 -0636  0635  0639
0476  02  -1.20500E-03  -0640 -0635  0639
0477  01  -8.00000E+00  -0639 -0638  0547  0637
0478  02  -1.20500E-03  -0639 -0637  0547
c
c Cell cards modeling beam port 4:
c --------------------------------
c
c Four cells are used to model beam port 4:
c (1) Cell 0491 represents the aluminum tube that forms
c     stage 1 of beam port 4.
c (2) Cell 0492 represents the air cavity in stage 1 of beam port 4.
c (3) Cell 0493 represents the stainless steel tube that forms
c     stage 2 of beam port 4.
c (4) Cell 0494 represents the air cavity in stage 2 of beam port 4.
c
c     m         d                   geom
c     --   -----------  ----------------------------
0491  09  -2.70000E+00  -0655 -0652  0439  0452  0651
0492  02  -1.20500E-03  -0655 -0651  0439  0452 #0504
0493  01  -8.00000E+00  -0654 -0549  0655  0653
0494  02  -1.20500E-03  -0653 -0549  0655
c
c Cell cards modeling the beam port tally spheres:
c ------------------------------------------------
c
c Five cell cards, cell cards 0501, 0502, 0503, 0504, and 0505, are used to
c model five spheres, one in each of the five beam ports. These spheres are
c not currently being used, but in some other, older MCNP runs they were
c used to evaluate tallies in the beam ports.
c
c     m         d       geom
c     --   -----------  -----
0501  02  -1.20500E-03  -0661  $ The sphere in beam port 1.
```

```
0502  02  -1.20500E-03  -0662  $ The sphere in beam port 2.
0503  02  -1.20500E-03  -0663  $ The sphere in beam port 3.
0504  02  -1.20500E-03  -0664  $ The sphere in beam port 4.
0505  02  -1.20500E-03  -0665  $ The sphere in beam port 5.
c
c Cell cards modeling the primary collimator in beam port 5:
c ---------------------------------------------------------
c
c Nine cells are used to model the primary collimator in beam port 5:
c (1) Cell 0511 represents the aluminum insert guide of the primary collimator.
c (2) Cell 0512 represents the boral inlet diaphram of the primary collimator.
c (3) Cell 0513 represents the first part of the iron moderating piece of the
c     primary collimator.
c (4) Cell 0514 represents the second part of the iron moderating piece of
c     the primary collimator.
c (5) Cell 0515 represents the gamma filter of the primary collimator.
c     The gamma filter is a single bismuth crystal.
c (6) Cell 0516 represents the polyethylene moderating piece of the
c     primary collimator.
c (7) Cell 0517 represents the boral primary diaphram of the primary collimator.
c (8) Cell 0518 represents the lead gamma shield of the primary collimator.
c (9) Cell 0519 represents the aluminum fixer disk of the primary collimator.
c
c    m        d               geom
c    --  -----------  ----------------------
0511 09 -2.70000E+00 -0604 -0561  0595  0603
0512 17 -2.53000E+00 -0603 -0561  0594  0602
0513 18 -7.87400E+00 -0602 -0561  0591  0601
0514 18 -7.87400E+00 -0601 -0561  0595  0600
0515 19 -9.74700E+00 -0601 -0595  0600
0516 20 -9.30000E-01 -0600 -0561  0591  0599
0517 17 -2.53000E+00 -0599 -0561  0593  0598
0518 10 -1.13500E+01 -0598 -0561  0592  0597
0519 09 -2.70000E+00 -0597 -0561  0592  0596
c
c
c Fission Chamber Exp Cell Cards (MBS)
c ================================================
c
0691    91 -19.1 -97 910                                          $ Fission Chamber HEU
0692    01 -8.05 -91 #0691 #0697 #0698                            $ Fission Chamber Case
0693    95 -2.7 -94                                               $ Fission Chamber Wire
0694    09 -2.7 (-95 96)                                          $ Billet
0696    09 -2.7 (-93 92):(-912):(-98 99) #0691 #0692 #0693 #0694  $ Fission Chamber
Holder
0697    96 -0.0018261048 (-910 911)                               $ Fission Chamber Gas
0698    01 -8.05 -911                                             $ Fission Chamber Inner
Electrode

c ===================
c MCNP SURFACE CARDS:
c ===================
c
c Surface cards defining the boundaries of
c the TRIGA fuel elements and control rods:
c ========================================
c
c Surface cards defining the boundaries of the TRIGA fuel elements:
c ------------------------------------------------------------------
c
c The following surface cards define the boundaries of the TRIGA fuel elements.
c
c    nnnn AAA  D.DDDDDE+DD  x.xxxxxE+xx  y.yyyyyE+yy  R.RRRRRE+RR
c    ---- ---  -----------  -----------  -----------  -----------
0001      C/Z               0.00000E+00  4.35356E+00  2.85000E-01
0002      C/Z               0.00000E+00  4.35356E+00  7.87400E-01
```

```
0003      C/Z               0.00000E+00  4.35356E+00  1.81610E+00
0004      C/Z               0.00000E+00  4.35356E+00  1.86690E+00
0005      PZ  -3.73474E+01
0006      PZ  -2.84974E+01
0007      PZ  -1.98106E+01
0008      PZ  -1.97319E+01
0009      PZ   1.83681E+01
0010      PZ   2.70549E+01
0011      PZ   2.76366E+01
0012      PZ   3.17387E+01
0013      PZ   3.59297E+01
0014      PZ   3.69297E+01
c
c Surface cards defining the boundaries of the
c fuel-followed regulating and shim control rods:
c ------------------------------------------------
c
c The following surface cards define the boundaries of the fuel-followed
c regulating and shim control rods.
c
c    nnnn AAA  D.DDDDDE+DD  x.xxxxxE+xx  y.yyyyyE+yy  R.RRRRRE+RR
c    ---- ---  -----------  -----------  -----------  -----------
0021      C/Z               0.00000E+00 -8.70712E+00  2.85000E-01
0022      C/Z               0.00000E+00 -8.70712E+00  1.50749E+00
0023      C/Z               0.00000E+00 -8.70712E+00  1.57460E+00
0024      C/Z               0.00000E+00 -8.70712E+00  1.66350E+00
0025      C/Z               0.00000E+00 -8.70712E+00  1.71450E+00
0026      PZ  -7.81519E+01
0027      PZ  -7.68819E+01
0028      PZ  -6.03719E+01
0029      PZ  -5.78319E+01
0030      PZ  -1.90969E+01
0031      PZ  -1.78269E+01
0032      PZ   2.02731E+01
0033      PZ   2.05781E+01
0034      PZ   2.18481E+01
0035      PZ   3.83581E+01
0036      PZ   3.96281E+01
c
c Surface cards defining the boundaries of
c the air-followed transient control rod:
c ---------------------------------------
c
c The following surface cards define the boundaries of the air-followed
c transient control rod.
c
c    nnnn AAA  D.DDDDDE+DD  x.xxxxxE+xx  y.yyyyyE+yy  R.RRRRRE+RR
c    ---- ---  -----------  -----------  -----------  -----------
0051      C/Z               0.00000E+00  8.70712E+00  1.51130E+00
0052      C/Z               0.00000E+00  8.70712E+00  1.55200E+00
0053      C/Z               0.00000E+00  8.70712E+00  1.58750E+00
0054      PZ  -7.40371E+01
0055      PZ  -7.27621E+01
0056      PZ  -1.71919E+01
0057      PZ   2.09081E+01
0058      PZ   2.47181E+01
c
c Surface cards defining the boundaries of the central thimble
c irradiation facility, the 3-element irradiation facility,
c and the pneumatic transfer system irradiation facility:
c ============================================================
c
c Surface cards defining the boundaries of
c the central thimble irradiation facility:
c -----------------------------------------
c
```

```
c The following surface cards define the boundaries of the central thimble
c irradiation facility. The positions of these surfaces were developed from
c information extracted from chapter eight of the Safety Analysis Report for
c the University of Texas at Austin's TRIGA Mark II nuclear research reactor
c (the version dated May 1991).
c
c    nnnn AAA  D.DDDDDE+DD  R.RRRRRE+RR
c    ---- ---  -----------  -----------
0071      CZ                1.18500E+00
0072      CZ                1.69000E+00
0073      CZ                1.90500E+00
0074      PZ               -5.55504E+01
0075      PZ               -5.53474E+01
0076      PZ  -2.50000E+00
0077      PZ   2.50000E+00
0078      PZ   3.15976E+01
c
c Surface cards defining the boundaries
c of the 3-element irradiation facility:
c --------------------------------------
c
c The following surface cards define the boundaries of the 3-element (3L)
c irradiation facility. The positions of these surfaces were developed from
c drawings of the 3L that I received as attachments to an email from Mr. Tracy
c Tipping, who is the health physicist at The University of Texas at Austin's
c Nuclear Engineering Teaching Lab. I received the email on 6 November 2015.
c
c    nnnn AAA  D.DDDDDE+DD  x.xxxxxE+xx  y.yyyyyE+yy  R.RRRRRE+RR
c    ---- ---  -----------  -----------  -----------  -----------
c 0081      C/Z               8.79798E+00 -1.52375E+01  1.93929E+00
c 0082      C/Z               8.79798E+00 -1.52375E+01  2.06375E+00
c 0083      C/Z               8.79798E+00 -1.52375E+01  2.16535E+00
c 0084      C/Z               8.79798E+00 -1.52375E+01  2.23393E+00
c 0085      C/Z               8.79798E+00 -1.52375E+01  2.38125E+00
c 0086      C/Z               8.79798E+00 -1.52375E+01  2.40000E+00
c 0087      PZ  -3.31723E+01
c 0088      PZ  -3.06324E+01
c 0089      PZ  -3.05308E+01
c 0090      PZ  -3.02133E+01
c 0091      PZ   8.75792E+01
c 0092      PZ   8.94842E+01
c 0093      PZ   9.16051E+01
c 0094      PZ   9.47801E+01
c
c 0700      RCC 9E+00 -1.5E+01 37.4  0 0 21  4.10000E+00 $Cd Shell x 8.79798E+00
c 0701      RCC 9E+00 -1.5E+01 37.5  0 0 20.9  4.00000E+00 $Al Shell y -1.52375E+01
c 0702      RCC 9E+00 -1.5E+01 38  0 0 20.38  3.50000E+00 $Boron-10 Powder Shell
c 0703      RCC 9E+00 -1.5E+01 40  0 0 18.38  1.50000E+00 $B-10 N Shell
c 0704      RCC 9E+00 -1.5E+01 41  0 0 17.26  0.50000E+00 $Air Shell
c 0706      RCC 9E+00 -1.5E+01 41.1 0 0 6.86 4.50000E-01 $borosilicate glass shell
c 0707      RCC 9E+00 -1.5E+01 41.2 0 0 6.66 4.30000E-01 $air or sample gas inside BSG
c 0705      RCC 9E+00 -1.5E+01 -30 0 0 60  2.00000E+00 $Vac Shell
c 0711      RCC 9E+00 -1.5E+01 -30.001 0 0 60.002  2.001000E+00 $Al Shell around air
c 0708      TRC 9E+00 -1.5E+01 58.4 0 0 28 4.1 0.5 $pneumatic part 1
c 0709      TRC 9E+00 -1.5E+01 58.4 0 0 28 3.5 0.5 $pneumatic part 2
c 0710      RCC 9E+00 -1.5E+01 58.4 0 0 35 0.5 $transfer Al tube 1
c
c Surface cards defining the boundaries of the Swagelok
c PFA plug valve in the 3L irradiation facility:
c -----------------------------------------------------
c
c The following surface cards define the boundaries of the Swagelok PFA plug
c valve in the 3L irradiation facility. The positions of these surfaces are
c calculated in the Excel workbook having the following file name:
c Swagelok_PFA_Plug_Valve_Surface_Position_Calculations.xlsx
c
```

```
c    nnnn AAA  D.DDDDDE+DD  x.xxxxxE+xx  y.yyyyyE+yy  z.zzzzzE+zz  R.RRRRRE+RR
c    ---- ---  -----------  -----------  -----------  -----------  -----------
c 0101      C/X                          -1.58421E+01 -2.69733E+01  1.97500E-01
c 0102      C/Y               8.79798E+00              -2.69733E+01  6.81500E-01
c 0103      C/Y               8.79798E+00              -2.69733E+01  1.07250E+00
c 0104      C/Z               8.79798E+00 -1.58421E+01               1.97500E-01
c 0105      C/Z               8.79798E+00 -1.58421E+01               3.14000E-01
c 0106      C/Z               8.79798E+00 -1.58421E+01               5.50500E-01
c 0107      C/Z               8.79798E+00 -1.58421E+01               7.83500E-01
c 0108      PY  -1.68001E+01
c 0109      PY  -1.48841E+01
c 0110      PY  -1.34751E+01
c 0111      PZ  -2.98063E+01
c 0112      PZ  -2.88723E+01
c 0113      PZ  -2.69733E+01
c 0114      PZ  -2.50743E+01
c 0115      PZ  -2.42903E+01
c
c Surface cards defining the boundaries of the
c pneumatic transfer system irradiation facility:
c -----------------------------------------------
c
c The following surface cards define the boundaries of the pneumatic transfer
c system irradiation facility.
c
c    nnnn AAA  D.DDDDDE+DD  x.xxxxxE+xx  y.yyyyyE+yy  R.RRRRRE+RR
c    ---- ---  -----------  -----------  -----------  -----------
0121      C/Z              -1.13106E+01  1.95910E+01  8.69950E-01
0122      C/Z              -1.13106E+01  1.95910E+01  1.11125E+00
0123      C/Z              -1.13106E+01  1.95910E+01  1.16205E+00
0124      C/Z              -1.13106E+01  1.95910E+01  1.53543E+00
0125      C/Z              -1.13106E+01  1.95910E+01  1.74625E+00
0126      PZ  -3.58275E+00
0127      PZ  -3.37193E+00
0128      PZ  -2.99855E+00
0129      PZ  -2.94775E+00
0130      PZ  -2.07645E+00
0131      PZ   5.00000E+01
c
c Surface cards defining the boundaries of the rotary specimen
c rack outer housing and the rotary specimen rack sample tubes:
c ============================================================
c
c Surface cards defining the boundaries of
c the rotary specimen rack outer housing:
c ---------------------------------------
c
c The following surface cards define the boundaries of the rotary specimen rack
c outer housing.
c
c    nnnn AAA  D.DDDDDE+DD  R.RRRRRE+RR
c    ---- ---  -----------  -----------
0141      CZ               2.75376E+01
0142      CZ               2.82727E+01
0143      CZ               3.02394E+01
0144      CZ               3.08745E+01
0145      CZ               3.60388E+01
0146      CZ               3.66737E+01
0147      PZ   8.90270E+00
0148      PZ   9.53770E+00
0149      PZ   3.40352E+01
0150      PZ   3.63538E+01
0151      PZ   4.36690E+01
0152      PZ   4.44627E+01
c
c Surface cards defining the boundaries of
```

```
c the rotary specimen rack sample tubes:
c ---------------------------------------
c
c The following surface cards define the boundaries of the rotary specimen rack
c sample tubes.
c
c    nnnn AAA  D.DDDDDE+DD  x.xxxxxE+xx  y.yyyyyE+yy  R.RRRRRE+RR
c    ---- ---  -----------  -----------  -----------  -----------
0161      C/Z               3.34563E+01  0.00000E+00  1.74625E+00
0162      C/Z               3.34563E+01  0.00000E+00  1.67259E+00
0163      PZ   1.08077E+01
0164      PZ   1.09550E+01
0165      PZ   4.01193E+01
c
c Surface cards defining the boundaries of four rotary specimen rack flux wires:
c ------------------------------------------------------------------------------
c
c The following surface cards define the boundaries of four rotary specimen rack
c flux wires. Note that the four flux wires are assumed to be located in four
c rotary specimen rack sample tubes spaced at equal intervals around the rotary
c specimen rack. It should also be noted that the flux wires are assumed to have
c diameters of 0.038 cm (0.015 in) in accordance with a Shieldwerx cobalt flux
c wire material analysis sheet provided by Shieldwerx (Don Hanna)
c on 16 July 2015. Furthermore, the flux wires are assumed to have lengths of
c 1 cm, and they are assumed to be sitting 0.5 cm above the bottom surface of
c the rotary specimen rack sample tubes.
c
c      nnnn AAA  D.DDDDDE+DD  x.xxxxxE+xx  y.yyyyyE+yy  R.RRRRRE+RR
c      ---- ---  -----------  -----------  -----------  -----------
0171        C/Z               3.34563E+01  0.00000E+00  1.90000E-02
0172        C/Z               0.00000E+00  3.34563E+01  1.90000E-02
0173        C/Z              -3.34563E+01  0.00000E+00  1.90000E-02
0174        C/Z               0.00000E+00 -3.34563E+01  1.90000E-02
0175        PZ   1.14550E+01
0176        PZ   1.24550E+01
c
c Surfaces cards defining the boundaries of the bottom and top grid plates:
c ==========================================================================
c
c Surface cards defining the outer boundaries of the bottom grid plate:
c ---------------------------------------------------------------------
c
c The following surface cards define the outer boundaries of the bottom
c grid plate.
c
c    nnnn AAA  A.AAAAAE+AA  B.BBBBBE+BB  C.CCCCCE+CC  D.DDDDDE+DD
c    ---- ---  -----------  -----------  -----------  -----------
0181      PX                                          2.47980E+01
0182      P    1.72325E+00  1.00000E+00  0.00000E+00  5.22533E+01
0183      P    5.77110E-01  1.00000E+00  0.00000E+00  2.86332E+01
0184      PY                                          2.61214E+01
0185      P   -5.77110E-01  1.00000E+00  0.00000E+00  2.86332E+01
0186      P   -1.72325E+00  1.00000E+00  0.00000E+00  5.22533E+01
0187      PX                                         -2.47980E+01
0188      P   -1.72325E+00 -1.00000E+00  0.00000E+00  5.22533E+01
0189      P   -5.77110E-01 -1.00000E+00  0.00000E+00  2.86332E+01
0190      PY                                         -2.61214E+01
0191      P    5.77110E-01 -1.00000E+00  0.00000E+00  2.86332E+01
0192      P    1.72325E+00 -1.00000E+00  0.00000E+00  5.22533E+01
0193      PZ                                         -3.63474E+01
0194      PZ                                         -3.31724E+01
c
c Surface cards defining the outer boundaries of the top grid plate:
c ------------------------------------------------------------------
c
c The following surface cards define the outer boundaries of the top grid plate.
```

```
c
c    nnnn AAA  D.DDDDDE+DD  R.RRRRRE+RR
c    ---- ---  -----------  -----------
0200      CZ                2.76225E+01
0201      PZ   3.08102E+01
0202      PZ   3.23850E+01
c
c Surface cards defining the boundaries of the
c bottom and top grid plate fuel element cut-outs:
c -----------------------------------------------
c
c The following surface cards define the boundaries of the bottom and top grid
c plate fuel element cut-outs. There is one cut-out in the bottom grid plate and
c one cut-out in the top grid plate for each of the 121 reactor core locations,
c and thus there are 121 cylindrical surfaces in the following list.
c
c    nnnn AAA  x.xxxxxE+xx  y.yyyyyE+yy  R.RRRRRE+RR
c    ---- ---  -----------  -----------  -----------
0211      CZ                             1.91135E+00 $ The A01 cut-out.
0212      C/Z  0.00000E+00  4.35356E+00  1.91135E+00 $ The B01 cut-out.
0213      C/Z  3.76936E+00  2.17678E+00  1.91135E+00 $ The B02 cut-out.
0214      C/Z  3.76936E+00 -2.17678E+00  1.91135E+00 $ The B03 cut-out.
0215      C/Z  0.00000E+00 -4.35356E+00  1.91135E+00 $ The B04 cut-out.
0216      C/Z -3.76936E+00 -2.17678E+00  1.91135E+00 $ The B05 cut-out.
0217      C/Z -3.76936E+00  2.17678E+00  1.91135E+00 $ The B06 cut-out.
0218      C/Z  0.00000E+00  8.70712E+00  1.91135E+00 $ The C01 cut-out.
0219      C/Z  3.76936E+00  6.53034E+00  1.91135E+00 $ The C02 cut-out.
0220      C/Z  7.54126E+00  4.35356E+00  1.91135E+00 $ The C03 cut-out.
0221      C/Z  7.54126E+00  0.00000E+00  1.91135E+00 $ The C04 cut-out.
0222      C/Z  7.54126E+00 -4.35356E+00  1.91135E+00 $ The C05 cut-out.
0223      C/Z  3.76936E+00 -6.53034E+00  1.91135E+00 $ The C06 cut-out.
0224      C/Z  0.00000E+00 -8.70712E+00  1.91135E+00 $ The C07 cut-out.
0225      C/Z -3.76936E+00 -6.53034E+00  1.91135E+00 $ The C08 cut-out.
0226      C/Z -7.54126E+00 -4.35356E+00  1.91135E+00 $ The C09 cut-out.
0227      C/Z -7.54126E+00  0.00000E+00  1.91135E+00 $ The C10 cut-out.
0228      C/Z -7.54126E+00  4.35356E+00  1.91135E+00 $ The C11 cut-out.
0229      C/Z -3.76936E+00  6.53034E+00  1.91135E+00 $ The C12 cut-out.
0230      C/Z  0.00000E+00  1.30607E+01  1.91135E+00 $ The D01 cut-out.
0231      C/Z  3.76936E+00  1.08839E+01  1.91135E+00 $ The D02 cut-out.
0232      C/Z  7.54126E+00  8.70712E+00  1.91135E+00 $ The D03 cut-out.
0233      C/Z  1.13106E+01  6.53034E+00  1.91135E+00 $ The D04 cut-out.
0234      C/Z  1.13106E+01  2.17678E+00  1.91135E+00 $ The D05 cut-out.
0235      C/Z  1.13106E+01 -2.17678E+00  1.91135E+00 $ The D06 cut-out.
0236      C/Z  1.13016E+01 -6.53034E+00  1.91135E+00 $ The D07 cut-out.
0237      C/Z  7.54126E+00 -8.70712E+00  1.91135E+00 $ The D08 cut-out.
0238      C/Z  3.76936E+00 -1.08839E+01  1.91135E+00 $ The D09 cut-out.
0239      C/Z  0.00000E+00 -1.30607E+01  1.91135E+00 $ The D10 cut-out.
0240      C/Z -3.76936E+00 -1.08839E+01  1.91135E+00 $ The D11 cut-out.
0241      C/Z -7.54126E+00 -8.70712E+00  1.91135E+00 $ The D12 cut-out.
0242      C/Z -1.13016E+01 -6.53034E+00  1.91135E+00 $ The D13 cut-out.
0243      C/Z -1.13106E+01 -2.17678E+00  1.91135E+00 $ The D14 cut-out.
0244      C/Z -1.13106E+01  2.17678E+00  1.91135E+00 $ The D15 cut-out.
0245      C/Z -1.13106E+01  6.53034E+00  1.91135E+00 $ The D16 cut-out.
0246      C/Z -7.54126E+00  8.70712E+00  1.91135E+00 $ The D17 cut-out.
0247      C/Z -3.76936E+00  1.08839E+01  1.91135E+00 $ The D18 cut-out.
0248      C/Z  0.00000E+00  1.74142E+01  1.91135E+00 $ The E01 cut-out.
0249      C/Z  3.76936E+00  1.52375E+01  1.91135E+00 $ The E02 cut-out.
0250      C/Z  7.54126E+00  1.30607E+01  1.91135E+00 $ The E03 cut-out.
0251      C/Z  1.13106E+01  1.08839E+01  1.91135E+00 $ The E04 cut-out.
0252      C/Z  1.50825E+01  8.70712E+00  1.91135E+00 $ The E05 cut-out.
0253      C/Z  1.50825E+01  4.35356E+00  1.91135E+00 $ The E06 cut-out.
0254      C/Z  1.50825E+01  0.00000E+00  1.91135E+00 $ The E07 cut-out.
0255      C/Z  1.50825E+01 -4.35356E+00  1.91135E+00 $ The E08 cut-out.
0256      C/Z  1.50825E+01 -8.70712E+00  1.91135E+00 $ The E09 cut-out.
0257      C/Z  1.13106E+01 -1.08839E+01  1.91135E+00 $ The E10 cut-out.
0258      C/Z  7.54126E+00 -1.30607E+01  1.91135E+00 $ The E11 cut-out.
```

```
0259      C/Z  3.76936E+00 -1.52375E+01  1.91135E+00 $ The E12 cut-out.
0260      C/Z  0.00000E+00 -1.74142E+01  1.91135E+00 $ The E13 cut-out.
0261      C/Z -3.76936E+00 -1.52375E+01  1.91135E+00 $ The E14 cut-out.
0262      C/Z -7.54126E+00 -1.30607E+01  1.91135E+00 $ The E15 cut-out.
0263      C/Z -1.13106E+01 -1.08839E+01  1.91135E+00 $ The E16 cut-out.
0264      C/Z -1.50825E+01 -8.70712E+00  1.91135E+00 $ The E17 cut-out.
0265      C/Z -1.50825E+01 -4.35356E+00  1.91135E+00 $ The E18 cut-out.
0266      C/Z -1.50825E+01  0.00000E+00  1.91135E+00 $ The E19 cut-out.
0267      C/Z -1.50825E+01  4.35356E+00  1.91135E+00 $ The E20 cut-out.
0268      C/Z -1.50825E+01  8.70712E+00  1.91135E+00 $ The E21 cut-out.
0269      C/Z -1.13106E+01  1.08839E+01  1.91135E+00 $ The E22 cut-out.
0270      C/Z -7.54126E+00  1.30607E+01  1.91135E+00 $ The E23 cut-out.
0271      C/Z -3.76936E+00  1.52375E+01  1.91135E+00 $ The E24 cut-out.
0272      C/Z  0.00000E+00  2.17678E+01  1.91135E+00 $ The F01 cut-out.
0273      C/Z  3.76936E+00  1.95910E+01  1.91135E+00 $ The F02 cut-out.
0274      C/Z  7.54126E+00  1.74142E+01  1.91135E+00 $ The F03 cut-out.
0275      C/Z  1.13106E+01  1.52375E+01  1.91135E+00 $ The F04 cut-out.
0276      C/Z  1.50825E+01  1.30607E+01  1.91135E+00 $ The F05 cut-out.
0277      C/Z  1.88519E+01  1.08839E+01  1.91135E+00 $ The F06 cut-out.
0278      C/Z  1.88519E+01  6.53034E+00  1.91135E+00 $ The F07 cut-out.
0279      C/Z  1.88519E+01  2.17678E+00  1.91135E+00 $ The F08 cut-out.
0280      C/Z  1.88519E+01 -2.17678E+00  1.91135E+00 $ The F09 cut-out.
0281      C/Z  1.88519E+01 -6.53034E+00  1.91135E+00 $ The F10 cut-out.
0282      C/Z  1.88519E+01 -1.08839E+01  1.91135E+00 $ The F11 cut-out.
0283      C/Z  1.50825E+01 -1.30607E+01  1.91135E+00 $ The F12 cut-out.
0284      C/Z  1.13106E+01 -1.52375E+01  1.91135E+00 $ The F13 cut-out.
0285      C/Z  7.54126E+00 -1.74142E+01  1.91135E+00 $ The F14 cut-out.
0286      C/Z  3.76936E+00 -1.95910E+01  1.91135E+00 $ The F15 cut-out.
0287      C/Z  0.00000E+00 -2.17678E+01  1.91135E+00 $ The F16 cut-out.
0288      C/Z -3.76936E+00 -1.95910E+01  1.91135E+00 $ The F17 cut-out.
0289      C/Z -7.54126E+00 -1.74142E+01  1.91135E+00 $ The F18 cut-out.
0290      C/Z -1.13106E+01 -1.52375E+01  1.91135E+00 $ The F19 cut-out.
0291      C/Z -1.50825E+01 -1.30607E+01  1.91135E+00 $ The F20 cut-out.
0292      C/Z -1.88519E+01 -1.08839E+01  1.91135E+00 $ The F21 cut-out.
0293      C/Z -1.88519E+01 -6.53034E+00  1.91135E+00 $ The F22 cut-out.
0294      C/Z -1.88519E+01 -2.17678E+00  1.91135E+00 $ The F23 cut-out.
0295      C/Z -1.88519E+01  2.17678E+00  1.91135E+00 $ The F24 cut-out.
0296      C/Z -1.88519E+01  6.53034E+00  1.91135E+00 $ The F25 cut-out.
0297      C/Z -1.88519E+01  1.08839E+01  1.91135E+00 $ The F26 cut-out.
0298      C/Z -1.50825E+01  1.30607E+01  1.91135E+00 $ The F27 cut-out.
0299      C/Z -1.13106E+01  1.52375E+01  1.91135E+00 $ The F28 cut-out.
0300      C/Z -7.54126E+00  1.74142E+01  1.91135E+00 $ The F29 cut-out.
0301      C/Z -3.76936E+00  1.95910E+01  1.91135E+00 $ The F30 cut-out.
0302      C/Z  3.76936E+00  2.39446E+01  1.91135E+00 $ The G02 cut-out.
0303      C/Z  7.54126E+00  2.17678E+01  1.91135E+00 $ The G03 cut-out.
0304      C/Z  1.13106E+01  1.95910E+01  1.91135E+00 $ The G04 cut-out.
0305      C/Z  1.50825E+01  1.74142E+01  1.91135E+00 $ The G05 cut-out.
0306      C/Z  1.88519E+01  1.52375E+01  1.91135E+00 $ The G06 cut-out.
0307      C/Z  2.26212E+01  8.70712E+00  1.91135E+00 $ The G08 cut-out.
0308      C/Z  2.26212E+01  4.35356E+00  1.91135E+00 $ The G09 cut-out.
0309      C/Z  2.26212E+01  0.00000E+00  1.91135E+00 $ The G10 cut-out.
0310      C/Z  2.26212E+01 -4.35356E+00  1.91135E+00 $ The G11 cut-out.
0311      C/Z  2.26212E+01 -8.70712E+00  1.91135E+00 $ The G12 cut-out.
0312      C/Z  1.88519E+01 -1.52375E+01  1.91135E+00 $ The G14 cut-out.
0313      C/Z  1.50825E+01 -1.74142E+01  1.91135E+00 $ The G15 cut-out.
0314      C/Z  1.13106E+01 -1.95910E+01  1.91135E+00 $ The G16 cut-out.
0315      C/Z  7.54126E+00 -2.17678E+01  1.91135E+00 $ The G17 cut-out.
0316      C/Z  3.76936E+00 -2.39446E+01  1.91135E+00 $ The G18 cut-out.
0317      C/Z -3.76936E+00 -2.39446E+01  1.91135E+00 $ The G20 cut-out.
0318      C/Z -7.54126E+00 -2.17678E+01  1.91135E+00 $ The G21 cut-out.
0319      C/Z -1.13106E+01 -1.95910E+01  1.91135E+00 $ The G22 cut-out.
0320      C/Z -1.50825E+01 -1.74142E+01  1.91135E+00 $ The G23 cut-out.
0321      C/Z -1.88519E+01 -1.52375E+01  1.91135E+00 $ The G24 cut-out.
0322      C/Z -2.26212E+01 -8.70712E+00  1.91135E+00 $ The G26 cut-out.
0323      C/Z -2.26212E+01 -4.35356E+00  1.91135E+00 $ The G27 cut-out.
0324      C/Z -2.26212E+01  0.00000E+00  1.91135E+00 $ The G28 cut-out.
```

```
0325      C/Z -2.26212E+01  4.35356E+00  1.91135E+00 $ The G29 cut-out.
0326      C/Z -2.26212E+01  8.70712E+00  1.91135E+00 $ The G30 cut-out.
0327      C/Z -1.88519E+01  1.52375E+01  1.91135E+00 $ The G32 cut-out.
0328      C/Z -1.50825E+01  1.74142E+01  1.91135E+00 $ The G33 cut-out.
0329      C/Z -1.13106E+01  1.95910E+01  1.91135E+00 $ The G34 cut-out.
0330      C/Z -7.54126E+00  2.17678E+01  1.91135E+00 $ The G35 cut-out.
0331      C/Z -3.76936E+00  2.39446E+01  1.91135E+00 $ The G36 cut-out.
c
c Surfaces cards defining the boundaries of the
c other cut-outs unique to the bottom grid plate:
c ------------------------------------------------
c
c The following surface cards define the boundaries of the other cut-outs that
c are unique to the bottom grid plate.
c
c    nnnn AAA  x.xxxxxE+xx  y.yyyyyE+yy  R.RRRRRE+RR
c    ---- ---  -----------  -----------  -----------
0351      C/Z  2.19964E+01  1.27000E+01  5.15940E-01
0352      C/Z  1.11252E+00  2.54000E+01  3.96870E-01
0353      C/Z  0.00000E+00  2.54000E+01  5.15940E-01
0354      C/Z -8.79856E+00  1.08839E+01  5.55620E-01
0355      C/Z -2.19964E+01  1.27000E+01  5.15940E-01
0356      C/Z -2.19964E+01 -1.27000E+01  5.15940E-01
0357      C/Z  0.00000E+00 -2.54000E+01  5.15940E-01
0358      C/Z  1.11252E+00 -2.54000E+01  3.96870E-01
0359      C/Z  8.79856E+00 -1.52375E+01  5.55620E-01
0360      C/Z  2.19964E+01 -1.27000E+01  5.15940E-01
c
c Surface cards defining the boundaries of the other cut-outs
c that are common to both the bottom and top grid plates:
c ------------------------------------------------------------
c
c The following surface cards define the boundaries of the other cut-outs that
c are common to both the bottom and top grid plates.
c
c    nnnn AAA  x.xxxxxE+xx  y.yyyyyE+yy  R.RRRRRE+RR
c    ---- ---  -----------  -----------  -----------
0371      C/Z -2.38785E+01 -2.17678E+00  2.57810E-01
0372      C/Z -2.00929E+01 -2.17678E+00  2.57810E-01
0373      C/Z -1.63398E+01 -2.17678E+00  2.57810E-01
0374      C/Z -1.38252E+01 -2.17678E+00  2.57810E-01
0375      C/Z -8.79856E+00 -2.17678E+00  2.57810E-01
0376      C/Z -6.28396E+00 -2.17678E+00  2.57810E-01
0377      C/Z -1.25730E+00 -2.17678E+00  2.57810E-01
0378      C/Z  1.25730E+00 -2.17678E+00  2.57810E-01
0379      C/Z  6.28396E+00 -2.17678E+00  2.57810E-01
0380      C/Z  8.79856E+00 -2.17678E+00  2.57810E-01
0381      C/Z  1.38252E+01 -2.17678E+00  2.57810E-01
0382      C/Z  1.63398E+01 -2.17678E+00  2.57810E-01
0383      C/Z  2.00929E+01 -2.17678E+00  2.57810E-01
0384      C/Z  2.38785E+01 -2.17678E+00  2.57810E-01
0385      C/Z  1.25730E+00 -2.39446E+01  2.57810E-01
0386      C/Z  1.25730E+00 -1.95910E+01  2.57810E-01
0387      C/Z  1.25730E+00 -1.52375E+01  2.57810E-01
0388      C/Z  1.25730E+00 -1.08839E+01  2.57810E-01
0389      C/Z  1.25730E+00 -6.53034E+00  2.57810E-01
0390      C/Z  1.25730E+00  2.17678E+00  2.57810E-01
0391      C/Z  1.25730E+00  6.53034E+00  2.57810E-01
0392      C/Z  1.25730E+00  1.08839E+01  2.57810E-01
0393      C/Z  1.25730E+00  1.52375E+01  2.57810E-01
0394      C/Z  1.25730E+00  1.95910E+01  2.57810E-01
0395      C/Z  1.25730E+00  2.39446E+01  2.57810E-01
c
c Surface cards defining the boundaries of the
c other cut-outs unique to the top grid plate:
c ---------------------------------------------
```

```
c
c The following surface cards define the boundaries of the other cut-outs that
c are unique to the top grid plate.
c
c    nnnn AAA  x.xxxxxE+xx  y.yyyyyE+yy  R.RRRRRE+RR
c    ---- ---  -----------  -----------  -----------
0411      C/Z  2.66700E+01 -1.11252E+00  3.17500E-01
0412      C/Z  2.66700E+01  0.00000E+00  5.15940E-01
0413      C/Z  1.33350E+01  2.30962E+01  5.15940E-01
0414      C/Z -1.33350E+01  2.30962E+01  5.15940E-01
0415      C/Z -2.17170E+01  1.25476E+01  7.93750E-01  $ 5/8 in Cut Out ***
0416      C/Z -2.66700E+01  0.00000E+00  5.15940E-01
0417      C/Z -2.66700E+01 -1.11252E+00  3.17500E-01
0418      C/Z -1.33350E+01 -2.30962E+01  5.15940E-01
0419      C/Z  1.33350E+01 -2.30962E+01  5.15940E-01
0420      C/Z  2.17170E+01 -1.25476E+01  7.93750E-01  $ 5/8 in Cut Out
c
c
c Fission Chamber Exp Surface Cards (MBS)
c ================================================
c
c   -- 91 is Outer cylinder representing Fission Chamber Case
c   -- 92 is Inner cylinder representing Fission Chamber Holder
c   -- 93 is Outer cylinder representing Fission Chamber Holder
c   -- 94 is cylinder representing Fission Chamber Wire
c   -- 95 is Outer cylinder representing Billet
c   -- 96 is Inner cylinder representing Billet
c   -- 97 is Outer cylinder representing 90%+ HEU
c   -- 98 is Outer cylinder representing Fission Chamber Top Holder
c   -- 99 is Inner cylinder representing Fission Chamber Top Holder
c   -- 910 is Fission Chamber Fill Gas
c   -- 911 is Fission Chamber Inner Electrode
c   -- 912 is Fission Chamber Holder Bottom
c
 91       RCC -2.17170E+01 1.25476E+01 -5.004   0 0 8.6    0.235
 92       RCC -2.17170E+01 1.25476E+01 -6.004   0 0 38.39  0.424
 93       RCC -2.17170E+01 1.25476E+01 -5.504   0 0 37.89  0.635
 94       RCC -2.17170E+01 1.25476E+01 3.596    0 0 35     0.05
 95       RCC -2.17170E+01 1.25476E+01 3.596    0 0 8.8    0.406
 96       RCC -2.17170E+01 1.25476E+01 3.596    0 0 8.8    0.177
 97       RCC -2.17170E+01 1.25476E+01 -3.454   0 0 2.7    0.000005
 98       RCC -2.17170E+01 1.25476E+01 32.386   0 0 5.08   1.27
 99       RCC -2.17170E+01 1.25476E+01 32.386   0 0 5.08   0.424
 910      RCC -2.17170E+01 1.25476E+01 -3.454   0 0 2.7    0.22
 911      RCC -2.17170E+01 1.25476E+01 -3.454   0 0 2.7    0.12
 912      RCC -2.17170E+01 1.25476E+01 -5.504   0 0 0.5    0.635
c
c
c Surface cards defining the boundaries of the
c reflector inner, outer, lower, and upper shrouds:
c ================================================
c
c Surface cards defining the boundaries of the reflector inner shroud:
c ---------------------------------------------------------------------
c
c The following surface cards define the outer and upper boundaries of the
c reflector inner shroud. The lower and inner boundaries of the reflector inner
c shroud are formed by the surface cards used to define the outer boundaries of
c the bottom grid plate.
c
c    nnnn AAA  A.AAAAAE+AA  B.BBBBBE+BB  C.CCCCCE+CC  D.DDDDDE+DD
c    ---- ---  -----------  -----------  -----------  -----------
0431      PX                                         2.54330E+01
0432      P    1.72325E+00  1.00000E+00  0.00000E+00  5.35234E+01
0433      P    5.77110E-01  1.00000E+00  0.00000E+00  2.93636E+01
0434      PY                                         2.67564E+01
```

```
0435      P   -5.77110E-01  1.00000E+00  0.00000E+00  2.93636E+01
0436      P   -1.72325E+00  1.00000E+00  0.00000E+00  5.35234E+01
0437      PX                                          -2.54330E+01
0438      P   -1.72325E+00 -1.00000E+00  0.00000E+00  5.35234E+01
0439      P   -5.77110E-01 -1.00000E+00  0.00000E+00  2.93636E+01
0440      PY                                          -2.67564E+01
0441      P    5.77110E-01 -1.00000E+00  0.00000E+00  2.93636E+01
0442      P    1.72325E+00 -1.00000E+00  0.00000E+00  5.35234E+01
0443      PZ                                           2.89052E+01
c
c Surface cards defining the boundaries of the reflector outer shroud:
c ---------------------------------------------------------------------
c
c The following surface cards define the boundaries of the reflector
c outer shroud.
c
c    nnnn AAA  D.DDDDDE+DD  R.RRRRRE+RR
c    ---- ---  -----------  -----------
0451      CZ                5.34988E+01
0452      CZ                5.47688E+01
0453      PZ  -3.22199E+01
0454      PZ   2.87401E+01
c
c Surface cards defining the boundaries of the reflector lower shroud:
c ---------------------------------------------------------------------
c
c The following surface cards define the boundaries of the reflector
c lower shroud.
c
c    nnnn AAA  D.DDDDDE+DD  R.RRRRRE+RR
c    ---- ---  -----------  -----------
0461      PZ  -2.92100E+01
0462      PZ  -2.79400E+01
0463      CZ                5.22288E+01
c
c Surface cards defining the boundaries of the reflector upper shroud:
c ---------------------------------------------------------------------
c
c The following surface cards define the boundaries of the reflector
c upper shroud.
c
c    nnnn AAA  D.DDDDDE+DD  R.RRRRRE+RR
c    ---- ---  -----------  -----------
0471      CZ                2.94481E+01
0472      CZ                3.00831E+01
0473      CZ                3.68300E+01
0474      CZ                3.74650E+01
0475      PZ   6.99770E+00
0476      PZ   7.63270E+00
0477      PZ   2.63652E+01
0478      PZ   3.39852E+01
0479      PZ   2.82702E+01
0480      PZ   2.95402E+01
c
c Surface cards defining the boundaries of the reflector
c shroud around the beam port 3 reflector penetration:
c -----------------------------------------------------
c
c The following surface cards define the boundaries of the reflector shroud
c around the beam port 3 penetration.
c
c    nnnn AAA  y.yyyyyE+yy  z.zzzzzE+zz  R.RRRRRE+RR
c    ---- ---  -----------  -----------  -----------
0491      C/X  0.00000E+00 -6.98500E+00  9.52500E+00
0492      C/X  0.00000E+00 -6.98500E+00  1.01600E+01
c
```

```
c Surface cards defining the boundaries of the
c reflector cut-out adjacent to beam ports 1 and 5:
c -------------------------------------------------
c
c The following surface cards define the boundaries of the reflector cut-out
c adjacent to beam ports 1 and 5.
c
c    nnnn AAA  D.DDDDDE+DD
c    ---- ---  -----------
0501      PX   3.52552E+01
0502      PZ  -1.53850E+01
0503      PZ   1.41500E+00
0504      PY  -9.52500E+00
0505      PY   9.52500E+00
c
c Surface cards defining the outer surfaces of the reactor pool water
c volumes, the aluminum reactor pool liner, and the biological shield:
c ====================================================================
c
c Surface cards defining the outer boundaries of the reactor pool water volumes:
c -------------------------------------------------------------------------------
c
c The following surface cards are used to define the outer boundaries of three
c reactor pool water volumes. The three water volumes collectively constitute
c the larger reactor pool water volume: surfaces 0511, 0518, and 0519 define
c the outer boundaries of one reactor pool water volume; surfaces 0512, 0513,
c 0518, and 0519 define the outer boundaries of a second reactor pool water
c volume; and surfaces 0512, 0513, 0514, 0515, 0516, 0517, 0518, and 0519
c define the outer boundaries of a third reactor pool water volume.
c
c    nnnn AAA  D.DDDDDE+DD  x.xxxxxE+xx  y.yyyyyE+yy  R.RRRRRE+RR
c    ---- ---  -----------  -----------  -----------  -----------
c
0511      CZ                                          2.70000E+01
0512      CZ                                          9.90600E+01
0513      C/Z               9.90600E+01  0.00000E+00  9.90600E+01
0514      PX   0.00000E+00
0515      PX   9.90600E+01
0516      PY  -9.90600E+01
0517      PY   9.90600E+01
0518      PZ  -9.71850E+01
0519      PZ   9.50000E+01
c
c Surface cards defining the outer boundaries
c of the aluminum reactor pool liner:
c -------------------------------------------
c
c The following surface cards are used to define the outer boundaries of the
c aluminum reactor pool liner that separates the reactor pool water from the
c biological shield.
c
c    nnnn AAA  D.DDDDDE+DD  x.xxxxxE+xx  y.yyyyyE+yy  R.RRRRRE+RR
c    ---- ---  -----------  -----------  -----------  -----------
0531      CZ                                          1.00330E+02
0532      C/Z               9.90600E+01  0.00000E+00  1.00330E+02
0533      PY  -1.00330E+02
0534      PY   1.00330E+02
c
c Surface cards defining the outer boundaries of the biological shield:
c ---------------------------------------------------------------------
c
c The following surface cards are used to define the outer boundaries of the
c biological shield.
c
c    nnnn AAA  A.AAAAAE+AA  B.BBBBBE+BB  C.CCCCCE+CC  D.DDDDDE+DD
c    ---- ---  -----------  -----------  -----------  -----------
```

```
0541      PX                                          3.88620E+02
0542      P    1.73212E+00  1.00000E+00  0.00000E+00  7.60924E+02
0543      P    5.77551E-01  1.00000E+00  0.00000E+00  4.22392E+02
0544      PY                                          3.42900E+02
0545      P   -5.77844E-01  1.00000E+00  0.00000E+00  3.96014E+02
0546      P   -1.74715E+00  1.00000E+00  0.00000E+00  6.89491E+02
0547      PX                                         -3.42900E+02
0548      P   -1.74715E+00 -1.00000E+00  0.00000E+00  6.89491E+02
0549      P   -5.77844E-01 -1.00000E+00  0.00000E+00  3.96014E+02
0550      PY                                         -3.42900E+02
0551      P    5.77551E-01 -1.00000E+00  0.00000E+00  4.22392E+02
0552      P    1.73212E+00 -1.00000E+00  0.00000E+00  7.60924E+02
c
c Surface cards defining the outer boundaries of five
c cylindrical volumes surrounding each of the five beam ports:
c -------------------------------------------------------------
c
c The following surface cards are used to define the outer boundaries of five
c cylindrical volumes surrounding each of the five beam ports.
c
c    nnnn AAA  x.xxxxxE+xx  y.yyyyyE+yy  z.zzzzzE+zz  R.RRRRRE+RR
c    ---- ---  -----------  -----------  -----------  -----------
0553      C/Y  3.52552E+01              -6.98500E+00  3.50000E+01 $ BP 1 and 5.
0554 0554 CX                                         3.50000E+01 $ BP 2.
0555      C/X               0.00000E+00 -6.98500E+00  3.50000E+01 $ BP 3.
0556 0556 CX                                         3.50000E+01 $ BP 4.
c
c Surface cards defining the boundaries of beam ports 1, 2, 3, 4, and 5:
c ======================================================================
c
c Surface cards defining the boundaries of beam ports 1 and 5:
c -------------------------------------------------------------
c
c The following surface cards define the boundaries of beam ports 1 and 5.
c
c    nnnn AAA -D.DDDDDE+DD -x.xxxxxE+xx -z.zzzzzE+zz -R.RRRRRE+RR
c    ---- ---  -----------  -----------  -----------  -----------
0561      C/Y               3.52552E+01 -6.98500E+00  7.77875E+00
0562      C/Y               3.52552E+01 -6.98500E+00  8.41375E+00
0563      C/Y               3.52552E+01 -6.98500E+00  1.03188E+01
0564      C/Y               3.52552E+01 -6.98500E+00  1.09538E+01
0565      C/Y               3.52552E+01 -6.98500E+00  1.55575E+01
0566      C/Y               3.52552E+01 -6.98500E+00  1.61925E+01
0567      C/Y               3.52552E+01 -6.98500E+00  1.96850E+01
0568      C/Y               3.52552E+01 -6.98500E+00  2.03200E+01
0569      PY  -2.51460E+02
0570      PY  -1.67640E+02
0571      PY  -1.23190E+02
0572      PY   1.80000E+02
c
c Surface cards defining the boundaries of the
c graphite scattering block in beam ports 1 and 5:
c ------------------------------------------------
c
c The following surface cards define the boundaries of the graphite scattering
c block in beam ports 1 and 5. The positions of these surfaces were developed
c from information extracted from the doctoral dissertation of Young Gyun Jo
c titled "Development of a Thermal Neutron Imaging Facility for Real Time
c Neutron Radiography and Computed Tomography."
c
c    nnnn AAA -D.DDDDDE+DD -x.xxxxxE+xx -z.zzzzzE+zz -R.RRRRRE+RR
c    ---- ---  -----------  -----------  -----------  -----------
0581      PY  -2.54000E+00
0582      C/Y               3.52552E+01 -6.98500E+00  6.35000E+00
c
c Surface cards defining the boundaries of
```

```
c the primary collimator in beam port 5:
c ---------------------------------------
c
c The following surface cards define the boundaries of the primary collimator
c in beam port 5. The positions of these surfaces were developed from
c information extracted from the doctoral dissertation of Young Gyun Jo
c titled "Development of a Thermal Neutron Imaging Facility for Real
c Time Neutron Radiography and Computed Tomography."
c
c    nnnn AAA  x.xxxxxE+xx  y.yyyyyE+yy  z.zzzzzE+zz  t.tttttE+tt  +/-1
c    ---- ---  -----------  -----------  -----------  -----------  ----
0591      K/Y  3.52552E+01 -1.86820E+02 -6.98500E+00  1.55000E-03  1
0592      K/Y  3.52552E+01 -1.10620E+02 -6.98500E+00  1.55000E-03 -1
c
c    nnnn AAA  D.DDDDDE+DD -x.xxxxxE+xx -z.zzzzzE+zz -R.RRRRRE+RR
c    ---- ---  -----------  -----------  -----------  -----------
0593      C/Y               3.52552E+01 -6.98500E+00  1.00000E+00
0594      C/Y               3.52552E+01 -6.98500E+00  2.63000E+00
0595      C/Y               3.52552E+01 -6.98500E+00  3.24000E+00
0596      PY  -1.56340E+02
0597      PY  -1.53800E+02
0598      PY  -1.48820E+02
0599      PY  -1.48080E+02
0600      PY  -1.20140E+02
0601      PY  -1.17220E+02
0602      PY  -1.10620E+02
0603      PY  -1.09340E+02
0604      PY  -1.01700E+02
c
c Surface cards defining the boundaries of beam port 2:
c -----------------------------------------------------
c
c The following surface cards define the boundaries of beam port 2.
c
c    nnnn AAA  D.DDDDDE+DD  R.RRRRRE+RR
c    ---- ---  -----------  -----------
0611 0611 CX                7.77875E+00
0612 0612 CX                8.41375E+00
0613 0613 CX                1.03188E+01
0614 0614 CX                1.09538E+01
0615 0615 PX   0.00000E+00
0616 0616 PX   0.00000E+00
0617 0617 PX   0.00000E+00
c
c Surface cards defining the boundaries of beam port 3:
c -----------------------------------------------------
c
c The following surface cards define the boundaries of beam port 3.
c
c    nnnn AAA  D.DDDDDE+DD  y.yyyyyE+yy  z.zzzzzE+zz  R.RRRRRE+RR
c    ---- ---  -----------  -----------  -----------  -----------
0631      C/X               0.00000E+00 -6.98500E+00  7.70255E+00
0632      C/X               0.00000E+00 -6.98500E+00  8.41375E+00
0633      C/X               0.00000E+00 -6.98500E+00  1.03188E+01
0634      C/X               0.00000E+00 -6.98500E+00  1.09538E+01
0635      C/X               0.00000E+00 -6.98500E+00  1.55575E+01
0636      C/X               0.00000E+00 -6.98500E+00  1.61925E+01
0637      C/X               0.00000E+00 -6.98500E+00  1.96850E+01
0638      C/X               0.00000E+00 -6.98500E+00  2.03200E+01
0639      PX  -2.51460E+02
0640      PX  -1.67640E+02
0641      PX  -1.23190E+02
c
c Surface cards defining the boundaries of beam port 4:
c -----------------------------------------------------
c
```

```
c The following surface cards define the boundaries of beam port 4.
c
c    nnnn AAA  A.AAAAAE+AA  B.BBBBBE+BB  C.CCCCCE+CC  D.DDDDDE+DD  R.RRRRRE+RR
c    ---- ---  -----------  -----------  -----------  -----------  -----------
0651 0651 CX                                                       7.77875E+00
0652 0652 CX                                                       8.41375E+00
0653 0653 CX                                                       1.03188E+01
0654 0654 CX                                                       1.09538E+01
0655 0655 P   -5.77110E-01 -1.00000E+00  0.00000E+00  2.86332E+01
c
c Surface cards defining the boundaries of five spheres that
c may be used to support evaluating beam port flux tallies:
c ---------------------------------------------------------
c
c The following surface cards define the boundaries of five spheres, one in
c each of the five beam ports. These spheres are not currently being used,
c but in some other, older MCNP runs they were used to evaluate tallies
c in each of the beam ports.
c
c    nnnn AAA  x.xxxxxE+xx  y.yyyyyE+yy  z.zzzzzE+zz  R.RRRRRE+RR
c    ---- ---  -----------  -----------  -----------  -----------
0661      S    3.52552E+01  5.40000E+01 -6.98500E+00  2.50000E+00
0662      S   -3.00000E+01  5.60000E+01 -6.98500E+00  2.50000E+00
0663      S   -6.50000E+01  0.00000E+00 -6.98500E+00  2.50000E+00
0664      S   -3.30000E+01 -5.60000E+01 -6.98500E+00  2.50000E+00
0665      S    3.52552E+01 -5.40000E+01 -6.98500E+00  2.50000E+00

c ================
c MCNP DATA CARDS:
c ================
c
c TR: Coordinate transformations:
c ================================
c
c Note that unless noted otherwise all of the control rod and fuel element
c coordinate transformations are relative to the fuel element in reactor core
c location B01. Also note that because the coordinate transformations are
c relative to the fuel element in reactor core location B01, the fuel element
c in reactor core location B01 does not require any coordinate transformations.
c
c B-ring fuel element coordinate transformations:
c ------------------------------------------------
c
c          o1           o2           o3
c       -----------  -----------  -----------
TR0082  3.76936E+00 -2.17678E+00  0.00000E+00 $ Fuel element in location B02.
TR0083  3.76936E+00 -6.53034E+00  0.00000E+00 $ Fuel element in location B03.
TR0084  0.00000E+00 -8.70712E+00  0.00000E+00 $ Fuel element in location B04.
TR0085 -3.76936E+00 -6.53034E+00  0.00000E+00 $ Fuel element in location B05.
TR0086 -3.76936E+00 -2.17678E+00  0.00000E+00 $ Fuel element in location B06.
c
c C-ring fuel element and control rod coordinate transformations:
c ---------------------------------------------------------------
c
c          o1           o2           o3
c       -----------  -----------  -----------
TR0087  0.00000E+00  0.00000E+00  2.26620E+01 $ Transient rod in location C01.
TR0088  3.76936E+00  2.17678E+00  0.00000E+00 $ Fuel element in location C02.
TR0089  7.54126E+00  0.00000E+00  0.00000E+00 $ Fuel element in location C03.
TR0090  7.54126E+00 -4.35356E+00  0.00000E+00 $ Fuel element in location C04.
TR0091  7.54126E+00 -8.70712E+00  0.00000E+00 $ Fuel element in location C05.
TR0092  3.76936E+00 -1.08839E+01  0.00000E+00 $ Fuel element in location C06.
TR0093  0.00000E+00  0.00000E+00  2.26810E+01 $ Regulating rod in location C07.
TR0094 -3.76936E+00 -1.08839E+01  0.00000E+00 $ Fuel element in location C08.
TR0095 -7.54126E+00 -8.70712E+00  0.00000E+00 $ Fuel element in location C09.
TR0096 -7.54126E+00 -4.35356E+00  0.00000E+00 $ Fuel element in location C10.
```

```
TR0097 -7.54126E+00  0.00000E+00  0.00000E+00 $ Fuel element in location C11.
TR0098 -3.76936E+00  2.17678E+00  0.00000E+00 $ Fuel element in location C12.
c
c D-ring fuel element and control rod coordinate transformations:
c ---------------------------------------------------------------
c
c Note that the coordinate transformations associated with shim rod 1 and
c shim rod 2, coordinate transformations TR325 and TR333, respectively,
c are relative to the regulating rod in reactor core location C07.
c
c          o1           o2           o3
c       -----------  -----------  -----------
TR0099  0.00000E+00  8.70714E+00  0.00000E+00 $ Fuel element in location D01.
TR0100  3.76936E+00  6.53034E+00  0.00000E+00 $ Fuel element in location D02.
TR0101  7.54126E+00  4.35356E+00  0.00000E+00 $ Fuel element in location D03.
TR0102  1.13106E+01  2.17678E+00  0.00000E+00 $ Fuel element in location D04.
TR0103  1.13106E+01 -2.17678E+00  0.00000E+00 $ Fuel element in location D05.
TR0104  1.13106E+01  6.53034E+00  2.26220E+01 $ Shim rod 1 in location D06.
TR0105  1.13016E+01 -1.08839E+01  0.00000E+00 $ Fuel element in location D07.
TR0106  7.54126E+00 -1.30607E+01  0.00000E+00 $ Fuel element in location D08.
TR0107  3.76936E+00 -1.52375E+01  0.00000E+00 $ Fuel element in location D09.
TR0108  0.00000E+00 -1.74143E+01  0.00000E+00 $ Fuel element in location D10.
TR0109 -3.76936E+00 -1.52375E+01  0.00000E+00 $ Fuel element in location D11.
TR0110 -7.54126E+00 -1.30607E+01  0.00000E+00 $ Fuel element in location D12.
TR0111 -1.13016E+01 -1.08839E+01  0.00000E+00 $ Fuel element in location D13.
TR0112 -1.13106E+01  6.53034E+00  2.26220E+01 $ Shim rod 2 in location D14.
TR0113 -1.13106E+01 -2.17678E+00  0.00000E+00 $ Fuel element in location D15.
TR0114 -1.13106E+01  2.17678E+00  0.00000E+00 $ Fuel element in location D16.
TR0115 -7.54126E+00  4.35356E+00  0.00000E+00 $ Fuel element in location D17.
TR0116 -3.76936E+00  6.53034E+00  0.00000E+00 $ Fuel element in location D18.
c
c E-ring fuel element coordinate transformations:
c -----------------------------------------------
c
c Note that the coordinate transformation associated with the fuel element
c in reactor core location E11, coordinate transformation TR348, should be
c commented out if the 3L is in the reactor core.
c
c          o1           o2           o3
c       -----------  -----------  -----------
TR0117  0.00000E+00  1.30606E+01  0.00000E+00 $ Fuel element in location E01.
TR0118  3.76936E+00  1.08839E+01  0.00000E+00 $ Fuel element in location E02.
TR0119  7.54126E+00  8.70714E+00  0.00000E+00 $ Fuel element in location E03.
TR0120  1.13106E+01  6.53034E+00  0.00000E+00 $ Fuel element in location E04.
TR0121  1.50825E+01  4.35356E+00  0.00000E+00 $ Fuel element in location E05.
TR0122  1.50825E+01  0.00000E+00  0.00000E+00 $ Fuel element in location E06.
TR0123  1.50825E+01 -4.35356E+00  0.00000E+00 $ Fuel element in location E07.
TR0124  1.50825E+01 -8.70712E+00  0.00000E+00 $ Fuel element in location E08.
TR0125  1.50825E+01 -1.30607E+01  0.00000E+00 $ Fuel element in location E09.
TR0126  1.13106E+01 -1.52375E+01  0.00000E+00 $ Fuel element in location E10.
c TR0127  7.54126E+00 -1.74143E+01  0.00000E+00 $ Fuel element in location E11.
TR0128  3.76936E+00 -1.95911E+01  0.00000E+00 $ Fuel element in location E12.
TR0129  0.00000E+00 -2.17678E+01  0.00000E+00 $ Fuel element in location E13.
TR0130 -3.76936E+00 -1.95911E+01  0.00000E+00 $ Fuel element in location E14.
TR0131 -7.54126E+00 -1.74143E+01  0.00000E+00 $ Fuel element in location E15.
TR0132 -1.13106E+01 -1.52375E+01  0.00000E+00 $ Fuel element in location E16.
TR0133 -1.50825E+01 -1.30607E+01  0.00000E+00 $ Fuel element in location E17.
TR0134 -1.50825E+01 -8.70712E+00  0.00000E+00 $ Fuel element in location E18.
TR0135 -1.50825E+01 -4.35356E+00  0.00000E+00 $ Fuel element in location E19.
TR0136 -1.50825E+01  0.00000E+00  0.00000E+00 $ Fuel element in location E20.
TR0137 -1.50825E+01  4.35356E+00  0.00000E+00 $ Fuel element in location E21.
TR0138 -1.13106E+01  6.53034E+00  0.00000E+00 $ Fuel element in location E22.
TR0139 -7.54126E+00  8.70714E+00  0.00000E+00 $ Fuel element in location E23.
TR0140 -3.76936E+00  1.08839E+01  0.00000E+00 $ Fuel element in location E24.
c
c F-ring fuel element coordinate transformations:
```

```
c ------------------------------------------------
c
c Note that the coordinate transformations associated with the fuel elements
c in reactor core locations F13 and F14, coordinate transformations TR374
c and TR375, respectively, should be commented out if the 3L is in the
c reactor core.
c
c          o1           o2           o3
c       -----------  -----------  -----------
TR0141  0.00000E+00  1.74142E+01  0.00000E+00 $ Fuel element in location F01.
TR0142  3.76936E+00  1.52374E+01  0.00000E+00 $ Fuel element in location F02.
TR0143  7.54126E+00  1.30606E+01  0.00000E+00 $ Fuel element in location F03.
TR0144  1.13106E+01  1.08839E+01  0.00000E+00 $ Fuel element in location F04.
TR0145  1.50825E+01  8.70714E+00  0.00000E+00 $ Fuel element in location F05.
TR0146  1.88519E+01  6.53034E+00  0.00000E+00 $ Fuel element in location F06.
TR0147  1.88519E+01  2.17678E+00  0.00000E+00 $ Fuel element in location F07.
TR0148  1.88519E+01 -2.17678E+00  0.00000E+00 $ Fuel element in location F08.
TR0149  1.88519E+01 -6.53034E+00  0.00000E+00 $ Fuel element in location F09.
TR0150  1.88519E+01 -1.08839E+01  0.00000E+00 $ Fuel element in location F10.
TR0151  1.88519E+01 -1.52375E+01  0.00000E+00 $ Fuel element in location F11.
TR0152  1.50825E+01 -1.74142E+01  0.00000E+00 $ Fuel element in location F12.
c TR0153  1.13106E+01 -1.95910E+01  0.00000E+00 $ Fuel element in location F13.
c TR0154  7.54126E+00 -2.17678E+01  0.00000E+00 $ Fuel element in location F14.
TR0155  3.76936E+00 -2.39446E+01  0.00000E+00 $ Fuel element in location F15.
TR0156  0.00000E+00 -2.61214E+01  0.00000E+00 $ Fuel element in location F16.
TR0157 -3.76936E+00 -2.39446E+01  0.00000E+00 $ Fuel element in location F17.
TR0158 -7.54126E+00 -2.17678E+01  0.00000E+00 $ Fuel element in location F18.
TR0159 -1.13106E+01 -1.95911E+01  0.00000E+00 $ Fuel element in location F19.
TR0160 -1.50825E+01 -1.74143E+01  0.00000E+00 $ Fuel element in location F20.
TR0161 -1.88519E+01 -1.52375E+01  0.00000E+00 $ Fuel element in location F21.
TR0162 -1.88519E+01 -1.08839E+01  0.00000E+00 $ Fuel element in location F22.
TR0163 -1.88519E+01 -6.53034E+00  0.00000E+00 $ Fuel element in location F23.
TR0164 -1.88519E+01 -2.17678E+00  0.00000E+00 $ Fuel element in location F24.
TR0165 -1.88519E+01  2.17678E+00  0.00000E+00 $ Fuel element in location F25.
TR0166 -1.88519E+01  6.53034E+00  0.00000E+00 $ Fuel element in location F26.
TR0167 -1.50825E+01  8.70714E+00  0.00000E+00 $ Fuel element in location F27.
TR0168 -1.13106E+01  1.08839E+01  0.00000E+00 $ Fuel element in location F28.
TR0169 -7.54126E+00  1.30606E+01  0.00000E+00 $ Fuel element in location F29.
TR0170 -3.76936E+00  1.52374E+01  0.00000E+00 $ Fuel element in location F30.
c
c G-ring fuel element coordinate transformations:
c ------------------------------------------------
c
c Note that there are no coordinate transformations associated with the G01,
c G07, G13, G19, G25, G31, G32, or G34 reactor core locations because there
c are not fuel elements in any of these reactor core locations. Reactor core
c locations G01, G07, G13, G19, G25, and G31 are the locations that would
c be at the outer corners of the G-ring if they were actual reactor core
c locations (they're not real), and reactor core locations G32 and G34
c sometimes contain the AmBe startup source and the pneumatic transfer
c system irradiation facility, respectively, depending on the reactor
c core configuration.
c
c          o1           o2           o3
c       -----------  -----------  -----------
TR0171  3.76936E+00  1.95910E+01  0.00000E+00 $ Fuel element in location G02.
TR0172  7.54126E+00  1.74142E+01  0.00000E+00 $ Fuel element in location G03.
TR0173  1.13106E+01  1.52374E+01  0.00000E+00 $ Fuel element in location G04.
TR0174  1.50825E+01  1.30606E+01  0.00000E+00 $ Fuel element in location G05.
TR0175  1.88519E+01  1.08839E+01  0.00000E+00 $ Fuel element in location G06.
TR0176  2.26212E+01  4.35356E+00  0.00000E+00 $ Fuel element in location G08.
TR0177  2.26212E+01  0.00000E+00  0.00000E+00 $ Fuel element in location G09.
TR0178  2.26212E+01 -4.35356E+00  0.00000E+00 $ Fuel element in location G10.
TR0179  2.26212E+01 -8.70712E+00  0.00000E+00 $ Fuel element in location G11.
TR0180  2.26212E+01 -1.30606E+01  0.00000E+00 $ Fuel element in location G12.
TR0181  1.88519E+01 -1.95911E+01  0.00000E+00 $ Fuel element in location G14.
```

```
TR0182  1.50825E+01 -2.17678E+01  0.00000E+00 $ Fuel element in location G15.
TR0183  1.13106E+01 -2.39446E+01  0.00000E+00 $ Fuel element in location G16.
TR0184  7.54126E+00 -2.61214E+01  0.00000E+00 $ Fuel element in location G17.
TR0185  3.76936E+00 -2.82982E+01  0.00000E+00 $ Fuel element in location G18.
TR0186 -3.76936E+00 -2.82982E+01  0.00000E+00 $ Fuel element in location G20.
TR0187 -7.54126E+00 -2.61214E+01  0.00000E+00 $ Fuel element in location G21.
TR0188 -1.13106E+01 -2.39446E+01  0.00000E+00 $ Fuel element in location G22.
TR0189 -1.50825E+01 -2.17678E+01  0.00000E+00 $ Fuel element in location G23.
TR0190 -1.88519E+01 -1.95911E+01  0.00000E+00 $ Fuel element in location G24.
TR0191 -2.26212E+01 -1.30607E+01  0.00000E+00 $ Fuel element in location G26.
TR0192 -2.26212E+01 -8.70712E+00  0.00000E+00 $ Fuel element in location G27.
TR0193 -2.26212E+01 -4.35356E+00  0.00000E+00 $ Fuel element in location G28.
TR0194 -2.26212E+01  0.00000E+00  0.00000E+00 $ Fuel element in location G29.
TR0195 -2.26212E+01  4.35356E+00  0.00000E+00 $ Fuel element in location G30.
TR0196 -1.50825E+01  1.30606E+01  0.00000E+00 $ Fuel element in location G33.
TR0197 -7.54126E+00  1.74142E+01  0.00000E+00 $ Fuel element in location G35.
TR0198 -3.76936E+00  1.95910E+01  0.00000E+00 $ Fuel element in location G36.
c
c Coordinate transformations supporting beam port 2 alignment:
c -------------------------------------------------------------
c
c Note that the values assigned to each of the keywords of the coordinate
c transformation cards that follow are provided to a precision of seven digits
c as opposed to six digits (most values in this MCNP input deck are provided
c to a precision of six digits) in order to prevent the generation of
c non-orthogonality warning messages.
c
*TR0554  0.000000E+00  3.959470E+01 -6.985000E+00 $ o1, o2, and o3 keywords.
        -3.000000E+01 -1.200000E+02  9.000000E+01 $ xx', yx', and zx' keywords.
         6.000000E+01 -3.000000E+01  9.000000E+01 $ xy', yy', and zy' keywords.
         9.000000E+01  9.000000E+01  0.000000E+00 $ xz', yz', and zz' keywords.
c
*TR0611  0.000000E+00  3.959470E+01 -6.985000E+00 $ o1, o2, and o3 keywords.
        -3.000000E+01 -1.200000E+02  9.000000E+01 $ xx', yx', and zx' keywords.
         6.000000E+01 -3.000000E+01  9.000000E+01 $ xy', yy', and zy' keywords.
         9.000000E+01  9.000000E+01  0.000000E+00 $ xz', yz', and zz' keywords.
c
*TR0612  0.000000E+00  3.959470E+01 -6.985000E+00 $ o1, o2, and o3 keywords.
        -3.000000E+01 -1.200000E+02  9.000000E+01 $ xx', yx', and zx' keywords.
         6.000000E+01 -3.000000E+01  9.000000E+01 $ xy', yy', and zy' keywords.
         9.000000E+01  9.000000E+01  0.000000E+00 $ xz', yz', and zz' keywords.
c
*TR0613  0.000000E+00  3.959470E+01 -6.985000E+00 $ o1, o2, and o3 keywords.
        -3.000000E+01 -1.200000E+02  9.000000E+01 $ xx', yx', and zx' keywords.
         6.000000E+01 -3.000000E+01  9.000000E+01 $ xy', yy', and zy' keywords.
         9.000000E+01  9.000000E+01  0.000000E+00 $ xz', yz', and zz' keywords.
c
*TR0614  0.000000E+00  3.959470E+01 -6.985000E+00 $ o1, o2, and o3 keywords.
        -3.000000E+01 -1.200000E+02  9.000000E+01 $ xx', yx', and zx' keywords.
         6.000000E+01 -3.000000E+01  9.000000E+01 $ xy', yy', and zy' keywords.
         9.000000E+01  9.000000E+01  0.000000E+00 $ xz', yz', and zz' keywords.
c
*TR0615  8.000000E+00  3.959470E+01 -6.985000E+00 $ o1, o2, and o3 keywords.
        -3.000000E+01 -1.200000E+02  9.000000E+01 $ xx', yx', and zx' keywords.
         6.000000E+01 -3.000000E+01  9.000000E+01 $ xy', yy', and zy' keywords.
         9.000000E+01  9.000000E+01  0.000000E+00 $ xz', yz', and zz' keywords.
c
*TR0616 -1.305640E+02  1.195947E+02 -6.985000E+00 $ o1, o2, and o3 keywords.
        -3.000000E+01 -1.200000E+02  9.000000E+01 $ xx', yx', and zx' keywords.
         6.000000E+01 -3.000000E+01  9.000000E+01 $ xy', yy', and zy' keywords.
         9.000000E+01  9.000000E+01  0.000000E+00 $ xz', yz', and zz' keywords.
c
*TR0617 -1.245640E+02  1.195947E+02 -6.985000E+00 $ o1, o2, and o3 keywords.
        -3.000000E+01 -1.200000E+02  9.000000E+01 $ xx', yx', and zx' keywords.
         6.000000E+01 -3.000000E+01  9.000000E+01 $ xy', yy', and zy' keywords.
         9.000000E+01  9.000000E+01  0.000000E+00 $ xz', yz', and zz' keywords.
```

```
c
c Coordinate transformations supporting beam port 4 alignment:
c -------------------------------------------------------------
c
c Note that the values assigned to each of the keywords of the coordinate
c transformation cards that follow are provided to a precision of seven digits
c as opposed to six digits (most values in this MCNP input deck are provided
c to a precision of six digits) in order to prevent the generation of
c non-orthogonality warning messages.
c
*TR0556  0.000000E+00  0.000000E+00 -6.985000E+00 $ o1, o2, and o3 keywords.
         5.986650E+01 -3.013350E+01  9.000000E+01 $ xx', yx', and zx' keywords.
         1.498665E+02  5.986650E+01  9.000000E+01 $ xy', yy', and zy' keywords.
         9.000000E+01  9.000000E+01  0.000000E+00 $ xz', yz', and zz' keywords.
c
*TR0651  0.000000E+00  0.000000E+00 -6.985000E+00 $ o1, o2, and o3 keywords.
         5.986650E+01 -3.013350E+01  9.000000E+01 $ xx', yx', and zx' keywords.
         1.498665E+02  5.986650E+01  9.000000E+01 $ xy', yy', and zy' keywords.
         9.000000E+01  9.000000E+01  0.000000E+00 $ xz', yz', and zz' keywords.
c
*TR0652  0.000000E+00  0.000000E+00 -6.985000E+00 $ o1, o2, and o3 keywords.
         5.986650E+01 -3.013350E+01  9.000000E+01 $ xx', yx', and zx' keywords.
         1.498665E+02  5.986650E+01  9.000000E+01 $ xy', yy', and zy' keywords.
         9.000000E+01  9.000000E+01  0.000000E+00 $ xz', yz', and zz' keywords.
c
*TR0653  0.000000E+00  0.000000E+00 -6.985000E+00 $ o1, o2, and o3 keywords.
         5.986650E+01 -3.013350E+01  9.000000E+01 $ xx', yx', and zx' keywords.
         1.498665E+02  5.986650E+01  9.000000E+01 $ xy', yy', and zy' keywords.
         9.000000E+01  9.000000E+01  0.000000E+00 $ xz', yz', and zz' keywords.
c
*TR0654  0.000000E+00  0.000000E+00 -6.985000E+00 $ o1, o2, and o3 keywords.
         5.986650E+01 -3.013350E+01  9.000000E+01 $ xx', yx', and zx' keywords.
         1.498665E+02  5.986650E+01  9.000000E+01 $ xy', yy', and zy' keywords.
         9.000000E+01  9.000000E+01  0.000000E+00 $ xz', yz', and zz' keywords.
c
*TR655 -8.000000E+01 -1.385640E+02 -6.985000E+00 $ o1, o2, and o3 keywords.
c
c Material data cards:
c ====================
c
c Stainless steel alloy 304 material data cards:
c ----------------------------------------------
c
c The following material data cards provide material data for stainless steel
c alloy 304. The material data reproduced below was extracted from the Pacific
c Northwest National Laboratory Compendium of Material Composition Data for
c Radiation Transport Modeling (PNNL-15870 Rev. 1).
c
c       ZAID      Fraction
c    ----------  -----------
M01  006000.80c  1.83000E-03 $ Natural C at T = 293.6 K.
     014000.60c  9.78100E-03 $ Natural Si at T = 293.6 K.
     015031.80c  4.08000E-04 $ P-31 at T = 293.6 K.
     016000.62c  2.57000E-04 $ Natural S at T = 293.6 K.
     024000.50c  2.00762E-01 $ Natural Cr at T = 293.6 K.
     025055.80c  1.00010E-02 $ Mn-55 at T = 293.6 K.
     026000.50c  6.90375E-01 $ Natural Fe at T = 293.6 K.
     028000.50c  8.65870E-02 $ Natural Ni at T = 293.6 K.
c
c Air material data cards:
c ------------------------
c
c The following material data cards provide material data for air, or, more
c specifically, for dry air near sea level. The material data reproduced below
c was extracted from the Pacific Northwest National Laboratory Compendium of
c Material Composition Data for Radiation Transport
```

```
c Modeling (PNNL-15870 Rev. 1).
c
c       ZAID      Fraction
c    ----------  -----------
M02  006000.80c  1.50000E-04 $ Natural C at T = 293.6 K.
     007014.80c  7.84431E-01 $ N-14 at T = 293.6 K.
     008016.80c  2.10748E-01 $ O-16 at T = 293.6 K.
     018000.59c  4.67100E-03 $ Natural Ar at T = 293.6 K.
c
c Graphite material data cards:
c ------------------------------
c
c The following material data cards provide material data for graphite.
c The material data reproduced below was extracted from the Pacific Northwest
c National Laboratory Compendium of Material Composition Data for Radiation
c Transport Modeling (PNNL-15870 Rev. 1).
c
c       ZAID      Fraction
c    ----------  -----------
M03  005010.80c  2.00000E-07 $ B-10 at T = 293.6 K.
     005011.80c  8.00000E-07 $ B-11 at T = 293.6 K.
     006000.80c  9.99999E-01 $ Natural C at T = 293.6 K.
c
MT03 grph.20t $ Thermal neutron scattering data for
c               natural carbon in graphite at T = 293.6 K.
c
c Zirconium material data cards:
c -------------------------------
c
c The following material data cards provide material data for natural zirconium.
c The material data reproduced below was extracted from the Pacific Northwest
c National Laboratory Compendium of Material Composition Data for Radiation
c Transport Modeling (PNNL-15870 Rev. 1).
c
c       ZAID      Fraction
c    ----------  -----------
M04  040000.66c  1.00000E+00 $ Natural Zr at T = 293.6 K.
c
c Uranium zirconium hydride material data cards:
c ----------------------------------------------
c
c The following material data cards provide material data for uranium
c ziconium hydride. The uranium, zirconium, and hydrogen isotope
c fractions on the material data cards were calculated in the
c Excel workbook having the following file name:
c UZrH_Material_Data_Calculations.xlsx
c
c       ZAID      Fraction
c    ----------  -----------
M05  001001.81c  6.06927E-01 $ H-1 at T = 600 K.
     040090.81c  1.95165E-01 $ Zr-90 at T = 600 K.
     040091.81c  4.25608E-02 $ Zr-91 at T = 600 K.
     040092.81c  6.50550E-02 $ Zr-92 at T = 600 K.
     040094.81c  6.59274E-02 $ Zr-94 at T = 600 K.
     040096.81c  1.06212E-02 $ Zr-96 at T = 600 K.
     092234.81c  6.00280E-07 $ U-234 at T = 600 K.
     092235.81c  2.70751E-03 $ U-235 at T = 600 K.
     092238.81c  1.10356E-02 $ U-238 at T = 600 K.
c
MT05 zr/h.23t $ Thermal neutron scattering data for natural ~~~~~~~made change
c               zirconium in zirconium hydride at T = 600 K.
     h/zr.23t $ Thermal neutron scattering data for H-1 in
c               zirconium hydride at T = 600 K.
c
c Molybdenum material data cards:
c --------------------------------
```

```
c
c The following material data cards provide material data for natural
c molybdenum. The material data reproduced below was extracted from the Pacific
c Northwest National Laboratory Compendium of Material Composition Data for
c Radiation Transport Modeling (PNNL-15870 Rev. 1).
c
c       ZAID      Fraction
c    ----------  -----------
M06  042000.66c  1.00000E+00 $ Natural Mo at T = 293.6 K.
c
c Water material data cards:
c --------------------------
c
c The following material data cards provide material data for liquid water.
c The material data reproduced below was extracted from the Pacific Northwest
c National Laboratory Compendium of Material Composition Data for Radiation
c Transport Modeling (PNNL-15870 Rev. 1).
c
c       ZAID      Fraction
c    ----------  -----------
M07  001001.80c  6.66657E-01 $ H-1 at T = 293.6 K.
     008016.80c  3.33343E-01 $ O-16 at T = 293.6 K.
c
MT07 lwtr.20t $ Thermal neutron scattering data for H-1 in water at T = 293.6 K.
c
c Boron carbide material data cards:
c ----------------------------------
c
c The following material data cards provide material data for boron carbide.
c The material data reproduced below was extracted from the Pacific Northwest
c National Laboratory Compendium of Material Composition Data for Radiation
c Transport Modeling (PNNL-15870 Rev. 1). Note that Pacific Northwest National
c Laboratory reports a single atom fraction for what is assumed to be natural
c boron, but the boron atom fractions below are broken down into B-10 and B-11
c atom fractions where the B-10 to B-11 ratio is the ratio associated with
c natural boron reported by the National Institue of Standards and Technology.
c
c       ZAID      Fraction
c    ----------  -----------
M08  005010.80c  1.59996E-01 $ B-10 at T = 293.6 K.
     005011.80c  6.39985E-01 $ B-11 at T = 293.6 K.
     006000.80c  2.00019E-01 $ Natural C at T = 293.6 K.
c
c Aluminum alloy 6061 material data cards:
c ----------------------------------------
c
c The following material data cards provide material data for aluminum
c alloy 6061. The material data reproduced below was extracted from the Pacific
c Northwest National Laboratory Compendium of Material Composition Data for
c Radiation Transport Modeling (PNNL-15870 Rev. 1).
c
c       ZAID      Fraction
c    ----------  -----------
M09  012000.66c  1.11620E-02 $ Natural Mg at T = 293.6 K.
     013027.80c  9.77325E-01 $ Al-27 at T = 293.6 K.
     014000.60c  5.79600E-03 $ Natural Si at T = 293.6 K.
     022000.62c  4.99000E-04 $ Natural Ti at T = 293.6 K.
     024000.50c  1.01700E-03 $ Natural Cr at T = 293.6 K.
     025055.80c  4.35000E-04 $ Mn-55 at T = 293.6 K.
     026000.50c  1.98700E-03 $ Natural Fe at T = 293.6 K.
     029000.50c  1.17400E-03 $ Natural Cu at T = 293.6 K.
     030000.70c  6.06000E-04 $ Natural Zn at T = 293.6 K.
c
MT09 al27.22t $ Thermal neutron scattering data for Al-27 at T = 293.6 K.
c
c Lead material data cards:
```

```
c -------------------------
c
c The following material data cards provide material data for natural lead.
c The material data reproduced below was extracted from the Pacific Northwest
c National Laboratory Compendium of Material Composition Data for Radiation
c Transport Modeling (PNNL-15870 Rev. 1).
c
c       ZAID      Fraction
c    ----------  -----------
M10  082000.50c  1.00000E+00 $ Natural Pb at T = 293.6 K.
c
c Perfluoroalkoxy alkane (PFA) material data cards:
c -------------------------------------------------
c
c The following material data cards provide material data for perfluoroalkoxy
c alkane (PFA). The carbon, oxygen, and fluorine isotope fractions on the
c material data cards were calculated in the Excel workbook having the
c following file name: PFA_Constituent_Atom_Fraction_Calc.xlsx
c
c       ZAID      Fraction
c    ----------  -----------
M11  006000.80c  3.12500E-01 $ Natural C at T = 293.6 K.
     008016.80c  6.25000E-02 $ O-16 at T = 293.6 K.
     009019.80c  6.25000E-01 $ F-19 at T = 293.6 K.
c
c Xenon gas material data cards:
c ------------------------------
c
c The following material data cards provide material data for each of the pure
c xenon gases of interest. Only one of the xenon material data cards should be
c active at a time; the other xenon material data cards should be commented out.
c
c       ZAID      Fraction
c    ----------  -----------
M12  054130.00c  1.00000E+00 $ Xe-130 at 293.6 K.
c M12  054131.00c  1.00000E+00 $ Xe-131 at 293.6 K.
c M12  054131.01c  1.00000E+00 $ Xe-131m at 293.6 K.
c M12  054132.00c  1.00000E+00 $ Xe-132 at 293.6 K.
c M12  054133.00c  1.00000E+00 $ Xe-133 at 293.6 K.
c M12  054133.01c  1.00000E+00 $ Xe-133m at 293.6 K.
c M12  054134.00c  1.00000E+00 $ Xe-134 at 293.6 K.
c M12  054135.00c  1.00000E+00 $  Xe-135 at 293.6 K.
c M12  054135.01c  1.00000E+00 $ Xe-135m at 293.6 K.
c
c Cadmium material data cards:
c ----------------------------
c
c The following material data cards provide material data for natural cadmium.
c The material data reproduced below was extracted from the Pacific Northwest
c National Laboratory Compendium of Material Composition Data for Radiation
c Transport Modeling (PNNL-15870 Rev. 1).
c
c       ZAID      Fraction
c    ----------  -----------
M13  048000.51c  1.00000E+00 $ Natural Cd at T = 293.6 K.
c
c Cobalt material data cards:
c ---------------------------
c
c The following material data cards provide material data for the cobalt
c flux wires. The cobalt flux wires are assumed to be pure, natural cobalt,
c which has a natural isotopic composition of 100 % Co-59. Note that the
c cobalt flux wires manufactured by Shieldwerx are 99.95 % pure cobalt
c according to the Shieldwerx material analysis report provided by
c Don Hanna on 16 July 2015.
c
```

```
c       ZAID      Fraction
c    ----------  -----------
M14  027059.80c  1.00000E+00 $ Co-59 at T = 293.6 K.
c
c Concrete material data cards:
c -----------------------------
c
c The following material data cards provide material data for the high density
c concrete that forms the first level of the biological shield. The Safety
c Analysis Report for the University of Texas at Austin's TRIGA Mark II nuclear
c research reactor (the version dated May 1991) states that the concrete is
c steel rebar reinforced high density concrete with a magnetite aggregate, but
c detailed composition information could not be located. The material data
c reproduced below was extracted from the Pacific Northwest National Laboratory
c Compendium of Material Composition Data for Radiation Transport
c Modeling (PNNL-15870 Rev. 1).
c
c       ZAID      Fraction
c    ----------  -----------
M15  001001.80c  8.60690E-02 $ H-1 at T = 293.6 K.
     008016.80c  3.14488E-01 $ O-16 at T = 293.6 K.
     012000.66c  5.51600E-03 $ Natural Mg at T = 293.6 K.
     013027.80c  1.40300E-02 $ Al-27 at T = 293.6 K.
     014000.60c  2.04990E-02 $ Natural Si at T = 293.6 K.
     020000.66c  5.07690E-02 $ Natural Ca at T = 293.6 K.
     022000.62c  1.21920E-02 $ Natural Ti at T = 293.6 K.
     023000.70c  4.64000E-04 $ Natural V at T = 293.6 K.
     026000.50c  4.95972E-01 $ Natural Fe at T = 293.6 K.
c
c Aluminum oxide material data cards:
c -----------------------------------
c
c The following material data cards provide material data for aluminum oxide.
c The material data reproduced below was extracted from the Pacific Northwest
c National Laboratory Compendium of Material Composition Data for Radiation
c Transport Modeling (PNNL-15870 Rev. 1).
c
c       ZAID      Fraction
c    ----------  -----------
M16  008016.80c  6.00000E-01 $ O-16 at T = 293.6 K.
     013027.80c  4.00000E-01 $ Al-27 at T = 293.6 K.
c
c Boral material data cards:
c --------------------------
c
c The following material data cards provide material data for Boral (65 % Al
c and 35 % boron carbide). The material data reproduced below was extracted
c from the Pacific Northwest National Laboratory Compendium of Material
c Composition Data for Radiation Transport Modeling (PNNL-15870 Rev. 1).
c Note that Pacific Northwest National Laboratory reports a single atom
c fraction for what is assumed to be natural boron, but the boron atom
c fractions below are broken down into B-10 and B-11 atom fractions where
c the B-10 to B-11 ratio is the ratio associated with natural boron reported
c by the National Institue of Standards and Technology.
c
c       ZAID      Fraction
c    ----------  -----------
M17  005010.80c  9.04469E-02 $ B-10 at T = 293.6 K.
     005011.80c  3.64060E-01 $ B-11 at T = 293.6 K.
     006000.80c  1.13475E-01 $ Natural C at T = 293.6 K.
     013027.80c  4.32018E-01 $ Al-27 at T = 293.6 K.
c
c Iron material data cards:
c -------------------------
c
c The following material data cards provide material data for natural iron.
```

```
c The material data reproduced below was extracted from the Pacific Northwest
c National Laboratory Compendium of Material Composition Data for Radiation
c Transport Modeling (PNNL-15870 Rev. 1).
c
c       ZAID      Fraction
c    ----------  -----------
M18  026000.50c  1.00000E+00 $ Natural Fe at T = 293.6 K.
c
c Bismuth material data cards:
c ----------------------------
c
c The following material data cards provide material data for bismuth.
c The material data reproduced below was extracted from the Pacific Northwest
c National Laboratory Compendium of Material Composition Data for Radiation
c Transport Modeling (PNNL-15870 Rev. 1).
c
c       ZAID      Fraction
c    ----------  -----------
M19  083209.80c  1.00000E+00 $ Natural Bi at T = 293.6 K.
c
c Polyethylene material data cards:
c ---------------------------------
c
c The following material data cards provide material data for non-borated
c polyethylene. The material data reproduced below was extracted from the
c Pacific Northwest National Laboratory Compendium of Material Composition
c Data for Radiation Transport Modeling (PNNL-15870 Rev. 1).
c
c       ZAID      Fraction
c    ----------  -----------
M20  001001.80c  6.66662E-01 $ H-1 at T = 293.6 K.
     006000.80c  3.33338E-01 $ Natural C at T = 293.6 K.
c
M21  13027.70c -1 $aluminum metal
M22  5010.60c  -0.9 5011.60c -0.1 $enriched boron 10 powder
M23  7014.60c  -0.58314  5010.60c  -0.41686 $BN enriched B10
M24  48106.70c -0.011777  48108.70c -0.008543  48110.70c -0.122116  & $Cd
     48111.70c -0.126284  48112.70c -0.24021  48113.70c -0.122734  &
     48114.70c -0.29111  48116.70c -0.077225
M25     5010 -0.007385   5011 -0.032681 $borosilicate glass
        8016 -0.539559   11023 -0.028191 $borosilicate glass
        13027 -0.011644  14028 -0.346565 $borosilicate glass
        14029 -0.018175  14030 -0.012481 $borosilicate glass
        19039 -0.003086  19041 -0.000234 $borosilicate glass
M26     5011 -0.8 5010 -0.2 $natural boron powder
c
c Fission Chamber Exp Material Cards (MBS)
c ============================================
c
c     -- 90% Enriched Uranium
c
M91    92235.70c 0.9
       92238.70c 0.1
c
c     -- MgO Mineral Cable
c
M95    12024.70c          0.5
        8016.70c          0.5
c
c     -- Fill Gas
c
M96    18036.70c          1
c
c XS: Cross-section evaluation files:
c ===================================
c
```

```
c The following XS cards direct MCNP to cross-section evaluations specific to
c each of the pure xenon gases of interest. Only the XS card associated with the
c active xenon material data card should be active; the other XS cards should
c be commented out. Note that the ACE formatted files associated with the
c cross-section evaluations are assumed to be located in the same directory
c as this MCNP input deck.
c
XS1 54130.00c 128.787600 054130.00c 0 1 1 459604 0 0 2.530E-08 ptable
c XS1 54131.00c 129.780500 054131.00c 0 1 1 881582 0 0 2.530E-08 ptable
c XS1 54131.01c 129.780500 054131.01c 0 1 1 350728 0 0 2.530E-08 ptable
c XS1 54132.00c 130.771000 054132.00c 0 1 1 500694 0 0 2.530E-08 ptable
c XS1 54133.00c 131.764200 054133.00c 0 1 1 489824 0 0 2.530E-08 ptable
c XS1 54133.01c 131.764200 054133.01c 0 1 1 357702 0 0 2.530E-08 ptable
c XS1 54134.00c 132.755100 054134.00c 0 1 1 423933 0 0 2.530E-08 ptable
c XS1 54135.00c 133.748300 054135.00c 0 1 1 545678 0 0 2.530E-08 ptable
c XS1 54135.01c 133.748300 054135.01c 0 1 1 337320 0 0 2.530E-08 ptable
c
c MODE: Specify which particle and photon types should be transported:
c ===================================================================
c
c Include only an "N" designator on the MODE card to
c specify that MCNP should transport only neutrons.
c
MODE N
c
c KCODE: Use the criticality source to determine keff:
c ====================================================
c
c Set the "nsrck" keyword equal to 100,000 to instruct MCNP to run 100,000
c source histories per KCODE cycle. Set the "rkk" keyword equal to 1.0 to
c specify that the initial guess at keff should be 1.0. Set the "ikz" keyword
c equal to 100 and the "kct" keyword equal to 200 to instruct MCNP to run
c a total of 200 KCODE cycles and ignore the first 100 KCODE cycles for
c purposes of calculating keff.
c
KCODE 10000 1.0 100 200 $modified 100000 to 1000000
c changed the total number of cycles from 200 to 300
c
c KSRC: Specify the initial source point locations:
c =================================================
c
c Note that the initial source point locations specified on the KSRC card
c that follows are only utilized by the first KCODE cycle of an initiate
c run. Subsequent initiate run KCODE cycles and all continue run KCODE
c cycles utilize the fission sites generated by previous KCODE cycles.
c
c Specify the initial source point locations associated with the B-ring
c fuel elements. These source point locations are at the centers of
c the B-ring fuel elements.
c
c          x            y           z
c     -----------  -----------  -----------
KSRC  0.00000E+00  4.35356E+00  0.00000E+00 $ Fuel Element B01.
      3.76936E+00  2.17678E+00  0.00000E+00 $ Fuel Element B02.
      3.76936E+00 -2.17678E+00  0.00000E+00 $ Fuel Element B03.
      0.00000E+00 -4.35356E+00  0.00000E+00 $ Fuel Element B04.
     -3.76936E+00 -2.17678E+00  0.00000E+00 $ Fuel Element B05.
     -3.76936E+00  2.17678E+00  0.00000E+00 $ Fuel Element B06.
c
c Specify the initial source point locations associated with the C-ring
c fuel elements. These initial source point locations are at the centers
c of the C-ring fuel elements. Note that there are no initial source point
c locations associated with the C01 or C07 reactor core locations because
c there are not fuel elements in either of these reactor core locations.
c
c          x            y           z
```

```
c     -----------  -----------  -----------
      3.76936E+00 -6.53034E+00  0.00000E+00 $ Fuel Element C02.
      7.54126E+00  4.35356E+00  0.00000E+00 $ Fuel Element C03.
      7.54126E+00  0.00000E+00  0.00000E+00 $ Fuel Element C04.
      7.54126E+00 -4.35356E+00  0.00000E+00 $ Fuel Element C05.
     -3.76936E+00 -6.53034E+00  0.00000E+00 $ Fuel Element C06.
     -3.76936E+00  6.53034E+00  0.00000E+00 $ Fuel Element C08.
     -7.54126E+00 -4.35356E+00  0.00000E+00 $ Fuel Element C09.
     -7.54126E+00  0.00000E+00  0.00000E+00 $ Fuel Element C10.
     -7.54126E+00  4.35356E+00  0.00000E+00 $ Fuel Element C11.
      3.76936E+00  6.53034E+00  0.00000E+00 $ Fuel Element C12.
c
c Specify the initial source point locations associated with the D-ring
c fuel elements. These initial source point locations are at the centers
c of the D-ring fuel elements. Note that there are no initial source point
c locations associated with the D06 or D14 reactor core locations because
c there are not fuel elements in either of these reactor core locations.
c
c          x           y           z
c     -----------  -----------  -----------
      0.00000E+00  1.30607E+01  0.00000E+00 $ Fuel Element D01.
      3.76936E+00  1.08839E+01  0.00000E+00 $ Fuel Element D02.
      7.54126E+00  8.70712E+00  0.00000E+00 $ Fuel Element D03.
      1.13106E+01  6.53034E+00  0.00000E+00 $ Fuel Element D04.
      1.13106E+01  2.17678E+00  0.00000E+00 $ Fuel Element D05.
      1.13016E+01 -6.53034E+00  0.00000E+00 $ Fuel Element D07.
      7.54126E+00 -8.70712E+00  0.00000E+00 $ Fuel Element D08.
      3.76936E+00 -1.08839E+01  0.00000E+00 $ Fuel Element D09.
      0.00000E+00 -1.30607E+01  0.00000E+00 $ Fuel Element D10.
     -3.76936E+00 -1.08839E+01  0.00000E+00 $ Fuel Element D11.
     -7.54126E+00 -8.70712E+00  0.00000E+00 $ Fuel Element D12.
     -1.13016E+01 -6.53034E+00  0.00000E+00 $ Fuel Element D13.
     -1.13106E+01  2.17678E+00  0.00000E+00 $ Fuel Element D15.
     -1.13106E+01  6.53034E+00  0.00000E+00 $ Fuel Element D16.
     -7.54126E+00  8.70712E+00  0.00000E+00 $ Fuel Element D17.
     -3.76936E+00  1.08839E+01  0.00000E+00 $ Fuel Element D18.
c
c Specify the initial source point locations associated with the E-ring
c fuel elements. These initial source point locations are at the centers
c of the E-ring fuel elements. Note that there may or may not be not an
c initial source point location associated with the E11 reactor core
c location because there may or may not be a fuel element in the E11
c reactor core location depending on the reactor core configuration.
c If there is not a fuel element in reactor core location E11 the
c initial source point location associated with the E11 reactor
c core location should be commented out.
c
c          x           y           z
c     -----------  -----------  -----------
      0.00000E+00  1.74142E+01  0.00000E+00 $ Fuel Element E01.
      3.76936E+00  1.52375E+01  0.00000E+00 $ Fuel Element E02.
      7.54126E+00  1.30607E+01  0.00000E+00 $ Fuel Element E03.
      1.13106E+01  1.08839E+01  0.00000E+00 $ Fuel Element E04.
      1.50825E+01  8.70712E+00  0.00000E+00 $ Fuel Element E05.
      1.50825E+01  4.35356E+00  0.00000E+00 $ Fuel Element E06.
      1.50825E+01  0.00000E+00  0.00000E+00 $ Fuel Element E07.
      1.50825E+01 -4.35356E+00  0.00000E+00 $ Fuel Element E08.
      1.50825E+01 -8.70712E+00  0.00000E+00 $ Fuel Element E09.
      1.13106E+01 -1.08839E+01  0.00000E+00 $ Fuel Element E10.
c     7.54126E+00 -1.30607E+01  0.00000E+00 $ Fuel Element E11.
      3.76936E+00 -1.52375E+01  0.00000E+00 $ Fuel Element E12.
      0.00000E+00 -1.74142E+01  0.00000E+00 $ Fuel Element E13.
     -3.76936E+00 -1.52375E+01  0.00000E+00 $ Fuel Element E14.
     -7.54126E+00 -1.30607E+01  0.00000E+00 $ Fuel Element E15.
     -1.13106E+01 -1.08839E+01  0.00000E+00 $ Fuel Element E16.
     -1.50825E+01 -8.70712E+00  0.00000E+00 $ Fuel Element E17.
```

```
     -1.50825E+01 -4.35356E+00  0.00000E+00 $ Fuel Element E18.
     -1.50825E+01  0.00000E+00  0.00000E+00 $ Fuel Element E19.
     -1.50825E+01  4.35356E+00  0.00000E+00 $ Fuel Element E20.
     -1.50825E+01  8.70712E+00  0.00000E+00 $ Fuel Element E21.
     -1.13106E+01  1.08839E+01  0.00000E+00 $ Fuel Element E22.
     -7.54126E+00  1.30607E+01  0.00000E+00 $ Fuel Element E23.
     -3.76936E+00  1.52375E+01  0.00000E+00 $ Fuel Element E24.
c
c Specify the initial source point locations associated with the F-ring
c fuel elements. These initial source point locations are at the centers
c of the F-ring fuel elements. Note that there may or may not be initial
c source point locations associated with the F13 and F14 reactor core
c locations because there may or may not be fuel elements in these
c reactor core locations depending on the reactor core configuration.
c If there are not fuel elements in reactor core locations F13 or F14
c the initial source point location associated with the F13 and F14
c reactor core locations should be commented out.
c
c          x           y           z
c     -----------  -----------  -----------
      0.00000E+00  2.17678E+01  0.00000E+00 $ Fuel Element F01.
      3.76936E+00  1.95910E+01  0.00000E+00 $ Fuel Element F02.
      7.54126E+00  1.74142E+01  0.00000E+00 $ Fuel Element F03.
      1.13106E+01  1.52375E+01  0.00000E+00 $ Fuel Element F04.
      1.50825E+01  1.30607E+01  0.00000E+00 $ Fuel Element F05.
      1.88519E+01  1.08839E+01  0.00000E+00 $ Fuel Element F06.
      1.88519E+01  6.53034E+00  0.00000E+00 $ Fuel Element F07.
      1.88519E+01  2.17678E+00  0.00000E+00 $ Fuel Element F08.
      1.88519E+01 -2.17678E+00  0.00000E+00 $ Fuel Element F09.
      1.88519E+01 -6.53034E+00  0.00000E+00 $ Fuel Element F10.
      1.88519E+01 -1.08839E+01  0.00000E+00 $ Fuel Element F11.
      1.50825E+01 -1.30607E+01  0.00000E+00 $ Fuel Element F12.
c     1.13106E+01 -1.52375E+01  0.00000E+00 $ Fuel Element F13.
c     7.54126E+00 -1.74142E+01  0.00000E+00 $ Fuel Element F14.
      3.76936E+00 -1.95910E+01  0.00000E+00 $ Fuel Element F15.
      0.00000E+00 -2.17678E+01  0.00000E+00 $ Fuel Element F16.
     -3.76936E+00 -1.95910E+01  0.00000E+00 $ Fuel Element F17.
     -7.54126E+00 -1.74142E+01  0.00000E+00 $ Fuel Element F18.
     -1.13106E+01 -1.52375E+01  0.00000E+00 $ Fuel Element F19.
     -1.50825E+01 -1.30607E+01  0.00000E+00 $ Fuel Element F20.
     -1.88519E+01 -1.08839E+01  0.00000E+00 $ Fuel Element F21.
     -1.88519E+01 -6.53034E+00  0.00000E+00 $ Fuel Element F22.
     -1.88519E+01 -2.17678E+00  0.00000E+00 $ Fuel Element F23.
     -1.88519E+01  2.17678E+00  0.00000E+00 $ Fuel Element F24.
     -1.88519E+01  6.53034E+00  0.00000E+00 $ Fuel Element F25.
     -1.88519E+01  1.08839E+01  0.00000E+00 $ Fuel Element F26.
     -1.50825E+01  1.30607E+01  0.00000E+00 $ Fuel Element F27.
     -1.13106E+01  1.52375E+01  0.00000E+00 $ Fuel Element F28.
     -7.54126E+00  1.74142E+01  0.00000E+00 $ Fuel Element F29.
     -3.76936E+00  1.95910E+01  0.00000E+00 $ Fuel Element F30.
c
c Specify the initial source point locations associated with the G-ring
c fuel elements. These initial source point locations are at the centers
c of the G-ring fuel elements. Note that there are no initial source point
c locations associated with the G01, G07, G13, G19, G25, G31, G32, and G34
c reactor core locations because there are not fuel elements in any of
c these reactor core locations.
c
c          x           y           z
c     -----------  -----------  -----------
      3.76936E+00  2.39446E+01  0.00000E+00 $ Fuel Element G02.
      7.54126E+00  2.17678E+01  0.00000E+00 $ Fuel Element G03.
      1.13106E+01  1.95910E+01  0.00000E+00 $ Fuel Element G04.
      1.50825E+01  1.74142E+01  0.00000E+00 $ Fuel Element G05.
      1.88519E+01  1.52375E+01  0.00000E+00 $ Fuel Element G06.
      2.26212E+01  8.70712E+00  0.00000E+00 $ Fuel Element G08.
```

```
      2.26212E+01  4.35356E+00  0.00000E+00 $ Fuel Element G09.
      2.26212E+01  0.00000E+00  0.00000E+00 $ Fuel Element G10.
      2.26212E+01 -4.35356E+00  0.00000E+00 $ Fuel Element G11.
      2.26212E+01 -8.70712E+00  0.00000E+00 $ Fuel Element G12.
      1.88519E+01 -1.52375E+01  0.00000E+00 $ Fuel Element G14.
      1.50825E+01 -1.74142E+01  0.00000E+00 $ Fuel Element G15.
      1.13106E+01 -1.95910E+01  0.00000E+00 $ Fuel Element G16.
      7.54126E+00 -2.17678E+01  0.00000E+00 $ Fuel Element G17.
      3.76936E+00 -2.39446E+01  0.00000E+00 $ Fuel Element G18.
     -3.76936E+00 -2.39446E+01  0.00000E+00 $ Fuel Element G20.
     -7.54126E+00 -2.17678E+01  0.00000E+00 $ Fuel Element G21.
     -1.13106E+01 -1.95910E+01  0.00000E+00 $ Fuel Element G22.
     -1.50825E+01 -1.74142E+01  0.00000E+00 $ Fuel Element G23.
     -1.88519E+01 -1.52375E+01  0.00000E+00 $ Fuel Element G24.
     -2.26212E+01 -8.70712E+00  0.00000E+00 $ Fuel Element G26.
     -2.26212E+01 -4.35356E+00  0.00000E+00 $ Fuel Element G27.
     -2.26212E+01  0.00000E+00  0.00000E+00 $ Fuel Element G28.
     -2.26212E+01  4.35356E+00  0.00000E+00 $ Fuel Element G29.
     -2.26212E+01  8.70712E+00  0.00000E+00 $ Fuel Element G30.
     -1.50825E+01  1.74142E+01  0.00000E+00 $ Fuel Element G33.
     -7.54126E+00  2.17678E+01  0.00000E+00 $ Fuel Element G35.
     -3.76936E+00  2.39446E+01  0.00000E+00 $ Fuel Element G36.
c
c Request that tallies be evaluated:
c ==================================
c
c e0: Specify the default energy bin structure to be used for all tallies:
c ------------------------------------------------------------------------
c
c Specify that the default energy bin structure to be used for
c all tallies should be the CINDER'90 63 energy bin structure.
c
e0   1.00000E-11 5.00000E-09 1.00000E-08 1.50000E-08 2.00000E-08 2.50000E-08
     3.00000E-08 3.50000E-08 4.20000E-08 5.00000E-08 5.80000E-08 6.70000E-08
     8.00000E-08 1.00000E-07 1.52000E-07 2.51000E-07 4.14000E-07 6.83000E-07
     1.12500E-06 1.85500E-06 3.05900E-06 5.04300E-06 8.31500E-06 1.37100E-05
     2.26000E-05 3.72700E-05 6.14400E-05 1.01300E-04 1.67000E-04 2.75400E-04
     4.54000E-04 7.48500E-04 1.23400E-03 2.03500E-03 2.40400E-03 2.84000E-03
     3.35500E-03 5.53100E-03 9.11900E-03 1.50300E-02 1.98900E-02 2.55400E-02
     4.08700E-02 6.73800E-02 1.11100E-01 1.83200E-01 3.02000E-01 3.88700E-01
     4.97900E-01 6.39279E-01 8.20850E-01 1.10803E+00 1.35335E+00 1.73774E+00
     2.23130E+00 2.86505E+00 3.67879E+00 4.96585E+00 6.06500E+00 1.00000E+01
     1.49182E+01 1.69046E+01 2.00000E+01 2.50000E+01
c
c Evaluate tallies in the central body section of the Swagelok PFA plug valve:
c ---------------------------------------------------------------------------
c
c Request a tally to evaluate the neutron flux profile in the gas trapped
c in the central body section of the Swagelok PFA plug valve (cell 0253):
c
c F0004:n 0253
c FC0004 The neutron flux profile in cell 0253.
c SD0004 0.167 $ This segment divisor card specifies that the volume of cell 0253
c              is 0.167 cm^3. The volume of cell 0253 is calculated in the
c              Excel workbook having the following file name:
c              Swagelok_PFA_Plug_Valve_Surface_Position_Calculations.xlsx
c
c Request a tally to evaluate the cross-section weighted neutron flux
c profile in the gas trapped in the central body section of the
c Swagelok PFA plug valve (cell 0253):
c
c F0014:n 0253
c FC0014 Cross-section weighted neutron flux profile in cell 0253.
c FM0014 1 12 102 $ This tally multiplier card specifies that the multiplicative
c                 constant should be one, the MCNP material number associated
c                 with the material filling cell 0253 should be 30, and the
```

```
c                reaction number of interest should be 102 (the radiative
c                capture reaction number).
c SD0014 0.167 $ This segment divisor card specifies that the volume of cell 0253
c              is 0.167 cm^3. The volume of cell 0253 is calculated in the
c              Excel workbook having the following file name:
c              Swagelok_PFA_Plug_Valve_Surface_Position_Calculations.xlsx
c
c Evaluate tallies in the end-cap section of the Swagelok PFA plug valve:
c ---------------------------------------------------------------------
c
c Request a tally to evaluate the neutron flux profile in the gas trapped
c in the end-cap section of the Swagelok PFA plug valve (cell 0251):
c
c F0024:n 0251
c FC0024 The neutron flux profile in cell 0251.
c SD0024 0.438 $ This segment divisor card specifies that the volume of cell 0251
c              is 0.438 cm^3. The volume of cell 0253 is calculated in the
c              Excel workbook having the following file name:
c              Swagelok_PFA_Plug_Valve_Surface_Position_Calculations.xlsx
c
c Request a tally to evaluate the cross-section weighted neutron flux
c profile in the gas trapped in the end-cap section of the
c Swagelok PFA plug valve (cell 0251):
c
c F0034:n 0251
c FC0034 Cross-section weighted neutron flux profile in cell 0251.
c FM0034 1 12 102 $ This tally multiplier card specifies that the multiplicative
c                constant should be one, the MCNP material number associated
c                with the material filling cell 0251 should be 30, and the
c                reaction number of interest should be 102 (the radiative
c                capture reaction number).
c SD0034 0.438 $ This segment divisor card specifies that the volume of cell 0251
c              is 0.438 cm^3. The volume of cell 0253 is calculated in the
c              Excel workbook having the following file name:
c              Swagelok_PFA_Plug_Valve_Surface_Position_Calculations.xlsx
c
c
c FLUX TALLIES FOR BRANDONS CRAP
c F0704:N     700
c F0714:N     701
c F0724:N     702
c F0734:N     703
c F0744:N     704
c F0754:N     711
c F0764:N     706
c F0774:N     707
c
c WWP and WWG: Set weight-window parameter and weight-window generator options:
c ============================================================================
c
c Set the particle designator keyword on the WWP card equal to N and set the
c "switchn" keyword on the WWP card equal to -1 to specify that the lower
c weight bounds for neutrons should be extracted from an external WWINP file.
c Accept the defaults for all of the other WWP card keywords.
c
WWP:N 4J -1 4J
c
c Set the "it" keyword on the WWG card equal to 0024 to specify that the
c weight-window generator should be optimized for tally number 0024 (the neutron
c flux profile tally evaluated in the gas trapped in the central body section of
c the Swagelok PFA plug valve). Also set the "ic" keyword equal to 0016 to
c specify that the cell based weight-window generator should be invoked with
c cell 0016 as the reference cell (the fact that the reference cell is specified
c as a positive number indicates that the cell-based weight-window generator
c should be invoked). Accept the defaults for all of the other
c WWG card keywords.
```

```
c
c WWG 0024 0016 6J
c
c PRINT: Request that optional output tables be printed:
c ======================================================
c
c Request that optional print table 128, the universe map table, be printed.
c This table must be printed to allow MCNP to determine if all repeated
c structures and lattice elements are sampled for fission neutron
c source points.
c
PRINT 128
c
c RAND: Set the psuedorandom number generation options:
c =====================================================
c
c Set the "GEN" keyword on the RAND card equal to 1 to specify that the MCNP
c Lehmer 48-bit congruential psuedorandom number generator should be used
c (this is the default psuedorandom number generator in MCNP 6.1.1b). Also,
c set the "SEED" keyword on the RAND card equal to 219,008,682,294,439 to set
c the psuedorandom number generator seed equal to 219,008,682,294,439.
c Accept the defaults for all the other RAND card keywords.
c
c Note that originally the default values were accepted for all of the RAND
c card keywords, but the execution of this MCNP input deck terminated because
c of "bad trouble" in the rotas subroutine encountered during the transport of
c particle history number 1,6096,186, which utilized a starting psuedorandom
c number of 219,008,682,294,437. I discussed this issue with Dr. Forrest Brown
c at Los Alamos National Lab in an email chain that originated on
c 10 November 2015. While the root issue in the rotas subroutine was not
c identified or flushed out, Dr. Brown agreed that setting the psuedorandom
c number seed manually might provide a work around. The "SEED" keyword is thus
c now set equal to the odd number immediately following the starting
c psuedorandom number associated with the offending particle history in an
c attempt to work around the aforementioned bad trouble encountered when the
c default values were accepted for all of the RAND card keywords.
c
RAND GEN=1 SEED=219008682294439
```

References

Antolínez, A., Rapisarda, D. (2006) *Fission chambers designer based on Monte Carlo techniques working in current mode and operated in saturation regime*. Nuclear Instruments and Methods in Physics.

ASTM Standard E 262-03. (2003) *Standard Test Method for Determining Thermal Neutron Reaction and Fluence Rates by Radioactivation Techniques*. ASTM International.

Braisted, J. (2008) *Design and Characterization of an Irradiation Facility with Real-Time Monitoring*. The University of Texas at Austin.

Century Spring Corp. (2018) *Compression Spring 3858 Product Information*. Accessed 15 March 2018 http://www.centuryspring.com/compression-spring-3858.html.

Chabod, S., Fioni, G., Letourneau, A., Marie, F. (2006) *Modelling of fission chambers in current mode-Analytical approach*. Nuclear Instruments and Methods in Physics Research.

Chen, C., Chai, Z., Gao, Y. (2010) *Nuclear Analytical Techniques for Metallomics and Metalloproteomics*. Cambridge: Royal Society of Chemistry.

Copple, B. (2014). *Development of a Fully Automated Rapid Irradiated Sample Transport System for Neutron Activation Analysis*. The University of Texas at Austin.

DeJuren, J., Rosenwasser, H. (1953) *Diffusion Length of Thermal Neutrons in Water.* Journal of Research of the National Bureau of Standards.

Di Luzio M, Oddone M, Prata M, et al. (2017) *Measurement of the neutron flux parameters f and α at the Pavia TRIGA Mark II reactor*. J Radioanal Nucl Chem

Eriksson, S., Mackey, E., Lindstrom, R., et al. (2013) *Delayed-neutron activation analysis at NIST.* J Radioanal Nucl Chem.

Frontasyeva, M.V., (2011) *Neutron Activation Analysis in the Life Sciences.* J Radioanal Nucl Chem. Physics of Particles and Nuclei.

Geslot, B., Berhouet, F., Oriol, L., et.al. (2009) *Development and Manufacturing of Special Fission Chambers for In-Core Measurement Requirements in Nuclear Reactors.* 1st International Conference on Advancements in Nuclear Instrumentation, Measurement Methods and their Applications.

Geslot, B., Vermeeren, L., Filliatre, P., et.al. (2011) *New measurement system for on line in core high-energy neutron flux monitoring in material testing reactor conditions.* Review of Scientific Instruments.

Gilmore, G. (2008). *Practical Gamma-Ray Spectrometry, 2nd Edition.* John Wiley & Sons, Ltd.

Glascock, M. (2017) *Overview of Neutron Activation Analysis*, University of Missouri Research Reactor, Accessed 12 November 2017 http://archaeometry.missouri.edu/naa_overview.html

Goricanec T, Zerovnik G, Barbot L, et al (2018) *Evaluation of neutron flux and fission rate distributions inside the JSI TRIGA Mark II reactor using multiple in-core fission chambers*. An Nucl Ene

Greenberg, R., Bode, P., De Nadai Fernandes, E. (2011) *Neutron activation analysis: A primary method of measurement.* Spectrochimica Acta.

Hancock, R. (2015). *Encyclopedia of Scientific Dating Methods: Neutron Activation Analysis*. Springer Science and Business Media.

Huang, C., Jiang, S. (2017). *Neutron activation analysis using a modified absolute calibration method.* J Radioanal Nucl Chem.

Kaiba T, Žerovnik G, Jazbe A, et al (2015) *Validation of neutron flux redistribution factors in JSI TRIGA reactor due to control rod movements*. Appl. Radiat. Isot

Khamis, I., Othman, I., Nasri, M., Bakkour, M. (2001) *Transfer time optimization of a rapid cyclic instrumental neutron activation analysis for trace element detection.* Review of Scientific Instruments.

Knoll, G. F. (2010). *Radiation Detection and Measurement*. John Wiley.

Landsberger S, Cizek W, Domagala P (1992) *NADA: A versatile PC based program for neutron activation data analysis*. J Radioanal Nucl Chem

Landsberger, S., Dayman, K. (2012). *Monitoring of Neutron Flux Changes in Short-Lived Neutron Activation Analysis*. J Radioanal Nucl Chem.

MilliporeSigma (2016) *Sulfur Product CAS 7704-34-9 Safety Data Sheet.* Accessed 15 March 2018 https://www.sigmaaldrich.com/catalog/product/sigald/13825?lang=en&region=US

Mosgovoy, W., Morgan, W., Ballowe, W., Russell, J. (1962) *Thermal neutron diffusion length measuments in lightwater from 20°C to 90°C*. Vallecitos Atomic Laboratory, U.S. Atomic Energy Commission.

National Instruments (2015) *National Instruments GPIB-USB-HS Product information*. Accessed 15 March 2018 http://www.ni.com/en-us/shop/select/gpib-instrument-control-device.

National Instruments (2017) *National Instruments LabVIEW 2017 User Manual*. Accessed 15 March 2018.

NETL Safety Analysis Report (SAR), Rev.1. (1991) The University of Texas at Austin Nuclear Engineering Teaching Laboratory.

Photonis Technologies S.A.S (2015) *CFUF 43/30 No. 3417 Quality Control Booklet*. Brive, France.

Photonis Technologies S.A.S (2018) *Photonis In-Core Fission Chamber Product Information*. Accessed 15 March 2018. https://www.photonis.com/product/fission-chambers-core-use.

Pneumatic System Design Schematics. (1997) The University of Texas at Austin Nuclear Engineering Teaching Laboratory.

Ravnik, M. (1991) *Nuclear safety parameters of mixed TRIGA cores, Workshop on reactor physics calculations*, World Scientific

Stopic A, Bennett J (2016) *Irradiation pneumatic system fine-tuning using accelerometers*. J Radioanal Nucl Chem.

Tektronix INC. (2015) *Keithley Picoammeter Product Information. Accessed 15 March 2018* https://www.tek.com/keithley-low-level-sensitive-and-specialty-instruments/keithley-series-6400-picoammeters.

TRIGA Reactor Technical Specifications, Rev. 1. (1990) The University of Texas at Austin Nuclear Engineering Teaching Laboratory.

Trkov, A., Radulovic, V. (2015). *Nuclear reactions and physical models for neutron activation analysis.* J Radioanal Nucl Chem.

U.S. Department of Energy. (1993) *DOE Fundamentals Handbook Nuclear Physics and Reactor Theory Volume 1*, Washington, D.C.

U.S. Department of Energy. (1993) *DOE Fundamentals Handbook Nuclear Physics and Reactor Theory Volume 2*, Washington, D.C.

Vieira B, Landsberger S, Freitas M (2006) *Evaluation of atmospheric airborne particles in Lisbon, Portugal using neutron activation analysis*. J Radioanal Nucl Chem.

Zerovnik, G., Kaiba, T., Radulovic, V., et.al. (2015) *Validation of the neutron and gamma fields in the JSI TRIGA reactr using in-core fission and ionization chambers.* Applied Radiation and Isotopes.

Vita

Major Matthew Stokley received his B.S. in Physics from Valdosta State University in Valdosta, GA in 2006. In October 2007, MAJ Stokley was commissioned as an Officer in the U.S. Army, Medical Service Corps as a Nuclear Medical Science Officer. His previous assignments include: Chief of Health Physics and Radiation Safety Officer, Carl R. Darnall Army Medical Center, Fort Hood, TX; Deputy Chief of Health Physics and Laser Safety Officer, Dwight David Eisenhower Army Medical Center, Fort Gordon, GA; Current Operations Officer and Assistant S-3, U.S. Army Public Health Command, Landstuhl, Germany; Industrial Health Physics Program Manager, U.S. Army Center for Health Promotion and Preventive Medicine-Europe, Landstuhl, Germany.

In 2016, MAJ Stokley was selected by the Army to pursue his graduate degree in Nuclear Engineering at the University of Texas at Austin while serving on active duty. He received his Master's Degree in Nuclear and Radiation Engineering in 2018. His next assignment is with the Defense Threat Reduction Agency's Defense Nuclear Weapons School where he will be serving as an instructor and Officer in Charge of Health Physics.

Permanent email address: mbstokle@gmail.com

This thesis was typed by the author.